UNIVERSITY OF ALBERTA

CELLULAR STUDIES OF NEUROTRANSMISSION WITHIN THE HORIZONTAL LIMB OF THE DIAGONAL BAND OF BROCA

by

JACOB CHIRAKKATTU EASAW ©

A THESIS SUBMITTED TO THE FACULTY OF GRADUATE STUDIES IN PARTIAL FULFILLMENT OF THE REQUIREMENTS FOR THE DEGREE OF

DOCTOR OF PHILOSOPHY

IN

MEDICAL SCIENCES - MEDICINE

EDMONTON, ALBERTA

FALL, 1996

National Library of Canada
Acquisitions and Bibliographic Services Branch
395 Wellington Street
Ottawa, Ontario
K1A 0N4

Bibliothèque nationale du Canada
Direction des acquisitions et des services bibliographiques
395, rue Wellington
Ottawa (Ontario)
K1A 0N4

Your file Votre référence

Our file Notre référence

The author has granted an irrevocable non-exclusive licence allowing the National Library of Canada to reproduce, loan, distribute or sell copies of his/her thesis by any means and in any form or format, making this thesis available to interested persons.

L'auteur a accordé une licence irrévocable et non exclusive permettant à la Bibliothèque nationale du Canada de reproduire, prêter, distribuer ou vendre des copies de sa thèse de quelque manière et sous quelque forme que ce soit pour mettre des exemplaires de cette thèse à la disposition des personnes intéressées.

The author retains ownership of the copyright in his/her thesis. Neither the thesis nor substantial extracts from it may be printed or otherwise reproduced without his/her permission.

L'auteur conserve la propriété du droit d'auteur qui protège sa thèse. Ni la thèse ni des extraits substantiels de celle-ci ne doivent être imprimés ou autrement reproduits sans son autorisation.

ISBN 0-612-18033-6

Canada

University of Alberta

Library Release Form

Author:	Jacob Easaw
Title of Thesis:	Cellular Studies of Neurotransmission within the Horizontal Limb of the Diagonal Band of Broca.
Degree:	Doctor of Philosophy
Year This Degree Granted:	1996

Permission is hereby granted to the University of Alberta Library to reproduce single copies of this thesis and to lend or sell such copies for private, scholarly, or scientific research purposes only.

The author reserves all other publication and other rights in association with the copyright in the thesis, and except as hereinbefore provided, neither the thesis nor any substantial portion thereof may be printed or otherwise reproduced in any material form whatever without the author's prior written permission.

Author:

Date Submitted: 12Aug96

University of Alberta

Faculty of Graduate Studies and Research

The undersigned certify that they have read, and recommended to the Faculty of Graduate Studies and Research for acceptance, a thesis entitled **Cellular Studies of Neurotransmission within the Horizontal Limb of the Diagonal Band of Broca** submitted by **Jacob Chirakkattu Easaw** in partial fulfilment of the requirements for the degree of **Doctor of Philosophy** in **Medical Sciences - Medicine (Neurology).**

J.H. Jhamandas, M.D., Ph.D., Supervisor

C. W. Bourque, Ph.D., External Examiner

P. A. Smith, Ph.D., Committee Member

W. F. Colmers, Ph.D., Committee Member

J. J. Greer, Ph.D., Committee Member

T. L. Krukoff, Ph.D., Committee Member

R. L. Jones, Ph.D., Committee Chair

June 7, 1996

Date

For my parents

Abstract

The horizontal limb of the diagonal band of Broca (hDBB) within the basal forebrain subserves important roles in memory mechanisms, theta rhythm, and central cardiovascular regulation. In addition to its role in physiological processes, it is implicated in pathophysiological conditions such as Alzheimer's disease (AD). The objective of this thesis was to examine the actions of specific neurotransmitters and neuromodulators that are believed to mediate the hDBB's role in these physiological and pathophysiological conditions.

Glutamate is a major central excitatory neurotransmitter that is localized within the hDBB. Using an *in vitro* forebrain slice preparation, I provide evidence for the participation of ionotropic glutamate receptor subtypes in mediating fast excitatory synaptic transmission in this nucleus. Metabotropic glutamate receptors are also present presynaptically and attenuate the release of glutamate. Furthermore, an analysis of cable properties of these neurons indicates that they are electrically compact and thus possess features for the efficient relay of signals to distal sites.

I also characterized a role for the inhibitory amino acid, GABA, within the hDBB using a brain slice preparation. $GABA_A$, $GABA_B$, but not $GABA_C$ receptors were identified on hDBB neurons.$GABA_A$ receptors mediate inhibitory postsynaptic transmission, whereas $GABA_B$ receptors attenuate glutamate release presynaptically. In some cases, $GABA_B$ receptors also work synergistically with presynaptic metabotropic glutamate receptors to reduce the release of glutamate.

As the neuropeptide vasopressin (VP) has also been shown to modulate glutamate

actions in this nucleus, I examined the cellular mechanisms underlying the actions of VP on acutely dissociated hDBB cells. VP application produced two distinct responses. In one group of cells, VP evoked a decrease in outward currents through a V_1 receptor-mediated mechanism that is coupled to the I_C channel. In a second group, it increased outward current through I_C channels via activation of V_2 receptors.

Zinc (Zn^{++}) subserves important physiological roles in the brain and has been implicated in neurodegeneration of the basal forebrain in AD. I studied Zn^{++} modulation of intrinsic ionic conductances in hDBB neurons. Zn^{++} influences transiently- and slowly-activating potassium conductances as well as calcium currents. Zn^{++} also has the capacity to alter the excitability of hDBB neurons.

Neurotransmitter and peptidergic modulation of hDBB neurons may have important consequences for physiological processes and in the context of pathophysiology within this region.

ACKNOWLEDGMENTS

There are many people I would like to acknowledge for without their support, this thesis could not have been completed.

First and foremost, I would like to extend my heartfelt thanks to Dr. Jack Jhamandas. Jack has seen me go through some of the best and some of the worst times in my life during my years in his lab. Through it all, he has stood beside me, rejoicing in my triumphs and providing a shoulder to lean on through my defeats. He is so much more than a supervisor to me. He is a mentor, a colleague, and most importantly, a friend. I cannot adequately express the depth of my devotion to him. Without his guidance and patience, there is no question in my mind that this thesis could not have been completed.

I would also like to thank the other members of my supervisory committee: Drs. Peter Smith, John Greer, and Teresa Krukoff for their support and insight. They consistently reminded me that we don't just live in a world where channels open and close and ensured that I didn't lose site of the physiological relevance of my observations. In particular, I'd like to thank John. I can remember too many times when experiments weren't working and I felt like I had the weight of the world on my shoulders. He always reminded me that it wasn't the end of the world and that things would get better. His quiet encouragement help me through many an experiment.

I wish to acknowledge Drs. Bill Colmers and Marek Duszyk for serving as "hired guns" for my candidacy exam. Somehow, we were also able to coerce Bill into also serving as an examiner for my thesis defence. I'd also like to thank Bill, Peter, and Dr. Charles Bourque for reading drafts of the EAA paper. Their input helped raise the quality of the paper to the point where it was publishable.

I wish to extend my thanks to my colleagues in the lab: Kim Harris, Balvinder Jassar, and David MacTavish. Kim is one the most talented people I know. He paints, he's an athlete, and technically in the lab, he is unmatched. In the last few days before this thesis was sent to the examiners, he stayed late in the lab and helped me get it done. Balvinder is a scientific genius. In my opinion, this is the best description of the guy. I

admire his intuitive feel for science and his ability to overcome what seem like insurmountable obstacles. He read countless drafts of Chapters 5 and 6. His comments were always insightful and thorough. Finally, I'd like to thank David for his friendship. His quick-witted, relaxed demeanor and our mutual love of hard rock have made him a valued friend.

I would also like to thank Rory McQuiston, Jeff Zidichouski, and Cynthia Krys for all of their help. Rory and Jeff each spent a great deal of time teaching me the various nuances of electrophysiology and I am truly indebted to them. Cynthia is one of the kindest people I have had the opportunity to meet. Like so many of the people I have met as a graduate student, she is a multi-talented individual. In addition to being a superb typist, she bakes one mean birthday cake.

My good friend Susan Patrick who wiled away many an hour with me eating ice cream and musing on the merits of life in and out of science. She is the only person who can truly capture the evil of Mr. Burn's (from the Simpson's T.V. show) classic phrase "Excellent".

To my family. They have supported me through the sometimes trying life of a grad student. They have sacrificed so much for me so that I could reach this point. I hope that they are proud of me and I dedicate this thesis to them.

To Jennifer Barnes, the love of my life. I could not have finished this without her. She has stood by me through the good and the bad and taught me that some things are more important than work. I will never be able to express how important she is to me. She is my soulmate, my confidant, and my best friend. Without a doubt, the absolute best thing about my years as a Ph.D student is that I was able to meet her.

SOLI DEO GLORIA

Table of Contents

CHAPTER 1

GENERAL INTRODUCTION 1

Overview 2

A Brief History 2

Anatomy of the DBB 3

Neurochemical Characteristics of DBB neurons 4

Acetylcholine 4

GABA 5

Other chemical phenotypes 6

Afferent and Efferent Connections and Their Relation to Function 7

Anatomical Connectivity of the DBB 7

Efferent Connections of the DBB 7

Afferent Connections of the DBB 9

Physiological Functions Mediated by the DBB 11

Central cardiovascular regulation 11

Fluid Balance 13

Theta Rhythm 15

Memory and Learning 17

Cellular Properties 23

Rationale and Objectives 25

REFERENCES 28

CHAPTER 2

METHODS AND MATERIALS 57

Methods and Materials for Recording from Rat Brain Slices 58

Dissection 58

Electrophysiological Recording 58

Data Acquisition and Analysis 59

Drugs Used 59

Excitatory Amino Acid Study (Chapter 3) 60

Agonists: 60

Antagonists 60

Morphology 60

Analysis of Membrane Properties 61

Analysis of Cable Properties 61

Inhibitory Modulation of hDBB Neurons (Chapter 4) 63

Agonists: 63

Antagonists 63

Voltage Protocols: 64

Methods and Materials for Recording from Acutely Dissociated hDBB

Cells 64

Dissection 64

Electrodes and Method of Recording 64

Vasopressin Study (Chapter 5) 66

Voltage Protocols 66

Pharmacological Agents Used 66

Zinc (Chapter 6) 67

Voltage Protocols 67

Pharmacological Agents Used 67

REFERENCES 68

CHAPTER 3

ELECTROPHYSIOLOGY OF NEURONS IN THE HORIZONTAL LIMB OF THE DIAGONAL BAND OF BROCA: INTRINSIC PROPERTIES AND EXCITATORY SYNAPTIC INPUTS 70

ABSTRACT 71

INTRODUCTION 72

RESULTS 72

Morphology 72

Passive and Active Properties of hDBB Neurons 73

Pharmacology of Glutamate Neurotransmission 74

AMPA\Kainate 74

NMDA 74

Metabotropic 75

TTX 76

DISCUSSION 76

Morphology 76

Intrinsic Membrane Properties 77

Cable properties of hDBB neurons 78

Analysis of glutamate agonist effects and glutamate-mediated synaptic transmission 80

Functional Considerations 81

REFERENCES 103

CHAPTER 4

INHIBITORY INPUTS ONTO NEURONS IN THE HORIZONTAL LIMB OF THE DIAGONAL BAND OF BROCA 106

ABSTRACT 107

INTRODUCTION 108

RESULTS 109

Postsynaptic Actions of GABA 109

$GABA_A$ Receptors 109

$GABA_B$ Receptors 110

$GABA_C$ 111

Presynaptic Inhibition 111

$GABA_B$ Receptors 111

DISCUSSION 113

Interactions of GABA with glutamate 114

$GABA_C$ Receptors 114

Sources of GABAergic inputs to the DBB 115

Identity and physiological function of hDBB cells receiving. 115

Pathophysiological implications 116

REFERENCES 129

CHAPTER 5

VASOPRESSIN RECEPTOR SUBTYPES DIFFERENTIALLY MODULATE CALCIUM-ACTIVATED POTASSIUM CURRENTS IN THE HORIZONTAL LIMB OF THE DIAGONAL BAND OF BROCA 132

ABSTRACT 133

INTRODUCTION 134

RESULTS 136

Actions of VP in a Forebrain Slice Preparation 136

Actions of VP in an Acutely Dissociated hDBB Cell Preparation . 137

Effects of VP on outward currents 137

Receptor pharmacology of VP responses 139

Ionic mechanisms of VP-mediated responses 141

Blockade of Ca^{++} occludes VP responses 141

VP modulation of I_C currents 142

Effect of VP on calcium currents 143

DISCUSSION 144

Whole cell recording and VP responses 144

Localization of VP receptor subtypes 146

Mechanism of action of VP receptors 146

Intrinsic properties of hDBB neurons 148

Functional role of I_C in hDBB neurons 148

REFERENCES 174

CHAPTER 6

ZINC MODULATION OF IONIC CURRENTS IN THE HORIZONTAL LIMB OF THE DIAGONAL BAND OF BROCA (hDBB) 185

ABSTRACT 186

INTRODUCTION 188

RESULTS 189

Zn^{++} effects on A-current 190

Modulation of I_K by Zn^{++} 192

Zn^{++} modulation of I_{Na} 193

Effects of Zn^{++} on I_{Ba} 194

Effects of Zn^{++} on the discharge rate of APs in the forebrain slice 195

DISCUSSION 195

Concentration of Zinc 196

Zinc modulation of A-current 196

Decrease in delayed rectifier by Zn^{++} 197

Sodium Current modulation by Zinc 198

Calcium Current modulation by Zinc 198

Modulation of I_C and I_{AHP} 199

Pathophysiological consequences of Zn^{++} actions on hDBB cells .. 200

REFERENCES 218

CHAPTER 7

GENERAL DISCUSSION 225

CONCLUSIONS AND FUTURE EXPERIMENTS 230

REFERENCES 238

List of Figures

Figure 3-1. Schematic drawing of the rat forebrain illustrating horizontal limb of the diagonal band of Broca (hDBB), where whole cell patch clamp recordings were obtained. 86

Figure 3-2. Recordings taken from different hDBB neurons using either the whole cell patch clamp method (top row) or the perforated patch technique (bottom row). 88

Figure 3-3. AMPA receptors mediate excitatory neurotransmission in hDBB. 90

Figure 3-4. Kainate receptors mediate excitatory neurotransmission in hDBB. 92

Figure 3-5. NMDA receptor involvement in excitatory neurotransmission in hDBB. . . 94

Figure 3-6. Metabotropic receptor involvement in excitatory neurotransmission in hDBB. 96

Figure 3-7. Presynaptic modulation of excitatory neurotransmission by metabotropic receptors. 98

Figure 3-8. trans-ACPD does not modulate postsynaptic AMPA responses. 100

Figure 3-9. trans-ACPD does not modulate postsynaptic NMDA responses. 102

Figure 4-1. $GABA_A$ receptors activation mediates inhibitory neurotransmission in the hDBB. 118

Figure 4-2. Postsynaptic responses mediated by activation of $GABA_B$ but not $GABA_C$ receptors. 120

Figure 4-3. Presynaptic blockade of glutamate-mediated EPSCs. 122

Figure 4-4. Differential distribution of $GABA_A$ and $GABA_B$ channels. 124

Figure 4-5. Dual actions of presynaptic $GABA_B$ and mGluR receptors on EPSC. ... 126

Figure 4-6. Lack of $GABA_B$ and mGluR receptor synergy in modulating excitatory synaptic responses 128

Figure 5-1. Vasopressin modulates excitabiility of hDBB cells. 151

Figure 5-2. Vasopressin modulation of outward currents in rat forebrain slices. 153

Figure 5-3. Effects of perfusion of VP on two populations of cells. 155

Figure 5-4. Vasopressin mediated decrease in outward currents in acutely dissociated neurons 157

Figure 5-5. Vasopressin mediated increase in outward currents. 159

Figure 5-6. V_1 receptor antagonist, MC, blocked VP-mediated decrease in outward currents. 161

Figure 5-7. V_2 receptor antagonist ($d(CH_2)_5^1$,D-Ile^2,Ile^4,Arg^8,Ala^9) blocked VP-mediated increase in outward currents. 163

Figure 5-8. Blockade of Ca^{++}-influx occluded VP-induced decrease in outward current. 165

Figure 5-9. Blockade of Ca^{++}-influx occluded VP-induced increase in outward current. 167

Figure 5-10. CTX (25nM) occluded VP-mediated decrease in outward currents. 169

Figure 5-11. CTX (25nM) occluded VP-mediated increase in outward currents. 171

Figure 5-12. VP does not affect barium currents (I_{Ba})in hDBB neurons. 173

Figure 6-1. Effect of Zn^{++}on I_A 203

Figure 6-2. Effect of Zn^{++} on I_A under control conditions and under conditions when Na^+ and Ca^{++} influx was blocked. 205

Figure 6-3. Effect of Zn^{++} on the kinetics of activation and inactivation of I_A. 207

Figure 6-4. Effect of Zn^{++} on I_K in hDBB cells. 209

Figure 6-5. Effect of Zn^{++} on whole cell currents evoked by brief voltage steps. ... 211

Figure 6-6. Effect of Zn^{++} on I_{Na}. 213

Figure 6-7. Effect of Zn^{++} on I_{Ba}. 215

Figure 6-8. Zn^{++} modulation of hDBB excitability. 217

Figure 7-1. Distribution of GABAergic and glutamatergic receptor subtypes within the hDBB. 233

Figure 7-2. VP released from presynaptic terminals acts at postsynaptic V_1 and V_2 receptors. 235

Figure 7-3. Zn^{++} released from presynaptic terminals modulates voltage-gated ion channels postsynaptically. 237

List of Tables

Table 3-I. Summary of active and passive properties of hDBB neurons. 83

Table 3-II. Electrotonic properties of hDBB neurons. 84

List of Abbreviations

λ	length constant
ρ	dendrite-to soma-conductance ratio
4-AP	4-aminopyridine
ACE	amygdala
AchE	acetylcholinesterase
ACSF	artificial cerebrospinal fluid
AD	Alzheimer's disease
AHP	afterhyperpolarization
AII	angiotensin II
AMPA	α-amino-3-hydroxy-5-methyl-4-isoxazolepropionate
AP	action potential
AP3	2-amino-3-phosphonopropionate
APV	(-)2-amino-7-phosphonopentanoate
BF	basal forebrain
BST	bed nucleus of the stria terminalis
CACA	cis-4-aminocrotonic acid
ChAT	choline acetyltransferase
C_m	specific membrane capacitance
CNQX	6-cyano-7-nitroquinoxaline-2,3-dione
CNS	central nervous system
CTX	charybdotoxin

DBB	diagonal band of Broca
HRP	horseradish peroxidase
DR	dorsal raphe
EAAs	excitatory amino acids
EPSCs	excitatory postsynaptic currents
EPSPs	excitatory postsynaptic potentials
FAHP	fast postspike afterhyperpolarization
ff	fimbria-fornix
FSH	follicle stimulating hormone
GABA	γ-aminobutyric acid
GAD	glutamate decarboxylase
G_i	input conductance
H	amount of current attenuation
hDBB	diagonal band of Broca, horizontal limb
I-V	current-voltage
I_A	transiently activating K^+ currents
I_{Ba}	barium currents
I_{Ca}	calcium currents
I_K	delayed rectifier
I_C, I_{AHP}, $I_{K(Ca)}$	calcium activated potassium currents
I_{Na}	sodium currents
IPSCs	inhibitory postsynaptic currents
IPSPs	inhbitory postsynaptic potentials

ITT	inter-trial intervals
KA	kainate
L	electrotonic length
LC	locus coeruleus
LH	luteinizing hormone
LHRH	luteinizing hormone releasing hormone
LY	Lucifer Yellow
MC	Manning Compound
ME	median eminence
mGluR	metabotropic glutamate receptors
MS-DBB	medial septum-diagonal band of Broca
NA	noradrenaline
NBQX	2,3-dihydroxy-6-nitro-7-sulfamoyl-benzo(f)quinoxaline
NGF	nerve growth factor
NMDA	N-methyl-D-aspartate
NO	nitric oxide
p75-NGFr	low-affinity NGF receptors
PNZ	perinuclear zone
PV	parvalbumin
R_m	Specific membrane resistance
rmp	resting membrane potential
s.e.m.	standard error of mean
SFO	subfornical organ

SON	hypothalamic supraoptic
TEA	tetraethylammonium chloride
trans-ACPD	trans-1-aminocyclopentane-1,3-dicarboxylic acid
TTX	tetrodotoxin
V_a	half-activation voltage
vDBB	diagonal band of Broca, vertical limb
V_f-V	charging function
V_h	holding potential
V_L	voltage at opposite end of the cable
V_o	voltage at site of current injection
VP	vasopressin
WCR	whole cell recordings
Zn^{++}	zinc

CHAPTER 1

GENERAL INTRODUCTION

I. *Overview*

The horizontal limb of the diagonal band of Broca (hDBB) together with the vertical limb comprise the nucleus of the diagonal band of Broca (DBB), a conspicuous, highly integrated part of the limbic system within the basal forebrain. The work performed in this thesis was conducted entirely in the hDBB. The rationale for choosing to focus on the hDBB is founded on our current knowledge that it contains well-defined cell types, its projections have been well characterized, and it is known to participate in specific physiological processes. However, despite this, many fundamental questions regarding the biophysical profile of these cells and the actions of important neurotransmitters and neuromodulatory compounds have not yet been addressed. The goal of this thesis is to examine these issues.

The purpose of this chapter is to summarize the current state of knowledge concerning the hDBB with particular reference to the following aspects: (1) the neurochemical characteristics, (2) the afferent and efferent projections, (3) the physiological functions, and (4) the cellular physiology of hDBB neurons. While the focus of this thesis is the hDBB, it is recognized that the actions of this nucleus are intimately linked with the actions of the DBB as a whole. As a consequence, this chapter will describe our current understanding of the anatomy, physiology, and electrophysiology of the DBB with a specific focus on the hDBB where this information is available.

II. *A Brief History*

The DBB was first described by Broca (1878) in a seminal study that formally identified several distinct nuclei withiin the forebrain. Surprisingly, despite its early

characterization, relatively few studies were conducted on the DBB. One of the earliest reports on this region was an anatomical study characterizing a projection from the hDBB to the olfactory cortex (Price and Powell, 1970). Subsequent reports examined the role of the DBB in the release of luteinizing hormone (Kubo et al., 1975) and mechanisms associated with thirst (Aghajanian and Davis, 1975). However, in the late 1970's and early 1980's, two discoveries marked a significant change in the level of interest in research related to DBB. The first was the observation that neurodegenerative diseases of memory such as Alzheimer's disease (AD) involved the degeneration of cholinergic neurons within the basal forebrain (Terry, 1978; Terry, 1983). The second was the discovery of new tracer molecules which greatly facilitated study of the chemical anatomy and connectivity of neurons within DBB (Heimer and RoBards, 1981). The first discovery gave researchers a reason to study the basal forebrain and the second gave researchers more refined anatomical tools to study this region. As a result, there has been a 100-fold increase in the number of publications on the DBB in the fifteen years after these two discoveries. One major consequence of the increased research concerning the DBB research was the realization of the complexity of this nucleus with respect to its cellular organization and role in a wide variety of physiological functions.

III. *Anatomy of the DBB*

The DBB is a telencephalic structure lying dorsal to the anterior and medial regions of the corpus callosum. The anterior portion of the DBB is aligned with the onset of the anterior commissure and ends where the right and left anterior commissure combine at the

level of the optic chiasm. The DBB is a large structure that extends over 1.5mm (rostral to caudal) and has a conspicuous inverted "Y" shape. Harkmark et al. (1975) further subdivided the rat DBB into the vertical (vDBB) and the horizontal limbs (hDBB) where the vDBB comprises the dorsal "stalk" and the hDBB forms the two ventrally-located "arms" of the inverted "Y".

IV. *Neurochemical characteristics of DBB neurons*

DBB neurons are heterogeneous in their neurotransmitter and neuropeptide content. The two principal cell populations in this region are the cholinergic and the γ-aminobutyric acid (GABA) neurons (Brashear et al., 1986). Both of these chemical phenotypes are represented as large and small diameter cell types. The large cells appear to serve as projection neurons whereas the smaller cells likely mediate the release of neurotransmitter locally.

A. Acetylcholine

Within the DBB, it has been demonstrated that 34-45% of all neurons are cholinergic using staining methods for either choline acetyltransferase (ChAT) (Rye et al., 1984) or acetylcholinesterase (AChE) (Mesulam et al., 1983; Jakab and Leranth, 1995; Eckenstein and Sofroniew, 1983). The hDBB in particular is identified as having one of the highest concentrations of cholinergic-positive perikarya within the BF (Senut et al., 1989)

Ultrastructurally, two types of ChAT-immunoreactive neurons have been distinguished (Milner, 1991a). The first type are magnocellular (20-30μm) neurons which are round and contain lamellar bodies. Lamellar bodies are thought to regulate intracellular

calcium levels in metabolically active projection neurons (Palacios, 1990; Mesulam and Van Hoesen, 1976). The second type are parvocellular (15-20μm) neurons which are round and lack lamellar bodies. These smaller cholinergic neurons may release acetylcholine locally within the septal area (Metcalf et al., 1988).

The magnocellular cell population functions as projection neurons and serves as the principal source for the release of acetylcholine in CNS regions to which the DBB projects (Mesulam and Van Hoesen, 1976). Cholinergic DBB neurons exhibit dense projections to the olfactory cortex, the hippocampus, and several nuclei in the neocortex (Senut et al., 1989). As will be discussed later, these neurons are implicated in a diverse array of physiological functions including memory (Waite et al., 1994) and theta rhythm (Bland and Colom, 1993). Under pathophysiologic conditions, these cells are selectively destroyed in diseases of memory and cognition such as AD (Arendt et al., 1994).

B. GABA

GABA-positive neurons constitute the second largest group of DBB cells (Panula et al., 1984; Onteniente et al., 1986; Brashear et al., 1986). Kiss et al. (1990b) estimated that 34% of all BF neurons were GABAergic as judged by immunohistochemistry for glutamate decarboxylase (GAD), an enzyme that synthesizes GABA (Kermer et al., 1995). GABAergic neurons are uniquely characterized by trigonal shaped nuclei (Dinopoulos et al., 1988); however, as with the cholinergic neurons, GABAergic cells are not uniform in size. On the basis of morphological data, GABAergic BF neurons are either large (>15μm) or small (<15μm) (Panula et al., 1984). It is postulated that the smaller neurons function as local interneurons whereas the larger cells act as projection neurons exerting inhibitory effects

outside of the BF (Gritti et al., 1993). Anterograde and retrograde tracer studies indicate that GABA-containing efferents from the DBB innervate the olfactory bulb (Kunze et al., 1991), the neocortex (Freund and Gulyas, 1991), and the hippocampus (Freund, 1989). These results suggest that the projection pattern of DBB GABAergic neurons mirrors that of the cholinergic hDBB cells.

One of the problems that has arisen regarding the immunocytochemistry of GABA is the need to use glutaraldehyde to optimally visualize GABA positive cells (Kiss et al., 1990). Glutaraldehyde creates a dark background on tissues making it difficult to visualize immunocytochemically GABA-stained cells. Kiss et al. (1990a, b) suggested that the Ca^{++}-binding protein, parvalbumin (PV), was highly localized within GABA-positive neurons in the MS-DBB and that staining for PV could be used indirectly to visualize GABA neurons. However, this assertion is controversial and is disputed by Alonso et al. (1990) who claim that there is no correlation between PV and GABA neuronal distribution. Cholinergic DBB neurons, however, contain neither GABA (Kosaka et al., 1988) nor parvalbumin (Kiss et al., 1990a, b)

C. *Other chemical phenotypes*

MS-DBB neurons contain a variety of other neuromodulatory compounds. These include galanin, luteinizing hormone releasing hormone (LHRH), nerve growth factor (NGF), nitric oxide (NO), and vasopressin. While they have been anatomically identified in these cell, their functional role is not well understood. One peptide which has recently become the focus of intense interest is galanin. It is present within the DBB in high concentrations (Evans et al., 1993) and is known to coexist within cholinergic magnocellular

cells in the rat MS-DBB (Melander et al., 1986). The co-localization of these two neurochemicals has led to the postulate that galanin may modulate cholinergic function. This hypothesis has been tested and confirmed by Fisone et al. (1987) who demonstrated that galanin inhibited the release of acetylcholine via a presynaptic mechanism.

V. *Afferent and Efferent Connections and Their Relation to Function*

This section is divided into two segments. The first segment briefly describes the connectivity of the DBB and will focus on the principal projections of the DBB; it is not meant to be exhaustive. As this thesis examines the actions of specific neurotransmitters and neuromodulators on hDBB neurons, the chemical identity of afferent inputs will be discussed in greater detail. The second segment examines the major physiological roles subserved by the DBB in the context of the anatomical connectivity discussed in the previous section.

A. Anatomical Connectivity of the DBB

1. Efferent Connections of the DBB

Anatomical and electrophysiological studies have identified dense efferent projections originating from the DBB to the hippocampus, olfactory bulb, neocortex, hypothalamic supraoptic (SON) and paraventricular (PVN) nuclei, amygdala (ACE), dorsal raphe (DR), locus coeruleus (LC) (Meibach and Siegel, 1977; Luiten et al., 1985; Luiten et al., 1987; Woolf et al., 1986; Gaykema et al., 1990; Tomimoto et al., 1987; Caffe et al., 1989; Donevan and Ferguson, 1988; Tribollet et al., 1985; Garris, 1979; Jhamandas et al., 1989; Kalen and Wiklund, 1989; Behzadi et al., 1990)

Efferent projections from the DBB to the cortical hippocampus, olfactory bulb, and

neocortex have been studied in great detail (Gaykema et al., 1990). Both cholinergic and GABAergic DBB neurons project to these cortical areas (Mesulam and Van Hoesen, 1976; Rye et al., 1984; Kunze et al., 1991; Crutcher et al., 1983). Studies using microinjection of cholinergic agonists and antagonists suggest that acetylcholine exerts excitatory effects on target neurons (Bland and Colom, 1993), whereas GABA mediates an inhibitory input to the target cells (Freund and Antal, 1988; Miettinen and Freund, 1992). The fact that the DBB is the origin of both excitatory and inhibitory projections is suggestive of an important modulatory role mediated by the DBB in these sites. The functional relevance of this innervation will be discussed in sections V.B.3, 4.

The hypothalamic SON and PVN synthesize both oxytocin and vasopressin, neuropeptides whose actions as neurohormones in the periphery are well documented (Kovacs and Versteeg, 1993; Oka and Yoshida, 1985). In addition to their peripheral actions, these neuropeptides also play critical roles in the regulation of neuronal behavior (Pittman et al., 1988; Landgraf and Ramirez, 1991). The DBB projections to these nuclei influence the release of vasopressin and may serve crucial roles in both central cardiovascular regulation and drinking behavior (Discussed in sections V.B.1, 2)

Meibach and Siegal (1977) described a "massive projection" from the DBB to ACE. The ACE is an important component of the limbic system and is associated with a myriad of physiological functions including memory mechanisms, reproduction, and control of blood pressure (Alheid et al., 1995; Davis et al., 1994; Numan, 1994; McGaugh et al., 1993; Sanders and Shekhar, 1991). It is postulated that the DBB projection to ACE maybe involved in learning behavior and blood pressure regulation (Discussed in section B.V).

Efferent projections from the DBB to the DR and LC in the brainstem have also been identified (Kalivas et al., 1985; Lynn et al., 1991; Lawson and Bland, 1993). These target regions contain high concentrations of biogenic amines. Specifically, the DR contains serotonin and the LC contains noradrenaline (Willis and Smith, 1985). While the function of these efferent projections is unclear, it may be related to autonomic cardiovascular regulation of which all three regions are involved (Discussed in section V.B.1).

2. Afferent Connections of the DBB

The DBB receives input from diverse regions in the CNS. However, the regions which provide the most dense innervation to the DBB are also recipients of DBB efferents. This reciprocal connectivity may have important implications in the context of specific physiologic processes. Anatomical data indicate that afferent input to the DBB comes from cortical regions such as the hippocampus and piriform cortex, medial hypothalamic nuclei, the ACE and the brainstem LC and DR.

Autoradiographic studies (Swanson and Cowan, 1977) as well as those utilizing anterograde tracer techniques (Toth et al., 1993; Gaykema et al., 1991) have shown that the hippocampal formation projects to the medial septum-DBB (MS-DBB) complex. These projections are both excitatory and inhibitory. The transmitter in the former projection is postulated to be glutamate (Lamour et al., 1985; Walaas and Fonnum, 1993) whereas the latter is GABA (Leranth and Frotscher, 1989). Toth et al. (1993) demonstrated that the vast majority of fibers from the hippocampus innervating the MS-DBB are GABAergic. These afferent fibers innervate both parvalbumin-containing and cholinergic MS-DBB neurons which in turn provide reciprocal projections to the hippocampus (Jakab and Leranth, 1995).

These findings provide evidence for the existence of a direct septo-hippocampo-septal loop. Fibers innervating the DBB originating from allocortical and neocortical regions have also been identified. Alonso and Kohler (1984) have identified fibers originating from the entorhinal cortex and terminating in the DBB. Furthermore, Zaborszky et al. (1991) have described a restricted neocortical input to the DBB originating primarily in the orbital areas, insular cortex, and the piriform cortex. The chemical identity of these inputs is not yet clear, however, both glutamate and GABA are considered to be prime candidates to mediate these excitatory and inhibitory inputs, respectively. Importantly, the specific receptor subtypes which mediate glutamate and GABA synaptic transmission within the DBB have not been characterized.

The DBB receives input from virtually all parts of the hypothalamus (Simerly and Swanson, 1988; Berk and Finkelstein, 1981), particularly regions within the medial hypothalamic areas such as the PVN (Cullinan and Zaborszky, 1991). The DBB also receives dense afferent inputs from the bed nucleus of the stria terminalis (BST) and the ACE (Pare and Smith, 1994; Wilkinson and Pittman, 1995). The unifying characteristic of the inputs to the DBB from these diverse regions is that the peptide vasopressin (VP) is contained in these projections (Caffe et al., 1989; Ulfig et al., 1993; Lakhdar-Ghazal et al., 1995). A study by Insel et al. (1994) revealed that the highest concentration of radiolabelled VP binding was in the DBB. Functionally, VP modulation of DBB neurons may underlie autonomic cardiovascular regulation and memory/learning mechanisms. As yet, however, the mechanism of action of VP on DBB cells remains unclear (See section V.B.1, 2, 4)

Biogenic amine-containing afferents of moderate to high density from the brainstem

LC (Kalivas et al., 1985) and DR (Semba et al., 1988) innervate the DBB. The chemical identity of the inputs from the LC and DR are likely noradrenaline, and serotonin, respectively. Functionally, these inputs may mediate actions associated with central cardiovascular functions (Section V.B.1).

B. Physiological Functions Mediated by the DBB

1. Central cardiovascular regulation

As discussed previously, the neurohormone VP is recognized as a potent pressor agent and antidiuretic in the periphery (Jard, 1983). The VP used to mediate these actions is synthesized primarily in two nuclei in the hypothalamus: the SON and the PVN (Jard, 1983). Both nuclei project to the neurohypophysis where they release this neurohormone into the blood. Clearly, the extrinsic synaptic modulation of neurons within the SON and PVN represents a potent mechanism whereby arterial blood pressure can be controlled.

Considerable evidence has accumulated to suggest that the MS-DBB modulates the activity of VP neurons within the SON and thus subserves an important role in central cardiovascular control of blood pressure (Jhamandas, 1991). Extracellular *in vivo* recordings from the SON reveal that stimulation of the MS-DBB reversibly inhibits 83% of the VP neurons in this nucleus (Jhamandas and Renaud, 1986a,b, 1987a). Furthermore, systemic intravenous administration of the α-adrenergic agonist metaraminol evokes baroreceptor activation that is coincident to a decrease in the firing of VP neurons in the SON. Metaraminol-induced baroreceptor activation also increases the firing of 50% of all DBB neurons that project to the SON. Therefore, it is postulated that baroreceptor activation which inhibits VP neuron activity may result from the activation of DBB neurons. (Renaud

et al., 1988).

Anatomical studies using retrogradely transported latex microspheres and the anterograde tracer horseradish peroxidase (HRP) indicate that the hDBB projects indirectly to the SON via a region adjacent to the SON called the perinuclear zone (PNZ) (Jhamandas et al., 1989). The PNZ, which contains GABA-positive perikarya (Herbison, 1994), in turn projects to the SON (Jhamandas et al., 1989). Local application of the $GABA_A$ antagonist bicuculline into the SON reversibly abolishes the inhibition of VP neurons evoked by DBB stimulation (Jhamandas and Renaud, 1987a). In addition, application of bicuculline into the SON also blocks the metaraminol-induced decrease in VP activity (Jhamandas and Renaud, 1987a). It has therefore been postulated that the DBB is the origin of an excitatory projection to GABAergic neurons within the PNZ which then serve to inhibit SON neurons (Jhamandas and Renaud, 1987b). Also, a direct GABAergic projection from the MS-DBB to the SON may also inhibit activity in VP neurons (Jhamandas, 1987c).

The question that has arisen from these studies concerns the identity of the neurotransmitter that activates DBB neurons in response to changes in blood pressure. The principal candidates that have emerged are the catecholamines. Catecholaminergic inputs from the LC (NA)(Kalivas et al., 1985) and the DR (serotonin) (Kalivas et al., 1985; Lynn et al., 1991) to the DBB have been described and ultrastructural studies demonstrate that catecholamine containing fibers synapse onto neurons within the hDBB (Milner, 1991b).

Particular attention has been focused on the action of NA within the DBB. Injection of noradrenaline (NA) into the DBB potently inhibits the activity of VP cells within the SON (Cunningham et al., 1993). Furthermore, Cunningham et al. (1992) observed that injection

of the NA uptake inhibitor desipramine into the DBB prevented metaraminol-induced increases in blood pressure from changing the firing of VP neurons (92% did *not* respond) whereas in control animals, peripheral injections of metaraminol decreased the firing of 100% of VP neurons. From these results, they postulated that the DBB may receive catecholaminergic inputs from the pons and brainstem which in turn regulates the DBB's ability to modulate VP activity.

2. Fluid Balance

The DBB together with the nucleus medianus, the median preoptic area and the organ vasculosum lamina terminalis (OVLT) comprise what is referred to as the AV3V region (Jhamandas, 1987c). The AV3V region forms a part of the central complex for the control of water intake (Wishart and Mogenson, 1970). Lesions of the AV3V region alter fluid balance and drinking behavior, and influence VP release (Mangiapane et al., 1983; Honda et al., 1987). The DBB itself plays a large role in drinking behavior. Electrical stimulation of the DBB reduces drinking in rodents (Iovino et al., 1983; Iovino and Steardo, 1985; Wishart and Mogenson, 1970). Furthermore, i.v. administration of the peptide angiotensin II (AII) (Donevan and Ferguson, 1988) or metaraminol (Jhamandas and Renaud, 1986b) increases the firing rate of DBB neurons projecting to the hypothalamic PVN resulting in a reduction of VP release and a decrease in drinking.

Lesions of the MS or DBB evoke polydipsia, polyuria, urine hypoosmolality (Iovino et al., 1983; Sullivan et al., 1991). In a manner analogous to lesions of the DBB, increased blood osmolarity (Hubbard et al., 1985; De Castro and Taggart, 1979) or hemorrhage (Pittman and Bagdan, 1992) also reduce the activity of DBB neurons resulting in an increase

in VP release and drinking. These studies suggest a close link between the DBB regulation of drinking and VP release.

Although many brain regions act cooperatively to regulate VP production and release, the DBB is an important structure in this context. In the absence of regulatory input from the DBB (e.g. DBB lesion, elevated blood osmolarity, haemorrhage), VP neurons in the hypothalamus are disinhibited, which facilitates the release VP into the blood. Since VP increases blood pressure and promotes water retention, stimulation of drinking also serves a complimentary role to restore intravascular volume. Alternatively, stimulation of the DBB either by elevating blood pressure, increasing plasma angiotensin (AII), or i.v. injections of metaraminol decreases the activity of VP neurons therefore reducing the release of VP into the blood.

Interestingly, Donevan and Ferguson (1988) report that animals with DBB lesion show increased drinking but a reduced level of VP over an extended period of time. In these same animals, the typical increase in VP release in response to systemic administration of AII is also blunted. This observation suggests that a compensatory mechanism is turned on in the absence of the DBB to regulate VP levels in the blood. The fact that the animals remain polydipsic suggests that the compensatory mechanism modulating systemic/plasma VP levels does not modulate drinking behavior over the long term.

It is possible that VP in central pathways may participate in a feedback loop whereby this peptide modulates the activity of DBB neurons which in turn influences the release of VP from hypothalamic nuclei. Ulfig et al. (1993) and Caffe et al. (1989) reported that dense VP-positive fibers were present in the DBB. There are several possible sources of VP to the

DBB. Electrophysiological stimulation of the hypothalamic PVN increases VP release in the DBB (Neumann et al., 1988). Furthermore, immunocytochemical studies indicate that VP-positive fibers in the DBB originate from the subfornical organ (SFO) (Summy-Long et al., 1985) which is a circumventricular organ and the BST (Caffe et al., 1989; Wilkinson and Pittman, 1995). Patch clamp recordings from SFO neurons indicate that external application of VP modulates the firing of these cells. Jurzak (1995) extrapolated from these results that VP SFO neurons likely respond to changes in VP concentration in the blood. It is also known that the SFO sends a principally excitatory projection to DBB cells (Lind et al., 1982; Miselis, 1981) antidromically identified as projecting to the SON (Ferguson et al., 1985). Neurons in the BST, antidromically identified as projecting to the DBB, respond to changes in blood pressure (Jhamandas and Renaud, 1987a). Collectively, these results suggest that specific nuclei, which contain VP-positive perikarya, and that respond to changes in blood pressure (SFO, PVN, BST) may provide vasopressinergic input to the DBB. VP would modulate the activity of DBB neurons which in turn would influence the release of VP from the hypothalamus. One problem with such a postulate, however, is the lack of data concerning the actions of VP on DBB neurons.

3. Theta Rhythm

Theta rhythm is a synchronized, low frequency (4-12Hz) oscillation that is recorded in limbic structures (Leung et al., 1982). It represents the largest amplitude rhythmical activity generated by the mammalian brain (2mV amplitude) (Bland and Colom, 1993). Although its functional role is not entirely clear, Bland (1986) postulates that systems involved in theta rhythm provide voluntary motor systems with continually updated feedback

on their own performance relative to changing sensory conditions, particularly with respect to the intensity with which motor programs are initiated and maintained.

Petsche et al. (1962) were one of the first groups to suggest that the MS-DBB paces hippocampal theta rhythm as they observed that ablation of the MS-DBB eliminated theta rhythm. Anatomical studies reveal a distinctive topographical projection from the MS-DBB to the hippocampus. The dentate hillus appears to receive input only from the MS and the CA1 region receives input principally from the hDBB with a lesser input from the vDBB (Easaw et al., 1992; Yoshida and Oka, 1990; Kiss et al., 1990b). Since theta rhythm is most often recorded in the CA1 region, the hDBB and vDBB have been the focus of considerable attention regarding this rhythm (Sainsbury and Bland, 1981; Oka and Yoshida, 1985). Double immunocytochemical staining revealed that approximately 66% of the DBB neurons projecting to the dorsal hippocampus were cholinergic and the rest stained for PV, the calcium-binding protein that may be colocalized in GABA neurons (Kiss et al., 1990a,b). Cholinergic DBB neurons excite hippocampal pyramidal neurons (Bland and Colom, 1993) whereas GABAergic projection neurons within the DBB inhibit hippocampal interneurons (Freund and Antal, 1988; Miettinen and Freund, 1992). Bland and Colom (1993) hypothesize that as theta frequencies fall below 5 Hz, hippocampal interneurons are disinhibited due to reduced inhibitory input from the MS-DBB. As a consequence, the interneurons exert a more pronounced inhibition of theta-on cells thereby reducing their activity. As theta frequencies rise above 5Hz, the contribution of cholinergic-mediated excitatory postsynaptic potentials (EPSPs) to pyramidal cells begins to dominate. This reinforces the importance of a balance between septal cholinergic and GABAergic inputs in

modulating theta activity.

4. Memory and Learning

The DBB is also known for its role in memory and learning mechanisms. Evidence accumulated thus far suggests that the DBB projection to both the hippocampus and the cortex subserves important roles in memory and learning processes. DBB neurons project to the hippocampus via the fimbria-fornix (ff). Lesions of the ff or the MS consistently interfere with the rats ability to learn and recall certain maze tasks (Murtha and Pappas, 1994; Yee and Rawlins, 1994). Furthermore, Crutcher et al. (1983) observed that lesions of the DBB or hippocampus induce parallel patterns of memory impairments and a positive relationship exists between the lesion size in the DBB and the degree of memory impairment.

Kievit and Kuypers (1975) first identified a projection from the DBB to the neocortex. Subsequent studies by Gaykema et al. (1990) and Senut et al. (1989) revealed that the hDBB, in particular, projects densely to the entire neocortex. Both GABAergic and cholinergic projection neurons in the DBB participate in this projection (Mesulam and Van Hoesen, 1976; Rye et al., 1984; Gritti et al., 1993). Approximately 70% of postsynaptic neocortical targets of GABAergic basal forebrain neurons are also GABAergic (Freund and Gulyas, 1991). Inhibition of cortical projection cells evoked by acetylcholine can be blocked by both bicuculline and muscarinic antagonists, indicating that inhibition by acetylcholine is caused by activation of local GABAergic interneurons (McCormick and Prince, 1985, 1986; Muller and Singer, 1989). Based on these observations, it is postulated that GABAergic basal forebrain neurons innervate cortical interneurons resulting in a disinhibition of neocortical pyramidal cells. On the other hand, acetylcholine released from

terminals of DBB neurons excites the cortical interneurons which leads to an inhibition of principal cell activity.

The hDBB also projects to the olfactory bulb, an allocortical region of the brain that comprises a part of the paleocortex (Martin, 1989). The afferents to the olfactory bulb course through the olfactory peduncle (Gaykema et al., 1990). Interestingly, DBB innervation of the olfactory bulb is conserved in all mammalian species (Nickell and Shipley, 1988) suggesting that this connection may subserve a critical, non-redundant function in all mammals. Physiologically, the hDBB projection to the olfactory bulb may subserve important roles in associative memory processes, a type of memory where an association is made between patterned stimuli and a reward. Roman et al. (1993) lesioned the hDBB in rats and trained them in a successive olfactory cue discrimination test using different inter-trial intervals (ITT). The rats learned the task but showed significant impairment in the performance of odor-reward associations when ITTs are greater than 15 seconds. Based on this observation, it was concluded that the hDBB is an essential relay between the hippocampal system and the olfactory complex. The hDBB allows associative memory storage when a limited duration short term memory system located elsewhere is overloaded.

The cholinergic basal forebrain system which includes the DBB has been implicated in mechanisms of learning and memory (Kesner, 1986). The majority of studies examining this have employed or studied the effects of DBB lesion on behavior. In rodents, lesion of the septal area results in severe impairments in spatial navigation (Kesner et al., 1992) and attentional processing (Dunnett and Isacson, 1989; Robbins et al., 1989). One of the most commonly used measures of spatial navigation is the Morris water maze which is essentially

a small tub filled with an opaque solution with a small platform placed just under the surface of the solution in a fixed position. An animal is placed in the solution and is timed to determine how long it takes to find the platform. In control animals, the time to find the platform decreases with repetition suggesting that they have learned the location of the platform. However, animals with lesions in the DBB show significant impairments in their ability to find the platform suggesting that the absence of DBB neurons impairs their ability to spatially navigate (Wenk et al., 1987). A study by Fischer et al. (1991a) confirmed this postulate. Their simple experiment was to examine the ability of rats of different ages to navigate the Morris water maze. They observed a progressive decrease in spatial navigation with age. Anatomical study of the aged rats indicated a significant reduction in the number of ChAT-positive cells in the DBB. Thus, this result extends the observations of lesion studies and specifically suggests that cholinergic cells in the DBB mediate memory and learning. Fischer's observations confirmed for the first time that decreases in the ChAT-containing cells occur in parallel with memory deficits over time. In the rat, the DBB serves an important role in spatial memory. However, in humans, the type of memory affected by the loss of the DBB may be different. Morris et al. (1992) observed that a human with a discrete lesion of the right DBB had persistent global anterograde and retrograde amnesia.

The chemical neuroanatomy of the basal forebrain and its termination sites have attracted much interest because of the involvement of cholinergic cells in memory and learning as well as in neurological diseases such as AD. AD is characterized by a massive loss of acetylcholine containing neurons in the basal forebrain and therefore a reduction in the cholinergic innervation of cortical and limbic areas. According to a study of AChE and

DBB in postmortem AD brains, the most severely afflicted regions were the MS which lost 50% and the DBB which lost 65% of their cholinergic cells, respectively (Henke and Lang, 1983). Furthermore, brains afflicted with AD show neurofibrillar tangles and senile plaques distributed throughout the neocortex and hippocampus which, as discussed previously, are targets of cholinergic DBB neurons (Carlsen et al., 1985; McKinney et al., 1983; Bartus et al., 1982; Coyle et al., 1983; Arendt et al., 1985).

Several studies have attempted to determine what causes the degeneration of cholinergic neurons within the BF. While no single theory has been proven to be correct, three hypotheses have come to the forefront: excitotoxic death of cholinergic neurons, the actions of specific heavy metals within the brain, and the loss of specific regulatory peptides in the DBB.

The first hypothesis is based on the consistent observation that high concentrations of glutamate can kill cells (Thomas, 1995; Rothman and Olney, 1995). One of the mechanisms of this glutamate mediated excitotoxicity is thought to be due to the excessive influx of Ca^{++} via glutamate channels or the activation of voltage-gated Ca^{++} channels. Excessive Ca^{++} influx may activate several processes that promote cell death (Mody and MacDonald, 1995). Excitotoxicity is believed to mediate the cell death observed in numerous neuropathological conditions such as Parkinsons (Schulz and Beal, 1994; Dykens, 1994), Huntington's (Shaw, 1992; Beal, 1994), and stroke (Lustig et al., 1992; Beal, 1992). Numerous studies have suggested a similar link exists between excitotoxicity and AD (Scott et al., 1995; Smith-Swintosky and Mattson, 1994; Barger et al., 1993; Shaw, 1992). Page and Everitt (1995) observed that cholinergic basal forebrain cells possess high concentrations

of AMPA receptors. From these results, they infer that excessive activation of these receptors may depolarize neurons sufficiently to remove Mg^{++} blockade of NMDA channels and allow influx of Ca^{++} into the cells. Alternatively, excessive activation of AMPA channels devoid of the GluR2 subunit would also allow Ca^{++} levels to rise to toxic levels intracellularly. As a result, the use of selective glutamatergic antagonists may be an effective therapeutic intervention for patients with AD (Lawlor and Davis, 1992). A possible reason for the onset of excitotoxicity may be the loss of intrinsic inhibitory mechanisms that keep excitation in check. The brains of patients with AD show significant reductions in GABA and GABA receptor levels (Mohanakrishnan et al., 1995; Sasaki et al., 1986; Young, 1987). A dimunition of GABA-mediated inhibition would consequently amplify the actions of glutamate on these cells resulting in excitotoxic death.

A second hypothesis relates to the actions of certain metals within the brains of AD patients (Olanow and Arendash, 1994). One metal which has been the focus of much attention is zinc (Zn^{++}). Zn^{++} is one of the most abundant divalent cations in the brain (Ebadi et al., 1995). This metal subserves integral roles in several enzymatic processes (Wallwork, 1987). It is also a potent neuromodulator as demonstrated by its ability to regulate NMDA (Smart et al., 1994; Peters et al., 1987; Mayer and Vyklicky, 1989) and GABA (Buhl et al., 1996; Smart, 1992a,b; Narahashi et al., 1994) receptors as well as voltage-gated Na^{+} (Gilly and Armstrong, 1982), K^{+} (Talukder and Harrison, 1995; Harrison and Gibbons, 1994), and Ca^{++} (Busselberg et al., 1991, 1992) channels. However, when released in excessive amounts, Zn^{++} is highly neurotoxic (Koh and Choi, 1988; Duncan et al., 1992; Choi et al., 1988). This metal is principally localized in glutamate cells (Moos, 1993; Beaulieu et al.,

1992) and, in some cases, potentiates the excitotoxic effects of glutamatergic agonists on neurons (Weiss et al., 1993). Furthermore, Zn^{++} levels are significantly reduced in brains from human patients with AD (Constantinidis, 1991). The loss of Zn^{++} from these brains is postulated to arise consequent to excessive stimulation resulting in the depletion of Zn^{++}-containing terminals (Pohle and Rauca, 1994). Zn^{++} may exert excitotoxic actions on hDBB neurons and therefore may play a significant role in the etiology of AD.

Finally, the role of two peptides has been called into question regarding the etiology of AD. The first is VP. Injection of VP into cerebral ventricles has been demonstrated to enhance mechanisms associated with learning and memory (DeWeid, 1971). Aged rats which typically show memory deficits (Fischer et al., 1987) also possess significantly decreased concentrations of VP-positive fibers within the DBB (Fliers et al., 1985). This correlation has led to the suggestion that reductions in VP inputs to the DBB may be associated with neurodegenerative impairments of memory such as AD (Fliers et al., 1985). In fact, desaminoarginine VP has been used as a therapeutic in patients who show memory loss specifically attributed to lesions of the DBB (Phillips et al., 1987).

Another peptide that has been implicated in neurodegenerative diseases of memory is NGF and its actions at p75-NGFr. The MS-DBB has one of the highest concentrations of p75-NGFr in the brain (Woolf et al., 1989). Culture studies of adult septal neurons indicate that NGF can rescue neurons that would otherwise die after axotomy of the septohippocampal projection (Hefti, 1986; Kromer, 1987; Lapchak and Hefti, 1991; Montero and Hefti, 1988) and partially ameliorates age-related cholinergic neuronal atrophy (Fischer et al., 1987, 1991a, b). Minger and Davies (1992a,b) examined the hypothesis that the loss

of NGF releasing neurons in the cortex and hippocampus may result in the death of cholinergic DBB cells. They ablated cortical neurons using methyl-azoxymethanol acetate but found no degeneration of basal forebrain cholinergic neurons. This observation indicated that cortically derived trophic factor is unnecessary for the survival of these cells. Furthermore, NGF-mRNA and NGF-like immunoreactivity have been identified in DBB neurons indicating that NGF may be an intrinsic trophic factor for these neurons (Gibbs et al., 1994; Jakab and Leranth, 1995; Conner et al., 1992). Therefore, the release of NGF from target sites may not be as important as once believed.

VI. Cellular Properties

Only within the last decade has there been a concerted effort to examine the intracellular properties of DBB neurons (Griffith and Mathews, 1986). Griffith's (1988) seminal study in guinea pig electrophysiologically characterized three different cell types in this region. The identifying feature of the first cell type (SAHP) was a slow afterhyperpolarization (AHP) (duration-600ms) with an amplitude of 10-20mV. The null potential of the AHP was approximately -90mV and shifted by 25mV in 9mM KCl, a value closely predicted for a potassium (K^+) conductance. The AHP was reversibly blocked by cadmium (Cd^{++}) suggesting the AHP was mediated by a calcium Ca^{++}-activated K^+ conductance. The SAHP cell type comprised 40% of all cells recorded. The second cell type identified was called FAHP because the AHP duration of these cells is faster (duration 5-50ms) and the amplitude is smaller (5-10mV) compared to SAHP cells. The FAHP cell type composed 53% of the cells recorded. The final cell type identified in this study was

observed infrequently (7%) and fired in a burst pattern. Cells were filled with Lucifer Yellow and immunocytochemically stained for AChE. Only the SAHP neurons stained for AChE suggesting that these are cholinergic cells and that FAHP neurons represent a non-cholinergic, likely GABAergic cell population (Griffith and Mathews, 1986; Griffith, 1988). These observations corroborate the results of Markram and Segal (Markram and Segal, 1990) who identified neurons resembling Griffith's SAHP and FAHP cell types in a slice preparation of rat DBB.

Few studies have examined intrinsic voltage-activated and ligand-activated currents in these neurons. Griffith and Sim (1990) characterized a transient outward current (A-current) in these cells that could be blocked by 100-300μM 4-aminopyridine. Also, Ca^{++} currents have been studied in a preparation of acutely dissociated MS-DBB cells (Griffith et al., 1994). Large acutely dissociated cells (20-30μm) were postulated to represent to the magnocellular cholinergic cells. These larger neurons possessed both high voltage-activated and low voltage-activated Ca^{++} currents. In contrast, the smaller neurons (10-15μm) which are thought to represent the non-cholinergic population only expressed high voltage-activated currents.

Frye et al. (1994) have examined the interactions of ethanol and $GABA_A$-activated current in acutely dissociated adult MS-DBB neurons as it is believed that these cells may be particularly sensitive to alcohol. CNS depressants such as barbiturates and benzodiazepines exert their effects by allosterically stimulating $GABA_A$ receptors (Sigel et al., 1990). Ethanol elicits many CNS depressant actions similar to those of barbiturates and benzodiazepines and can also enhance $GABA_A$ receptor activity (Deitrich et al., 1989). It

is observed that the ethanol sensitivity of $GABA_A$ receptors on DBB cells varies considerably depending on the strain of rat used. In Sprague Dawley rats, $GABA_A$ currents were mostly insensitive to external applications of 3-300mM ethanol.

VII. Rationale and Objectives

The goals of this thesis were two-fold. The first was to gain insight into the actions of specific neurotransmitter and neuromodulatory agents on hDBB neurons. Since the hDBB participates in several physiological processes, it is important to understand how certain neurochemicals modulate the behavior of neurons in this region and therefore regulate their participation in these processes. In order to achieve this goal, I utilized the whole cell patch clamp technique to record from both rat forebrain slices which contained the hDBB and acutely dissociated hDBB neurons. Second, a detailed biophysical analysis of hDBB neurons was conducted to understand the mechanism of information transfer of these cells.

hDBB neurons are recipients of a wide array of chemical inputs. Functionally, these inputs are likely associated with memory/learning mechanisms, theta rhythm, and central autonomic responses. As discussed previously, these cells receive glutamatergic inputs principally from allocortical and neocortical regions. However, the nature and extent of glutamate's participation in neurotransmission in this region remains unclear. I examined the hypothesis that glutamate modulates excitatory synaptic transmission at both pre- and postsynaptic levels. The data presented in Chapter 3 describes the role of specific glutamate receptor subtypes in excitatory synaptic transmission. Furthermore, I characterized certain biophysical properties in order to understand how hDBB neurons may integrate synaptic

information and transmit inputs to target brain regions. This study was conducted in an *in vitro* rat slice preparation.

GABAergic innervation of the hDBB likely originates from allo- and neocortical sites. These inputs may underlie the hDBB's participation in memory and in theta rhythm. Also, the conspicuous loss of GABA and GABA receptors in AD may be associated with the onset of excitotoxicity in this region. In Chapter 4, the role of GABA-mediated inhibition of hDBB cells was examined in the forebrain slice preparation. The actions of $GABA_A$, $GABA_B$, and $GABA_C$ receptors on pre- and postsynaptic membranes as well as their contribution to inhibitory synaptic transmission are described.

The neuropeptide, VP, is found in fibers which densely innervate the hDBB (Ulfig et al., 1993; Caffe et al., 1989). The sources of VP appears to principally be brain regions that are involved in blood pressure regulation. Thus, this peptide may underlie the hDBB's participation in central cardiovascular activity. Also, VP is observed to enhance memory in rodents and may mediate mechanisms associated with memory and learning. A preliminary report by van Eerdenburg and Pittman (1991) has suggested that VP may modulate the actions of glutamate on MS-DBB neurons. However, the effect of specific actions of VP on hDBB neurons has not yet been addressed. The actions of this peptide were initially examined on cells in the rat brain slice. Based on our findings of a dual action of VP on hDBB neurons, we hypothesized that V_1 or V_2 receptors could mediate these actions. A comprehensive pharmacological analysis was then conducted in an acutely dissociated hDBB cell preparation to study the specific ionic conductances and receptors underlying VP's actions in the hDBB. Chapter 5 presents our observations of VP modulation of hDBB cells.

The whole cell patch clamp method was utilized in this study.

As discussed previously, the hDBB is one of the regions most severely affected in diseases of cognition such as AD. One of the principle hypotheses to explain the etiology of this disease centers upon the loss of Zn^{++} in the brain. Since Zn^{++} is known to modulate the neuronal behavior by specific actions upon various ion channels, I endeavored to examine the actions of this divalent cation on voltage-gated ion channels. The work on Zn^{++} was conducted in both the slice and the acutely dissociated cell preparations. These findings and their implications are discussed in Chapter 6.

The final chapter of this thesis summarizes the results of this study and examine them in the context of the specific physiological roles mediated by the hDBB. In addition, future studies which will need to be conducted as a result of the conclusions from this thesis will be discussed.

REFERENCES

Aghajanian, G. K. and Davis, M. A direct chemical brain stimulation in behavioral studies using microiontophoresis. *Pharmacol. Biochem. Beh.* 3(1):127-131, 1975.

Alheid, G. F., de Olmos, J. S., and Beltramino, C. A. Amygdala and Extended Amygdala. In: *The Rat Brain*, edited by G. Paxinos. New York: Academic Press, 1995, p. 495-578.

Alonso, A. and Kohler, C. A study of the reciprocal connections between the septum and the entorhinal area using anterograde and retrograde axonal transport methods in the rat brain. *J. Comp. Neurol.* 225:327-343, 1984.

Alonso, J. R., Covenas, R., Lara, J., and Aijen, J. Distribution of parvalbumin immunoreactivity in the rat septal area. *Br. Res. Bull.* 24(1):41-48, 1990.

Anderson, P., Bland, B. H., Myhrer, T., and Schwarzkrion, A. Septohippocampal pathway necessary for dentate theta production. *Brain Res.* 165:13-22, 1979.

Arendt, T., Bigl, V., Tennstedt, A., and Arendt, A. Neuronal loss in different parts of the nucleus basalis is related to neuritic plaque formation in cortical target areas in Alzheimer's disease. *Neurosci.* 14:1-14, 1985.

Arendt, T., Bruckner, M. K., Bigl, V., and Marcova, L. Dendritic reorganization in the basal forebrain under degenerative conditions and its defects in Alzheimer's disease. III. The basal forebrain compared with other subcortical areas. *J. Comp. Neurol.* 351(2):223-246, 1994.

Barger, S. W., Smith-Swintosky, V. L., Rydel, R. E., and Mattson, M. P. Beta-amyloid precursor protein mismetabolism and loss of calcium homeostasis in Alzheimer's

disease. *Ann. N.Y. Acad. Sci.* 695:158-164, 1993.

Bartus, R. T., Dean, R. L. I., Beer, B., and Lippa, A. S. Cholinergic hypothesis of geriatric memory dysfunction. *Science* 217:408-417, 1982.

Beal, M. F. Mechanisms of excitotoxicity in neurologic diseases. *FASEB* 6(15):3338-3344, 1992.

Beal, M. F. Huntington's disease, energy, and excitotoxicity. *Neurobiol. Aging* 15(2):275-276, 1994.

Beaulieu, C., Dyck, R., and Cynader, M. Enrichment of glutamate in zinc-containing terminals of the cat visual cortex. *Neuroreport* 3:861-864, 1992.

Behzadi, G., Kalen, P., Parvopass, F., and Wiklund, L. Afferents to the median raphe nucleus of the rat: retrograde cholera toxin and wheat germ conjugated horseradish peroxidase tracing, and selective d-[^{3}H]-aspartate labelling of possible excitatory amino acid inputs. *Neurosci.* 37:77-100, 1990.

Berk, M. L. and Finkelstein, J. A. Afferent projections to the preoptic area and hypothalamic regions in the rat brain. *Neurosci.* 6:1601-1624, 1981.

Bland, B. H. The physiology and pharmacology of hippocampal formation theta rhythms. *Prog. Neurobiol.* 26:1-54, 1986.

Bland, B. H. and Colom, L. V. Extrinsic and intrinsic properties underlying oscillation and synchrony in limbic cortex. *Prog. Neurobiol.* 41:157-208, 1993.

Brashear, H. R., Zaborszky, L., and Heimer, L. Distribution of GABAergic and cholinergic neurons in the rat diagonal band. *Neurosci.* 17(2):439-451, 1986.

Broca, P. Anatomie comparee des circonvolutions cerebrales. Le grad lobe limbique et la

scissure dans la serie des mammiferes. *Rev. Anthrop. Paris* 2:285-498, 1878.

Buhl, E. H., Otis, T. S., and Mody, I. Zinc-induced collapse of augmented inhibition by GABA in a temporal lobe epilepsy model. *Science* 271:369-372, 1996.

Burke, M. A., Mobley, W. C., Cho, J., Wiegand, S. J., Lindsay, R. M., Mufson, E. J., and Kordower, J. H. Loss of developing cholinergic basal forebrain neurons following excitotoxic lesions of the hippocampus: rescue by neurotrophins. *Exp. Neurol.* 130(2):178-195, 1994.

Busselberg, D., Evans, M. L., Rahmann, H., and Carpenter, D. O. Lead and zinc block a voltage-activated calcium channel of *Aplysia* neurons. *J. Neurophys.* 65(4):786-795, 1991.

Busselberg, D., Michael, D., Evans, M. L., Carpenter, D. O., and Haas, H. L. Zinc blocks voltage gated calcium channels in cultured rat dorsal root ganglion cells. *Brain Res.* 593:77-81, 1992.

Caffe, A. R., Van Ryen, P. C., Van der Woude, T. P., and Van Leeuwen, F. W. Vasopressin and oxytocin systems in the brain and upper spinal cord of *Macaca fascicularis*. *J.Comp.Neurol.* 287(3):302-325, 1989.

Carlsen, J. L., Zaborszky, L., and Heimer, L. Cholinergic projections from the basal forebrain to the basolateral amygdaloid complex: A combined retrograde fluorescent an immunohistochemical study. *J.Comp.Neurol.* 234:155-165, 1985.

Caverson, M. M., Ciriello, J., Calaresu, F. R., and Krukoff, T. L. Distribution and morphology of vasopressin-, neurophysin II-, and oxytocin-immunoreactive cell bodies in the forebrain of the cat. *J. Comp. Neurol.* 259(2):211-236, 1987.

Choi, D. W., Yokoyama, M., and Koh, J. Zinc neurotoxicity in cortical cell culture. *Neurosci.* 24:67-79, 1988.

Colom, L. V., Ford, R. D., and Bland, B. H. Hippocampal formation neurons code the level of activation of the cholinergic septo-hippocampal pathway. *Brain Res.* 410:12-20, 1987.

Colom, L. V., Roquet, S., and Bland, B. H. Behavioral correlates and cholinergic manipulations of hippocampal phasic linear theta-on cells. *Soc. Neurosci. Abstr.* 17:1036, 1989.

Conner, J. M., Muir, D., Varon, S., Hagg, T., and Manthorpe, M. The localization of nerve growth factor-like immunoreactivity in the adult rat basal forebrain and hippocampal formation. *J. Comp. Neurol.* 319(3):454-462, 1992.

Constantinidis, J. Hypothesis regarding amyloid and zinc in the pathogenesis of Alzheimer disease: potential for preventive intervention. *Alzh. Dis. Assoc. Dis.* 5(1):31-35, 1991.

Coyle, J. T., Price, D. L., and DeLong, M. R. Alzhiemer's disease: A disorder of cortical cholinergic innervation. *Science* 219:1184-1190, 1983.

Crutcher, K. A., Kesner, R. P., and Novak, J. M. Medial septal lesions, radial arm maze performance and sympathetic sprouting: A study of recovery of function. *Brain Res.* 262:91-98, 1983.

Cullinan, W. E. and Zaborszky, L. Organization of ascending hypothalamic projections to the rostral forebrain with special reference to the innervation of cholinergic projection neurons. *J. Comp. Neurol.* 306:631-667, 1991.

Cunningham, J. T., Nissen, R., and Renaud, L. P. Catecholamine depletion of the diagonal band reduces baroreflex inhibition of supraoptic neurons. *Am. J. Physiol. Regul. Integr. Comp. Physiol.* 263:R363-R367, 1992.

Cunningham, J. T., Nissen, R., and Renaud, L. P. Injections of norepinephrine (NE) in the diagonal band of Broca (DBB) attenuate the activity of rat supraoptic (SON) vasopressin neurons. *Soc. Neurosci. Abstr.* 17:1189, 1993.

Davis, M., Rainnie, D., and Cassel, M. Neurotransmission in the rat amygdala related to fear and anxiety. *TINS* 17(5):208-214, 1994.

De Castro, J. M. and Taggart, D. Medial septal lesions: body weight loss and its relationship to polyuria in rats. *Physiol. Behav.* 22(5):855-859, 1979.

Deitrich, R. A., Dunwiddie, T. V., Harris, R. A., and Erwin, V. G. Mechanism of action of ethanol: initial central nervous system actions. *Pharmacol. Rev.* 41:491-537, 1989.

DeWeid, D. Long term effect of vasopressin on the maintenance of a conditioned avoidance response in rats. *Nature* 232:58-60, 1971.

Dinopoulos, A., Parnavelas, J. G., Uylings, H. B. M., and Van Eden, C. G. Morphology of neurons in the basal forebrain nuclei of the rat: a Golgi study. *J. Comp. Neurol.* 272:461-474, 1988.

Donevan, S. D. and Ferguson, A. V. Subfornical organ and cardiovascular influences on identified septal neurons. *Am. J. Physiol. (Regulatory Integrative Comp. Physiol. 23)* 254:R544-R551, 1988.

Duncan, M. W., Marini, A. M., Watters, R., Kopin, I. J., and Markey, S. P. Zinc, a neurotoxin to cultured neurons, contaminates cycad flour prepared by traditional

Guamanian methods. *J. Neurosci.* 12:1523-1537, 1992.

Dunnett, S. and Isacson, O. Trophic mechanisms are not enough. *TINS* 12(7):257, 1989.

Dykens, J. A. Isolated cerebral and cerebellar mitochondria produce free radicals when exposed to elevated Ca^{2+} and Na^{+}: implications for neurodegeneration. *J. Neurochem.* 63(2):584-591, 1994.

Easaw, J. C., Petrov, T., and Jhamandas, J. H. Electrophysiological and anatomical characterization of a projection from the parabrachial nucleus to the diagonal band of Broca in the rat.. *Soc. Neurosci. Abst.* 18(2):1173, 1992.

Ebadi, M., Iverson, P. L., Hao, R., Cerutis, D. R., Rojas, P., Happe, H. K., Murrin, L. C., and Pfeiffer, R. F. Expression and regulation of brain metallothionein. *Neurochem. Int.* 27(1):1-22, 1995.

Eckenstein, F. and Sofroniew, M. V. Identification of central cholinergic neurons containing both choline acetyltransferase and acetylcholinesterase and of central neurons containing only acetylcholinesterase. *J. Neurosci.* 3:2286-2291, 1983.

Evans, H. F., Huntley, G. W., Morrison, J. H., and Shine, J. Localization of mRNA encoding the protein precursor of galanin in the monkey hypothalamus and basal forebrain. *J.Comp.Neurol.* 328:203-212, 1993.

Feenstra, B. W. A. and Holsheimer, J. Dipole-like neuronal sources of theta rhythm in dorsal hippocampus, dentate gyrus and cingulate cortex of the urethane-anesthetized rat. *Electroencephalogr. Clin. Neurophysiol.* 47:532-538, 1979.

Ferguson, A. V., Bourque, C. W., and Renaud, L. P. Subfornical organ and supraoptic nucleus connections with septal neurons in rats. *Am. J. Physiol.(Regulatory*

Integrative Comp. Physiol.) 18:R214-R218, 1985.

Fischer, W., Wictorin, K., Bjorklund, A., Williams, L. R., Varon, S., and Gage, F. H. Amelioration of cholinergic neuron atrophy and spatial memory impairment in aged rats by nerve growth factor. *Nature* 329:65-68, 1987.

Fischer, W., Chen, K. S., Gage, F. H., and Bjorklund, A. Progressive decline in spatial learning and integrity of forebrain cholinergic neurons in rats during aging. *Neurobiol. Aging* 13:9-23, 1991a.

Fischer, W., Wictorin, K., Bjorklund, A., Williams, L. R., Varon, S., and Gage, F. H. NGF improves spatial memory in aged rodents as a function of age. *J. Neurosci.* 11:1889-1906, 1991b.

Fisone, G., Wu, C. F., Consolo, S., Nordstrom, O., Brynne, N., Bartfai, T., Mendler, T., and Hokfelt, T. Galanin inhibits acetylcholine release in the ventral hippocampus of the rat: histochemically, autoradiographic *in vivo* and *in vitro* studies. *Proc. Natl. Acad. Sci.* 84:7339-7343, 1987.

Fliers, E., DeVries, G. J., and Swaab, D. F. Changes with aging in the vasopressin and oxytocin innervation of the rat brain. *Brain Res.* 348(1):1-8, 1985.

Freund, T. F. GABAergic septohippocampal neurons contain parvalbumin. *Brain Res.* 478:375-381, 1989.

Freund, T. F. and Antal, M. GABA-containing neurons in the septum control inhibitory interneurons in the hippocampus. *Nature* 336(6195):170-173, 1988.

Freund, T. F. and Gulyas, A. I. GABAergic interneurons containing calbindin D28K or somatostatin are major targets of GABAergic basal forebrain afferents in the rat

neocortex. *J. Comp. Neurol.* 314(1):187-199, 1991.

Frye, G. D., Fincher, A. S., Grover, C. A., and Griffith, W. H. Interaction of ethanol and allosteric modulators with $GABA_A$-activated currents in adult medial septum/diagonal band neurons. *Brain Res.* 635:283-292, 1994.

Garris, D. R. Direct septo-hypothalamic projections in the rat. *Neurosci. Lett.* 13(1):83-90, 1979.

Gaykema, R. P. A., Luiten, P. G. M., Nyakas, C., and Traber, J. Cortical projection patterns of the medial septum-diagonal band complex. *J. Comp. Neurol.* 293:103-124, 1990.

Gaykema, R. P. A., Van Weeghel, R., Hersh, L. B., and Luiten, P. G. M. Prefrontal Cortical Projections to the Cholinergic Neurons in the Basal Forebrain. *J. Comp. Neurol.* 303:563-583, 1991.

Gibbs, R. B., Chaso, M. V., and Pfaff, D. W. Effects of fimbria-fornix and angular bundle transection on NGFR mRNA-expressing cells located in the medial septum and diagonal band of Broca. *Soc. Neurosc. Abstr.* 17:20, 1994.

Gilly, W. M. F. and Armstrong, C. M. Slowing of sodium channel opening kinetics in squid axon by extracellular zinc. *J. Gen. Physiol.* 79:935-964, 1982.

Gould, E., Woolf, N. J., and Butcher, L. L. Cholinergic projections to the substantia nigra from the pedunculopontine and laterodorsal tegmental nuclei. *Neurosci.* 28(3):611-623, 1989.

Griffith, W. H. Membrane properties of cell types within guinea pig basal forebrain nuclei *in vitro*. *J. Neurophysiol.* 59(5):1590-1610, 1988.

Griffith, W. H. and Mathews, R. T. Electrophysiology of AchE-positive neurons in basal

forebrain slices. *Neurosci. Lett.* 71:169-174, 1986.

Griffith, W. H. and Sim, J. A. Comparison of 4-aminopyridine and tetrahyroaminoacridine on basal forebrain neurons. *J. Pharm. Exp. Ther.* 255(3):986-993, 1990.

Griffith, W. H., Taylor, L., and Davis, M. J. Whole-cell and single-channel calcium currents in guinea pig basal forebrain neurons. *J. Neurophysiol.* 71(6):2359-2376, 1994.

Gritti, I., Mainville, L., and Jones, B. E. Codistribution of GABA-with acetylcholine-synthesizing neurons in the basal forebrain of the rat. *J. Comp. Neurol.* 329(4):438-457, 1993.

Harkmark, W., Mellgren, S. I., and Srebro, B. Acetylcholinesterase histochemistry of the region in rat and human: distribution of enzyme activity. *Brain Res.* 95(2-3):281-289, 1975.

Harrison, N. L. and Gibbons, S. J. Zn^{2+}: an endogenous modulator of ligand- and voltage-gated ion channels. *Neuropharm.* 33(8):935-952, 1994.

Hawkins, R. D., Zhuo, M., and Arancio, O. Nitric oxide and carbon monoxide as possible retrograde messengers in hippocampal long-term potentiation. *J. Neurobiol.* 25(6):652-665, 1994.

Hefti, F. Nerve growth factor promotes survival of septal cholinergic neurons after fimbrial transections. *J. Neurosci.* 6(8):2155-2162, 1986.

Heimer, L. and RoBards, M. J. Neuroanatomical tract-tracing methods. New York: Plenum Press, 1981. p.1.

Henke, H. and Lang, W. Cholinergic enzymes in neocortex, hippocampus, and basal forebrain of non-neurological and senile dementia of Alzheimer-type patients. *Brain*

Res. 267(2):281-291, 1983.

Herbison, A. E. Immunocytochemical evidence for oestrogen receptors within GABA neurones located in the perinuclear zone of the supraoptic nucleus and $GABA_A$ receptor beta 2/beta 3 subunits on supraoptic oxytocin neurones. *J. Neuroendo.* 6(1):5-11z, 1994.

Hermes, M. L., Buijs, R. M., Masson-Pevet, M., and Pevet, P. Seasonal changes in vasopressin in the brain of the garden dormouse (*Eliomys quercinus L.*). *J.Comp.Neurol.* 293(3):340-346, 1990.

Honda, K., Negoro, H., Higuchi, T., and Tadokoro, Y. Activation of neurosecretory cells by osmotic stimulation of anteroventral third ventricle. *Am. J. Physiol.* 252 (6 Pt 2):R1039-R1045, 1987.

Hubbard, J. I., Hyland, B. I., and Sirett, N. E. Luteinizing hormone release in the anesthetized cal following stimulation in the diagonal band of Broca, dorsal septum, and fornix. *Neuroendo.* 52:434-440, 1990.

Hubbard, J. I., Mills, R. G., and Sirett, N. E. Distribution of osmosensitive cells in the preoptic and adjacent regions of cat brains. *Brain Res.* 345(2):402-405, 1985.

Inase, Y. and Machida, T. Differential effects of right-sided and left-sided orchidectomy on lateral asymmetry of LHRH cells in the mouse brain. *Brain Res.* 580:338-340, 1992.

Insel, T. R., Wang, Z. X., and Ferris, C. F. Patterns of brain vasopressin receptor distribution associated with social organization in microtine rodents. *J. Neurosci.* 14(9):5381-5392, 1994.

Iovino, M., Poenaru, S., and Annunziato, L. Basal and thirst-evoked vasopressin secretion

in rats with electrolytic lesion of the medio-ventral septal area. *Brain Res.* 258:123-126, 1983.

Iovino, M. S. and Steardo, L. Thirst and vasopressin secretion following central administration of angiotensin II in rats with lesions of the septal area and subfornical organ. *Neurosci.* 15:61-67, 1985.

Jacklet, J. W. Nitric oxide is used as an orthograde co-transmitter at identified histaminergic synapses. *J. Neurophysiol.* 74(2):891-895, 1995.

Jakab, R. L. and Leranth, C. Septum. In: *The Rat Nervous System*, edited by G. Paxinos. New York: Academic Press, 1995, p. 405-442.

Jard, S. Vasopressin isoreceptors in mammals: Relation to cyclic AMP-independent transduction mechanisms. *Curr. Topics Membr. Transp.* 18:255-285, 1983.

Jhamandas, J. H. and Renaud, L. P. Diagonal band neurons may mediate arterial baroreceptor input to hypothalamic vasopressin-secreting neurons. *Neurosci. Lett.* 65:214-218, 1986a.

Jhamandas, J. H. and Renaud, L. P. A gamma-amminobutyric-acid mediated baroreceptor input to supraoptic vasopressin neurons in the rat. *J. Physiol.* 381:595-606, 1986b.

Jhamandas, J. H. and Renaud, L. P. Bicuculline blocks an inhibitory baroreflex input to supraoptic vasopressin neurons. *Am. J. Physiol.* 252(5 Pt2):R947-R952, 1987a.

Jhamandas, J. H. and Renaud, L. P. Neurophysiology of a central baroreceptor pathway projecting to hypothalamic vasopressin neurons. *Can. J. Neurol. Sci.* 14(1):17-24, 1987b.

Jhamandas, J. H. Characterization of cardiovascular afferents to the hypothalamic supraoptic

nucleus in the rat. *Ph. D Thesis, McGill University* 1987c.

Jhamandas, J. H., Raby, W., Rogers, J., Buijs, R. M., and Renaud, L. P. Diagonal band projection towards the hypothalamic supraoptic nucleus: light and electron microscopic observations in the rat. *J. Comp. Neurol.* 282(1):15-23, 1989.

Jhamandas, J. H. Mapping Central Cardiovascular Pathways That Influence Vasopressin Secretion. *Annals RCPSC* 24:51-57, 1991.

Jurzak, M., Muller, A. R., and Gerstberger, R. Characterization of vasopressin receptors in cultured cells derived from the region of rat brain circumventricular organs. *Neurosci.* 65(4):1145-1159, 1995.

Kalen, P. and Wiklund, L. Projections from the medial septum and diagonal band of Broca to the dorsal and central superior raphe nuclei: A non-cholinergic pathway. *Exp. Br. Res.* 75:401-416, 1989.

Kalivas, P. W., Jennes, L., and Miller, J. S. A catecholaminergic projection from the ventral tegmental area to the diagonal band of Broca: modulation by neurotensin. *Brain Res.* 326:229-238, 1985.

Karmis, R. C., Vanderwolf, C. H., and Bland, B. H. Two types of hippocampal rhythmical slow activity in both the rabbit and the rat: Relations to behavior and effects of atropine, diethylether, urethane, and pentobarbitol. *Expl. Neurol.* 49:58-85, 1979.

Kermer, P., Naumann, T., Bender, R., and Frotscher, M. Fate of GABAergic septohippocampal neurons after fimbria-fornix transection as revealed by in situ hybridization for glutamate decarboxylase mRNA and parvalbumin immunocytochemistry. *J. Comp. Neurol.* 362(3):385-399, 1995.

Kesner, R. P. Reevaluation of the contribution of the basal forebrain cholinergic system to memory. *Neurobiol. Aging* 7:287-295, 1986.

Kesner, R. P., Berman, R. F., and Tardif, R. Place and taste aversion learning: role of basal forebrain, parietal cortex, and amygdala. *Br. Res. Bull.* 29:345-353, 1992.

Kievit, J. and Kuypers, H. G. J. M. Basal forebrain and hypothalamic connections to frontal and parietal cortex in the rhesus monkey. *Science* 187:660-662, 1975.

Kiss, J., Patel, A. J., Baimbridge, K. G., and Freund, T. F. Topographical localization of neurons containing parvalbumin and choline acetyltransferase in the medial septum-diagonal band region of the rat. *Neurosci.* 36:61-72, 1990a.

Kiss, J., Patel, A. J., and Freund, T. F. Distribution of septohippocampal neurons contain parvalbumin or choline acetyltransferase in the rat brain. *J. Comp. Neurol.* 298:362-372, 1990b.

Kiss, J., Shooter, E. M., and Patel, A. J. A low-affinity nerve growth factor receptor antibody is internalized and retrogradely transported selectively into cholinergic neurons of the rat basal forebrain. *Neurosci.* 57(2):297-305, 1993.

Kitchener, P. D. and Diamond, J. Distribution and colocalization of choline acetyltransferase immunoreactivity and NADPH diaphorase reactivity in neurons within the medial septum and diagonal band of Broca in the rat basal forebrain. *J. Comp. Neurol.* 335:1-15, 1993.

Koh, J. and Choi, D. W. Zinc alters excitatory amino acid neurotoxicity on cortical neurons. *J. Neurosci.* 8:2164-2171, 1988.

Kosaka, T., Tauchi, M., and Dahl, J. L. Cholinergic neurons containing GABA-like and/or

glutamic acid decarboxylase-like immunoreactivity in various brain regions of the rat. *Exp. Br. Res.* 70:606-617, 1988.

Kovacs, G. L. and Versteeg, D. H. Neurohypophysial peptides and brain neurochemistry. *Ann. N.Y. Acad. Sci.* 689:309-319, 1993.

Kromer, L. F. Nerve growth factor treatment after brain injury prevents neuronal death. *Science* 235:214-216, 1987.

Kubo, K., Mennin, S. P., and Gorski, R. A. Similarity of plasma LH release in androgenized and normal rats following electrochemical stimulation of the basal forebrain. *Endo.* 96(2):492-500, 1975.

Kunze, W. A. A., Shafton, A. D., Kemm, R. E., and McKenzie, J. S. Effect of stimulating the nucleus of the horizonal limb of the diagonal band on single unit activity in the olfactory bulb. *Neurosci.* 40(1):21-27, 1991.

Lakhdar-Ghazal, N., Dubois-Dauphin, M., Hermes, M. L., Buijs, R. M., Bengelloun, W. A., and Pevet, P. Vasopressin in the brain of a desert hibernator, the jerboa (Jaculus orientalis): presence of sexual dimorphism and seasonal variation. *J. Comp. Neurol.* 258(4):499-517, 1995.

Lamour, Y., Dutar, P., and Jobert, A. Effects of TRH, cyclo-(HIs-Pro) and (3-Me-His2)TRH on identified septohippocampal neurons in the rat. *Brain Res.* 331(2):343-347, 1985.

Landgraf, R. and Ramirez, A. D. The positive feedback action of vasopressin on its own release from rat septal tissue *in vitro* is receptor-mediated. *Brain Res.* 545:137-141, 1991.

Lapchak, P. A. and Hefti, H. Effect of recombinant human nerve growth factor on

presynaptic cholinergic function in rat hippocampal slices following partial septohippocampal lesions: measures of [^{3}H]acetylcholine release and choline acetyltransferase activity. *Neurosci.* 42:639-649, 1991.

Lawlor, B. A. and Davis, K. L. Does modulation of glutamatergic function represent a viable therapeutic strategy in Alzheimer's disease?. *Biol. Psychiatry* 31(4):337-350, 1992.

Lawson, V. H. and Bland, B. H. The role of the septohippocampal pathway in the regulation of hippocampal field activity and behavior: analysis by the intraseptal microinfusion of carbachol, atropine, and procaine. *Exp. Neurol.* 120(1):132-144, 1993.

Lechan, R. M., Nestler, J. L., and Jacobson, S. The tuberoinfundibular system of the rat as demonstrated by immunohistochemical localization of retrogradely transported wheat germ agglutinin (WGA) from the median eminence. *Brain Res.* 245(1):1-15, 1982.

Leranth, C. and Frotscher, M. Organization of the septal region in the rat brain: cholinergic-GABAergic interconnections and the termination of hippocampo-septal fibers. *J. Comp. Neurol.* 289:304-314, 1989.

Leung, L. -W. S., Lopes da Silva, F. H., and Wadman, W. J. Spectral characteristics of the hippocampal EEG in the freely moving rat.. *Electroencephalog. Clin. Neurophysiol.* 54:203-219, 1982.

Lind, R., Van Hoesen, G. W., and Johnson, A. K. An HRP study of the connections of the subfornical organ of the rat. *J. Comp. Neurol.* 210:265-277, 1982.

Luiten, P. G. M., Gaykema, R. P. A., Traber, J., and Spencer, D. J. J. Cortical projection patterns of magnocellular basal nucleus subdivisions as revealed by anterogradely transported *Phaseolus vulgaris* leucoagglutinin. *Brain Res.* 413:229-250, 1987.

Luiten, P. G. M., Spencer, D. G., Traber, J., and Gaykema, R. P. A. The pattern of cortical projections from the intermediate parts of the magnocellular nucleus of basalis in the rat demonstrated by tracing with *Phaseolus vulgaris* leucoagglutinin. *Neurosci. Lett.* 57:137-142, 1985.

Lustig, H. S., von Brauchitsch, K. L., Chan, J., and Greenberg, D. A. A novel inhibitor of glutamate release reduces excitotoxic injury *in vitro*. *Neurosci. Lett.* 143(1-2):229-232, 1992.

Lynn, R. B., Kreider, M. S., and Miselis, R. R. Thyrotropin-releasing hormone-immunoreactive projections to the dorsal motor nucleus and the nucleus of the solitary tract of the rat. *J. Comp. Neurol.* 311:271-288, 1991.

Macrides, F., Eichenbaum, H. B., and Forbes, W. B. Temporal relationship between sniffing and the limbic theta rhythm during odor discrimination reversal learning. *J. Neurosci.* 2(12):1705-1717, 1982.

Mangiapane, M. L., Thrasher, T. N., Keil, L. C., Simpson, J. B., and Ganong, W. F. Deficits in drinking and vasopressin secretion after lesions of the nucleus medianus. *Neuroendo.* 37:73-77, 1983.

Markram, H. and Segal, M. Electrophysiological characteristics of cholinergic and non-cholinergic neurons in the rat medial septum-diagonal band complex. *Brain Res.* 513:171-174, 1990.

Martin, J. H. The gustatory and olfactory systems. In: *Neuroanatomy: Text and Atlas*, Norwalk, Connecticut: Appleton and Lange, 1989, p. 187-206.

Mayer, M. L. and Vyklicky, L. The action of zinc on synaptic transmission and neuronal

excitability in cultures of mouse hippocampus. *J. Physiol.* 415:315-365, 1989.

McCormick, D. A. and Prince, D. A. Two types of muscarinic responses to acetylcholine in mammalian cortical neurons. *PNAS* 82(18):6344-6348, 1985.

McCormick, D. A. and Prince, D. A. Mechanisms of action of acetylcholine in the guinea-pig cerebral cortex *in vitro*. *J. Physiol.* 375:169-194, 1986.

McGaugh, J. L., Introini-Collison, I. B., Cahill, L. F., Castellano, C., Dalmaz, C., Parent, M. B., and Williams, C. L. Neuromodulatory systems and memory storage: role of the amygdala. *Beh. Br. Res.* 58(1-2):81-90, 1993.

McKinney, M., Coyle, J. T., and Hedreen, J. C. Topographic analysis of the innervation of the rat neocortex and hippocampus by the basal forebrain cholinergic system. *J.Comp.Neurol.* 217:103-121, 1983.

Meibach, R. C. and Siegel, A. Efferent connections of the septal area in the rat: an analysis utilizing retrograde and anterograde transport methods. *Brain Res.* 119(1):1-20, 1977.

Melander, T., Hokfelt, T., Rokaeus, A., Cuello, A. C., Oertel, W. H., Verhofstad, A., and Goldstein, M. Coexistence of galanin-like immunoreactivity with catecholamines, 5-hydroxytryptamine, GABA and neuropeptides in the rat CNS. *J. Neurosci.* 6(12):3640-3654, 1986.

Merchenthaler, I., Lopez, F. J., Lennard, D. E., and Negro-Vilar, A. Sexual differences in the distribution of neurons coexpressing galanin and luteinizing hormone releasing hormone in the rat brain. *Endo.* 129(4):1977-1986, 1991.

Merchenthaler, I., Lopez, F. J., and Negro-Vilar, A. Colocalization of galanin and luteinizing

hormone-releasing hormone in a subset of preoptic hypothalamic neurons: anatomical and functional correlates. *Proc. Natl. Acad. Sci. USA* 87:6326-6330, 1990.

Mesulam, M. -M. and Van Hoesen, G. W. Acetylcholinesterase-rich projections from the basal forebrain of the rhesus monkey to neocortex. *Brain Res.* 109:152-157, 1976.

Mesulam, M. M., Mufson, E. J., Wainer, B. H., and Levey, A. I. Central cholinergic pathways in the rat: an overview based on an alternative nomenclature (Ch1-Ch6). *Neurosci.* 10(4):1185-1201, 1983.

Metcalf, R. H., Boegman, R. J., Riopelle, R. J., and Ludwin, S. K. The release of endogenous acetylcholine from the medial septum/diagonal band of rat brain. *Neurosci. Lett.* 93:85-90, 1988.

Miettinen, R. and Freund, T. F. Convergence and segregation of septal and median raphe inputs onto different subsets of hippocampal inhibitory interneurons. *Brain Res.* 594(2):263-272, 1992.

Milner, T. A. Cholinergic neurons in the rat septal complex: Ultrastructural characterization and synaptic relations with catecholaminergic terminals. *J. Comp. Neurol.* 314:37-54, 1991a.

Milner, T. A. Ultrastructural localization of tyrosine hydroxylase immunoreactivity in the rat diagonal band of Broca. *J. Neurosci. Res.* 30:498-511, 1991b.

Minger, S. L. and Davies, P. Persistent innervation of the rat neocortex by basal forebrain cholinergic neurons despite the massive reduction of cortical target neurons. I. Morphometric analysis. *Exp. Neurol.* 117:124-138, 1992a.

Minger, S. L. and Davies, P. Persistent innervation of the rat neocortex by basal forebrain cholinergic neurons despite the massive reduction of cortical target neurons. II. Neurochemical analysis. *Exp. Neurol.* 117:139-150, 1992b.

Miselis, R. R. The efferent projections of the subfornical organ of the rat: a circumventricular organ within a neural network subserving water balance. *Brain Res.* 230:1-23, 1981.

Mitchell, S. J. and Ranck, J. B. Generation of theta rhythm in medial entorhinal cortex of freely moving rat. *Brain Res.* 189:49-66, 1980.

Mody, I. and MacDonald, J. F. NMDA receptor-dependent excitotoxicity: the role of intracellular Ca^{++} release. *TIPS* 16(10):356-359, 1995.

Mohanakrishnan, P., Fowler, A. H., Vonsattel, J. P., Husain, M. M., Jolles, P. R., Liem, P., and Komoroski, R. A. An *in vitro* 1H nuclear magnetic resonance study of the temporopatietal cortex of Alzheimer brains. *Exp. Br. Res* 102(3):503-510, 1995.

Montero, C. N. and Hefti, F. Rescue of lesioned septal cholinergic neurons by nerve growth factor: specificity and requirement for chronic treatment. *J. Neurosci.* 8:2986-2999, 1988.

Moos, T. Simultaneous application of Timm's sulphide silver method and immunoflurorescence histochemistry. *J. Neurosci. Meth.* 48:149-156, 1993.

Morris, M. K., Bowers, D., Chatterjee, A., and Heilman, K. M. Amnesia following a discrete basal forebrain lesion. *Brain* 115:1827-1847, 1992.

Muller, C. M. and Singer, W. Acetylcholine-induced inhibition in the cat visual cortex is mediated by a GABAergic mechanism. *Brain Res.* 487(2):335-342, 1989.

Murtha, S. J. and Pappas, B. A. Neurochemical, histopathological, and mnemonic effects of

combined lesions of the medial septal and serotonin afferents to the hippocampus. *Brain Res.* 651(1-2):16-26, 1994.

Narahashi, T., Ma, J. Y., Arakawa, O., Reuveny, E., and Nakahiro, M. GABA receptor-channel complex as a target site of mercury, copper, zinc, and lanthanides. *Cell. Mol. Neurobiol.* 14(6):599-620, 1994.

Neumann, I., Schwarzberg, H., and Landgraf, R. Measurement of septal release of vasopressin and oxytocin by the push-pull technique following electrical stimulation of the paraventricular nucleus of rats. *Brain Res.* 462:181-184, 1988.

Nickell, W. T. and Shipley, M. T. Neurophysiology of magnocellular forebrain inputs to the olfactory bulb in the rat: frequency potentiation of field potentials and inhibition of output neurons. *J. Neurosci.* 8(12):4492-4502, 1988.

Numan, M. A neural circuitry analysis of maternal behavior in the rat. *Acta Peadiatica Suppl.* 397:19-28, 1994.

Oka, H. and Yoshida, K. Septohippocampal connections to field CA1 of the rat identified with field potential analysis and retrograde labeling by horseradish peroxidase. *Neurosci. Lett.* 58:19-24, 1985.

Olanow, C. W. and Arendash, G. W. Metals and free radicals in neurodegeneration. *Curr. Op. Neurol.* 7(6):548-558, 1994.

Onteniente, B., Tago, H., Kimura, H., and Maeda, T. Distribution of gamma-aminobutyric acid-immunoreactive neurons in the septal region of the rat brain. *J. Comp. Neurol.* 248:422-430, 1986.

Pare, D. and Smith, Y. GABAergic projection from the intercalated masses of the amygdala

to the basal forebrain. *J. Comp. Neurol.* 344(1):33-49, 1994.

Page, K. J. and Everitt, B. J. The distribution of neurons coexpressing immunoreactivity to AMPA-sensitive glutamate receptor subtypes (gluR1-4) and nerve growth factor receptor in the rat basal forebrain. *Eur. J. Neurosci.* 7(5):1022-1033, 1995.

Palacios, G. The endomembrane system of cholinergic and non-cholinergic neurons in the medial septal nucleus and vertical limb of the diagonal band of Broca: A cytochemical and immunocytochemical study. *J. Histochem. Cytochem.* 38:563-571, 1990.

Panula, P., Revuelata, A. V., Cheney, D. L., Wu, J. -Y., and Costa, E. An immunohistochemical study on the location of GABAergic neurons in rat septum. *J.Comp.Neurol.* 222:69-80, 1984.

Pasqualotto, B. A. and Vincent, S. R. Galanin and NADPH-diaphorase coexistence in cholinergic neurons in the rat basal forebrain. *Brain Res.* 551(1-2):78-86, 1991.

Peters, S., Koh, J., and Choi, D. W. Zinc selectively blocks the action f N-methyl-D-aspartate on cortical neurons. *Science* 236:589-593, 1987.

Peterson, G. M., Ginn, S. R., and Lanford, G. W. Fibers immunoreactive for nerve growth factor receptor in adult rat cortex and hippocampus mimic the innervation pattern of AchE-positive fibers. *Br. Res. Bull.* 33(2):129-136, 1994.

Petsche, H., Stumpf, G., and Gogolak, G. The significance of the rabbits septum as a relay station between the midbrain and the hippocampus. I. The control of the hippocampus arousal activity by the septum cells. *Electroenceph. Clin. Neurophysiol.* 14:202-211, 1962.

Phillips, S., Sangalang, V., and Sterns, G. Basal forebrain infarction. A clinicopathologic correlation.. *Arch. Neurol.* 44(11):1134-1138, 1987.

Pittman, Q. J. and Bagdan, B. Vasopressin involvement in central control of blood pressure. In: *Progress in Brain Research*, edited by A. Ermisch, R. Lnadgraf and H. -J. Ruhle. Elsevier Science, 1992, p. 69-74.

Pittman, Q. J., Naylor, A., Poulin, P., Disturnal, J., Veale, W. L., Martin, S. M., Malkinson, T. J., and Mathieson, B. The role of vasopressin as an antipyretic agent in the ventral septal area and its possible involvement in convulsive disorders.. *Br. Res. Bull.* 20:887-892, 1988.

Planas, B., Kolb, P. E., Raskind, M. A., and Miller, M. A. Vasopressin and galanin mRNAs coexist in the nucleus of the horizontal diagonal band: a novel site of vasopressin gene expression. *J. Comp. Neurol.* 361(1):48-56, 1995.

Pohle, W. and Rauca, C. Hypoxia protects against the neurotoxicity of kainic acid. *Brain Res.* 644:297-304, 1994.

Price, J. L. and Powell, T. P. The effect connections of the nucleus of the horizontal limb of the diagonal band of Broca. *J. Anat.* 107(2):239-256, 1970.

Renaud, L. P., Jhamandas, J. H., Buijs, R., Raby, W., and Randle, J. C. Cardiovascular input to hypothalamic neurosecretory neurons. *Br. Res. Bull.* 20(6):771-777, 1988.

Robbins, T. W., Everitt, B. J., Marston, H. M., Wilkinison, J., Jones, G. H., and Page, K. J. Comparative effects of ibotenic acid- and quisqualic acid-induced lesions of the substantia innominata on attentional function in the rat: further implications for the role of the cholinergic neurons of the nucleus of basalis in cognitive processes.

Behav. Br. Res. 35(3):221-240, 1989.

Roman, F. S., Simonetto, I., and Soumireu-Mourat, B. Learning and memory of odor-reward association: selective impairment following horizontal diagonal band lesions. *Behav. Neurosci.* 107(1):72-81, 1993.

Rothman, S. M. and Olney, J. W. Excitotoxicity and the NMDA receptor - still lethal after eight years. *TINS* 18(2):57-58, 1995.

Rye, D. B., Wainer, B. H., Mesulam, M. M., Mufson, E. J., and Saper, C. P. Cortical projections arising from the basal forebrain: a study of cholinergic and non-cholinergic components employing combined retrograde tracing and immunohistochemical localization of choline acetyltransferase.. *Neurosci.* 13(3):627-643, 1984.

Sainsbury, R. S. and Bland, B. H. The effects of selective septal lesions on theta production in CA1 and the dentate gyrus of the hippocampus. *Physiol. Behav.* 26:1097-1101, 1981.

Sanders, S. K. and Shekhar, A. Blockade of $GABA_A$ receptors in the region of the anterior basolateral amygdala of rats elicits increases in heart rate and blood pressure. *Brain Res.* 567(1):101-110, 1991.

Sasaki, H., Muramoto, O., Kanazawa, I., Arai, H., Kosaka, K., and Iizuka, R. Regional distribution of amino acid transmitters in postmortem brains of presenile and senile dementia of Alzheimer type. *Ann. Neurol.* 19(3):263-269, 1986.

Schulz, J. B. and Beal, M. F. Mitochondrial dysfunction in movement disorders. *Curr. Op. Neurol.* 7(4):333-339, 1994.

Scott, H. L., Tannenberg, A. E., and Dodd, P. R. Variant forms of neuronal glutamate transporter sites in Alzheimer's disease cerebral cortex. *J. Neurochem.* 64(5):2193-2202, 1995.

Semba, K., Reiner, P. B., McGeer, E. G., and Fibiger, H. C. Brainstem afferents to the magnocellular basal forebrain studied by axonal transport, immunohistochemistry, and electrophysiology in the rat. *J. Comp. Neurol.* 267:433-453, 1988.

Senut, M. C., Menetrey, D., and Lamour, Y. Cholinergic and peptidergic projections from the medial septum and the nucleus of the diagonal band of Broca to dorsal hippocampus, cingulate cortex and olfactory bulb: a combined wheatgerm agglutinin-apohorseradish peroxidase-gold immunohistochemical study. *Neurosci.* 30(2):385-403, 1989.

Shaw, P. J. Excitatory amino acid neurotransmission, excitotoxicity, and excitotoxins. *Curr. Op. Neurol. Neurosurg.* 5(3):383-390, 1992.

Shute, C. C. and Lewis, P. R. The ascending cholinergic reticular system: neocortical, olfactory, and subcortical projections. *Brain* 90(3):497-520, 1967.

Sigel, E., Baur, R., Trube, G., Mohler, H., and Malherbe, P. The effect of subunit composition of rat brain $GABA_A$ receptors on channel function. *Neuron* 5:703-711, 1990.

Silverman, A. J., Jhamandas, J., and Renaud, L. P. Localization of luteinizing hormone-releasing hormone (LHRH) neurons that project to the median eminence. *J. Neurosci.* 7(8):2312-2319, 1987.

Simerly, R. B. and Swanson, L. W. Projections of the medial preoptic nucleus: A *phaseolus*

vulgaris leucoagglutinin anterograde tract-tracing study in the rat. *J. Comp. Neurol.* 270:209-242, 1988.

Smart, T. G. A novel modulatory binding site for zinc on the $GABA_A$ receptor complex in cultured rat neurones. *J. Physiol.* 447:587-625, 1992a.

Smart, T. G., Xie, X., and Krishek, B. J. Modulation of inhibitory and excitatory amino acid receptor ion channels by zinc. *Prog. Neurobiol.* 42:393-441, 1994.

Smith-Swintosky, V. L. and Mattson, M. P. Glutamate, beta-amyloid precursor proteins, and calcium mediated neurofibrillary degeneration. *J. Neural Transm. Suppl.* 44:29-45, 1994.

Smythe, J. W., Colom, L. V., and Bland, B. H. The extrinsic modulation of hippocampal theta depends on the coactivation of cholinergic and GABA-ergic medial septal inputs. *Neurosci. Biobehav. Rev.* 16:289-308, 1992.

Snyder, S. H. Nitric oxide: first in a new class of neurotransmitters. *Science* 257(5069):494-496, 1992.

Sobreviela, T., Clary, D. O., Reichardt, L. F., Brandabur, M. M., and Kordower, J. H. TrkA-immunoreactive profiles in the central nervous system: colocalization with neurons containing p75 nerve growth factor receptor, choline actyltransferase, and serotonin. *J. Comp. Neurol.* 350(4):587-611, 1994.

Sullivan, M. J., Cunningham, J. T., Nissen, R., Allen, A. M., Coderre, E., and Renaud, L. P. Ibotenic acid lesions of the diagonal band of Broca result in exaggerated polyethylene glycol-induced drinking behavior. *Soc. Neurosci. Abstr.* 17:885, 1991.

Summy-Long, J. Y., Emmert, S. E., and Rosella-Dampman, L. The subfornical organ:

biochemical and neuroendocrine comparisons with the hypothalamo-neurohypophysial system. *Br. Res. Bull.* 15(1):87-97, 1985.

Swanson, L. W. and Cowan, W. M. An autoradiographic study of the organization of the efferent connections of the hippocampal formation in the rat. *J. Comp. Neurol.* 172(1):49-84, 1977.

Talukder, G. and Harrison, N. L. On the mechanism of modulation of transient outward current in cultured rat hippocampal neurons by di- and trivalent cations. *J. Neurophys.* 73(1):73-79, 1995.

Terry, R. D. Senile Dementia. *Fed. Proc.* 37(14):2837-2840, 1978.

Terry, R. D. Senile dementia of the Alzheimer's type. *Ann. Neurol.* 14(5):497-506, 1983.

Thomas, R. J. Excitatory amino acids in health and disease. *J. Amer. Ger. Soc.* 43(11):1279-1289, 1995.

Tomimoto, H., Kamo, H., Kameyama, M., McGeer, P. L., and Kimura, H. Descending projections of the basal forebrain in the rat demonstrated by the anterograde neural tracer *Phaseolus vulgaris* leucoagglutinin(PHA-L). *Brain Res.* 425:248-255, 1987.

Toth, K., Borhegyi, Z., and Freund, T. F. Postsynaptic targets of GABAergic hippocampal neurons in the medial septum-diagonal band of Broca complex. *J. Neurosci.* 13(9):3712-3724, 1993.

Tribollet, E., Armstrong, W. E., Dubois-Dauphin, M., and Dreifuss, J. J. Extra-hypothalamic afferent inputs to the supraoptic nucleus area of the rat as determined by retrograde and anterograde tracing techniques. *Neurosci.* 15(1):135-148, 1985.

Ulfig, N., Braak, E., Ohm, T., and Pool, C. W. Vasopressinergic neurons in the

magnocellular nuclei of the human basal forebrain. *Brain Res.* 530:176-180, 1993.

van Eerdenburg, F. J. C. M. and Pittman, Q. J. Vasopressin modulates glutamate action in the medial septum and diagonal band of Broca of the rat. *Soc. Neurosci. Abstr.* 18:805, 1991.(Abstract)

Waite, J. J., Chen, A. D., Wardlow, M. L., and Thal, L. J. Behavioral and biochemical consequences of combined lesions of the medial septum/diagonal band and nucleus basalis in the rat when ibotenic acid, quisqualic acid, and AMPA are used. *Exp. Neurol.* 130(2):214-229, 1994.

Walaas, I. and Fonnum, F. Biochemical evidence for glutamate as a transmitter in hippocampal efferents to the basal forebrain and hypothalamus in the rat brain. *Neurosci.* 5:1691-1698, 1993.

Wallwork, J. C. Zinc and the central nervous system. *Prog. Food Nutr. Sci.* 11(2):203-247, 1987.

Weiss, J. H., Hartley, D. M., Koh, J. Y., and Choi, D. W. AMPA receptor activation potentiates zinc neurotoxicity. *Neuron* 10(1):43-49, 1993.

Wenk, G., Hughey, D., Boundry, V., Kim, A., and Walker, L. Neurotransmitters and memory: role of cholinergic, serotonergic, and noradrenergic systems. *Behav. Neurosci.* 101:325-332, 1987.

Wilkinson, M. F. and Pittman, Q. J. Changes in arterial blood pressure alter activity of electrophysiologically identified single units of the bed nucleus of the stria terminalis. *Neurosci.* 64(3):835-844, 1995.

Willis, G. L. and Smith, G. C. Amine accumulation in behavioral pathology. *Brain Res.*

356(2):109-132, 1985.

Wishart, T. B. and Mogenson, G. J. Effects of food deprivation on water intake in rats with septal lesions. *Physiol. Behav.* 5:1481-1486, 1970.

Woolf, N. J., Gould, E., and Butcher, L. L. Nerve growth factor receptor is associated with cholinergic neurons of the basal forebrain but not the pontomesencephalon. *Neurosci.* 30(1):143-152, 1989.

Woolf, N. J., Hermit, M. C., and Butcher, L. L. Cholinergic and non-cholinergic projections from the rat basal forebrain revealed by combined choline acetyltransferase and *Phaseolus vulgaris* leucoagglutinin immunohistochemistry. *Neurosci. Lett.* 66:281-286, 1986.

Yee, B. K. and Rawlins, J. N. The effects of hippocampal formation ablation or fimbria-fornix section on performance of a nonspatial radial arm maze task by rats. *J. Neurosci.* 14(6):3766-3774, 1994.

Yoshida, K. and Oka, H. Topographical distribution of septohippocampal projections demonstrated by the PHA-L immunohistochemical method in rats. *Neurosci. Lett.* 113(3):247-252, 1990.

Young, A. B. Cortical amino acidergic pathways in Alzheimer's disease. *J. Neural Transm. Suppl.* 24:147-152, 1987.

Zaborszky, L., Cullinan, W. E., and Braun, A. Afferents to basal forebrain cholinergic projection neurons: an update. In: *The Basal Forebrain*, edited by T.C.Napier et al., New York: Plenum Press, 1991, p. 43-100.

Zhuo, M., Hu, Y., Schultz, C., Kandel, E. R., and Hawkins, R. D. Role of guanylyl cyclase

and cGMP-dependent protein kinase in long-term potentiation. *Nature* 368(6472):635-639, 1994.

CHAPTER 2

METHODS AND MATERIALS

Methods and Materials for Recording from Rat Brain Slices

Dissection

The dissection utilized for this study is similar to the method described previously (Collingridge and Singer, 1990; Zidichouski et al., in press). In brief, male Sprague-Dawley rats (100-200g) were decapitated, their brains quickly excised and placed in ice cold artificial cerebrospinal fluid (ACSF)(126mM NaCl, 2.5mM KCl, 1.2mM $MgCl_2 \cdot 6H_2O$, 1.2mM NaH_2PO_4, 2.4mM $CaCl_2 \cdot 6H_2O$, 25mM $NaHCO_3$, 11mM Glucose). For studies examining NMDA receptor activation, $MgCl_2$ was omitted from the ACSF solution. The brain was trimmed, glued to a plastic block with cyanoacrylate glue, and 400μm coronal slices containing the DBB were cut using a Vibratome (Series 1000). The slices were placed into small oxygenated (95% O_2, 5% CO_2) vials containing ACSF at 30-32°C. Sections were cropped to remove extraneous tissue around the DBB and the tissue was mounted into the recording chamber where it was perfused with ACSF (3mL/min).

Electrophysiological Recording

Electrophysiological recordings were made from cells using either the whole cell patch clamp or the perforated patch clamp techniques. Cells were recorded using either current clamp or voltage clamp configurations. The internal pipette solution was composed of the following (mM): K-gluconate 140, EGTA 10, HEPES 40, $MgCl_2$ 3.5, Na-ATP 2.2, Na-GTP 0.3. The pH was adjusted to 7.2 with 1M KOH. Patch clamp electrodes (World Precision Instruments - Thin Wall with Filament, 1.5mm) were pulled with a Sutter Instrument (Model P-87) puller to yield electrodes with resistances of 4-8MΩ. Recordings were made from the basal-medial portion of the hDBB where seals of 1GΩ or greater were

obtained using a water-driven Narishige micromanipulator (WR-89 3-D Aqua Purificate). Using an Axoclamp 2A (Axon Instruments) amplifier, cells were initially acquired in current clamp mode and then switched to continuous voltage clamp mode where cells were typically held at approximately -80mV, the typical resting membrane potential (rmp) observed when cells were acquired. The measurement of membrane potential was corrected for liquid junction potential. Recordings were made at a bandwidth of 30kHz and data was filtered using the filtering programs in pClamp version 5.7 (Axon Instruments). Bipolar electrodes (stimulus of 200μs duration @ 2Hz, range 10-70V) placed in the ventromedial aspect of the hDBB were used to evoke synaptic currents or potentials. Pharmacological characterization of these synaptic inputs was carried out by application of specific glutamate receptor agonists and antagonists (see "Drugs Used" below).

Perforated patch clamp recordings were also performed on hDBB cells using the antibiotic Amphotericin B (450μg/mL) which was added to the internal patch solution.

Data Acquisition and Analysis

Cells with action potential heights less than 50mV or rmp less than 60mV were not analyzed. Additional analysis was performed using Quattro Pro For Windows (ver 1.0, 6.0), Origin (ver. 2.5), and Axum (version 3). All data were analyzed on a 486 IBM personal computer.

Drugs Used

All drugs used in this study were applied to cells via bath perfusion using a four-way valve delivery system.

Excitatory Amino Acid Study (Chapter 3)

Agonists: The glutamate agonists utilized were AMPA (α-amino-3-hydroxy-5-methyl-4-isoxazolepropionate; 5μM; RBI), kainate (5μM; Cambridge Research Biochemicals), NMDA (N-methyl-D-aspartate; 15μM; RBI), and the metabotropic receptor agonist, trans-ACPD (trans-1-aminocyclopentane-1,3-dicarboxylic acid; 10μM; RBI).

Antagonists: NBQX (2,3-dihydroxy-6-nitro-7-sulfamoyl-benzo(f)quinoxaline; 1μM; NovoNordisk), L-APV ((-)2-amino-7-phosphonovalerate; 60μM; CRB), and L-AP3 (2-amino-3-phosphonopropionate; 200μM; RBI), were used to antagonize the AMPA, NMDA, and metabotropic receptors respectively. NBQX and CNQX (6-cyano-7-nitroquinoxaline-2,3-dione; 1μM; CRB) were agents used to block kainate and AMPA receptor.

Agonist studies were also repeated in the presence of 1μM tetrodotoxin (TTX; Sigma). In order to eliminate possible contamination of excitatory postsynaptic currents (EPSCs) by GABA-evoked inhibitory postsynaptic currents (IPSCs), experiments examining synaptic responses were also carried out in ACSF containing a cocktail of bicuculline (10μM, Sigma), a $GABA_A$ antagonist, and CGP35348 (10μM, Ciba-Geigy), a $GABA_B$ antagonist.

Morphology

Recordings from hDBB neurons were made using electrodes filled with an internal solution with 0.5% Lucifer Yellow (LY). After filling the neurons, the slice was fixed overnight in 4% paraformaldehyde. Tissues were dehydrated by sequential application of ethanol solutions (10%, 30%, 50%, 70%, 100%) and then cleared with methylsalicylate. Subsequently they were mounted on microscope slides, coverslipped with cytoseal (Stephens

Scientific). Neurons were then observed with a confocal microscope (Leitz Aristoplan attached to Leica CLSM system, ArKr light source) equipped with a filter combination for the detection of FITC fluorescence. The image was optically sectioned at 2.0μm intervals and extended focus was applied in order to obtain details of the neuronal arborization at different focal planes. Photomicrographs were taken directly from the screen of the monitor.

Analysis of Membrane Properties

Action potentials (APs) were generated by applying brief current pulse (300ms; 0.05-0.3nA) through recording electrodes with the use of the Master 8 pulse generator (A.M.P.I.). AP characteristics examined included spike height (measured from threshold), width (measured at threshold), and duration of the AHP (measured from baseline). Voltage ramps from -120 to -20mV (9.2mV/sec) were applied to the cell and input conductance (G_i) was measured between -60 to -80mV. The effects of exogenously applied glutamate receptor agonists and antagonists on G_i were also assessed using voltage ramps.

Analysis of Cable Properties

Passive membrane cable properties were assessed from small hyperpolarizing current pulses (-0.09nA; 400ms; voltage range: -60 to -80mV) according to the methods of Rall (1969) and Taube (1993). Hyperpolarizing responses were transformed to the charging function (V_f-V) and expressed as a sum of exponentials:

$$V_f\text{-}V=C_o e^{-t/\tau o} + C_1 e^{-t/\tau 1} + \ldots$$

where: V = membrane potential at time t, V_f = final steady state voltage, τ_0= first order time constant, τ_1 = second order time constant, C_o= first order coefficient (amplitude), and C_1= second order coefficient (amplitude). Estimates for τ_0, τ_1, C_o, and C_1 calculated using the

curve fitting program (pClamp vesion. 5.7, Axon Instruments). Rall's (1969) idealized neuron model, consisting of a cell body as a lumped resistor and capacitor in parallel and the dendrites as a single cylinder of finite length, can be used to calculate the electrotonic length (L) and the dendrite-to soma-conductance ratio (ρ). This model makes several assumptions including: 1) the membrane is passive and that there are no active conductances; 2) dendrites are represented as one uniform cylinder; 3) extracellular space has infinite conductivity; 4) dendritic branching pattern that conforms to Rall's 3/2 power rule. Application of the equivalent cylinder analysis to our data enables a comparison to be made between electrical constants in hDBB neurons and other central neurons where the Rall model has also been applied (Rall, 1969; Griffith, 1988; Taube, 1993). Brown et al. (1981) and Taube (1993) calculated the dendrite-to-soma conductance ratio as follows:

$$\rho = [\frac{\tau_0}{V_f} \cdot (\frac{C_0}{\tau_0} + \frac{C_1}{\tau_1})] - 1$$

where ρ is the dendrite- to-soma conductance ratio. The electrotonic length (L) was estimated according to the method of Rall (Schoepp et al., 1990):

$$L = \pi \cdot \frac{(\frac{\rho}{\sqrt{\rho + 1}})}{(\frac{\tau_0}{\tau_1} - 1)}$$

Since τ_0 represents the product of the specific membrane resistance (R_m) and the specific membrane capacitance (C_m) of the neuron, values of R_m can be estimated assuming C_m to be fixed at $1 \mu F/cm^2$ (Christie and North, 1988). Also, estimates can be made regarding the percentage of current attenuation as it passes from the dendrite to the soma. This value is

described as:

$$(1-\frac{1}{H})\times 100\%$$

where

$$H=\frac{V_o}{V_L}=\cosh(L)$$

where (H=amount of current attenuation, V_o= voltage at site of current injection at one end of the cable; V_L=voltage at the other end of the cable (Sternweis and Pang, 1990).

Inhibitory Modulation of hDBB Neurons (Chapter 4)

Agonists: The GABA agonists utilized in this study were the $GABA_A$ agonist muscimol (10μM, Sigma), the $GABA_B$ agonist, baclofen (10μM, Sigma), and the $GABA_C$ agonist CACA (cis-4-aminocrotonic acid, 5-100μM, RBI). To activate presynaptic metabotropic receptors, we utilized trans-ACPD (see previous section).

Antagonists: The antagonists used in this study were the $GABA_A$ agonist, bicuculline (10μM, Sigma) and the $GABA_B$ antagonist, CGP-35348 (10μM, Ciba-Geigy). Also, the non-NMDA antagonist, NBQX (see previous section) was used to block glutamate-mediated EPSCs.

Studies examining postsynaptic actions of GABA agonists were repeated in the presence of 1μM TTX. Also, studies examining some IPSPs synaptic responses were repeated in CNQX/APV solutions.

Voltage Protocols: Voltage ramps were applied to hDBB cells. The voltage ranges of these ramps varied between different cells. The specific values are indicated within the text of Chapter 4. Input conductance was measured in a manner similar to that described above. Furthermore, synaptic currents and potentials were evoked using the method described above.

Methods and Materials for Recording from Acutely Dissociated hDBB Cells

Dissection

Male Sprague-Dawley rat pups (15-23 days old) were decapitated, their brains rapidly excised, and placed into oxygenated ice-cold ACSF (in mM): NaCl 140, KCl 2, $CaCl_2$ 1.5, $MgCl_2$ 5, HEPES 10, D-Glucose 33 (pH 7.4). The brains were trimmed, glued to a plastic chuck with cyanoacrylate glue. 350μm slices containing the DBB were cut using a Vibratome (Series 1000). The slices were then placed into oxygenated ACSF where the hDBB was dissected out. Acutely dissociated neurons were prepared by enzymatic treatment of the slices with trypsin (0.65mg/ml) for 23-35 minutes (exposure to enzyme was increased by one minute per day increase in the age of animal) at 32°C, followed by mechanical trituration for dispersion of individual cells. Cell were then plated on Poly-L-lysine coated cover slips (0.005% w/v) and viewed using an inverted microscope (Zeiss-Axiovert 135). Continuous perfusion was maintained at 3-5mL/min during recording which allowed complete exchange of bath solution in less than one minute.

Electrodes and Method of Recording

The whole-cell patch clamp recording (WCR) technique was used to record from

acutely dissociated hDBB neurons using an Axopatch-1D amplifier (Axon Instruments). Patch electrodes (World Precision Instruments - Thin Wall with Filament, 1.5mm diameter) were flame polished to yield resistances of 3-6MΩ. The internal patch pipette solution used for recording contained (in mM): K-methylsulfate 140, $MgCl_2$ 5, $CaCl_2$ 1, HEPES 10, EGTA 10, Na_2-ATP 2.2, Na-GTP 0.3 (pH 7.2). After whole-cell configuration was acquired, a "run-up" of potassium currents often occurred within 1-2 minutes (c.f. Kang et al., 1995). Consequently, we waited at least 5 minutes for steady state currents to stabilize so as to avoid discrepancies which could result from the "run-up" of currents.

To examine the effects of VP and Zn^{++} on the contribution of Ca^{++} to voltage-dependent ionic currents, we utilized an external solution which contained 0mM Ca^{++} and 50μM Cd^{++} was utilized. In this solution $CaCl_2$ was replaced with equimolar amounts of $MgCl_2$.

Sodium currents (I_{Na}) were recorded in isolation for studying the effects of Zn^{++} on these currents. For recording I_{Na}, the internal patch pipette solution contained (in mM): cesium-methanesulfonate 130, $MgCl_2$ 2, HEPES 10, BAPTA 10, Mg-ATP 5, Na_2-GTP 0.3 (pH 7.2 with Cs-OH) and the external perfusing solution was composed of (in mM): NaCl 125, TEA-Br 20, $MgCl_2$ 2, $MnCl_2$ 5, HEPES 10, glucose 20 (pH 7.4 with Tris-OH).

Modulation of Ca^{++} currents by VP and Zn^{++} was investigated by recording currents through calcium channels using Ba^{++} as charge carrier. The use of Ba^{++} has advantages over Ca^{++} as it avoids Ca^{++}-induced inactivation of Ca^{++} channels (Chad and Eckert, 1986) and is considered a better charge carrier (Griffith et al., 1994). The external solution for recording I_{Ba} contained (in mM): TEA-Br 150, $BaCl_2$ 2, glucose 30, HEPES 10 (pH 7.4 with TEA-OH)

and the internal solution was the same as that described above for I_{Na}.

The cells were held at -80mV which was close to their rmp. Cell size was measured electronically using the whole cell capacitance compensation circuit on the Axopatch-1D amplifier. The signals were filtered between 20kHz and 100kHz on the amplifier and capacitance compensation (>80%) was continuously monitored. Maximum voltage clamp error in recording a current of 6nA using a patch electrode with an electrode resistance of 5MΩ was 6mV. All recordings were made at room temperature (20-22^0 C). Data were acquired using pClamp6 (version 6.02, Axon Instruments) and analyzed using Origin (version 3.5, Microcal) and Quattro Pro (version 6.0, Novell) software packages. Data are presented as mean±standard error of mean (s.e.m.) and Student's two-tailed t-test was utilized for determining significance of effect.

Vasopressin Study (Chapter 5)

Voltage Protocols

Depolarizing voltage steps of 100ms duration were applied (increment 10mV per step) to evoke whole cell currents. In the experiments on K^+ currents, the maximum depolarizing step command was to +30mV and in the case of Ba^{++} currents, it was +70 mV. Steady state currents evoked by voltage steps were normalized to the cell size and plotted as current density-voltage relationships in order to assess the effects of VP and its antagonists.

Pharmacological Agents Used

All solutions were applied via bath perfusion. Vasopressin (300nM, Bachem),

Manning Compound (MC;V_1 receptor antagonist;1μM,Bachem,), d(CH2)5)[1],D-Ile[2],Ile[4],Arg[8],Ala[9]) (V_2 receptor antagonist; 1μM, Bachem), charybdotoxin (CTX; 25nM; Sigma), and apamin (50nM; Sigma) were utilized in this study. The concentrations of all chemicals used in this study are based upon previous studies that have examined the actions of these agents on other cell types: VP (Tanaka et al., 1994)); MC (Brinton and McEwen, 1989); V_2 antagonist (Manning and Sawyer, 1989); CTX (Goh et al., 1989); apamin (Womble and Moises, 1993).

Zinc (Chapter 6)

Voltage Protocols

All protocols used in this study are described in detail in the results section of Chapter 6.

Pharmacological Agents Used

The cation Zn^{++} ($ZnCl_2$; 50μM; Fischer), TTX (tetrodotoxin,1μM; Sigma), TEA (tetraethylammonium chloride; 5mM; Sigma); and 4-AP (4-aminopyridine; 0.05-1mM, Sigma) were all utilized in this study. All pharmacological agents were applied through bath perfusion.

REFERENCES

Brinton, R. E. and McEwen, B. S. Vasopressin neuromodulation in the hippocampus. *J. Neurosci.* 9(3):752-759, 1989.

Chad, J. E. and Eckert, R. An enzymatic mechanism for calcium current inactivation in dialyzed Helix neurones. *J. Physiol.* 378:31-51, 1986.

Christie, M. J. and North, R. A. Agonists at μ-opioid, M_2-muscarinic and $GABA_B$-receptors increase the same potassium conductance in rat lateral parabrachial neurones. *Br. J. Pharmacol.* 95:896-902, 1988.

Collingridge, G. L. and Singer, W. Excitatory amino acid receptors and synaptic plasticity. *TIPS* 11:290-296, 1990.

Goh, J. W., Kelly, M. E., and Pennefather, P. S. Electrophysiological function of the delayed rectifier (IK) in bullfrog sympathetic ganglion neurones. *Pflugers Arch Eur. J. Physiol.* 413(5):482-486, 1989.

Griffith, W. H., Taylor, L., and Davis, M. J. Whole-cell and single-channel calcium currents in guinea pig basal forebrain neurons. *J. Neurophysiol.* 71(6):2359-2376, 1994.

Kang, J., Sumners, C., and Posner, P. Modulation of net outward current in cultured neurons by angiotensin II: involvement of AT1 and AT2 receptors. *Brain Res.* 580:317-324, 1992.

Manning, M. and Sawyer, W. H. Discovery, development, and some uses of vasopressin and oxytocin antagonists. *J. Lab. Clin. Med.* 114(6):617-632, 1989.

Rall, W. Time constants and electrotonic length of membrane cylinder and neurons. *Biophys. J.* 9: 1483-1508, 1969.

Schoepp, D., Bockaert, J., and Sladeczek, F. Pharmacological and functional characteristics of metabotropic excitatory amino acid receptors. *TIPS* 11:508-515, 1990.

Sternweis, P. C. and Pang, I. The G protein-channel connection. *TINS* 13:83-87, 1990.

Tanaka, T., Shishido, Y., Shigenobu, S., and Watanabe, S. Facilitatory effect of vasopressin on the ischemic decrease of the CA1 presynaptic fiber spikes in rat hippocampal slices. *Brain Res.* 644:343-346, 1994.

Taube, J.S. Electrophysiological properties of neurons in the rat subiculum *in vitro*. *Exp. Brain Res.* 96: 304-318, 1993.

Womble, M. D. and Moises, H. C. Muscarinic modulation of conductances underlying the afterhyperpolarization in neurons of the rat basolateral amygdala. *Brain Res.* 621:87-96, 1993.

Zidichouski, J.A., J.C. Easaw and J.H. Jhamandas. Glutamate receptor subtypes mediate excitatory synaptic responses of rat lateral parabrachial neurons. *Am. J. Physiol.* (in press).

CHAPTER 3

ELECTROPHYSIOLOGY OF NEURONS IN THE HORIZONTAL LIMB OF THE DIAGONAL BAND OF BROCA: INTRINSIC PROPERTIES AND EXCITATORY SYNAPTIC INPUTS

A version of this Chapter has recently been accepted for publication in the American Journal of Physiology: Cell Physiology Section

ABSTRACT

We examined the morphological and electrophysiological properties of neurons within the horizontal limb of the diagonal band of Broca (hDBB) and investigated the role of excitatory amino acid-mediated synaptic transmission in this region. Whole cell patch clamp recordings were obtained from hDBB neurons in rat forebrain slices. The hDBB cells examined in this study display a morphological and electrophysiological profile that is consistent with the type B, non-cholinergic cell type. Cable analysis reveals that hDBB neurons are electrotonically compact and may therefore function as efficient relays for transmission of inputs to other forebrain target sites. Application of agonists for AMPA, kainate, NMDA, and metabotropic receptors all evoke inward currents in hDBB neurons. Pharmacological analysis of synaptic events indicate that evoked excitatory postsynaptic currents (EPSCs) are either mediated by non-NMDA receptors alone or a combination of non-NMDA and NMDA receptors. In some neurons, the metabotropic receptor agonist, trans-ACPD, reduced EPSC amplitude without altering postsynaptic input conductance, thus, suggesting a presynaptic locus of action. The electrical and pharmacological properties described for hDBB neurons may be physiologically relevant for the effective transmission of excitatory synaptic inputs to sites that receive projections from the hDBB.

INTRODUCTION

We have identified a cell type in the hDBB that morphologically resembles rat Type B neurons (Barrenechia et al., 1995) and shares the electrophysiological profile of the non-cholinergic neurons characterized by a fast postspike afterhyperpolarization (FAHP) (Griffith, 1988). In this study, we examined two specific issues concerning these putative Type B/FAHP neurons. First, we investigated both the active and passive electrical properties to better understand the characteristics of information transfer in these neurons. Second, since previous *in vivo* studies suggest that hDBB neurons receive a predominantly excitatory input (Jhamandas and Renaud, 1986a,b), we examined actions of putative transmitters that mediate excitation in these neurons. Anatomical evidence reveals the presence of aspartate and glutamate in terminals contacting hDBB cells suggesting that excitatory amino acids (EAAs) may serve as neurotransmitter candidates within this region (Carnes et al., 1990). Therefore, we investigated the role of specific EAA receptor subtypes in excitatory synaptic transmission within the hDBB.

RESULTS

Morphology

We identified 5 neurons by LY intracellular staining (Fig. 3-1). Cells stained with LY exhibited a polygonal cell body (diameter 12-20μm) with numerous processes. These processes appeared to contact the cerebrospinal fluid in the medioventral surface of the brain, or penetrated the adjacent neuropile. The processes could be followed at a distance of 100-120μm. These stained cells share the same morphology as Type B

neurons identified by Barrenechea et al. (1995). Our anatomical data also suggest that hDBB neurons are not damaged by the slice procedure.

Passive and Active Properties of hDBB Neurons

We examined several passive and active electrophysiological characteristics of hDBB neurons. The passive properties examined were the rmp and G_t. The active properties examined were the height, width, and the duration of the afterhyperpolarization of single APs evoked with a brief depolarizing pulse (Table 3-1). As indicated in Fig. 3-2, we observed similar passive properties in these neurons using either WCR or perforated patch clamp recordings suggesting that the passive properties are not altered using WCR.

To examine the intrinsic cable properties of these neurons, hyperpolarizing pulses (-0.09nA) were applied according to the methods of Rall (1969) and Taube (1993). The pulses were applied at the rmp which typically lay between -60 and -80mV. As indicated in Fig. 3-2, step data and voltage ramp data are linear between -60 and -80mV suggesting that there are no voltage-dependent currents in this range. Cable properties for hDBB cells calculated using the data and equations (see Methods) are shown in Table 3-2. An additional observation was that the charging curve of 16 neurons could be fit by a single exponential as shown in Fig. 3-2C_1 and C_2 using either whole cell patch or perforated patch clamp recordings. This indicates that the dendrites and soma essentially function as a single capacitor in these neurons thus, suggesting that the dendrites are isopotential with the soma.

Pharmacology of Glutamate Neurotransmission

a) *AMPA\Kainate*

In 22 of 23 cells, exogenous application of 5μM AMPA evoked an inward current that reversed at approximately 0mV (Fig. 3-3A). This inward current is attenuated by NBQX (1μM), an antagonist for the AMPA receptor, by 67% (range: 28.7-100%; 5/5 cells). The inset of Fig. 3-3A further illustrates the net inward AMPA current and its attenuation by NBQX. Application of 1μM NBQX, the same concentration used to block agonist-induced inward current, also attenuates evoked fast EPSCs (mean=61.4%; range: 32-100%; 29/35 cells) (Fig. 3-3B).

Exogenous superfusion of 5μM kainate induces an inward current in 22 out of 26 cells (Fig. 3-4A). Similar to AMPA, kainate-induced current reverses at approximately 0mV. CNQX (1μM) is able to attenuate kainate-induced inward current in all cases (mean=66.7% attenuation; range: 52.3-100%; 5/5 cells). The net current generated by kainate and the effect of CNQX on this current are illustrated in the inset of Fig. 3-4A. Furthermore, application of 1μM CNQX also antagonizes EPSCs (mean=54.1%; range: 46.5-100%; n=3 cells)(Fig. 3-4B).

b) *NMDA*

Application of 15μM NMDA in the absence of $[Mg^{++}]_o$ generates a large inward current (15/15 cells) that can be blocked by application of the NMDA receptor antagonist, APV (60μM)(7/7 cells)(Fig. 3-5A). The contribution of NMDA receptor activation to synaptic currents was examined by application of APV on evoked EPSCs in control and 0 Mg^{++} ACSF solutions. As shown in Fig. 3-5B, APV typically only

blocks the latter component of the EPSC (mean-39.3%; range: 18.3-44.4%) (9/11 cells) and the application of NBQX is able to further attenuate the synaptic current under normal conditions. When hDBB cells are superfused with a 0 Mg^{++} ACSF solution, EPSC duration was typically observed to increase by 80% (n=6)(Fig. 3-5C) compared to those observed in normal ACSF (Fig. 3-5B). This increased duration is due to an enhanced contribution from NMDA channels as indicated in Fig. 3-5C where 60μM APV attenuates the larger late component of the EPSC. Application of 1μM NBQX with APV completely blocks the EPSC.

c) *Metabotropic*

In 9 of 22 cells, application of 10μM trans-ACPD increased postsynaptic G_i (E_{rev}= -35mV) which would be consistent with an underlying mixed ionic conductance in these neurons. Furthermore, this postsynaptic response can be attenuated by the metabotropic antagonist, AP3 (42%; range: 15-89%) (Fig. 3-6A). Interestingly, in 13 of 22 cells, trans-ACPD did not evoke a change in postsynaptic G_i (Fig. 3-6B). However in these cells, trans-ACPD was able to attenuate the amplitude of EPSCs (42.2%; range: 32-100%; 13/22 cells) (Fig. 3-7A and B). These observations suggest an additional presynaptic locus of action for trans-ACPD (Fig. 3- 7A and B).

We considered the possibility that the putative presynaptic modulation of synaptic transmission by trans-ACPD may in fact be due to a possible postsynaptic blockade of AMPA or NMDA receptors. In order to address this issue, agonists for AMPA or NMDA receptors were superfused onto the cell followed by application of the agonist with trans-ACPD. If trans-ACPD was acting at postsynaptic AMPA or NMDA

receptors, the direct response of these glutamate receptor agonists would be expected to be reduced in the presence of trans-ACPD. However, as shown in Fig. 3-8 and Fig. 3-9, the inward current generated in the presence and absence of the metabotropic receptor agonist is the same for AMPA and NMDA in the presence of trans-ACPD.

TTX

All agonist studies performed in ACSF were repeated in the presence of TTX. We observed no change in the effects of agonists on hDBB cells in the presence of TTX (NMDA n=7; AMPA n=5; kainate n=4) which suggests that exogenously applied glutamate receptor agonists exert their effects directly at the postsynaptic level.

DISCUSSION

The present study provides two important observations related to the physiology and pharmacology of hDBB neurons. First, our electrophysiological analysis of identified hDBB neurons indicates these cells to be electronically compact. This may have implications for the functional role of hDBB neurons in the transfer of synaptic inputs to target sites. Second, glutamate receptor subtypes mediate excitatory synaptic transmission in the hDBB at pre- and postsynaptic levels.

Morphology

The morphological characteristics of Lucifer yellow filled neurons in the present study resemble Type B neurons reported by Berrenechea et al. (1995). Specifically, the similarities we observed related to soma shape, size, and dendritic branching. The position of the processes of these neurons suggests that they may influence the activity

of cells in an area with a diameter of at least 200μm. *In vivo* intracellular recordings from DBB indicate that Type B neurons are characterized by a fast postspike AHP (Berrenechea et al., 1995). A similar type of cell with a fast postspike AHP (FAHP cell type) has also been observed *in vitro* DBB preparations (Griffith, 1988; Mathews and Lee, 1991). Rat type B/FAHP neurons do not stain positively for AchE or ChAT (Griffith and Mathews, 1991) suggesting that these cells are likely non-cholinergic. Importantly, the preserved morphological characteristics of the LuciferYellow-filled cells we recorded from suggests that they are not damaged by the slice procedure.

Intrinsic Membrane Properties

The intrinsic membrane properties examined in this study were the rmp, G_i, and the height, width, and afterhyperpolarization of the action potential. In Griffith's (1988) analysis of guinea pig medial septum-diagonal band (MS-DBB) neurons, he observed three cell types in this region: 1) cells with a slow postspike afterhyperpolarization (~600ms) 2) cells with a fast postspike afterhyperpolarization (5-50ms) (FAHP) and 3) a bursting cell type. Assuming a similar compartmentalization for the rat, our results suggest that we are recording principally from FAHP-like cells. We observe AHPs for these hDBB cells to have a mean value of 48±8.82 ms (Table 3-1), which falls in the range reported by Griffith (1988) for the FAHP cell type. However, not all of the intrinsic properties measured in hDBB cells correlate with guinea pig FAHP cells including rmp, AP width, and G_i. These differences are likely attributable to the fact that studies reported by Griffith (1988) were done in guinea pig and utilized sharp

microelectrode recording as opposed to our studies performed in the rat and utilizing the whole cell patch configuration. In particular, the higher G_i observed in our study can be explained by our use of WCR. Since WCR requires the formation of a high resistance seal, there is less leakage of current where the electrode has access to the cell interior compared to sharp microelectrodes. Thus, the voltage deflection elicited by a current step will be larger as a result of a larger G_i. Our use of perforated patch clamp revealed similar observations as with WCR suggesting that the use of WCR did not alter the electrophysiological characteristics of the cell (Fig. 3-2).

Cable properties of hDBB neurons

In comparison with other central neurons, where similar analyses have been carried out, our data on passive cable properties (H, R_m, ρ, and L) of hDBB neurons suggest that these cells are electrically compact (Griffith, 1988; Tanaka et al., 1991). The calculated value of H was 1.34 which is consistent with a current attenuation of only 25% from the dendrite to the soma. This relatively low value of current attenuation also implies that hDBB neurons are electrically compact (Griffith, 1988).

Since τ_0 represents the product of specific membrane resistance (R_m) and specific membrane capacitance (C_m), the average τ_0 value in Table 3-2 and 1μF/cm^2 for C_m were inserted into the equation:

$$\tau_0 = R_m \cdot C_m$$

producing an R_m value of 24 930Ωcm^2. This value is more than 1/3 larger than the R_m value calculated using Griffith's (1988) τ_0 value of 16.15ms for FAHP cells measured

with sharp microelectrodes. This difference may be due to the fact that Griffith's measurements were made using sharp electrodes unlike ours which were made using WCR. The formation of a high resistance seal using low resistance electrodes permits a low access resistance into the cell, therefore, a given current injection will likely elicit a larger voltage deflection and thus, yield a larger τ_0 value. Physiologically, a large R_m value would be important because it would be indicative of a large length constant (λ) as given by the equation:

$$\lambda = \sqrt{\left(\frac{R_m}{R_i} \cdot \frac{d}{4}\right)}$$

where R_i is the specific internal resistance and d is the diameter of the dendritic cable. Thus, a given current pulse would be able to propagate a greater distance along the cable through electrotonic spread (Pongracz et al, 1991).

Analysis of ρ and L values calculated in this study also suggest that hDBB cells are electrotonically compact. The value of ρ is the ratio of dendritic conductance to somatic conductance. The calculated ρ value of 1.84 suggests that there may be conductances in the dendritic regions (Lacaille and Williams, 1990). L is the average electrotonic length of equivalent cylinder dendrites with sealed ends and is representative of the ratio of physical length of the dendrite to its length constant. A ratio of 1.08 suggests that hDBB dendrites terminate approximately 1 length constant from the soma.

Furthermore, 16 hDBB neurons also showed charging curves that could be fitted by a single exponential suggesting that the dendrites are isopotential with the soma further demonstrating the electrical compactness of hDBB cells (Coleman and Miller,

1989). These electrophysiological and morphological properties of hDBB neurons should permit distal synaptic potentials to be faithfully transmitted to target neurons. hDBB cells appear to act as highly efficient relay neurons for the transmittal of their inputs to their projection sites with high fidelity.

Analysis of glutamate agonist effects and glutamate-mediated synaptic transmission

Immunocytochemical data reveal that cells in the hDBB are recipients of dense glutamatergic input (Carnes et al., 1990). We have observed the presence of AMPA, kainate, NMDA, and metabotropic receptor subtypes in these cells. As illustrated in Fig. 3-3 and 3-4, single receptor subtypes such as AMPA and kainate receptors mediate fast excitatory synaptic transmission entirely on their own. However, it appears that glutamate-mediated synaptic transmission may also involve different receptor subtypes working in concert as indicated by our observation that the AMPA and NMDA receptors together mediated synaptic transmission (Fig. 3-5c). Thus, the AMPA-mediated early phase of the EPSC may serve to depolarize the cell and, thereby, activate NMDA channels by relieving the voltage-dependent Mg^{++} block of these channels.

Metabotropic receptor activation was observed at both pre- and postsynaptic levels. Postsynaptically, however, we observed fewer responses. As metabotropic receptors mediate their effects via G-proteins (Manzoni et al., 1990), it might be argued that this small number of postsynaptic receptors is due to our use of the whole cell patch clamp technique where washout of the second messenger components from the cell could occur. However, we feel that this is unlikely as the use of amphotericin B in perforated patch technique did not reveal an increase in the number of metabotropic-mediated

postsynaptic responses (unpublished observations). In addition, we have also observed that application of baclofen, a $GABA_B$ receptor agonist whose actions are also mediated via a G-protein mechanism, evokes postsynaptic hyperpolarizing responses (Easaw and Jhamandas, 1994). The presence of the metabotropic receptor presynaptically such as we have observed in the hDBB is consistent with that reported in regions including the hippocampus (Baskys and Malenka, 1991) and the cingulate cortex (Sheardown, 1992). This autoreceptor attenuates excitatory synaptic transmission which suggests that glutamate release can be modulated.

Functional Considerations

Transmitters that mediate excitation in the hDBB have been the focus of considerable interest on account of the fact that activation of peripheral arterial baroreceptors results in an increase in the excitability of hDBB neurons (Jhamandas and Renaud, 1986a). An excitation of hDBB neurons in turn inhibits VP-secreting neurons of the hypothalamic supraoptic nucleus (Jhamandas and Renaud, 1986b). Two neurotransmitter candidates, noradrenaline (NA) and glutamate have been postulated to activate hDBB neurons. While infusions of NA *in vivo* into the MS-DBB complex result in a depression of VP neuronal activity (Cunningham et al., 1993), applications of NA *in vitro* do not appear to excite hDBB neurons (unpublished observations). Our observations indicates that these cells possess AMPA, kainate, NMDA, and metabotropic receptors and that all of these receptors participate in excitatory neurotransmission in the hDBB. We postulate that glutamate may be the putative neurotransmitter that excites baroreceptor-sensitive hDBB neurons.

In summary, the results presented in this study provide a characterization of electrotonic properties of hDBB cells that may explain their role in information transfer within this forebrain nucleus. EAA-mediated neurotransmission may subserve important roles in central autonomic responses and other physiological functions.

Table 3-I: Summary of passive and active properties of hDBB neurons.

RMP (mV) (n=111)	G_i (nS) (n=88)	AP height (mV) (n=96)	AP width (ms) (n=98)	AHP duration (ms) (n=95)
-79±0.84mV	3.21±0.06	80.87±2.0	1.89±0.07ms	48.52±3.55

Abbreviations:

RMP- resting membrane potential; G_i - input conductance; AP - action potential.

Table 3-II: Electrotonic properties of hDBB neurons.

Neurons (n)	τ_0 (ms)	τ_1 (ms)	C_0	C_1	ρ	L	R_m ($\Omega \cdot cm^2$)	H
n=11	24.93±7.34	3.78±0.97	7.46±1.30	4.6±1.83	1.8	1.09	24930	1.34

Abbreviations:

τ_0 - first time constant; τ_1 - second time constant; C_0 - first order coefficient; and C_1 - second order coefficient; ρ - soma-to-conductance ratio; R_m - specific membrane resistance; H - current attenuation.

Figure 3-1. Schematic drawing of the rat forebrain illustrating horizontal limb of the hDBB, where whole cell patch clamp recordings were obtained. Abbreviations: AC - anterior commissure, CC - corpus callosum, ON- optic nerve, vDBB - vertical limb of diagonal band of Broca. **Inset:** Typical hDBB neuron filled with Lucifer Yellow using the whole cell patch clamp protocol. The morphology of these neurons appears to be similar to the Type B neuron described by Barrenechea et al. (1995) and the non-cholinergic FAHP cell type identified by Griffith (1988).

hDBB
vDBB
AC
ON
CC

Figure 3-2. Recordings taken from different hDBB neurons using either the whole cell patch clamp method (top row) or the perforated patch technique (bottom row). **A_1 and A_2:** representative APs generated using either the whole cell or perforated patch techniques. APs were generated by 300ms current pulse applications (0.05-0.3nA). **B_1 and B_2**: current-voltage (I-V) relationships in hDBB neurons were examined using ramps from -120 to -20mV. G_i was measured between -60 to -80mV from I-V plot. **C_1 and C_2:** Voltage pulses to hyperpolarizing current steps (-0.09nA; 400ms), rmp=-75mV and -78mV for C_1 and C_2 respectively. Each of these pulses could be fit by a single exponential using pClamp fitting program.

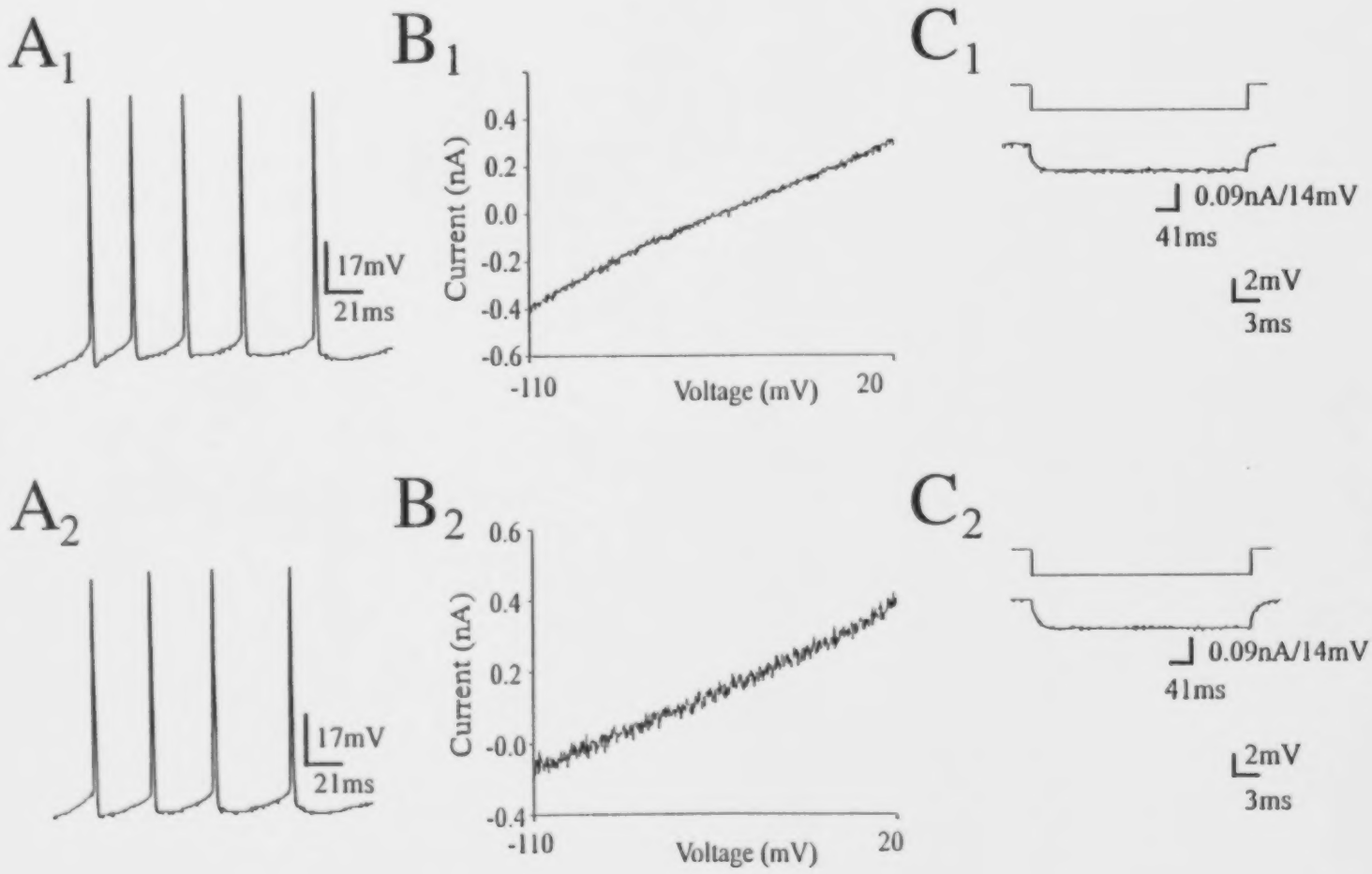
A1
17mV
21ms
B1
Current (nA)
0.4
0.2
0.0
-0.2
-0.4
-0.6
-110
Voltage (mV)
20
C1
0.09nA/14mV
41ms
2mV
3ms
A2
17mV
21ms
B2
Current (nA)
0.6
0.4
0.2
-0.0
-0.4
-110
Voltage (mV)
20
C2
0.09nA/14mV
41ms
2mV
3ms

Figure 3-3. AMPA receptors mediate excitatory neurotransmission in hDBB. A: Currents generated by voltage ramps under control conditions, in the presence of 5μM AMPA, and in the presence of 5μM AMPA + 1μM NBQX. By extrapolation, the AMPA induced current reverses at approximately 0mV. Inset shows net current in the presence of AMPA and AMPA+NBQX. **B:** EPSC is attenuated by 1μM NBQX with partial recovery (V_h=-80mV).

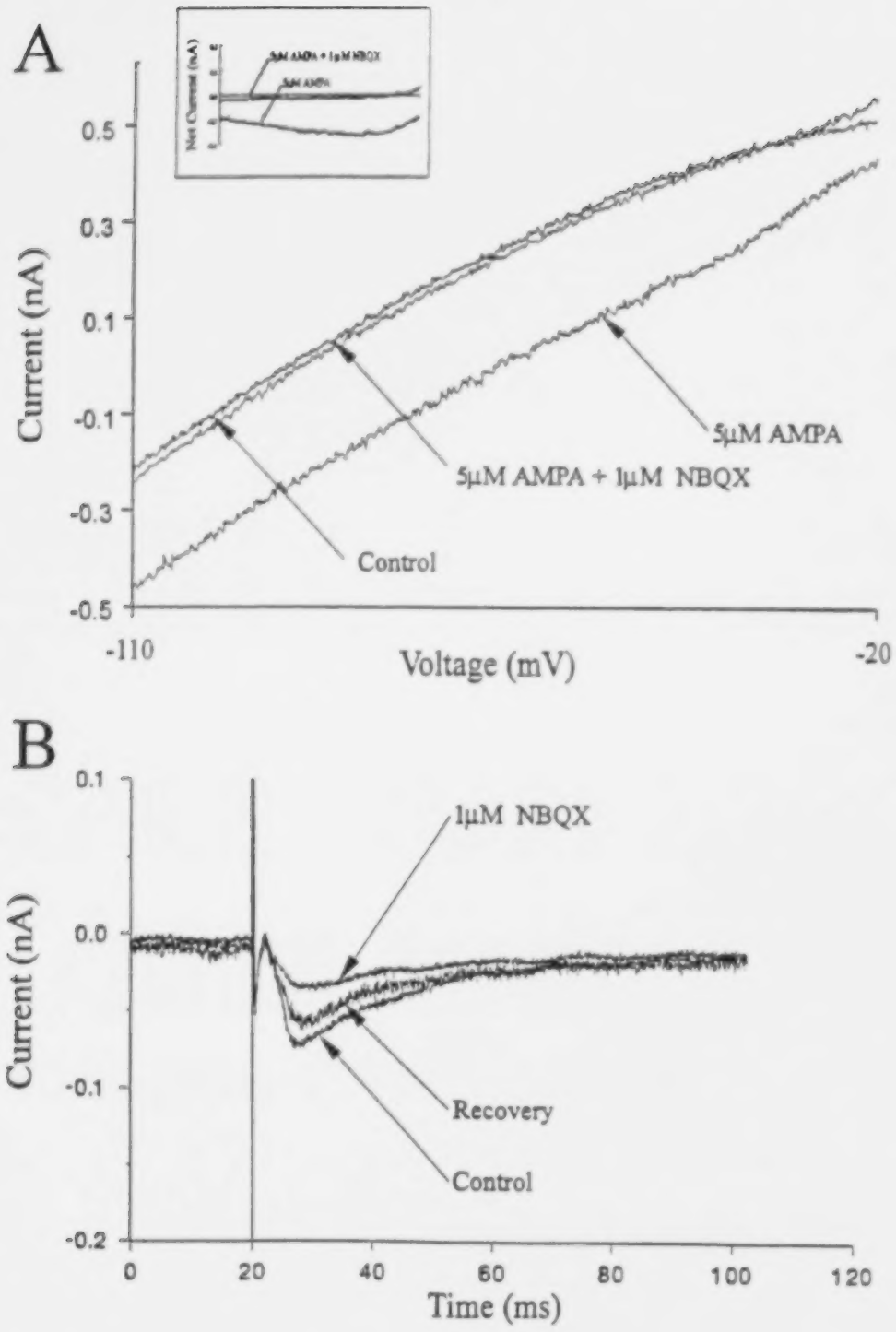
A
Current (nA)
0.5
0.3
0.1
-0.1
-0.3
-0.5
-110
-20
Voltage (mV)
5μM AMPA
5μM AMPA + 1μM NBQX
Control
B
Current (nA)
0.1
0.0
-0.1
-0.2
1μM NBQX
Recovery
Control
0
20
40
60
80
100
120
Time (ms)

Figure 3-4. Kainate receptors mediate excitatory neurotransmission in hDBB. A: Currents generated by voltage ramps under control conditions, in the presence of 5μM kainate (KA), and in the presence of 5μM KA + 1μM CNQX. By extrapolation, the KA induced current reverses at approximately 0mV. Inset shows net current in the presence of KA and KA+CNQX. **B:** EPSC is attenuated by 1μM CNQX with recovery (V_h=-75mV).

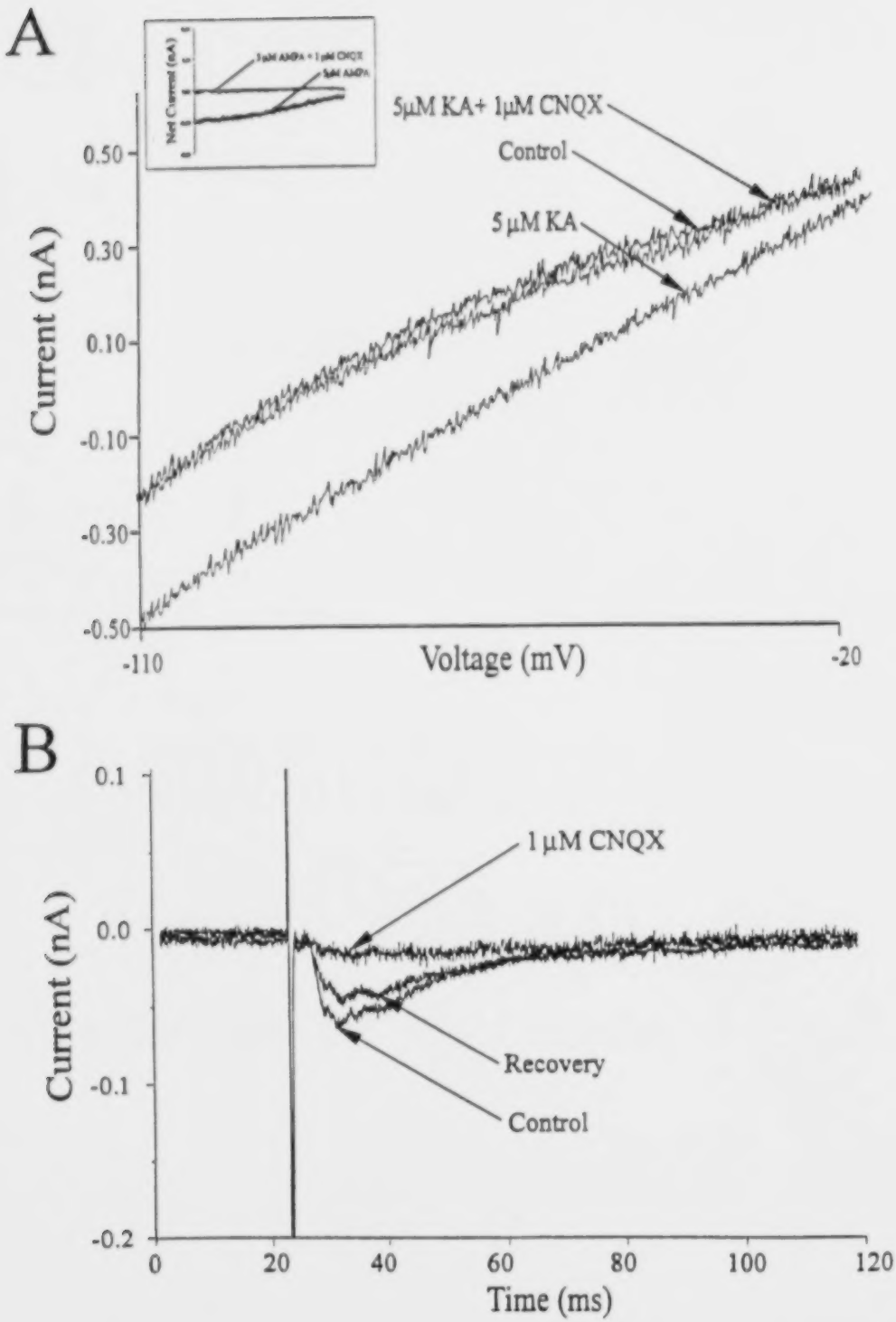
A
5μM KA+ 1μM CNQX
Control
5 μM KA
Current (nA)
0.50
0.30
0.10
-0.10
-0.30
-0.50
-110
Voltage (mV)
-20
B
1 μM CNQX
Recovery
Control
Current (nA)
0.1
0.0
-0.1
-0.2
0
20
40
60
80
100
120
Time (ms)

Figure 3-5. NMDA receptor involvement in excitatory neurotransmission in hDBB. These data are from three separate cells. **A:** Currents generated by voltage ramps in 0 Mg^{++} ACSF. 15μM NMDA induces an inward current that reverses at approximately 0mV and is attenuated by application of 60μM APV. Inset shows net current in the presence of NMDA and NMDA+APV. **B:** Late component of the EPSC is attenuated by 60μM APV. Application of 1μM NBQX further attenuates the EPSC indicating that this synaptic current is mediated by the activation of multiple glutamate receptor subtypes. Cell is perfused in normal ACSF (1.2mM Mg^{++}) (V_h=-78mV). **C:** In 0 Mg^{++} ACSF, the EPSC is over 80% longer in duration compared to B. 60μM APV attenuates the larger late component of the EPSC. Application of 1μM NBQX with 60μM APV completely attenuates EPSC. The small upward deflection at the onset of the NBQX +APV trace is a part of the stimulus transient (V_h=-75mV).

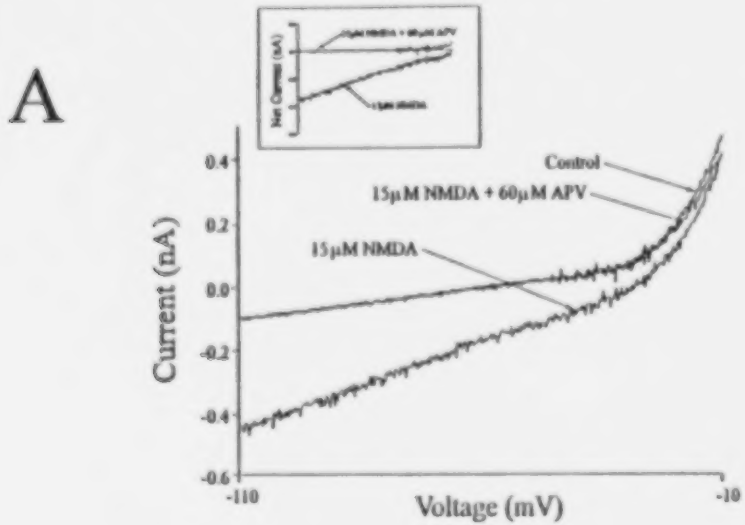
A
Control
15μM NMDA + 60μM APV
15μM NMDA
Current (nA)
Voltage (mV)
0.4
0.2
0.0
-0.2
-0.4
-0.6
-110
-10

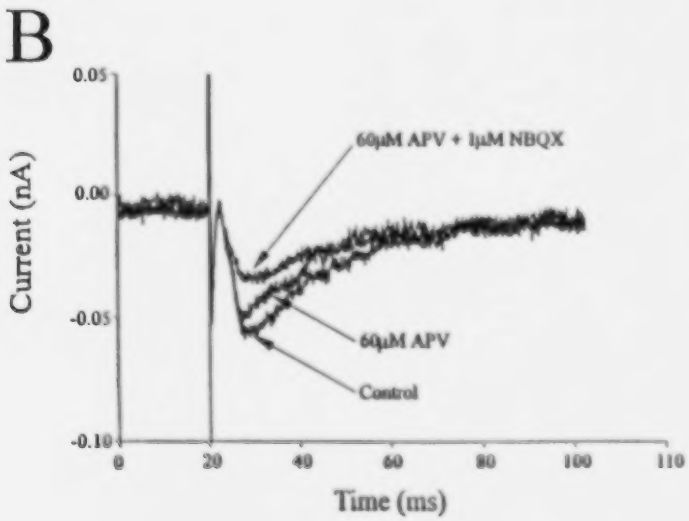
B
60μM APV + 1μM NBQX
60μM APV
Control
Current (nA)
Time (ms)
0.05
0.00
-0.05
-0.10
0
20
40
60
80
100
110

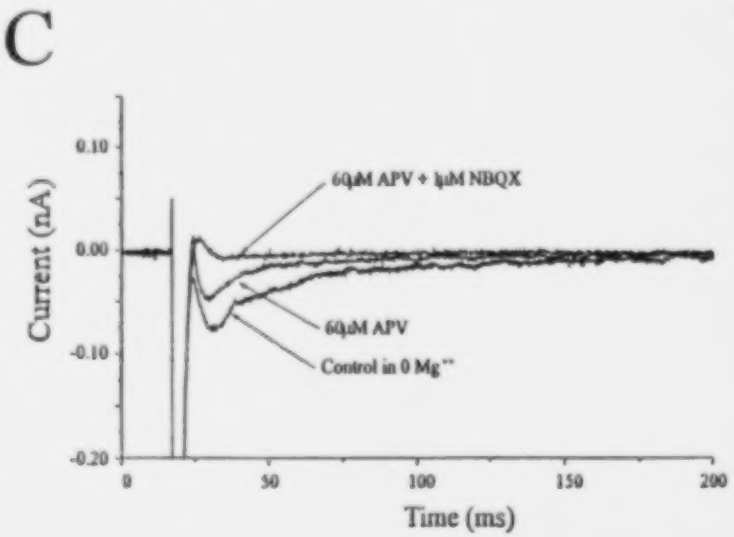
C
60μM APV + 1μM NBQX
60μM APV
Control in 0 Mg++
Current (nA)
Time (ms)
0.10
0.00
-0.10
-0.20
0
50
100
150
200

Figure 3-6. Metabotropic receptor involvement in excitatory neurotransmission in hDBB. **A:** Currents generated by voltage ramps under control conditions, in the presence of 10μM trans-ACPD, and in the presence of 10μM trans-ACPD + 200μM AP3. The trans-ACPD induced current reverses at approximately -35mV. Inset shows net current in the presence of trans-ACPD and trans-ACPD + AP3. **B:** 10μM trans-ACPD did not evoke postsynaptic changes in input G_i in 13 of 22 neurons. Inset shows net current in the presence of trans-ACPD.

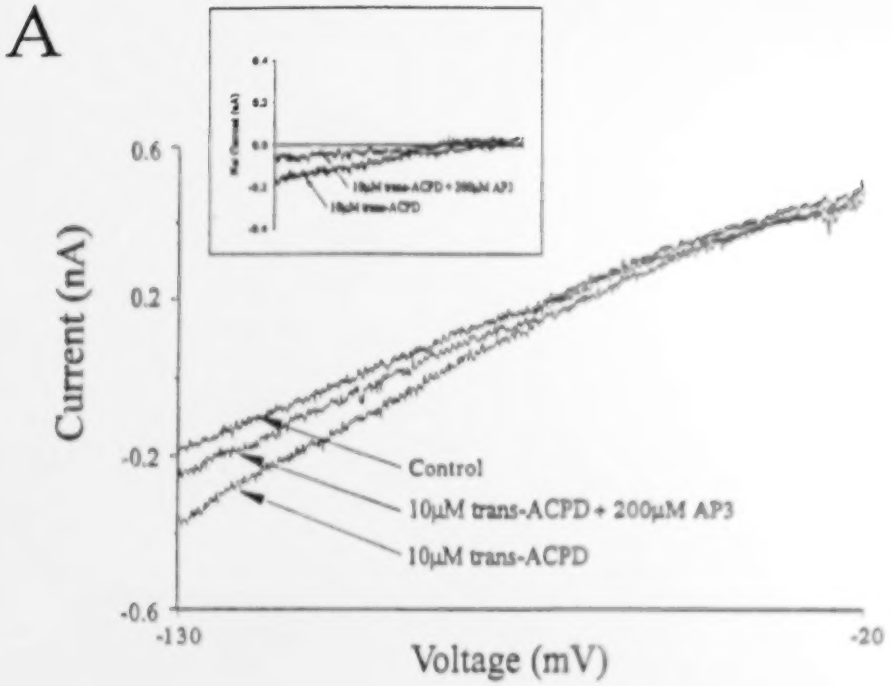
A
0.6
0.2
-0.2
-0.6
Current (nA)
-130
-20
Voltage (mV)
Control
10μM trans-ACPD + 200μM AP3
10μM trans-ACPD

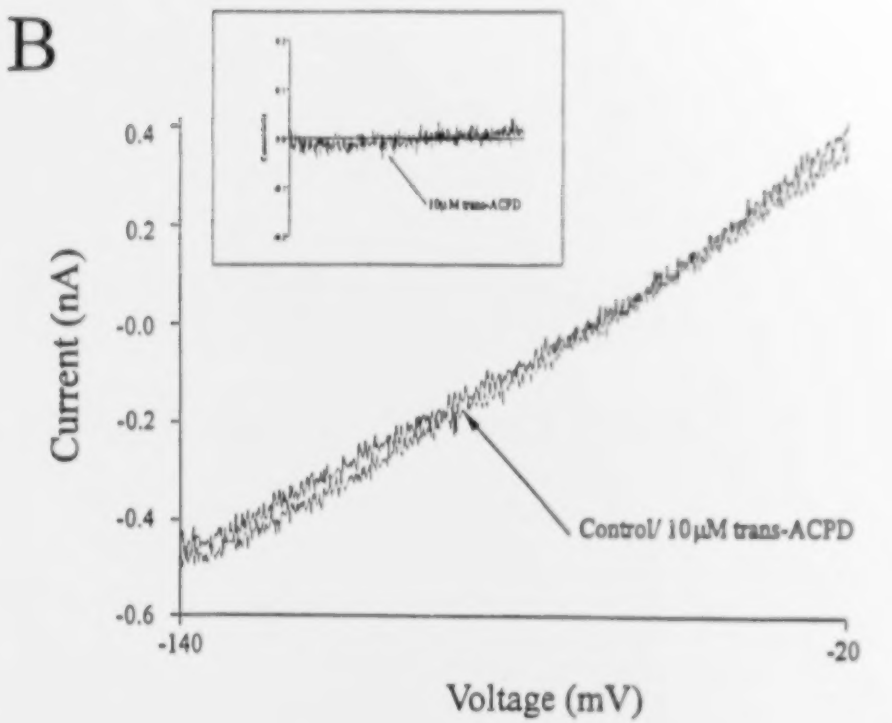
B
0.4
0.2
-0.0
-0.2
-0.4
-0.6
Current (nA)
-140
-20
Voltage (mV)
Control/ 10μM trans-ACPD

Figure 3-7. Presynaptic modulation of excitatory neurotransmission by metabotropic receptors. A: In the same cell, there is no net change in current in the presence of 10μM trans-ACPD, thus, no change in postsynaptic G_t. Inset shows currents generated by voltage ramps under control conditions and in the presence of 10μM trans-ACPD. **B:** EPSC is attenuated by 10μM trans-ACPD with a complete recovery.

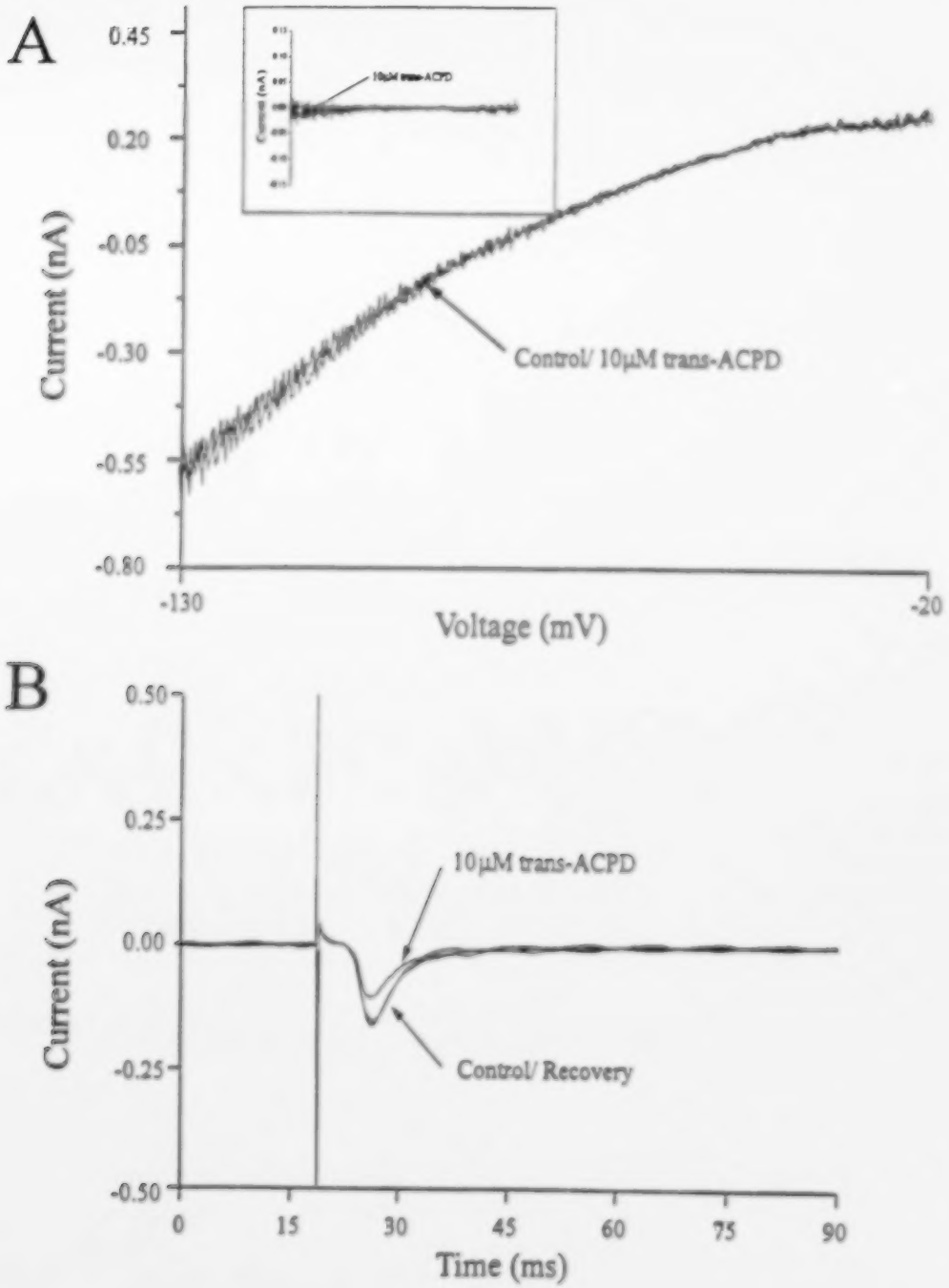
A
0.45
0.20
-0.05
-0.30
-0.55
-0.80
Current (nA)
-130
-20
Voltage (mV)
Control/ 10μM trans-ACPD
B
0.50
0.25
0.00
-0.25
-0.50
Current (nA)
10μM trans-ACPD
Control/ Recovery
0
15
30
45
60
75
90
Time (ms)

Figure 3-8. trans-ACPD does not modulate postsynaptic AMPA responses. A: Current generated by voltage ramps. The first ramp is a control, the second ramp is in the presence of 10μM AMPA, the third ramp is in the presence of 10μM AMPA+10μM trans-ACPD, and the final ramp is a recovery. **B:** No change in G_t is observed when the cell is superfused with AMPA alone and AMPA + trans-ACPD thus suggesting that trans-ACPD is not exerting an effect at postsynaptic AMPA receptors.

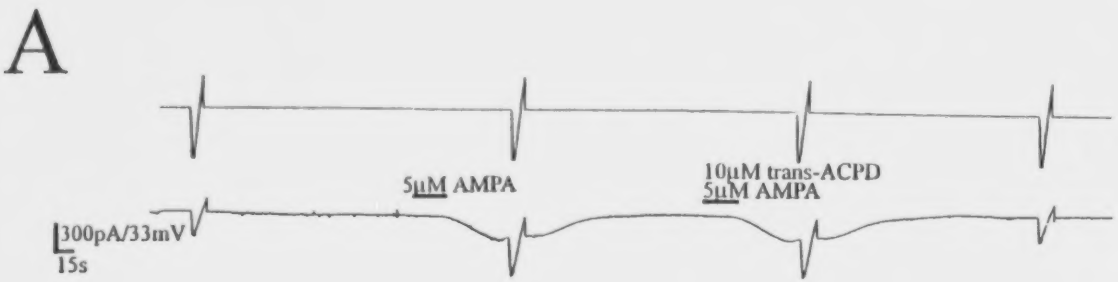
A
5μM AMPA
10μM trans-ACPD
5μM AMPA
300pA/33mV
15s

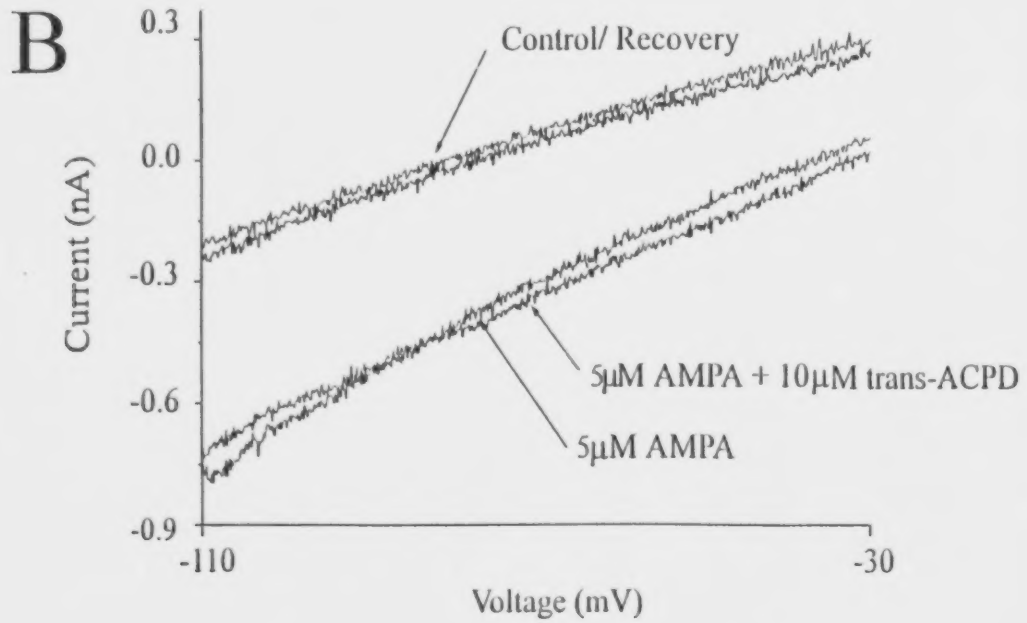
B
0.3
0.0
-0.3
-0.6
-0.9
Current (nA)
Control/ Recovery
5μM AMPA + 10μM trans-ACPD
5μM AMPA
-110
-30
Voltage (mV)

Figure 3-9. trans-ACPD does not modulate postsynaptic NMDA responses. A: Current generated by voltage ramps. The first ramp is a control, the second ramp is in the presence of 15μM NMDA, the third ramp is in the presence of 15μM NMDA+10μM trans-ACPD, and the final ramp is a recovery. All experiments performed in 0 Mg^{++}. **B:** No change in G_i is observed when the cell is superfused with NMDA alone and NMDA + trans-ACPD thus suggesting that trans-ACPD is not exerting an effect at postsynaptic NMDA receptors.

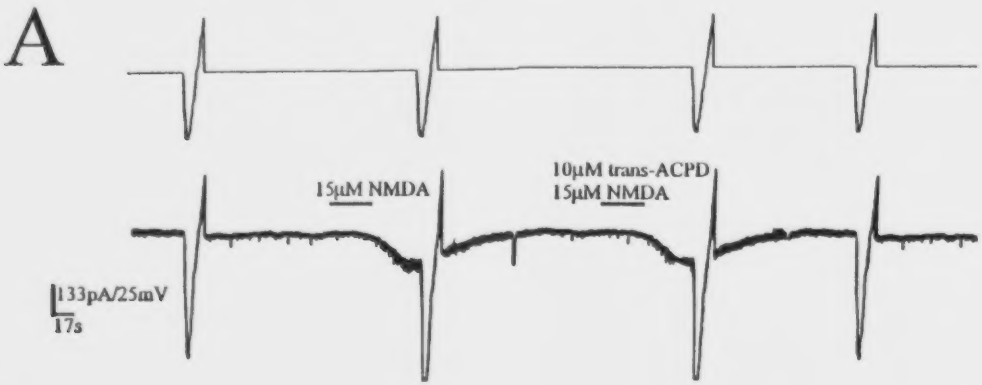
A
15μM NMDA
10μM trans-ACPD
15μM NMDA
133pA/25mV
17s

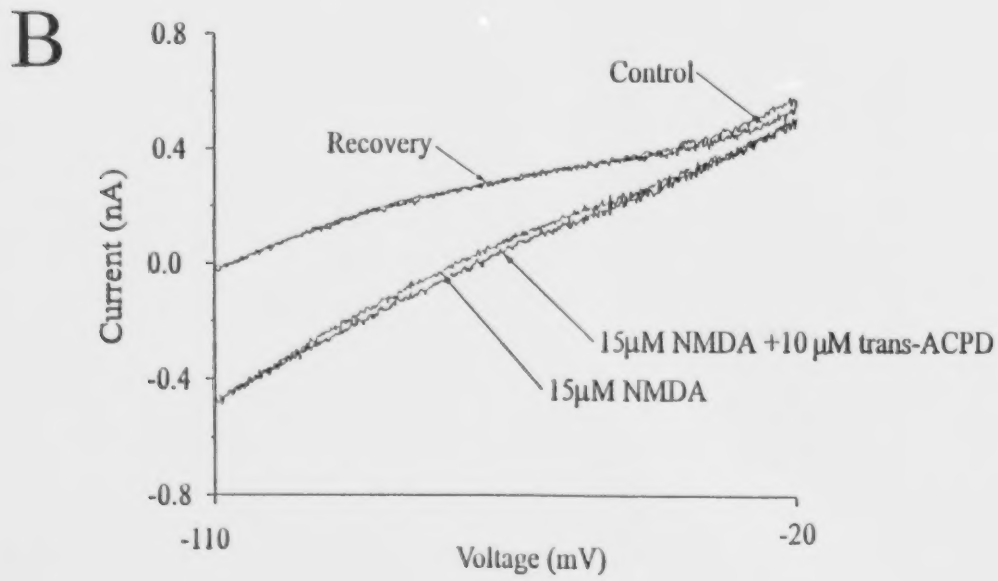
B
0.8
0.4
0.0
-0.4
-0.8
Current (nA)
Control
Recovery
15μM NMDA +10 μM trans-ACPD
15μM NMDA
-110
-20
Voltage (mV)

REFERENCES

Barrenechia, C., M. Pedemonte, A. Nunez, and E. Garcia-Austt. *In vivo* intracellular recordings of medial septal and diagonal band of Broca neurons: relationships with theta rhythm. *Exp. Br. Res.* 103: 31-40, 1995.

Baskys, A. and R.C. Malenka. Agonists at metabotropic glutamate receptors presynaptically inhibit EPSC's in neonatal rat hippocampus. *J. Physiol.* 444: 687-701 1991.

Carnes, K. M., T.A. Fuller and J.L. Price. Sources of presumptive glutamatergic/aspartatergic afferents to the magnocellular basal forebrain in the rat. *J. Comp.Neurol.* 302: 824-852, 1990.

Coleman, P. A. and R.F. Miller. Measurement of passive membrane parameters with whole-cell recording from neurons in the intact amphibian retina. *J. Neurophysiol.* 61(1): 218-230, 1989.

Cunningham, J. T., R. Nissen, and L.P. Renaud. Injections of norepinephrine (NE) in the diagonal band of Broca (DBB) attenuate the activity of rat supraoptic (SON) vasopressin neurons. *Soc. Neurosci. Abstr.* 17: 1189, 1993.

Easaw, J.C. and J.H. Jhamandas. Presynaptic modulation of glutamatergic neurotransmission by $GABA_B$ and metabotropic receptors in the horizontal limb of the diagonal band of Broca (hDBB) *in vitro*. *Soc. Neurosci. Abstr.* 20: 1119, 1994.

Griffith, W.H. and R.T. Mathews. Electrophysiology of AchE-positive neurons in basal forebrain slices. *Neurosci. Lett.* 71 (2): 169-74, 1986.

Griffith, W. H. Membrane properties of cell types within guinea pig basal forebrain nuclei *in vitro*. *J. Neurophysiol.* 59(5): 1590-1610, 1988.

Jhamandas, J.H. and L.P. Renaud. A GABA-mediated baroreceptor input to supraoptic vasopressin neurones in the rat. *J. Physiol.* 381: 595-606, 1986a.

Jhamandas, J.H. and L.P. Renaud. Diagonal band neurons may mediate arterial baroreceptor input to hypothalamic vasopressin-secreting neurons. *Neurosci.Lett.*65:214-218, 1986b.

Lacaille, J-C. and S. Williams. Membrane properties of interneurons in stratum oriens-alveus of the CA1 region of rat hippocampus *in vitro*. *Neurosci.* 36(2):349-359,1990.

Manzoni, O.J., F. Finiels-Marlier, I. Sassetti, J. Blockaert, C. la Peuch, and F.A. Saldeczek. The glutamate receptor of the Qp-type activates protein kinase C and is regulated by protein kinase C. *Neurosci. Lett.* 109(1-2): 146-151, 1990.

Mathews, R.T. and W.L. Lee. A comparison of extracellular and intracellular recordings from medial septum/diagonal band neurons *in vitro*. *Neurosci.* 42(2): 451-462, 1991.

Pongracz, F., S. Firestein, and G.M. Shepherd. Electrotonic structure of olfactory sensory neurons analyzed by intracellular and whole cell patch clamp techniques. *J. Neurophysiol.* 65(3): 747-758, 1991.

Rall, W. Time constants and electrotonic length of membrane cylinder and neurons. *Biophys J.* 9: 1483-1508, 1969.

Sheardown, M.J. Metabotropic glutamate receptor agonists reduce epileptiform activity

in the rat cortex. *Neuroreport* 3(10): 916-918, 1992.

Tanaka, E., H. Higashi, and S. Nishi. Membrane properties of guinea pig cingulate cortical neurons *in vitro*. *J. Neurophysiol.* 65(4): 808-821, 1991.

Taube, J.S. Electrophysiological properties of neurons in the rat subiculum *in vitro*. *Exp. Brain Res.* 96: 304-318, 1993.

CHAPTER 4

INHIBITORY INPUTS ONTO NEURONS IN THE HORIZONTAL LIMB OF THE DIAGONAL BAND OF BROCA

ABSTRACT

In the previous chapter, we characterized a pronounced glutamatergic excitatory input onto hDBB neurons. In many neuronal systems, it is known that excitatory input is often balanced by a concomitant inhibitory input. In this study, we endeavored to identify and characterize an inhibitory input onto these neurons. Since GABA is the most common inhibitory neurotransmitter within the CNS, we investigated the role of this neurotransmitter in inhibitory neurotransmission within the hDBB. Our results indicate that $GABA_A$ and $GABA_B$ receptors but not $GABA_C$ receptors are present on these cells. Exogenous application of 10μM muscimol, the $GABA_A$ agonist, elicits a decrease in postsynaptic input resistance with a reversal potential, which is consistent with an underlying chloride conductance. Furthermore, inhibitory postsynaptic potentials (IPSPs) can be blocked by 10μM bicuculline, the $GABA_A$ antagonist. Application of 10μM baclofen, the $GABA_B$ agonist elicited a postsynaptic response, however, its more common effect was to presynaptically inhibit glutamate-mediated excitatory postsynaptic currents (EPSCs). We also observed that activation of both presynaptic $GABA_B$ and metabotropic receptors act synergistically to reduce EPSC amplitude. Overall, our results suggest the presence of a multi-layered inhibitory system in this region with the presence of $GABA_A$ and to a lesser extent, $GABA_B$ receptors postsynaptically. $GABA_B$ and metabotropic receptors are also present on presynaptic terminals where they serve to inhibit glutamate release.

INTRODUCTION

In the course of our study of excitatory amino acid transmission within the hDBB, inhibitory postsynaptic currents and potentials (IPSC/IPSP) were also observed. We attempted to characterize the chemical identity of the neurotransmitter mediating this inhibitory input. GABA, which is the principal inhibitory neurotransmitter within the CNS (Krnjevic, 1974), is localized in fibers within the hDBB (Pare and Smith, 1994; Toth et al., 1993). Furthermore, *in situ* studies indicate that mRNA for specific GABA receptor subunits are also present in this region. Therefore, we hypothesized that GABA may mediate inhibitory synaptic events within the hDBB.

In the preceding chapter, we identified a prominent excitatory input to hDBB neurons using an *in vitro* rat DBB slice preparation. Systems where such excitatory influences impinge on neurons often possess an equivalent inhibitory mechanism as a means of balancing the excitatory input (Moore, 1993). In certain pathological conditions, the absence of inhibition can result in neuropathological disorders, as in AD. AD is characterized by the presence of neurofibrillary tangles, amyloid plaques, and by pronounced loss of cholinergic cells in the BF. The hDBB is amongst the regions most severely affected in this disease. It has been postulated that cholinergic neurons in the BF may be selectively prone to excitotoxic insult which may arise consequent to a loss of inhibitory inputs (Sasaki et al, 1986; Krogsgaard-Larsen, 1992). This is corroborated by NMR studies which indicate 60-70% decreases in GABA receptors (Young, 1987) and concomitant decreases in GABA levels (Mohanakrishnan et al., 1995; Klunk et al., 1992) within the brains of patients with AD. In light of these observations, inhibitory

inputs may meditate essential roles in the normal physiological function of the hDBB and the loss of these inputs may result in the onset of certain pathological conditions.

GABA exerts its effects via three pharmacologically distinct receptor subtypes: ionotropic $GABA_A$ and $GABA_C$ receptors present at the postsynaptic level and G-protein coupled $GABA_B$ receptors which exert effects both pre- and postsynaptically. We identified the role of each of these receptor subtypes in inhibitory neurotransmission within the hDBB using whole cell patch clamp recordings from cells in a forebrain slice preparation.

RESULTS

GABA-mediated postsynaptic and presynaptic inhibition of hDBB neurons were investigated in this study. Analysis of the passive and active electrophysiological properties of 41 hDBB neurons examined in this study reveal an average rmp of -71±9mV, an G_i of 3.21±0.06nS, AP height of 80.01±2.4mV, width of 1.87±0.08ms, and AHP duration of 46.30±3.05ms. These parameters are consistent with those reported for cells studied in Chapter 3.

I. Postsynaptic Actions of GABA

A. $GABA_A$ Receptors

Fig. 4-1A shows the current evoked by a voltage ramp from -130 to -10mV (9.2mV/sec) from a representative hDBB neuron under control conditions and the presence of the $GABA_A$ agonist, muscimol (10μM)(inset in Fig. 4-1A). Muscimol elicited an increase in G_i which reversed near -73mV which coincides with the Nernstian

reversal potential for chloride in these cells (E_{Cl}=-75mV). This response was observed in 12 cells with an average reversal potential of -74±2mV. Subsequent applications of muscimol were equally effective and desensitization was not observed in any of the cells perfused with muscimol.

IPSCs and IPSPs were elicited by passing current through bipolar stimulating electrodes placed adjacent to the recording site. Fig. 4-1B shows an IPSP recorded from an hDBB cell which reversed at -75mV. The average IPSP reversal potential of 6 cells was -74±4mV suggesting that these responses are likely mediated by a chloride conductance. As indicated in Fig. 4-1C, IPSPs could be attenuated by application of 10μM bicuculline, a $GABA_A$ receptor antagonist (average blockade: 91%; 10/10 cells). In some cases, application of bicuculline unmasked slow EPSPs (3/10 cells)(Fig. 4-1C). These results indicate the presence of a Cl^--mediated, bicuculline-sensitive IPSP in hDBB neurons. The $GABA_A$ receptor-mediated response may blunt postsynaptic excitatory responses.

B. $GABA_B$ Receptors

$GABA_B$ receptors are G-protein coupled and are known to attenuate Ca^{++} currents in some neuronal systems (Huston et al., 1995) and increase K^+ currents in others (Jiang et al., 1995). Fig. 4-2A shows the current generated by a voltage ramp from -130 to -20mV in a representative hDBB neuron. In 5/32 cells, the $GABA_B$ agonist, baclofen (10μM) increased postsynaptic G_i compared to the control. This increased G_i reversed at approximately -93mV which is close to the reversal potential of K^+ in hDBB cells (E_K=-99mV). Furthermore, none of the IPSPs examined in this study could be

modulated by 10 μM CGP-35348, a $GABA_B$ receptor antagonist (0/10 cells).

C. $GABA_C$

Similar to the $GABA_A$ channel, $GABA_C$ is an ionotropic channel which conducts Cl^-. Pharmacologically, $GABA_C$ receptors are activated by cis-4-aminocrotonic acid (CACA) and are relatively insensitive to blockade by bicuculline (Feigenspan and Bormann, 1994). As indicated in Fig. 4-2B, application of 100μM CACA on hDBB cells had no effect, suggesting that $GABA_C$ channels are not be present on postsynaptic membranes of hDBB cells (0/19 cells).

II. Presynaptic Inhibition

$GABA_B$ Receptors

While activation of postsynaptic $GABA_B$ receptors elicited only modest postsynaptic responses, activation of these receptors was more commonly observed to presynaptically inhibit synaptic transmission. However, the presynaptic actions of $GABA_B$ receptors appear to be directed exclusively towards excitatory neurotransmission (17/27) with no effect on $GABA_A$-mediated IPSPs (0/10 cells). Fig. 4-3A and 4-3B show that perfusion of 10μM baclofen had no effect on the postsynaptic G_i, yet, reversibly attenuated the amplitude of EPSCs. This response was observed in 17 neurons with an average decrease of 67% in the peak synaptic current (range 21-100%). The observation that EPSC amplitude can be reduced with no concomitant change in postsynaptic G_i suggests that baclofen may exert its action via a presynaptic mechanism. We subsequently attempted to characterize the chemical identity of the neurotransmitter underlying the baclofen-sensitive EPSC. Exogenous perfusion of baclofen reduced

EPSC amplitude (Fig. 4-3D) but had no effect on G_i (Fig. 4-3C). After the cell had recovered, 1μM NBQX, the AMPA/kainate receptor antagonist, was able to completely block the EPSC (Fig. 4-3D; 6/6 cells; mean: 74%; range: 34-100%). This observation demonstrates that baclofen presynaptically modulates glutamate-mediated EPSCs in hDBB neurons.

In some hDBB neurons, $GABA_A$ and $GABA_B$ receptors are clearly differentially distributed. As illustrated in Fig. 4-4A and 4-4B, exogenous perfusion of 10μM baclofen reversibly decreased EPSC amplitude with no effect on postsynaptic G_i. After recovery of this response, application of 10μM muscimol reversibly increased postsynaptic G_i indicating that $GABA_A$ receptors are localized on postsynaptic membranes (Fig. 4-4C; n=5). These results support the dual participation of $GABA_A$ and $GABA_B$ receptors in direct (postsynaptic) and indirect (presynaptic) inhibition of hDBB neurons respectively.

Glutamate release can also be attenuated presynaptically by activation of metabotropic glutamate receptors (mGluR). Previously, we had observed that 10μM trans-ACPD (TA), an mGluR agonist, reduced EPSC amplitude without altering postsynaptic G_i in the hDBB (Fig. 3-7). Since EPSC amplitude can also be decreased by activation of presynaptic $GABA_B$ receptors, we examined whether both mGluR and $GABA_B$ receptors could modulate the same EPSC. Fig. 4-5A and 4-5B show data from a representative neuron where exogenous application of 10μM baclofen reduced EPSC amplitude by 58% with no change in postsynaptic G_i. In the presence of baclofen, TA was subsequently applied. The mGluR agonist elicited no postsynaptic effect (Fig. 4-5A), but it further reduced the amplitude of the EPSC by 25% (Fig. 4-5B). After the cell

had recovered, NBQX was applied and completely eliminated the EPSC thus confirming glutamate as the transmitter underlying this synaptic response. This additive effect was observed in 5 hDBB cells where the average blockade exerted by baclofen was 55% (range: 44-63%) and the average TA-mediated blockade in the presence of baclofen was 23% (range: 12-34%). The data from these occlusion studies reveal that EPSCs can be modulated presynaptically by both GABA and glutamate receptor subtypes.

In some hDBB neurons, we did not observe the EPSC modulation by both baclofen and TA. As shown in Fig. 4-6A_1 and 4-6A_2, application of 3μM NBQX attenuated EPSC amplitude confirming that the synaptic response under study is mediated by glutamate. In this same cell, applications of baclofen presynaptically reduced EPSC amplitude (Fig. 4-6B_1 and 4-6B_2) whereas TA had no effect on the synaptic current (Fig. 4-6C_1 and 4-6C_2; n=3). From these data, we conclude that the dual effects of mGluR and $GABA_B$ receptor activation are not present on all excitatory synaptic inputs to the hDBB.

DISCUSSION

Our results suggest the presence of well developed GABA-mediated inhibitory mechanisms within the hDBB. The activation of $GABA_A$ receptors provides postsynaptic inhibitory control of hDBB neurons. In contrast, while $GABA_B$ receptors evoke postsynaptic inhibitory responses in some cells, their primary role appears to be the presynaptic inhibition of glutamate release. Furthermore, our results provide evidence for a synergistic action of $GABA_B$ and mGluR receptors to presynaptically

attenuate excitatory synaptic currents in some neurons.

Interactions of GABA with glutamate

GABA and glutamate represent the most common inhibitory and excitatory neurotransmitters within the CNS, respectively. Our results indicate that the hDBB possesses a multi-layered inhibitory system designed to regulate the excitatory actions of glutamate. In addition to its already well-defined role as a potent and rapid inhibitor of cellular activity, our results demonstrate that postsynaptic $GABA_A$ receptors are capable of masking postsynaptic activation of glutamate receptors (Fig. 4-1C). This observation confirms the work by McCormick et al. (1993) who observed a similar phenomenon in neocortical neurons. Since the reversal potential of Cl^- lies within the average rmp range of the cells examined in this study, it is likely that activation of $GABA_A$ channels masks postsynaptic excitatory responses by shunting the inward current elicited by glutamate.

Although activation of $GABA_B$ receptors results in postsynaptic K^+-mediated inhibitory effects, we did not observe such a response frequently. However, $GABA_B$ receptors alone, or in combination with mGluR receptors represent a potent presynaptic inhibitory mechanism whereby glutamate release from presynaptic terminals is regulated. A recent study has identified presynaptic $GABA_B$ and mGluR modulation of GABA release in hippocampus (Jouvenceau et al., 1995), but to our knowledge, this is the first observation of a synergistic $GABA_B$ and mGluR regulation of glutamate release.

$GABA_C$ Receptors

$GABA_C$ receptors represent a pharmacologically distinct family of receptors

(Johnston, 1994). The principal agonist for this receptor, CACA, elicits a Cl^--mediated conductance in other cells which is insensitive to bicuculline. These receptors, however, appear to have a limited distribution within the CNS. Thus far, they have only been described in the retina and suprachiasmatic nucleus (O'Hara et al., 1995). We tested the possibility that $GABA_C$ receptors are present in the hDBB and found no evidence for this.

Sources of GABAergic inputs to the DBB

GABA-positive inputs have been shown to originate from the CA1 hippocampal region (Toth et al., 1993) and the intercalated masses of the ACE (Pare and Smith, 1994). In turn, hDBB neurons project to these same nuclei to suggest reciprocal linkages between these forebrain structures (Meibach and Siegel, 1977; Gaykema et al., 1990). Functionally, these connections may influence the hDBB's role in both mechanisms associated with memory and learning as well as central cardiovascular control.

Identity and physiological function of hDBB cells receiving GABAergic input

hDBB neurons comprise a heterogeneous population of cell types as identified by both immunocytochemical and electrophysiological studies. Detailed electrophysiological studies by Griffith (1988) and Markram and Segal (1990) characterized specific cell types within the DBB. The first cell type examined was identified as being AchE-positive and was characterized by a long duration AHP (~600ms). The second population of hDBB cells does not stain for AchE and likely represents the GABAergic cell type within the hDBB (Griffith, 1988). Electrophysiologically, this non-cholinergic cell population is primarily characterized by

a shorter AHP duration (5-50ms). Given that the cells examined in this study possess an AHP duration of approximately 46ms, it is possible that these cells represent the non-cholinergic cell population. However, anatomical studies are required to confirm the chemical identity of these cells.

Pathophysiological implications

The hDBB has also been implicated in pathophysiological disorders of memory such as AD. While most forms of AD are idiopathic, excitotoxic death has been postulated as a possible explanation for the neuronal degeneration of neurons in the basal forebrain (Scott et al., 1995; Smith-Swintosky and Mattson, 1994; Barger et al., 1993; Shaw, 1992). One possible explanation for the development of excitotoxicity is the loss of intrinsic inhibitory mechanisms which may normally serve to control over-excitation of neurons by glutamate (Mohanakrishnan et al., 1995; Sasaki et al., 1986; Young, 1987). In the present study, we have identified four possible sources of inhibition in these neurons, postsynaptic $GABA_A$ and $GABA_B$-receptor mediated inhibition, a presynaptic $GABA_B$-mediated attenuation of glutamate release, and a presynaptic metabotropic receptor-induced reduction of glutamate release. This inhibitory system may represent an intrinsic defence against excitotoxic actions of glutamate. It is postulated that the loss of any one of these inhibitory systems could result in aberrant neurotransmission leading to excitotoxicity.

Figure 4-1. $GABA_A$ receptor activation mediates inhibitory neurotransmission in the hDBB. A: Currents generated by voltage ramps from -120 to -10mV (inset) under control conditions and in the presence of 10μM muscimol, a $GABA_A$ receptor agonist. The muscimol induced response reversed at -73mV. (V_h=-69mV) **B:** Current clamp recordings of IPSP which reverses at -75mV, close to E_{Cl}. When the cell is depolarized to -59mV, the amplitude of the IPSP is large. Hyperpolarization of the cell to -83mV caused the IPSP to reverse. (rmp=-70mV). **C.** Current clamp recordings showing that IPSP is reversibly blocked by 10μM bicuculline, the $GABA_A$ receptor antagonist. Blockade of the IPSP "unmasks" a slow EPSP.(rmp=-65mV).

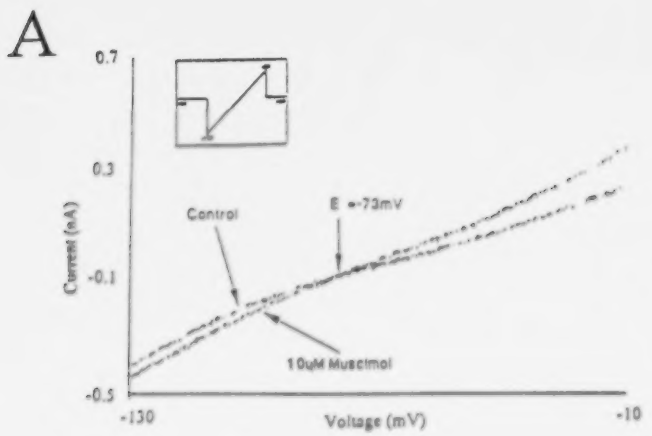
A
0.7
0.3
-0.1
-0.5
Current (nA)
Control
E =-73mV
10uM Muscimol
-130
Voltage (mV)
-10

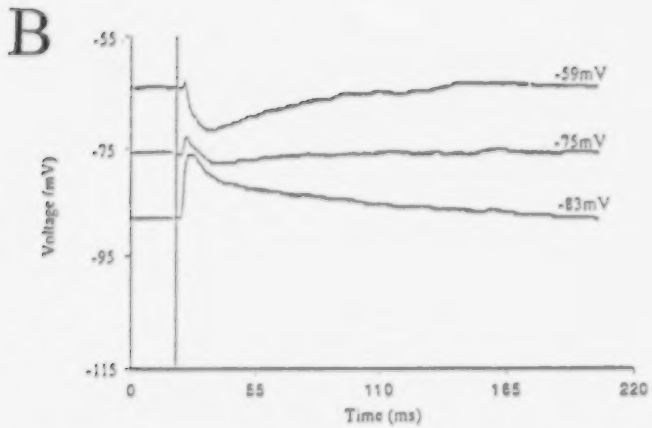
B
-55
-75
-95
-115
Voltage (mV)
-59mV
-75mV
-83mV
0
55
110
165
220
Time (ms)

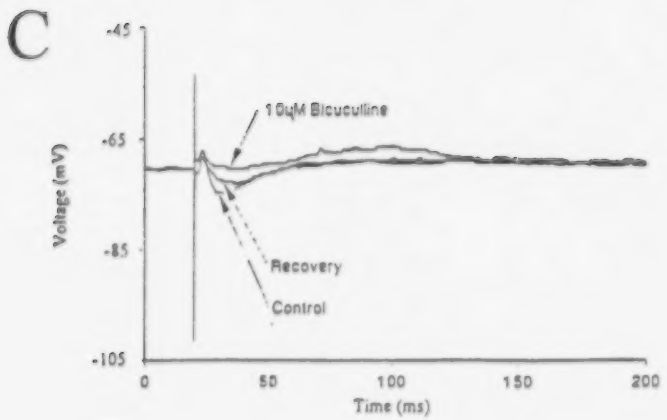
C
-45
-65
-85
-105
Voltage (mV)
10uM Bicuculline
Recovery
Control
0
50
100
150
200
Time (ms)

Figure 4-2. Postsynaptic responses mediated by activation of $GABA_B$ but not $GABA_C$ receptors. A. Currents generated by voltage ramps from -130 to -20mV in the presence and absence of 10μM baclofen, the $GABA_B$ receptor agonist. This response reversed at -90mV, close to E_K (V_h=-72mV). **B.** Currents generated by voltage ramps from -120 to -20mV in the presence and absence of 100μM CACA, the $GABA_C$ receptor agonist. The lack of response suggests that $GABA_C$ are not present on these cells (V_h=-73mV).

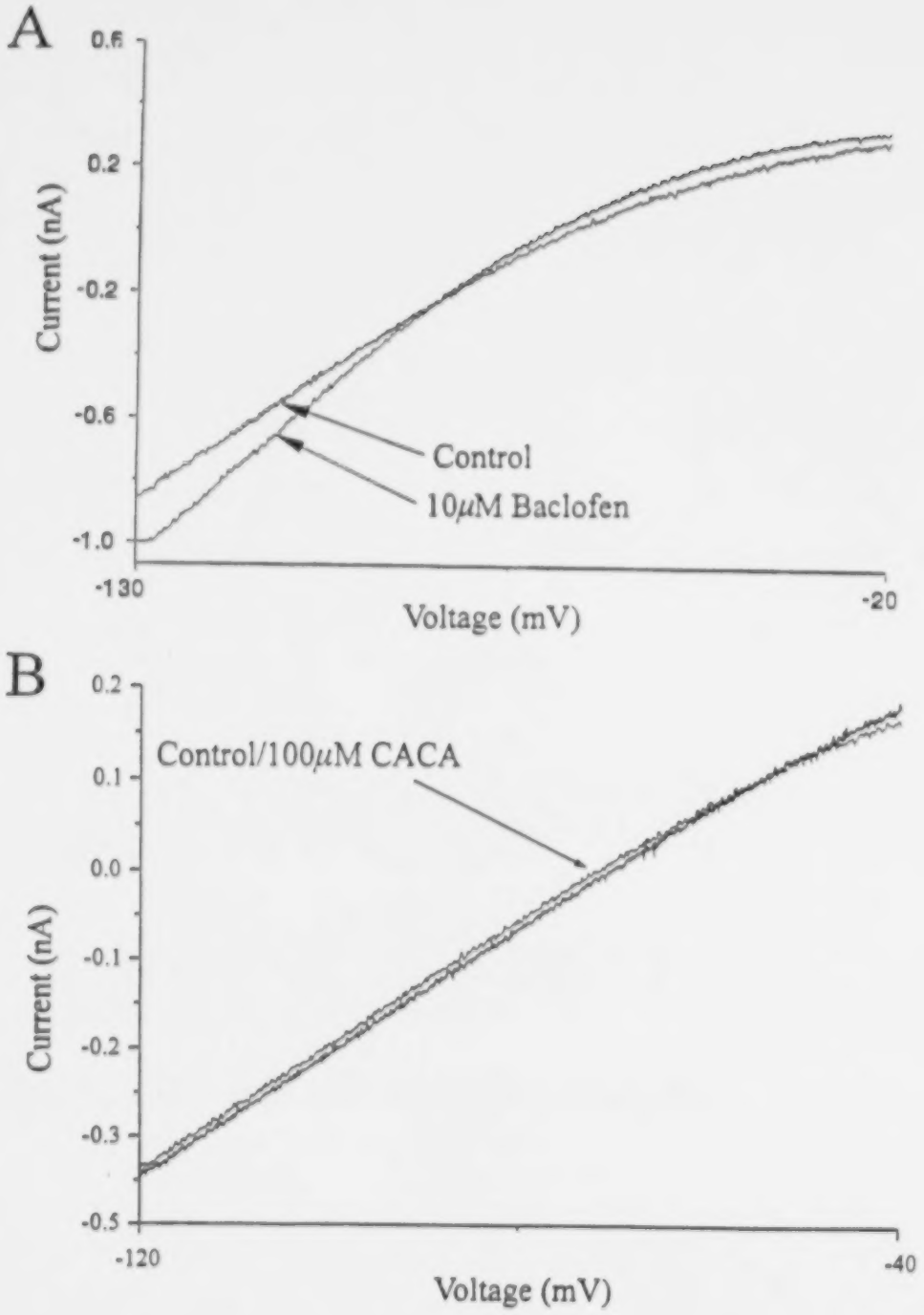
A
0.6
0.2
-0.2
-0.6
-1.0
Current (nA)
Control
10μM Baclofen
-130
-20
Voltage (mV)
B
0.2
0.1
0.0
-0.1
-0.2
-0.3
-0.5
Current (nA)
Control/100μM CACA
-120
-40
Voltage (mV)

Figure 4-3. Presynaptic blockade of glutamate-mediated EPSCs. A,B. Voltage ramps from -120 to -20mV in the presence and absence of 10μM baclofen failed to elicit a change in postsynaptic G_t. In the same cell, baclofen reversibly reduced the amplitude of the EPSC. These results suggest a presynaptic locus of action for baclofen (V_h=-71mV). **C, D.** In a different cell, voltage ramps from -120 to -20mV failed to elicit a change in postsynaptic G_t, however, in the same cell, baclofen reversibly attenuated the EPSC amplitude. After this response had recovered, application of 1μM NBQX reversibly eliminated the EPSC indicating that the EPSC is glutamatergic (V_h=-75mV).

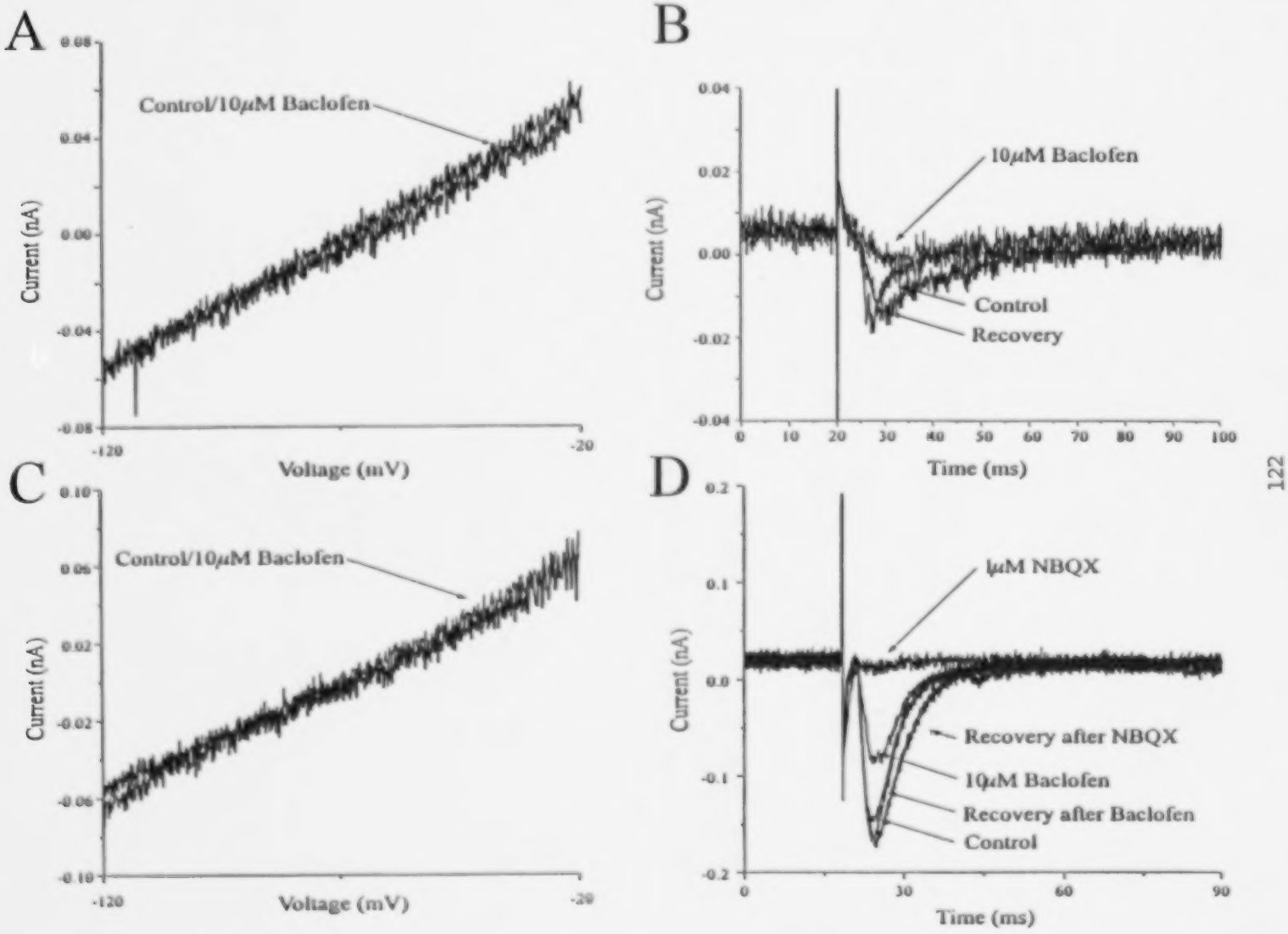
A
Control/10μM Baclofen
Current (nA)
Voltage (mV)
B
10μM Baclofen
Control
Recovery
Current (nA)
Time (ms)
C
Control/10μM Baclofen
Current (nA)
Voltage (mV)
D
1μM NBQX
Recovery after NBQX
10μM Baclofen
Recovery after Baclofen
Control
Current (nA)
Time (ms)

Figure 4-4. Differential distribution of $GABA_A$ and $GABA_B$ channels. A,B. 10μM baclofen reversibly reduced EPSC amplitude with no change on postsynaptic G_t indicating a presynaptic site of action for $GABA_B$ receptors (V_h=-69mV). **C.** In this same cell, application of 10μM muscimol elicited a postsynaptic change in G_t which reversed at -73mV, which is near E_{Cl}. This response indicates that $GABA_A$ receptors are present postsynaptically.

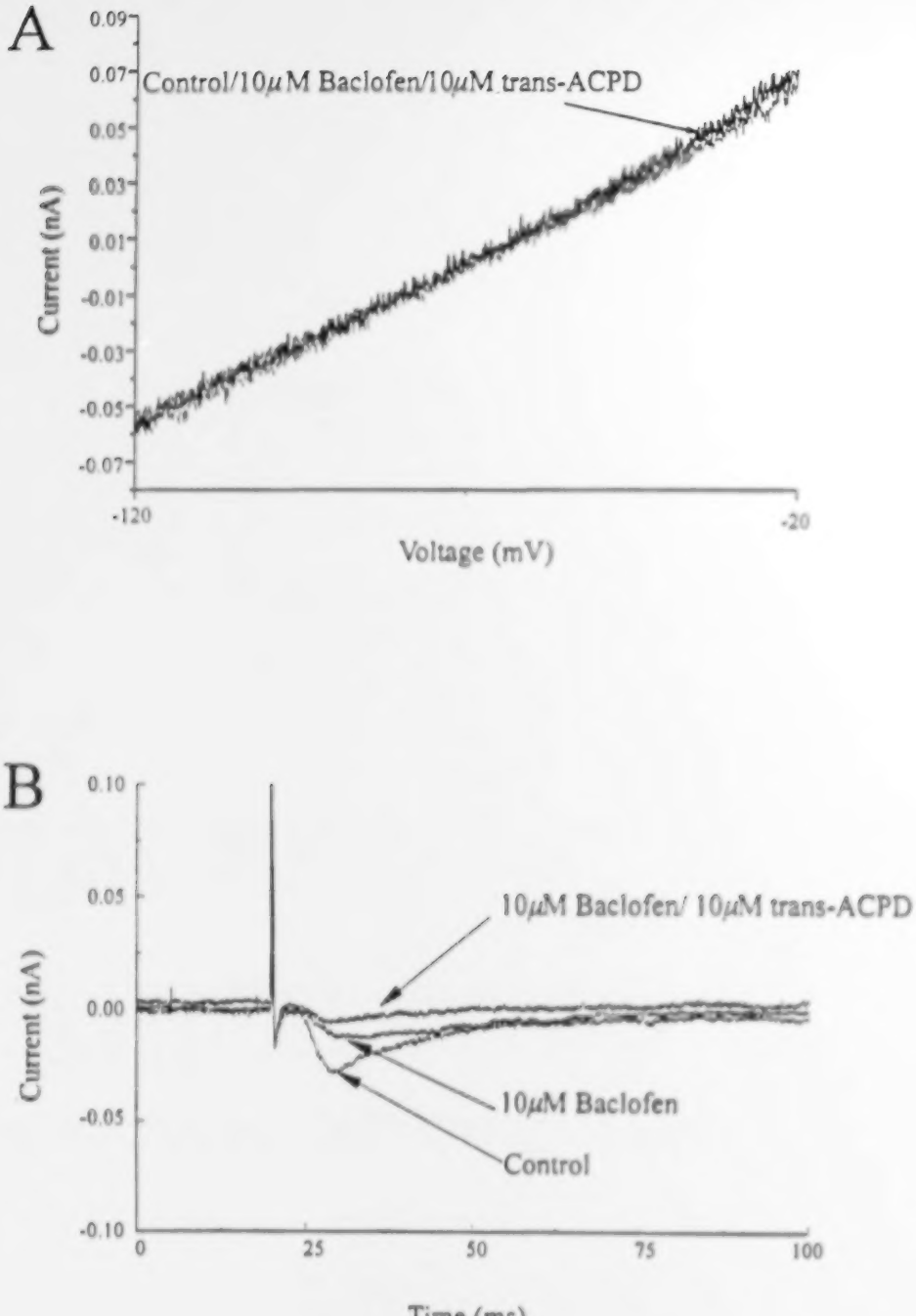
A
0.09
0.07
0.05
0.03
0.01
-0.01
-0.03
-0.05
-0.07
Current (nA)
Control/10μM Baclofen/10μM trans-ACPD
-120
-20
Voltage (mV)
B
0.10
0.05
0.00
-0.05
-0.10
Current (nA)
10μM Baclofen/ 10μM trans-ACPD
10μM Baclofen
Control
0
25
50
75
100
Time (ms)

Figure 4-5. Dual actions of presynaptic $GABA_B$ and mGluR receptors on EPSC. A,B. Perfusion of 10μM baclofen did not change postsynaptic G_o, however, it did reduce EPSC amplitude. In the presence of baclofen, 10μM TA was applied. TA failed to alter postsynaptic G_i but further reduced the amplitude of the EPSC (V_h=-72mV).

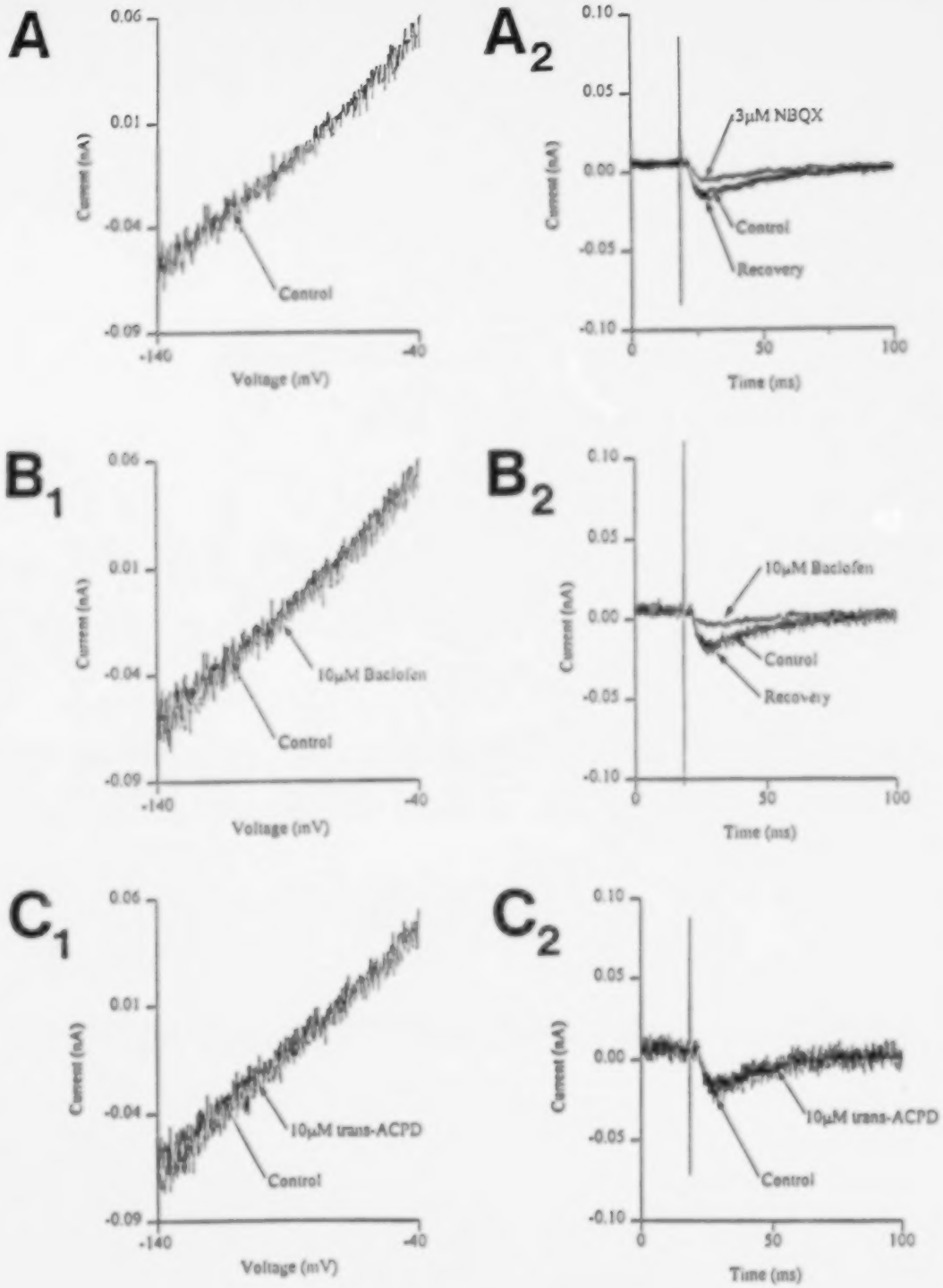
A
0.06
0.01
-0.04
-0.09
Current (nA)
Control
-140
-40
Voltage (mV)
A2
0.10
0.05
0.00
-0.05
-0.10
3μM NBQX
Control
Recovery
0
50
100
Time (ms)
B1
10μM Baclofen
Control
B2
C1
10μM trans-ACPD
C2

Figure 4-6. Lack of $GABA_B$ and mGluR receptor synergy in modulating excitatory synaptic responses. A_1A_2. Perfusion of 1μM NBQX reversibly attenuated EPSC amplitude. Voltage ramp performed on the cell was from -140 to -40mV. B_1B_2. In the same cell, 10μM baclofen elicited no postsynaptic change in G_i reduced EPSC amplitude. C_1C_2. In the same cell, 10μM TA had no effect on postsynaptic G_i nor did it reduce EPSC amplitude (V_h=-75mV).

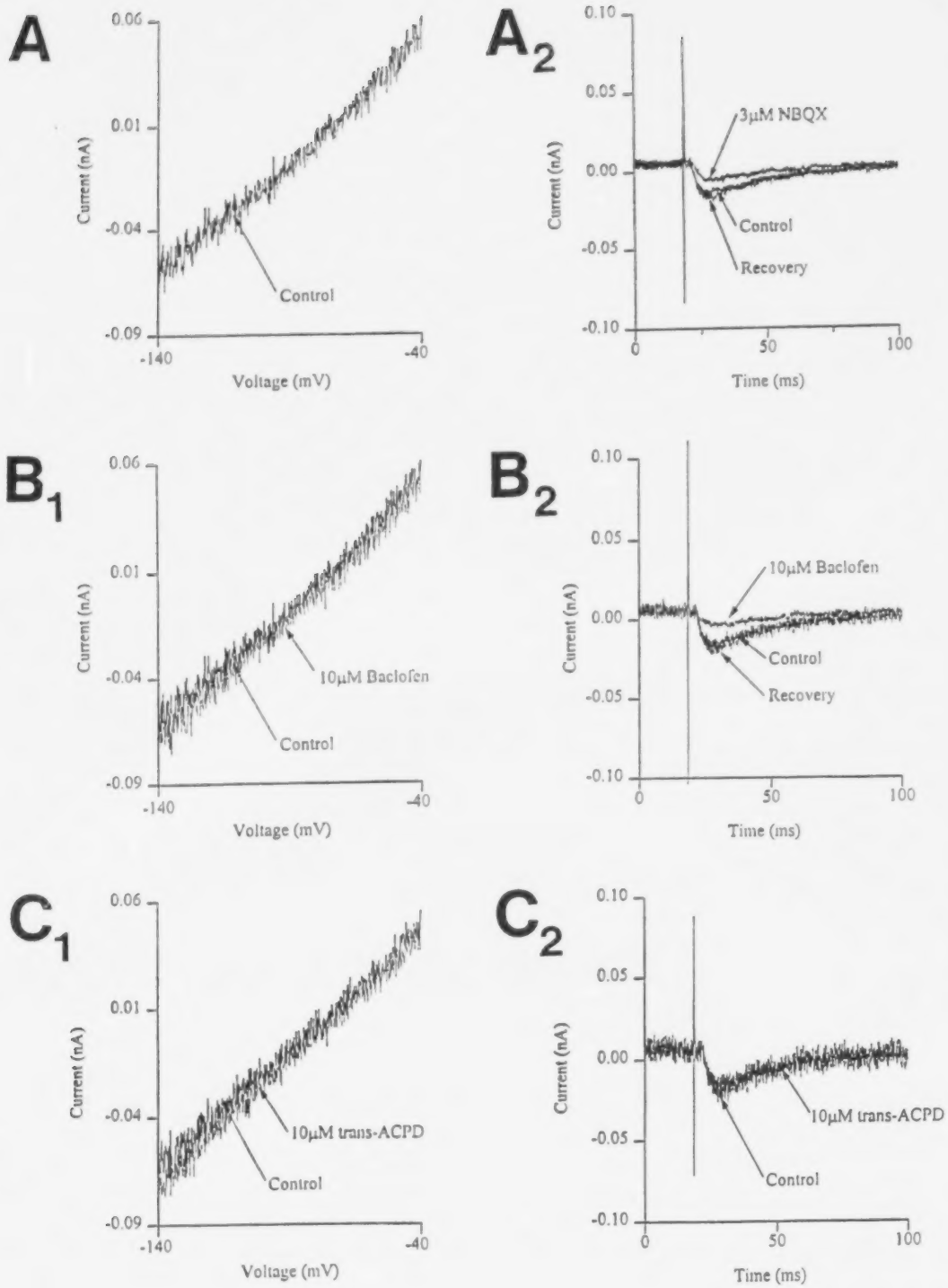
A
0.06
0.01
-0.04
-0.09
Current (nA)
Control
-140
-40
Voltage (mV)
A2
0.10
0.05
0.00
-0.05
-0.10
Current (nA)
3μM NBQX
Control
Recovery
0
50
100
Time (ms)
B1
0.06
0.01
-0.04
-0.09
Current (nA)
10μM Baclofen
Control
-140
-40
Voltage (mV)
B2
0.10
0.05
0.00
-0.05
-0.10
Current (nA)
10μM Baclofen
Control
Recovery
0
50
100
Time (ms)
C1
0.06
0.01
-0.04
-0.09
Current (nA)
10μM trans-ACPD
Control
-140
-40
Voltage (mV)
C2
0.10
0.05
0.00
-0.05
-0.10
Current (nA)
10μM trans-ACPD
Control
0
50
100
Time (ms)

REFERENCES

Barger, S. W., Smith-Swintosky, V. L., Rydel, R. E., and Mattson, M. P. Beta-amyloid precursor protein mismetabolism and loss of calcium homeostasis in Alzheimer's disease. *Ann. N.Y. Acad. Sci.* 695:158-164, 1993.

Feigenspan, A. and Bormann, J. Differential pharmacology of $GABA_A$ and $GABA_C$ receptors on rat retinal bipolar cells. *Eur. J. Pharm.* 288(1):97-104, 1994.

Gaykema, R. P. A., Luiten, P. G. M., Nyakas, C., and Traber, J. Cortical projection patterns of the medial septum-diagonal band complex. *J. Comp. Neurol.* 293:103-124, 1990.

Griffith, W. H. Membrane properties of cell types within guinea pig basal forebrain nuclei in vitro. *J. Neurophysiol.* 59(5):1590-1610, 1988.

Huston, E., Cullen, G. P., Burley, J. R., and Dolphin, A. C. The involvement of multiple calcium channel sub-types in gluamate release from cerebellar granule cells and its modualtion by $GABA_B$ receptor activation. *Neurosci.* 68(2):465-478, 1995.

Johnston, G.A. $GABA_C$ receptors. *Prog. Br. Res.* 100:61-65.

Jiang, Z. G., Allen, C. N., and North, R. A. Presynaptic inhibition by baclofen of retinohypothalamic excitatory synaptic transmission in rat suprachiasmatic nucleus. *Neurosci.* 64(3):813-819, 1995.

Jouvenceau, A., Dutar, P., and Billard, J. M. Presynaptic depression of inhibitory postsynaptic potentials by metabotropic glutamate receptors in rat hippocampal CA1 pyramidal cells. *Eur. J. Pharm.* 281(2):131-139, 1995.

Klunk, W. E., Panchalingam, K., Moosy, J., McClure, R. J., and Pettegrew, J. W. N-acety-L-aspartate and other amino acid metabolites in Alzheimer's disease brain:

a preliminary proton nuclear magnetic resonance study. *Neurology* 42(8):1578-1585, 1992.

Krnjevic, K. Some neuroactive compounds in the substantia nigra. *Advances in Neurology* 5:145-152, 1974.

Krogsgaard-Larsen, P. GABA and glutamate receptors as therapeutic targets in neurodegenerativedisorders. *Pharm. Tox.* 70(2):95-104, 1992.

Markram, H. and Segal, M. Electrophysiological characteristics of cholinergic and non-cholinergic neurons in the rat medial septum-diagonal band complex. *Brain Res.* 513:171-174, 1990.

McCormick, D. A., Wang, Z., and Huguenard, J. Neurotransmitter control of neocortical neuronal activity and excitability. *Cerebral Cortex* 3(5):387-398, 1993.

Meibach, R. C. and Siegel, A. Efferent connections of the septal area in the rat: an analysis utilizing retrograde and anterograde transport methods. *Brain Res.* 119(1):1-20, 1977.

Mohanakrishnan, P., Fowler, A. H., Vonsattel, J. P., Husain, M. M., Jolles, P. R., Liem, P., and Komoroski, R. A. An *in vitro* 1H nuclear magnetic resonance study of the temporopatietal cortex of Alzheimer brains. *Exp. Br. Res.* 102(3):503-510, 1995.

Moore, R. Y. Principles of synaptic transmission. *Ann. N.Y. Acad. Sci.* 695:1-9, 1993.

O'Hara, B. F., Andretic, R., Heller, H. C., Carter, D. B., and Kilduff, T. S. $GABA_A$, $GABA_C$, and NMDA receptor subunit expression in the suprachiasmatic nucleus and other brain regions. *Br. Res. Mol. Br. Res.* 28(2):239-250, 1995.

Pare, D. and Smith, Y. GABAergic projection from the intercalated masses of the amygdala

to the basal forebrain. *J. Comp. Neurol.* 344(1):33-49, 1994.

Sasaki, H., Muramoto, O., Kanazawa, I., Arai, H., Kosaka, K., and Iizuka, R. Regional distribution of amino acid transmitters in postmortem brains of presenile and senile dementia of Alzheimer type. *Ann. Neurol.* 19(3):263-269, 1986.

Scott, H. L., Tannenberg, A. E., and Dodd, P. R. Variant forms of neuronal glutamate transporter sites in Alzheimer's disease cerebral cortex. *J. Neurochem.* 64(5):2193-2202, 1995.

Shaw, P. J. Excitatory amino acid neurotransmission, excitotoxicity, and excitotoxins. *Curr. Opin. Neurol. Neurosurg.* 5(3):383-390, 1992.

Smith-Swintosky, V. L. and Mattson, M. P. Glutamate, beta-amyloid precursor proteins, and calcium mediated neurofibrillary degeneration. *J. Neural Transm. Suppl.* 44:29-45, 1994.

Toth, K., Borhegyi, Z., and Freund, T. F. Postsynaptic targets of GABAergic hippocampal neurons in the medial septum-diagonal band of Broca complex. *J. Neurosci.* 13(9):3712-3724, 1993.

Young, A. B. Cortical amino acidergic pathways in Alzheimer's disease. *J. Neural Transm. Suppl.* 24:147-152, 1987.

CHAPTER 5

VASOPRESSIN RECEPTOR SUBTYPES DIFFERENTIALLY MODULATE CALCIUM-ACTIVATED POTASSIUM CURRENTS IN THE HORIZONTAL LIMB OF THE DIAGONAL BAND OF BROCA

ABSTRACT

The actions of vasopressin (VP) on acutely dissociated neurones within the rat horizontal limb of the diagonal band of Broca (hDBB) were examined using the whole-cell patch clamp method.

VP elicited two distinct responses in 45 of 62 neurons. In one group of cells, 300nM VP decreased voltage-activated outward currents (26/45 cells) whereas in a second group, VP increased outward currents (19/45 cells). The VP-mediated decrease in outward current was blocked by 1μM Manning compound, a V_1 receptor antagonist, suggesting that this response was mediated via V_1 receptors. In contrast, the VP-induced increase in outward was blocked by 1μM $d(CH_2)_5)^1$,D-Ile^2,Ile^4,Arg^8,Ala^9, a V_2 receptor antagonist, indicating that V_2 receptor activation underlies this second response.

VP was unable to elicit any change in voltage-activated outward currents when cells were perfused with 0 Ca^{++}/50μM Cd^{++} solution suggesting that VP modulates a calcium-dependent conductance. In the presence of 25nM charybodotoxin, an I_C channel antagonist, VP was unable to alter outward currents therefore indicating that VP modulates I_C. Currents through calcium channels which are responsible for activation of I_C were unaffected by VP suggesting a direct effect of VP on I_C channels.

These observations demonstrate the differential modulation of I_C channels by VP via V_1 and V_2 receptors in the hDBB.

INTRODUCTION

Vasopressin (VP) was the first peptidergic neurotransmitter system detected in the mammalian brain (Bargmann and Scharrer, 1951). Early work on this peptide focused almost exclusively on its peripheral actions as an antidiuretic and as a pressor agent (Jard, 1983). As a consequence, the physiological roles subserved by VP within the CNS were not as well understood. DeWied's (1971) studies of VP-induced enhancement of conditioned learning were the first observations of a role for this peptide within the CNS. Subsequently, important physiological roles for the vasopressinergic system in the context of central cardiovascular regulation (Noszczyk et al., 1993), fluid balance (Iovino and Steardo, 1985) and antipyresis (Pittman et al., 1988) were characterized.

VP mediates its effects via V_1 and V_2 receptors which are coupled to phospholipase C and adenylate cyclase, respectively (Brinton and Brownson, 1993). V_1 receptors are located principally on postsynaptic membranes and exert excitatory effects on CNS neurones. In rat facial and hypoglossal motoneurones, activation of postsynaptic V_1 receptors elicits a TTX-insensitive, voltage-gated Na^+ current leading to depolarization of these cells (Palouzier-Paulignan et al., 1994; Raggenbass et al., 1991). Stimulation of V_1 receptors also excites lateral horn neurones in the rat, but this excitation is the result of a reduction in a postsynaptic potassium current (Ma and Dun, 1985).

V_2 receptors within the CNS evoke more heterogeneous responses. V_2 receptor activation in the rat septum increased excitatory neurotransmitter and vasopressin release through a presynaptic mechanism (Urban and DeWeid, 1986). In contrast, activation of presynaptic V_2 receptors reduced VP release from rat hypothalamus (Cheng and North,

1989). V_2 receptor actions have also been observed postsynaptically. Pretreatment of rodent ventral septal neurones with a V_2 agonist attenuated the efficacy of subsequent applications of glutamate via a postsynaptic mechanism (van Eerdenburg and Pittman, 1991).

Both V_1 and V_2 receptors are expressed throughout the septal region in the rat brain (Urban and DeWeid, 1986; Shewey and Dorsa, 1988; van Eerdenburg and Pittman, 1991). High concentrations of VP-positive fibers have been identified in the DBB, a basal forebrain region that is located within the septal area (Ulfig et al, 1993; Caffe et al., 1989). Anatomically, the DBB is subdivided into the vertical limb and the horizonal limb (hDBB). The hDBB, which contains a high complement of cholinergic and GABAergic neurones, has been of particular interest because of its integral roles in autonomic cardiovascular regulation (Jhamandas and Renaud, 1986a,b, 1987), fluid balance (Iovino and Steardo, 1985), and mechanisms associated with memory and learning (Chrobak et al., 1989; Givens and Olton, 1990). Despite the presence of VP-positive fibers and receptors within the hDBB and the clear overlap in physiological functions ascribed to both the hDBB and VP, studies investigating neuromodulation by VP in this nucleus are lacking.

In the present sudy, the cellular mechanisms underlying VP actions were examined on acutely dissociated rat hDBB neurones. The receptor pharmacology and the ionic mechanisms underlying VP responses were investigated with whole cell patch clamp recordings. Our results suggest that VP differentially modulates a calcium-activated K^+ current via V_1 and V_2 receptors.

RESULTS

Actions of VP in a Forebrain Slice Preparation

Application of 300nM VP produced two responses with regard to the excitability of hDBB cells recorded in forebrain slices. During a depolarizing pulse, VP application evoked an increase in AP discharge rate in one population (2/4 cells; Fig. 5-1A), and a reduction in the firing frequency of a second group of hDBB neurons (2/4 cells; Fig. 5-1B).

We subsequently examined the effects of VP on ionic conductances elicited using both voltage step and voltage ramp protocols. Applications of VP also elicited two distinct responses. In one group of cells, the neuropeptide caused a decrease in outward current (n=5) whereas in a second group, VP increased outward current (n=4). The I-V plot in Fig. 5-2A shows a VP-mediated decrease in outward current in an hDBB cell. Fig. 5-2B shows the increase in outward current generated by VP in an hDBB neuron. This plot was generated by a voltage ramp from -110 to +30mV.

To examine whether the V_1 or V_2 receptor subtypes mediated these two responses, single voltage steps were applied every 30 seconds to cells recorded using the perforated patch method and the steady state currents were plotted versus time (see inset of Fig. 5-3A). As shown in Fig. 5-3A, VP was applied in the presence and absence of the V_1 receptor antagonist, MC. In the absence of MC, VP decreased outward currents (44±9% reduction; n=5). However, this effect was blocked when VP was applied in the presence of MC. This observation suggests that the VP-induced reduction in outward current is mediated by the V_1 receptor.

Fig. 5-3B shows data from a representative hDBB cell where application of VP

elicited a prolonged increase in outward current (45±8%; n=4). This response did not completely recover even though the recording was conducted for over one hour. Two problems became apparent with this approach to study VP responses in the brain slice. First, VP responses consistently took upwards of one hour to recover. This prolonged recovery time hampered our efforts to pharmacologically characterize the VP receptor subtypes mediating each of the above responses. Prolonged duration of response to peptide applications have been observed in other preparations (R. McQuiston, personal communication) and it has been suggested that this may be the result of the larger peptides becoming enmeshed in the tissue thereby requiring more time to washout. Secondly, in spite of the use of perforated patch method of recordings, there was a progressive "rundown" of baseline current (Fig. 5-3A). Although it may be possible to qualitatively identify the nature of VP responses in presence of antagonists, we were also concerned at our inability to study ionic conductances underlying VP's actions using this approach. The use of an acutely dissociated cell preparation could eliminate this problem as the cells are dispersed on a coverslip in a petri dish, an approach that facilitates washout of applied peptides. With this rationale, we utilized an acutely dissociated preparation of rat hDBB neurons to conduct further pharmacological studies to examine the actions of VP on these cells.

Actions of VP in an Acutely Dissociated hDBB Cell Preparation

Effects of VP on outward currents

Exogenous application of 300nM VP on 62 acutely dissociated hDBB neurones produced two distinct responses in 45 neurones. In one group of neurones, VP caused a

decrease in voltage-activated outward currents (26/45 cells). This is demonstrated in Fig. 5-4A which is an I-V plot from a representative hDBB cell. Under control conditions, no current is observed until the cell is depolarized beyond -40mV. In this same cell, application of VP reversibly decreased the outward current. The inset in Figure 5-4A shows the currents evoked by depolarizing this cell from a holding potential of -80mV to +30mV under control conditions and in the presence of VP. Figure 5-4B illustrates the VP-induced decrease in outward current-density in the voltage range from -40 to +30mV. At +30mV, the current density under control conditions (0.33 ± 0.02nA/pF) was significantly different from that in the presence of VP (0.25 ± 0.02nA/pF; $P<0.01$; Figure 5-4B). The average capacitance of these cells was 17 ±1.2pF. These data show that VP decreases voltage-activated outward current in this group of hDBB neurones.

In a second population of cells, application of VP generated an increase in voltage-activated outward currents (19/45 cells). Figure 5-5A shows a representative VP-induced increase in the outward current of an hDBB neurone. This increase in current started typically at -40mV and continued to increase as cells were depolarized. The inset of Figure 5-5A shows the currents evoked by this cell in response to a depolarizing step from -80 to +30mV in the presence and absence of VP. Figure 5-5B is a current density plot in which the voltage-activated outward currents were increased by VP. The current density at +30mV under control conditions (0.33 ± 0.02nA/pF) increased in the presence of VP (0.40 ± 0.02nA/pF; $P<0.01$). The average capacitance of these cells was 18.7 ± 1.3pF. The data from this population of cells illustrate a VP-mediated increase in the voltage-activated outward currents.

VP did not induce desensitization in either cell population and responses were reproducible with repeated VP applications. We also noted that the time required for recovery in the acutely dissociated cell preparation was much shorter compared to the brain slice. Using the acutely dissociated cells, the decrease in outward current induced by VP usually recovered in less than 10 minutes after drug application was terminated, whereas the VP-induced outward current typically required ≥25 minutes to recover to control levels.

Receptor pharmacology of VP responses

Since VP receptors comprise a heterogeneous group of V_1 and V_2 receptor subtypes, we hypothesized that the two distinct VP mediated responses might result from selective activation of specific receptor subtypes. Therefore, we examined the identity of receptors underlying specific VP responses using selective V_1 and V_2 receptor antagonists.

Figure 5-6A shows data from an hDBB neurone where VP reversibly decreased voltage-activated outward current. Subsequent applications of VP in the presence of the V_1 receptor antagonist, MC (1μM), were unable to reduce outward current (Figure 5-6B). This is further illustrated in the insets of Figures 5-6A and 5-6B which show currents evoked by voltage steps from -80 to +30mV. Under control conditions, VP decreased the current elicited by the step whereas in the presence of MC, the VP effect is blocked. The plot in Figure 5-6C is the average current density-voltage relationship obtained from 8 hDBB neurones under control conditions, in the presence of MC, and VP application in the presence of MC. The current density at +30mV under control conditions (0.31 ± 0.03nA/pF) was not significantly different from that observed when VP and MC were applied together (0.31 ± 0.03nA/pF; $P>0.99$; $n=8$). Thus, MC blocked the VP-induced decrease in outward currents

suggesting that this particular response is mediated via V_1 receptors.

Figure 5-7A shows a typical I-V plot obtained from an hDBB neurone where VP caused an increase in the outward current. Subsequent increases were blocked by the selective V_2 antagonist, $d(CH_2)_5{}^1$,D-Ile^2,Ile^4,Arg^8,Ala^9 (1μM) (Figure 5-7B). The insets of Figure 5-7A and 4B are the recordings of currents evoked by voltage steps to +30mV from a holding potential of -80mV. They further confirm that the increase in current elicited by VP can be blocked by the V_2 antagonist. The average current density-voltage relationships obtained in 8 cells under control conditions and V_2 antagonist applications in the presence and absence of VP are shown in Figure 5-7C. The current density measured at +30mV under control conditions (0.34 ± 0.03nA/pF) was not significantly different ($P>0.99$) from that observed when $d(CH_2)_5{}^1$,D-Ile^2,Ile^4,Arg^8,Ala^9 blocked the VP-induced increase in voltage-activated currents (0.33 ± 0.03nA/pF). These data demonstrate that the VP-induced increase in outward currents is mediated via V_2 receptors.

Although the V_1 antagonist blocked the VP-induced decrease in outward currents and the V_2 antagonist blocked the VP-induced increase in outward currents, there remains the possibility of a non-selective antagonism of the VP receptor and cross reactivity of antagonists between the two receptor subtypes. We examined this possibility by applying MC to block VP mediated increases in outward current and the V_2 receptor antagonist to block VP-mediated decreases in outward current. The changes in current induced by VP were unaffected by these cross applications of antagonists (data not shown), indicating that VP mediates its effects on hDBB neurones via specific receptor subtypes.

Ionic mechanisms of VP-mediated responses

a) *Blockade of Ca^{++} occludes VP responses*

Mammalian CNS neurones exhibit a variety of K^+ currents. The K^+ currents that modulate AP shape and firing rates include the voltage-activated transient outward current, I_A; the classical Hodgkin-Huxley type delayed rectifier, I_K ; and the calcium-activated potassium currents, $I_{K(Ca)}$. Since VP affects currents evoked from holding potentials positive to -40mV, it is unlikely that VP affects I_A as this current is inactivated at this potential. Given that VP modulates outward currents that are activated at voltages beyond -40mV, we postulated that it may exert its effects on other K^+ currents.

To examine whether VP responses were mediated via I_K or $I_{K(Ca)}$, a 0 Ca^{++}/50μM Cd^{++} ACSF solution was perfused to block the Ca^{++} influx responsible for activation of $I_{K(Ca)}$. Figure 5-8A and B represent data from a typical cell. As shown in Figure 5-8A and inset, application of VP generated a decrease in outward current. After the VP response had recovered, the cell was perfused with the 0 Ca^{++}/50μM Cd^{++} ACSF solution and VP was then re-applied under these conditions. The calcium-free solution reduced outward current compared to the control and subsequent application of VP in the presence of calcium-free solution did not induce a further decrease in outward current (Figure 5-8B and inset). The current density plot in Figure 5-8C confirms that Ca^{++}-free solution reduced outward currents compared to that under control conditions at +30mV (control: 0.33 ± 0.02nA/pF; 0 Ca^{++}/50μM Cd^{++}: 0.26 ± 0.02nA/pF; $P<0.01$; n=10). Furthermore, VP-induced reduction of outward currents was not reproducible in the Ca^{++}-free solutions (VP+0 Ca^{++}: 0.25 ± 0.02 nA/pF; n=10). Our data also indicate that perfusion of the Ca^{++}-free solution reduced

outward current to similar levels as those by VP in control ACSF (0.26 ± 0.02nA/pF; P>0.99; see Figure 5-8-4C). These observations suggest that the V_1-receptor mediated decrease in outward current occurs via a Ca^{++}-activated current.

Figure 5-9A and inset show data acquired from a neurone where application of VP generated an increase in outward current. In this same cell, perfusion of 0 Ca^{++}/50μM Cd^{++} ACSF reduced the outward current and the subsequent addition of VP in 0 Ca^{++} ACSF did not elicit an increase in outward current (Figure 5-9B and inset). This response was observed in 9 neurones where current density at +30mV was significantly reduced to 0.27 ± 0.02 nA/pF in 0 Ca^{++} ACSF compared to 0.34 ± 0.02nA/pF in control solutions (P<0.01; Figure 5-9C). VP in the presence of 0 Ca^{++} external solution did not induce any change in current density (0.28 ± 0.02nA/pF; P>0.99) compared to 0 Ca^{++} alone at +30mV (Figure 5-9C). Thus, as observed with the V_1-receptor mediate response, the V_2-receptor mediated increase in outward current also occurs via a Ca^{++}-activated current.

b) *VP modulation of I_C currents*

There are two major families of $I_{K(Ca)}$, the large, voltage-dependent current referred to as I_C and the smaller, voltage-insensitive current referred to I_{AHP}. I_C can be selectively blocked by the scorpion toxin, CTX, (Goh et al., 1992) whereas I_{AHP} is selectively blocked by apamin, an active ingredient in bee venom (Womble and Moises, 1993). In dissociated hDBB neurones, application of 50nM apamin had little effect on currents evoked by the voltage steps whereas application of 25nM CTX reduced outward current. This indicates that apamin-sensitive I_{AHP} does not contribute significantly to the voltage-activated steady-state outward currents generated by applying depolarizing voltage commands.

Consequently, we examined the ability of CTX to occlude both the VP-induced increase and decrease in outward currents. As shown in Figure 5-10A and inset, VP evokes a readily reversible decrease in outward current. After recovery, CTX decreases outward current compared to control (Figure 5-10B). Application of VP in the presence of CTX does not decrease current as compared to CTX alone (Figure 5-10B and inset.). Examination of Figure 5-10C reveals that at +30mV, the current density is 0.34 ± 0.01nA/pF in control cells. This is reduced to 0.28 ± 0.02nA/pF in CTX and 0.27 ± 0.02nA/pF in the VP+CTX solution ($P<0.01$; n=8). CTX reduces the outward current by the same amount as VP under control conditions ($P>0.99$; see Figure 5-4C) and 0 Ca^{++} ($P>0.99$; see Figure 5-8C). These data further confirm that VP likely blocks I_C in hDBB cells.

Figure 5-11A and inset show data from a neurone where application of VP increased outward current. In this same cell, application of CTX reduced outward current and subsequent application of VP with CTX did not elicit any further increase in current (Figure 5-11B). The current-density at +30mV was 0.35 ± 0.01nA/pF and 0.30 ± 0.02nA/pF in control and VP/CTX solutions, respectively ($P<0.01$; n=9; Figure 5-11C). This observation indicates that the VP-induced outward current is mediated by an increase in I_C.

In summary, these results demonstrate that VP modulates I_C currents in hDBB neurones via the differential activation of distinct VP receptor subtypes.

c) Effect of VP on calcium currents

The influx of Ca^{++} required for the activation of I_C channels is derived from the activation of voltage-gated Ca^{++} channels (Augustine and Charlton, 1986). The effects of VP on I_C current could result either from a direct effect on the I_C channel itself or on the Ca^{++}

channels. To address this question, we examined the effects of VP on current through calcium channels in hDBB neurones. Ba^{++} was used as the charge carrier. Figure 5-12 illustrates the I-V relationship of I_{Ba} evoked by applying 20ms steps to different depolarizing voltage commands from a holding potential of -80mV under control conditions and in the presence of VP. VP did not significantly alter I_{Ba} (n=14; P>0.99). In these same cells, we have observed that applications of neurotensin and Zn^{++}caused approximately 30% and 85% decreases in I_{Ba}, respectively, (unpublished observations) which indicates that I_{Ba} is capable of being modulated in these neurones. These data suggest VP is likely to modulate the I_C channel directly rather than exert its effects at the level of calcium channels.

DISCUSSION

Our data suggest that VP modulates conductance through I_C channels in hDBB neurones. Specifically, activation of the V_1 receptor decreases I_C current in one set of neurones, whereas V_2 receptor activation increases I_C current in a second population of cells within this basal forebrain region. The inability of VP to modulate I_{Ba} suggests that V_1 and V_2 receptors directly modulate the I_C channel. In the context of currently known actions of VP effects on central mammalian neurones, our results appear to be the first demonstration of a differential modulation of an ionic current, I_C, by different VP receptor subtypes.

Whole cell recording and VP responses

Under our recording conditions in the acutely dissociated preparation, I_C accounted for approximately 20% of the total outward current at +30mV. However, the internal patch pipette solution contained 10mM EGTA. This can result in significant attenuation of Ca^{++}-

activated conductances due to intracellular calcium buffering. This may have led to underestimation of the contribution of I_C to the total voltage-activated outward current. Nonetheless, we were able to evoke I_C under these conditions as evident from the decrease in total outward current when external calcium was removed. The voltage range within which VP affects currents (Fig. 5-4, 5-5), and the occlusion of the VP-response by blocking calcium influx (Figs. 5-6, 5-7) and by CTX (Figs. 5-10, 5-11) are consistent with the notion that VP modulates I_C. If significant intracellular calcium buffering by EGTA had occurred, this would result in an underestimation of the contribution of I_C and thus, of the effect of VP on I_C. Therefore, under normal physiological conditions, I_C may make a much larger contribution to the voltage-activated outward current and VP may have a larger effect.

We also attempted to address this issue by lowering the concentration of EGTA in the internal solution to as low as 0.5mM. However, we observed that low EGTA concentrations rendered hDBB neurones non-viable for recording. It is likely that low concentrations of EGTA are unable to properly buffer calcium influx, consequently allowing intracellular calcium concentration to rise to toxic levels.

Another issue that must be addressed was the observation that the relative effects of VP in the slice were typically greater that those observed in the acutely dissociated preparation. Although the reason for this is not clear, it may be due to the fact that some of the VP receptors were damaged in the acute dissociation procedure and therefore rendered non-functional. This would further suggest that the responses recorded in the acutely dissociated preparation may underestimate of the actual VP effect in these cells.

Localization of VP receptor subtypes

The data from this study suggest that exogenous applications of VP on individual hDBB neurones activates either the V_1 or V_2 receptor but not both. If both receptor subtypes were present on the same cell, then in the presence of one of the VP receptor antagonists, VP might be expected to evoke an effect via the unblocked receptor. However, as illustrated in Figs. 5-6 and 5-7, VP effects could be completely blocked by application of a single antagonist. A possible explanation for this observation may be that the VP antagonists are nonselective. We examined this possibility and did not observe nonselective actions of either VP receptor antagonist. Furthermore, others have examined the selectivity of these antagonists ad also determined that they are highly specific for their respective receptor subtypes at the concentrations used in this study (Brinton and McEwen, 1989; Manning and Sawyer, 1989).

There are two main cell types within the hDBB: magnocellular cholinergic neurones and parvocellular GABAergic cells. The possibility exists that each chemically distinct cell type may possess one of the VP receptor subtypes. However, this seems less likely as we observed no difference in the membrane capacitance between cells demonstrating either of the VP responses which suggest that the cells which contain the VP receptors comprise a homogeneous population of hDBB neurones. The possibility also exists that the enzymatic and mechanical processes used to separate the neurones may have resulted in the loss of neuronal arborization and artifactually rendered cells of a uniform size.

Mechanism of action of VP receptors

The V_1 and V_2 receptors make up two distinct receptor families where V_1

receptors activate the phospholipase C pathway and the V_2 receptors typically act via adenylyl cyclase (Brinton and McEwen, 1989). V_1 receptors have been further delineated into two distinct subtypes: V_{1a} receptors which are localized in the CNS, liver, and vasculature (Kirk and Mitchell, 1981; Bone et al., 1984; Shewey and Dorsa, 1988; and Morel et al., 1992) and V_{1b} receptors which are present primarily in the anterior pituitary (Baertschi and Friedli, 1985). The V_2 receptor family also has two members: V_{2a} receptors found in the kidney (Jard, 1983) and the putative V_{2b} receptors distributed within the brain (Brinton and Brownson, 1993). If this subdivision of V_1 and V_2 receptor holds, then hDBB neurones likely express V_{1a} and V_{2b} receptor subtypes. However, this specific classification of VP actions cannot be confirmed until specific antagonists are developed to distinguish between the various V_1 and V_2 receptor subtypes. At present, MC and $d(CH_2)_5^1$,D-Ile^2,Ile^4,Arg^8,Ala^9 are only able to delineate between V_1 and V_2 receptors.

The signal transduction mechanism that underlies the effects of VP on I_C was not investigated. It is possible that the actions of the V_1 and V_2 receptors identified in this study are mediated via activation of specific G-protein coupled second messenger pathways. We consider this to be unlikely since the use of the whole cell patch clamp technique would have resulted in the washout of several important cytosolic components thereby attenuating responses in long term recordings (Penner et al., 1987). In most cases in this study, electrophysiological recordings lasted longer than 30 minutes which suggests it is more likely that VP's effects may be a result of a membrane-delimited mechanism such as direct activation of G-protein(s) coupled to the I_C channel itself.

Intrinsic properties of hDBB neurones

As our study is the one of the first to examine hDBB cells in the acutely dissociated cell preparation, some aspects of intrinsic properties of these neurones deserve comment. Intracellular recordings from DBB neurones in the slice have shown the presence of a slow afterhyperpolarization that follows action potentials in cholinergic neurones (Markram and Segal, 1990), but not in non-cholinergic, putative GABAergic cells (Griffith, 1988). The concentration of apamin used to block I_{AHP} in our experiments was well above the effective concentration required to block I_{AHP} in other CNS neurones (IC_{50} 1.3nM; Bourque and Brown, 1987). Based on the lack of effect of apamin, I_{AHP} channels are not present in sufficiently large concentration to contribure to currents generated by depolarizing steps. This suggests that these cells likely belong to the non-cholinergic, putative GABAergic cell population. Alternatively, the possibility that I_{AHP} channels may not survive the enzymatic treatment and the trituration procedure cannot be discounted.

Functional role of I_C in hDBB neurones

The I_C channels identified in hDBB neurones appear to be similar to those characterized in other CNS neurones, namely, their activation is positive to -40mV and they are highly sensitive to Ca^{++} influx (Belluzzi, 1985). Functionally, the I_C channel is observed to modulate AP repolarization (Sah and McLachlan, 1992) and contribute to the initial component of the AHP (Zhang and McBain, 1995). In particular, regulation of the I_C contribution to the AHP may modulate the AP firing frequency of these cells. Blockade of I_C can lead to a dramatic increase in the firing rate (Goh et al., 1989) by decreasing the amplitude and duration of the AHP, whereas an increase in I_C would have opposite effects

on the AHP and therefore reduce the AP discharge rate. Thus, the differential modulation of I_C by VP may confer upon this peptide the ability to fine tune the excitability of hDBB neurones. Specifically, VP may preferentially increase the discharge rate of those cells through V_1 receptor activation by decreasing I_C. On the other hand, activation of the V_2 receptor would likely restrict their firing rate consequent to an I_C-mediated increase in AHP duration. In this manner, VP may be able to differentially regulate the behavior of hDBB neurones and therefore control how this region interacts with target neurones.

Physiologically, we speculate that the differential modulation of I_C receptors subserves an integral role in the hDBB's regulation of central cardiovascular functions. Dense VP projections to the DBB have been identified to originate from the bed stria of the nucleus terminalis and the amygdala (Pare and Smith, 1994; Wilkinson and Pittman, 1995). Each of these regions responds to extrinsic signals related to changes in blood pressure (Alheid, de Olmos, and Beltramino, 1995; Negoro et al., 1973) and likely relays these inputs to the DBB, through identified pathways. In turn, this innervation may mediate DBB regulation of VP release from the supraoptic nucleus (Jhamandas and Renaud, 1986a,b, 1987).

Figure 5-1. Vasopressin modulates excitability of hDBB cells. A,B. In a cell resting at -75mV, perfusion of 300nM VP increased the firing frequency of hDBB neurons (*control*: AP height: 56±4mV; AP width: 2.4±0.3ms; AHP duration: 57.6±8.0ms; AHP amplitude: 5.86±1.2mV; *VP*: AP height: 54mV±5mV; AP width: 4.0±0.8ms; AHP duration: 29.6±10.1ms; AHP amplitude: 2.93±1.4mV; n=2). The depolarizing step was 0.18nA in amplitude and 1600ms in duration. **C,D.** In another hDBB cell (rmp=-71mV), perfusion of 300nM reduced the AP firing frequency (*control*: AP height: 67±8mV; AP width: 4.2±1.8ms; AHP duration: 156.6±12.4ms; AHP amplitude: 10.7±2.5mV; *VP*: AP height: 68±7.2mV; AP width: 3.0±1.2ms; AHP duration: 178.8±25.4ms; AHP amplitude: 8.79±4.7mV; n=2). The depolarizing step was 1000 ms in duration and 0.16nA in amplitude.

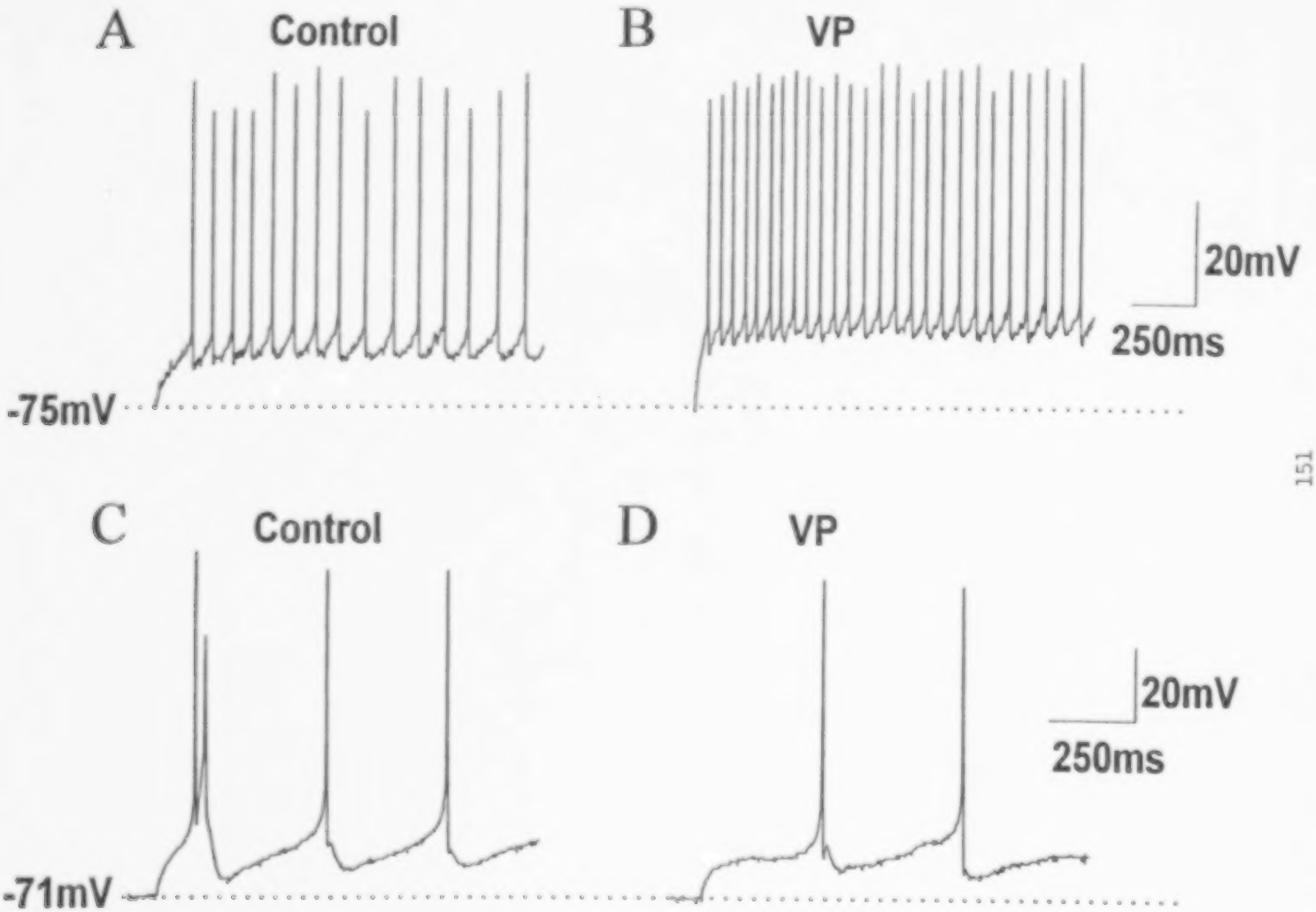
A
Control
B
VP
20mV
250ms
-75mV
C
Control
D
VP
20mV
250ms
-71mV

Figure 5-2. Vasopressin modulation of outward currents in rat forebrain slices. A. Cells were held at -80mV and depolarizing step commands were applied to +30mV (increment 10mV/step; 100ms) to evoke currents. Steady state currents were measured and I-V relationships were plotted. The plot represents an I-V relationship from a neuron where application of 300nM VP reversibly decreased outward current. **B.** Currents evoked from voltage ramps from -110 to +30mV (9mV/s) generated under control conditions and in the presence of 300nM VP. VP reversibly increased outward currents in this cell. The VP-mediated responses indicated in both A and B were acquired in the presence of 1μM TTX.

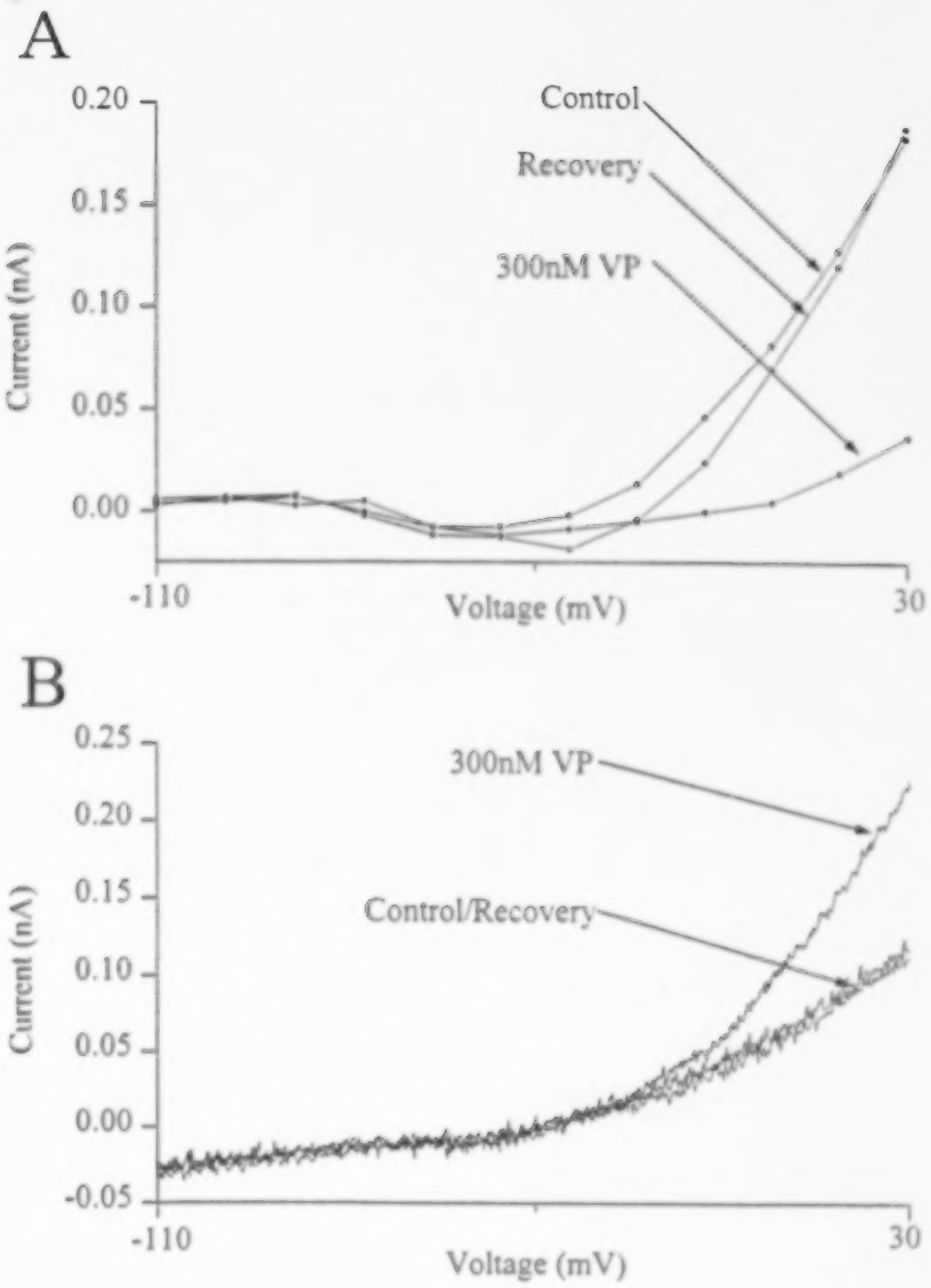
A
0.20
0.15
0.10
0.05
0.00
Current (nA)
Control
Recovery
300nM VP
-110
Voltage (mV)
30
B
0.25
0.20
0.15
0.10
0.05
0.00
-0.05
Current (nA)
300nM VP
Control/Recovery
-110
Voltage (mV)
30

Figure 5-3. Effects of perfusion of VP on two populations of cells. Single voltage steps were applied every 30 seconds and the steady state currents were plotted against time. **A.** In the presence of 1μM MC, a V_1 receptor antagonist, VP was unable to elicit a decrease in outward currents. However, in the absence of this antagonist, VP reversibly reduced outward currents. **B.** VP-induced outward currents in a representative hDBB cell. The response had not completely recovered after 1 hour of recording.

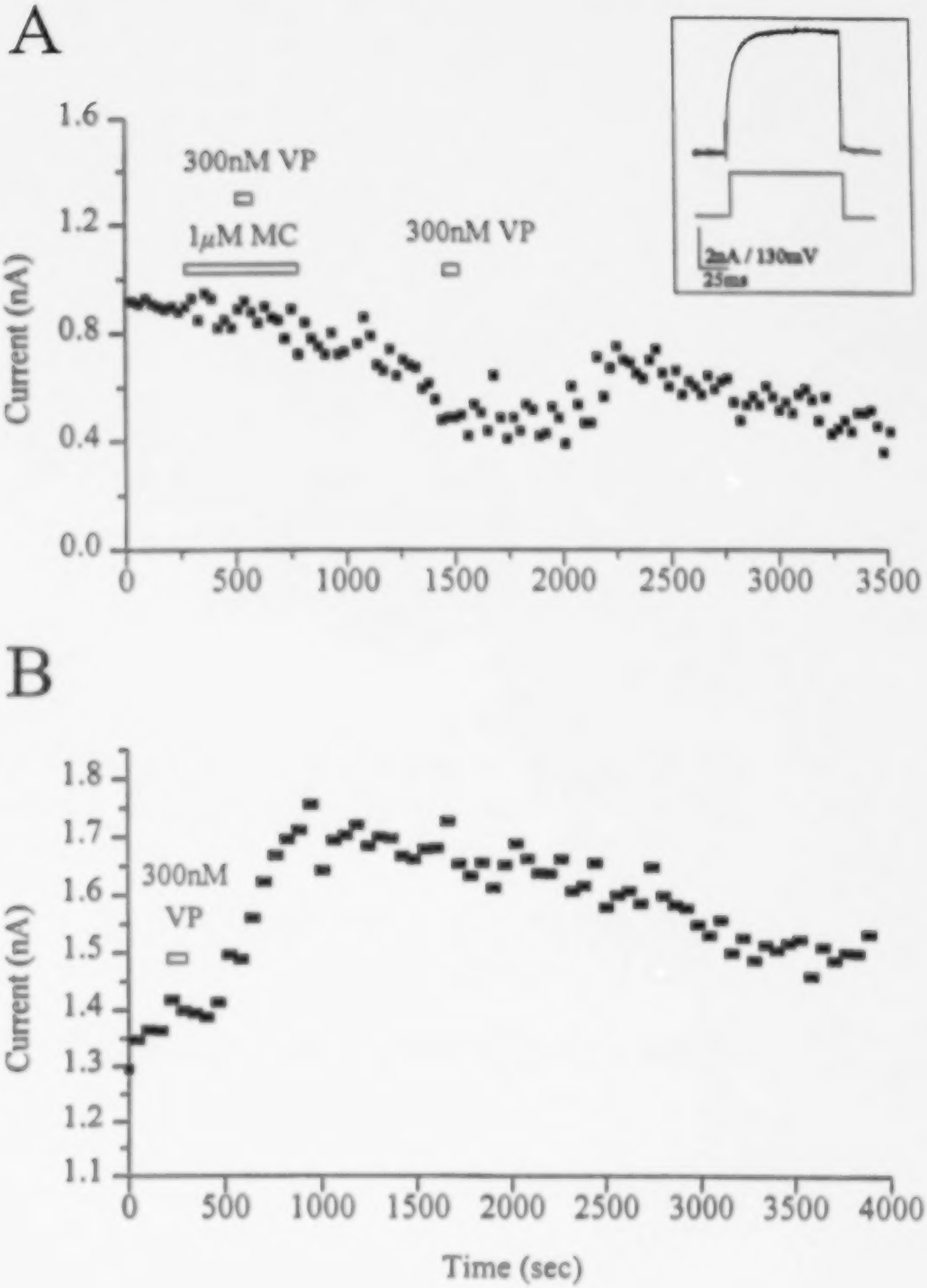
A
1.6
1.2
0.8
0.4
0.0
Current (nA)
300nM VP
1μM MC
300nM VP
2nA / 130mV
25ms
0
500
1000
1500
2000
2500
3000
3500
B
1.8
1.7
1.6
1.5
1.4
1.3
1.2
1.1
Current (nA)
300nM
VP
0
500
1000
1500
2000
2500
3000
3500
4000
Time (sec)

Figure 5-4. Vasopressin mediated decrease in outward currents in acutely dissociated neurons. Cells were held at -80mV and depolarizing step commands were applied to +30mV (increment 10mV/step; 100ms) to evoke currents. Steady state currents were measured and I-V relationships were plotted. **A.** Graph showing I-V relationships from an hDBB neuron where application of 300nM VP reversibly decreased outward current. The inset shows currents evoked by applying a voltage step from to +30mV from a holding potential of -80mV under control conditions and in the presence of VP. **B.** Current density-voltage plot of the averaged data obtained from 26 hDBB cells. VP reduced the outward current in the voltage range from -40mV to +30mV. Error bars show s.e.m.

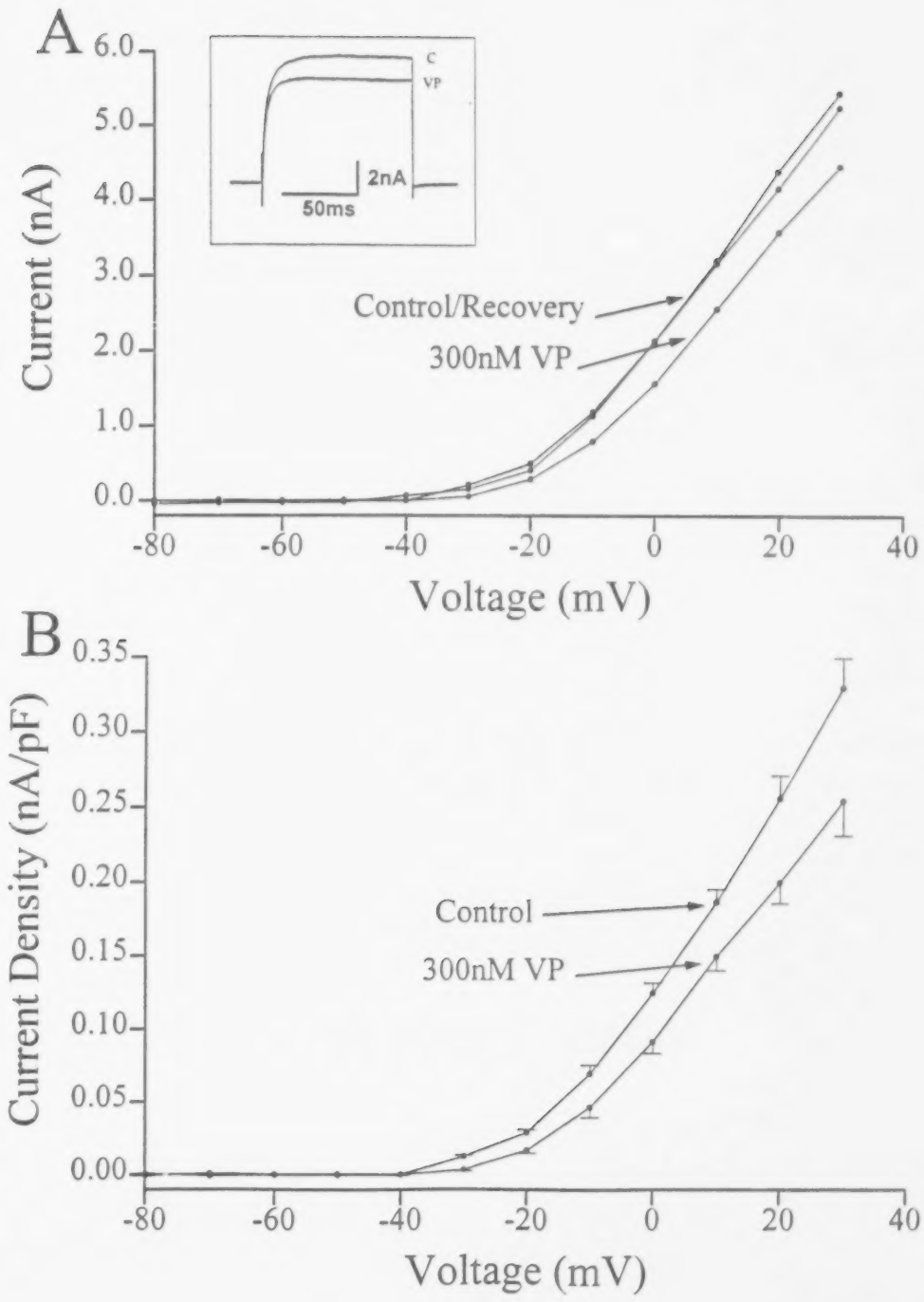
A
6.0
5.0
4.0
3.0
2.0
1.0
0.0
Current (nA)
C
VP
2nA
50ms
Control/Recovery
300nM VP
-80
-60
-40
-20
0
20
40
Voltage (mV)
B
0.35
0.30
0.25
0.20
0.15
0.10
0.05
0.00
Current Density (nA/pF)
Control
300nM VP
-80
-60
-40
-20
0
20
40
Voltage (mV)

Figure 5-5. Vasopressin mediated increase in outward currents. Cells were held at -80mV and depolarizing step commands were applied to +30mV (increment 10mV/step; 100ms) to evoke currents. Steady state currents were measured and I-V relationships were plotted. **A.** Graph showing I-V relationships from an hDBB neuron where application of 300nM VP reversibly increased outward current. The inset shows currents evoked by applying a voltage step from to +30mV from a holding potential of -80mV under control conditions and in the presence of VP. **B.** Current density-voltage plot of the averaged data obtained from 19 hDBB cells. VP increased outward current in the voltage range from -40mV to +30mV. Error bars show s.e.m.

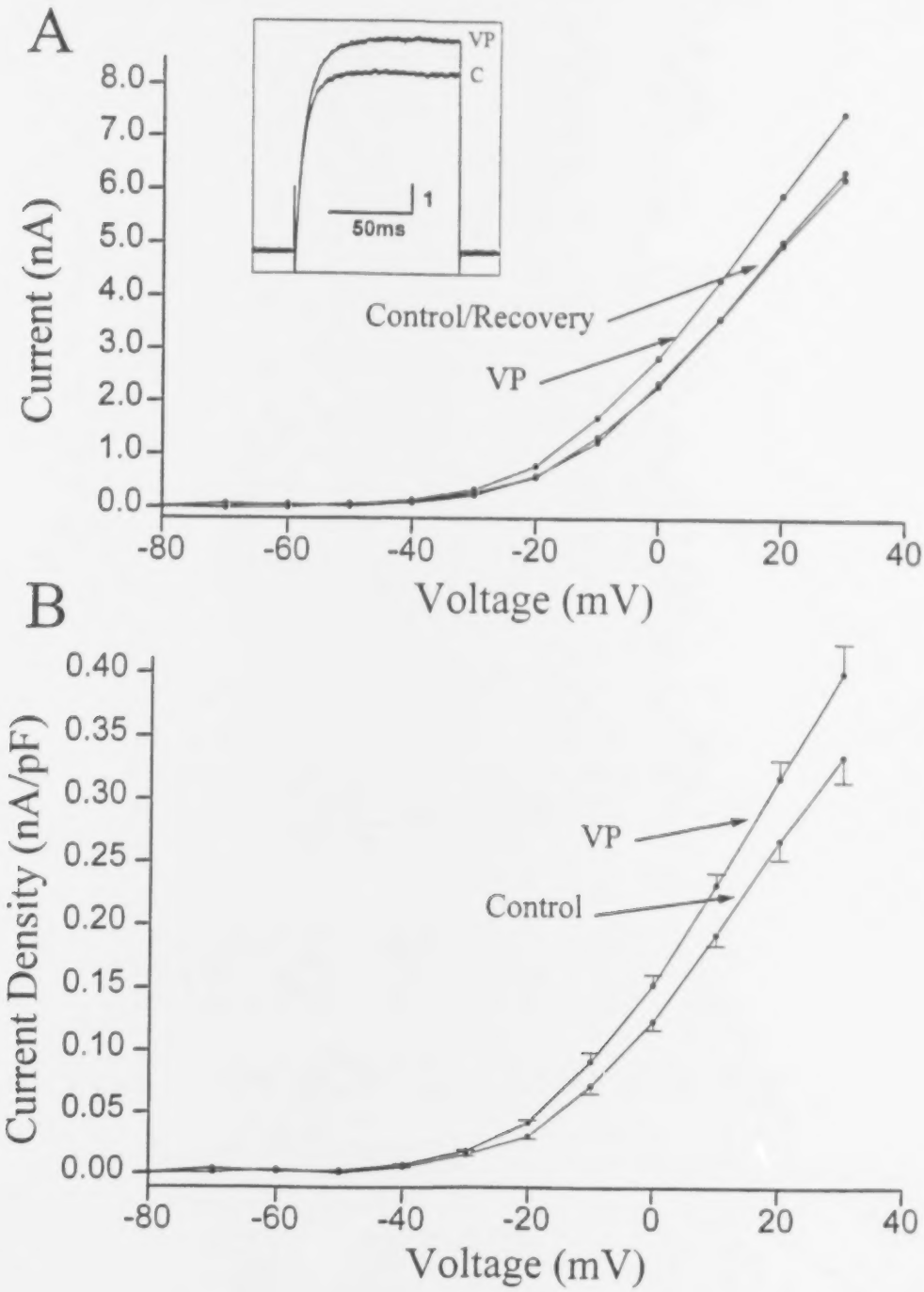
A
VP
C
1
50ms
Current (nA)
8.0
7.0
6.0
5.0
4.0
3.0
2.0
1.0
0.0
Control/Recovery
VP
-80
-60
-40
-20
0
20
40
Voltage (mV)
B
Current Density (nA/pF)
0.40
0.35
0.30
0.25
0.20
0.15
0.10
0.05
0.00
VP
Control
-80
-60
-40
-20
0
20
40
Voltage (mV)

Figure 5-6. V_1 receptor antagonist, MC, blocked VP-mediated decrease in outward currents. A. A typical I-V relationship illustrating VP-induced decrease in outward currents in an hDBB neuron (similar to that shown in Fig. 5-4A). **B.** I-V relationship of currents evoked under control conditions and in the presence of MC and VP in the same neuron. This graph illustrates a complete blockade of VP-mediated reduction in outward current by the V_1 antagonist. **C.** Current density-voltage relationships obtained from 8 cells under control conditions, in the presence of MC, and MC in the presence of VP.

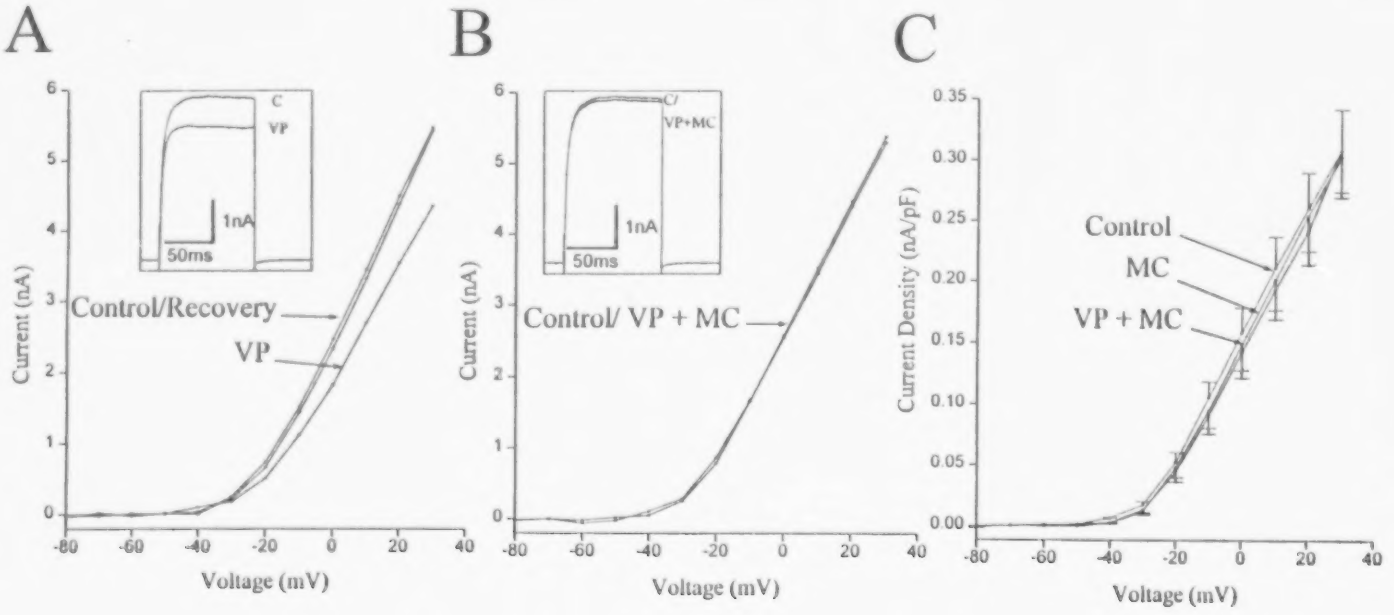
A
B
C
Current (nA)
Voltage (mV)
Control/Recovery
VP
1nA
50ms
Control/ VP + MC
Current Density (nA/pF)
Control
MC
VP + MC

Figure 5-7. V_2 receptor antagonist (d(CH_2)$_5$ [1],D-Ile [2],Ile [4],Arg [8],Ala [9]) blocked VP-mediated increase in outward currents. **A.** A typical I-V relationship showing a VP-induced increase in outward currents in an hDBB neuron (similar to that shown in Fig. 5-5A). **B.** I-V relationship of currents evoked under control conditions and in the presence of the V_2 receptor antagonist and VP in the same neuron. This graph illustrates a complete blockade of VP-mediated increase in outward current by the V_2 receptor antagonist. **C.** Current density-voltage relationships obtained from 8 cells under control conditions, in the presence of the V_2 receptor antagonist, and the V_2 receptor antagonist in the presence of VP.

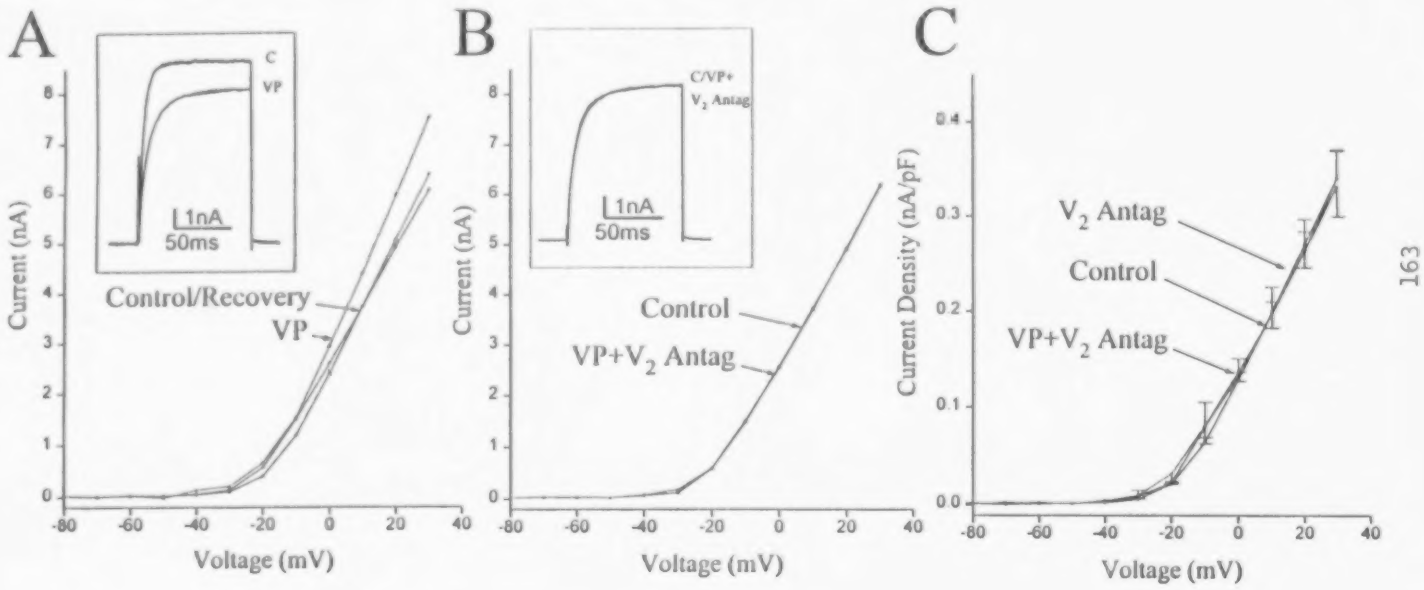
A
C
VP
1nA
50ms
Control/Recovery
VP
Current (nA)
Voltage (mV)
B
C/VP+
V2 Antag
1nA
50ms
Control
VP+V2 Antag
Current (nA)
Voltage (mV)
C
V2 Antag
Control
VP+V2 Antag
Current Density (nA/pF)
Voltage (mV)

Figure 5-8. Blockade of Ca^{++}-influx blocked VP-induced decrease in outward current. **A.** A typical I-V relationship depicting a VP-induced decrease in outward currents in an hDBB neuron (similar to that shown in Fig. 5-4A). **B.** I-V plot of the currents evoked under control conditions, and in 0 Ca^{++} external solution in the presence and absence of VP. This graph illustrates that in the absence of Ca^{++} influx, VP response was abolished. Inset shows the currents evoked by applying voltage steps from -80mv (holding potential) to +30mV under control conditions (C), in 0 Ca^{++}, and 0 Ca^{++} with VP. **C.** Current density-voltage plots obtained from 10 cells under conditions, and in 0 Ca^{++} external solution in the presence and absence of VP.

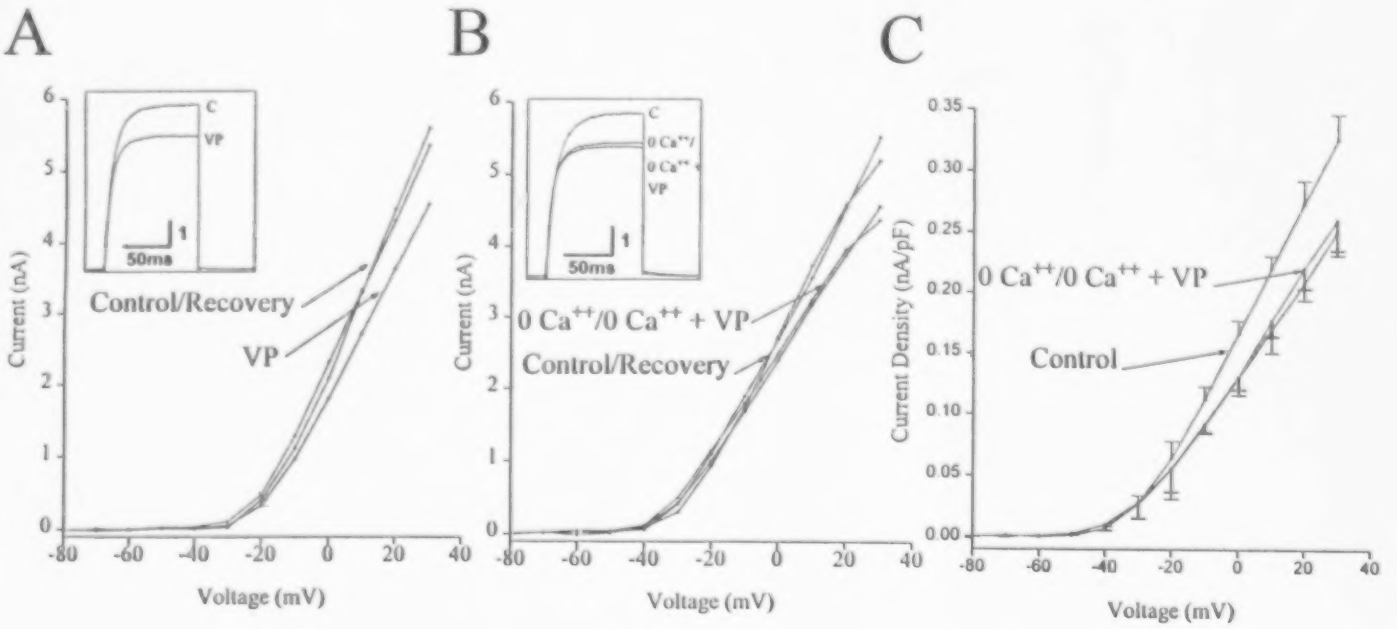
A
B
C
Current (nA)
Voltage (mV)
Control/Recovery
VP
0 Ca++/0 Ca++ + VP
Current Density (nA/pF)
Control
50ms
1

Figure 5-9. Blockade of Ca^{++}-influx blocked VP-induced increase in outward current. **A.** A typical I-V relationship depicting a VP-induced increase in outward currents in an hDBB neuron (similar to that shown in Fig. 5-5A). **B.** I-V plot of the currents evoked under control conditions, and in 0 Ca^{++} external solution in the presence and absence of VP. This graph illustrates that in the absence of Ca^{++} influx, VP response was blocked. Inset shows the currents evoked by applying voltage steps from -80mv (holding potential) to +30mV under control conditions (C), in 0 Ca^{++}, and 0 Ca^{++} with VP. **C.** Current density-voltage plots obtained from 9 cells under conditions, and in 0 Ca^{++} external solution in the presence and absence of VP.

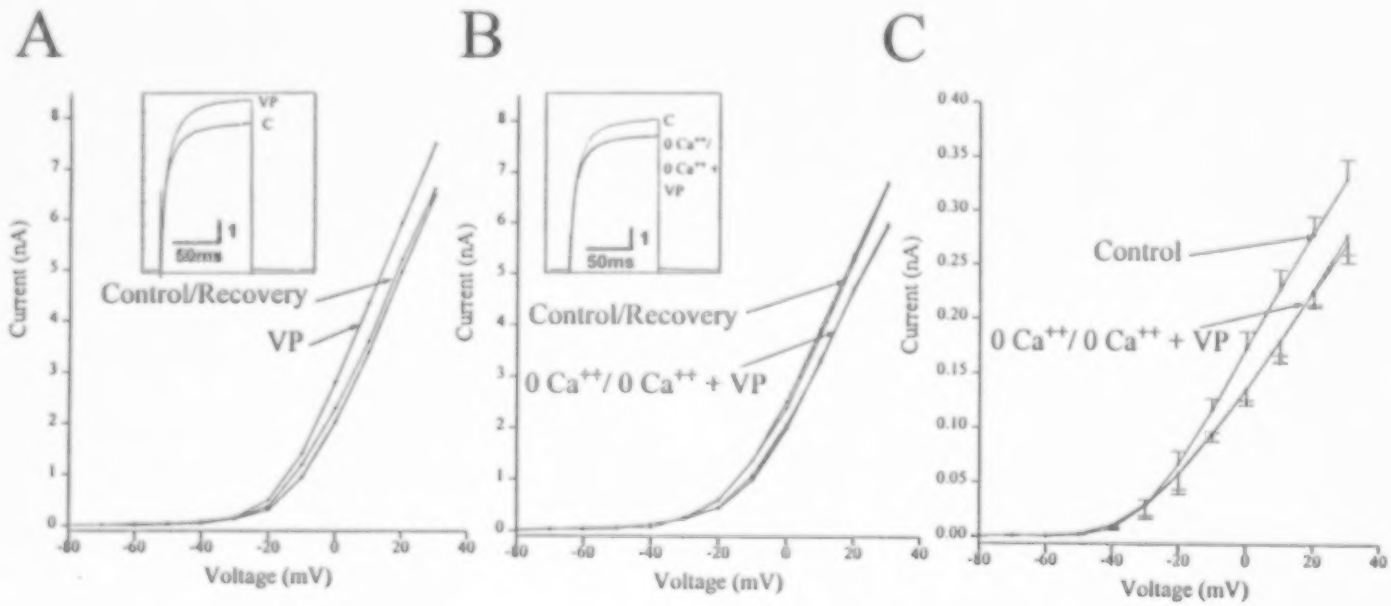
A
B
C
VP
C
50ms
Control/Recovery
VP
Current (nA)
Voltage (mV)
C
0 Ca++/
0 Ca++ +
VP
50ms
Control/Recovery
0 Ca++/ 0 Ca++ + VP
Current (nA)
Voltage (mV)
Control
0 Ca++/ 0 Ca++ + VP
Current (nA)
Voltage (mV)

Figure 5-10. CTX (25nM) blocked VP-mediated decrease in outward currents. A. I-V plots depicting a decrease in outward currents by VP in a representative hDBB cell. **B.** I-V relationships of the currents evoked under control conditions, and CTX in the presence and absence of VP. CTX eliminated the decrease in outward currents elicited by VP **C.** Current density-voltage relationships obtained from 8 cells illustrating that VP failed to decrease outward currents in the presence of CTX.

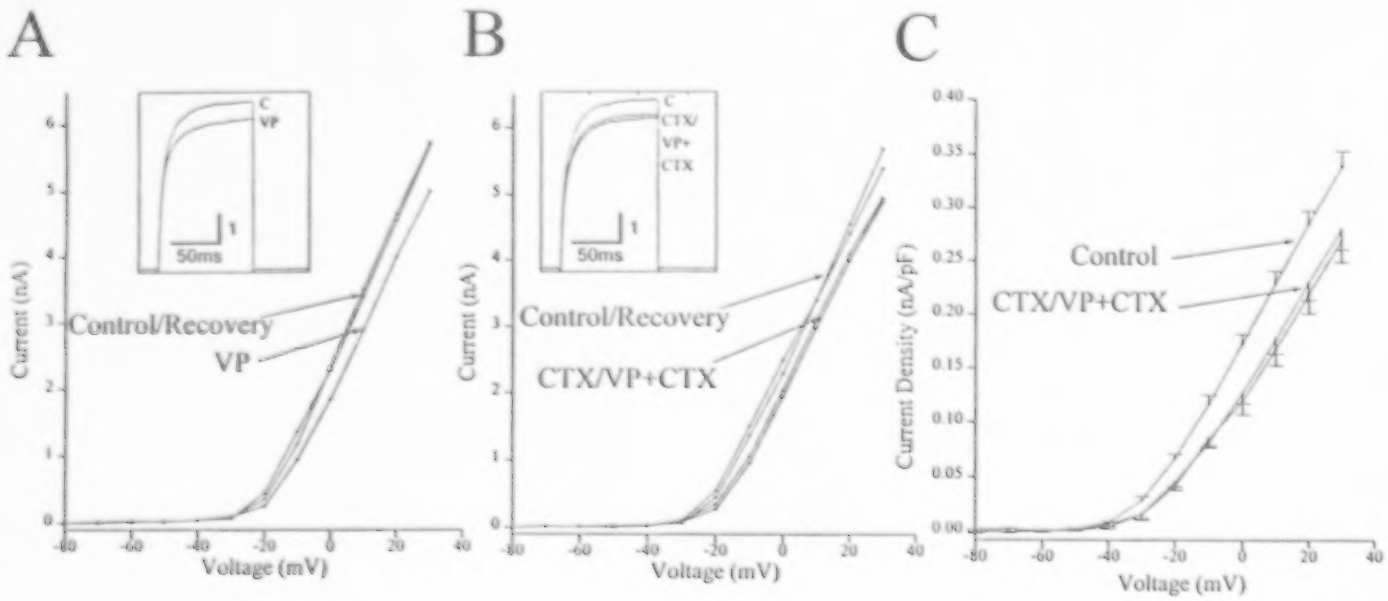
A
B
C
Current (nA)
Voltage (mV)
Control/Recovery
VP
CTX/VP+CTX
50ms
Current Density (nA/pF)
Control
CTX/VP+CTX

Figure 5-11. CTX (25nM) blocked VP-mediated increase in outward currents. **A.** I-V plots depicting an increase in outward currents by VP in a representative hDBB cell. **B.** I-V relationships of the currents evoked under control conditions, and CTX in the presence and absence of VP. CTX eliminated the increase in outward currents elicited by VP **C.** Current density-voltage relationships obtained from 9 cells illustrating that VP failed to increase outward currents in the presence of CTX.

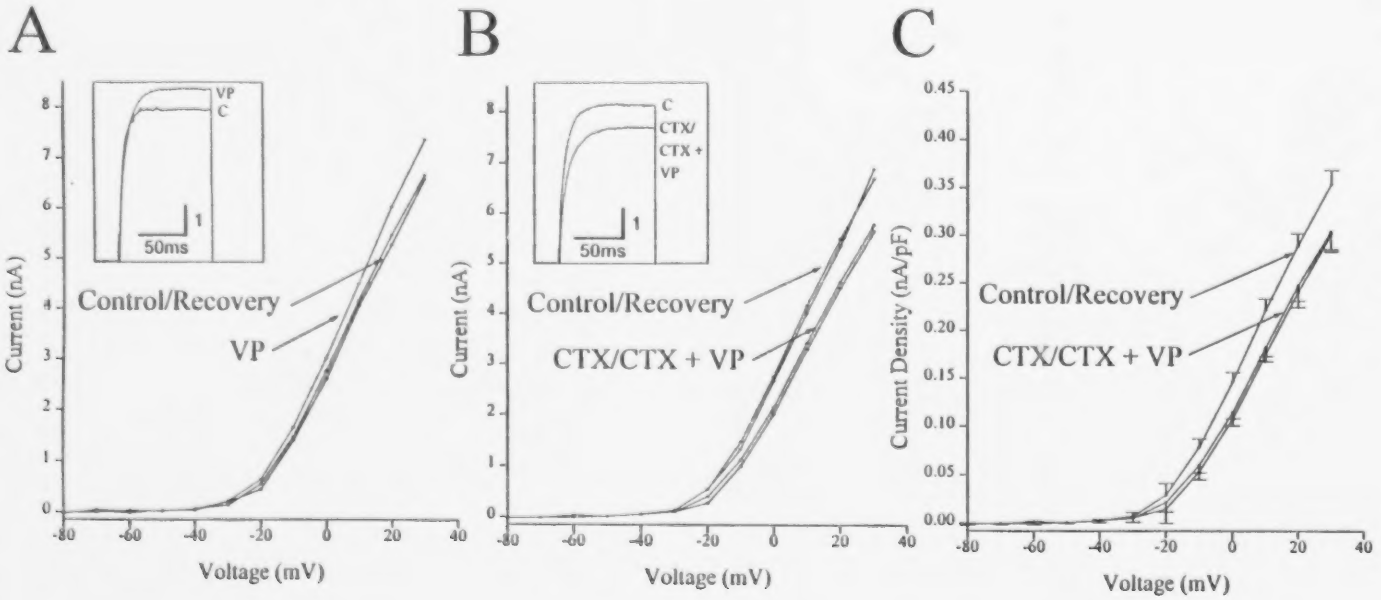
A
B
C
VP
C
50ms
1
Control/Recovery
VP
Current (nA)
Voltage (mV)
C
CTX/
CTX +
VP
CTX/CTX + VP
Current Density (nA/pF)

Figure 5-12. VP does not affect barium currents (I_{Ba})in hDBB neurons. I_{Ba} was evoked in 14 cells by applying depolarizing voltage steps from a holding potential of -80mV to +70mV (increment 10mV/step; 20ms). Steady state currents were plotted against command voltage. I-V relationships obtained under control conditions and in the presence of VP demonstrate that VP does not affect I_{Ba}.

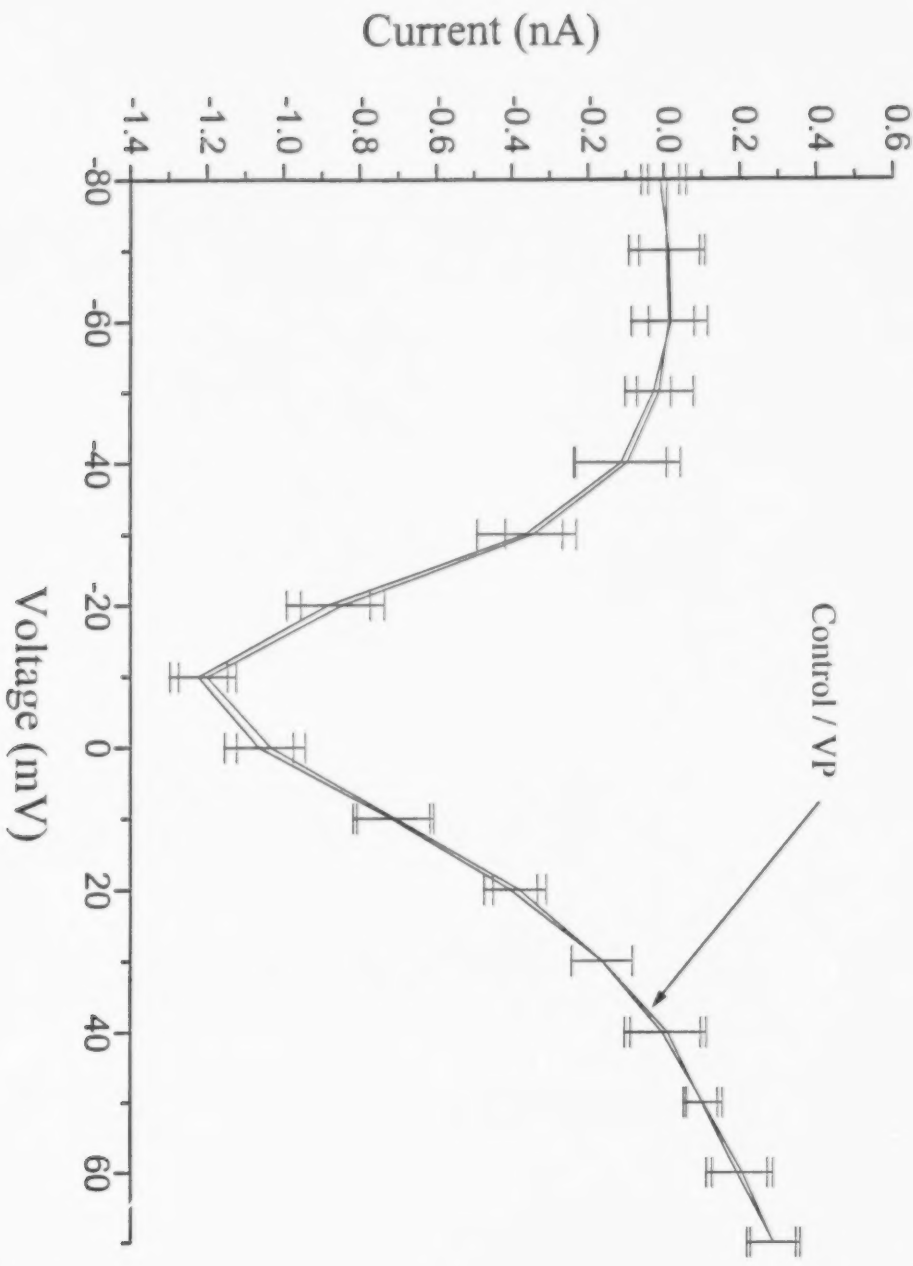
Current (nA)
0.6
0.4
0.2
0.0
-0.2
-0.4
-0.6
-0.8
-1.0
-1.2
-1.4
-80
-60
-40
-20
0
20
40
60
Voltage (mV)
Control / VP

REFERENCES

Abe, H., Inoue, M., Mats, T., Ogata, N. The effects of vasopressin on electrical activity in the guinea-pig supraoptic nucleus *in vitro*. *J. Physiol.* 337:665-685, 1983.

Adams, P. R., Brown, D. A., and Constanti, A. M-currents and other potassium currents in bullfrog sympathetic neurones. *J. Physiol.* 330:537-572, 1982.

Assaf, S. Y. and Chung, S. -H. Release of endogenous Zn^{2+} from brain tissue during activity. *Nature* 308:734-736, 1984.

Augustine, G.J., Charlton, M.P. Calcium dependence of presynaptic calcium currents and postsynaptic response at the squid giant axon. *J.Physiol.* 381: 619-640, 1986.

Baertschi, A.J. and Friedli, M. A novel type of vasopressin receptor on anterior pituitary corticotrophs? *Endocrinol.* 116:499-502, 1985.

Bargmann,W. and Scharrer, H. The site of origin of the homrones of the posterior pituitary. *Amer. Scient.* 39, 255-259, 1951.

Beaulieu, C., Dyck, R., and Cynader, M. Enrichment of glutamate in zinc-containing terminals of the cat visual cortex. *Neuroreport* 3:861-864, 1992.

Belluzzi, O., Sacchi, O., and Wanke, E. A fast transient outward current in the rat sympathetic neurone studied under voltage-clamp conditions. *J. Physiol.* 358:91-108, 1985a.

Belluzzi, O., Sacchi, O., and Wanke, E. Identification of delayed potassium and calcium currents in the rat sympathetic neurone under voltage clamp. *J. Physiol.*358:109-129, 1985b.

Bone, E.A., Fretten, P., Palmer, S., Kirk, C.J., Mitchell, R.H. Rapid accumulation of inositol

phosphates in isolated rat superior cervical sympathetic ganglia exposed to V_1-receptor and muscarinic cholinergic stimuli. *Biochem J.*, 221:803-811, 1984.

Bourque, C.W. and Brown, D.A. Apamin and d-tubocurarine block the afterhyperpolarization of rat supraoptic neurosecretory neurons. *Neurosci. Lett.* 82(2): 185-190, 1987.

Brinton, R.D. and Brownson, E.A. Vasopressin-induction of cyclic AMP in cultured hippocampal neurons. *Dev. Br. Res.* 71:101-105, 1993.

Busselberg, D., Evans, M. L., Rahmann, H., and Carpenter, D. O. Lead and Zinc block a voltage-activated calcium channel of *Aplysia* neurons. *J. Neurophys.* 65(4):786-795, 1991.

Busselberg, D., Michael, D., Evans, M. L., Carpenter, D. O., and Haas, H. L. Zinc blocks voltage gated calcium channels in cultured rat dorsal rool ganglion cells. *Brain Res.* 593:77-81, 1992.

Caffe, A.R., Van Ryen, P.C., Van der Woude, T.P., Van Leeuwen, F.W. Vasopressin and oxytocin systems in the brain and upper spinal cord of *Macaca fascicularis*. *J.Comp.Neurol.* 287(3):302-325, 1989.

Cheng, S.W., and North, W.G. Vasopressin reduces release from vasopressin-neurons and oxytocin-neurons by actingon V2-like receptors. *Br. Res.* 479(1):35-39, 1989.

Choi, D. W., Yokoyama, M., and Koh, J. Zinc neurotoxicity in cortical cell culture. *Neurosci.* 24:67-79, 1988.

Chrobak, J.J., Stackman, R.W., Walsh, T.J. Intraseptal administation of muscimol produces dose-dependent memory impairments in the rat. Beh. Neural Biol. 52(3):357-369,

1989.

Conner, J. A. and Stevens, C. F. Voltage clamp studies of a transient outward membrane current in gastropod neural somata. *J. Physiol.* 299:289-307, 1971.

Constanti, A. and Smart, T. G. Zinc blocks the A-current in cultured rat sympathetic neurones. *J. Physiol.* 396:159P, 1987.

Constantinidis, J. Hypothesis regarding amyloid and zinc in the pathogenesis of Alzheimer disease: potential for preventive intervention. *Alzhiemer Disease and Associated Disorders* 5(1):31-35, 1991.

DeWeid, D. Long term effect of vasopressin on the maintencance of a conditioned avoidance response in rats. *Nature* 232:58-60, 1971.

Dorsa, D.M., Brot, M.D., Shewey, L.M., Meyers, K.M. Szot, P. And Miller, M.A. Interaction of a vasopressin antagonist with vasopressin receptors in the septum of the rat brain. *Synapse*. 2:205-211, 1988.

Duncan, M. W., Marini, A. M., Watters, R., Kopin, I. J., and Markey, S. P. Zinc, a neurotoxin to cultured neurons, contaminates cycad flour prepared by traditional Guamanian methods. *J. Neurosci.* 12:1523-1537, 1992.

Ebadi, M., Iverson, P. L., Hao, R., Cerutis, D. R., Rojas, P., Happe, H. K., Murrin, L. C., and Pfeiffer, R. F. Expression and regulation of brain metallothionein. *Neurochem. Int.* 27(1):1-22, 1995.

Erdelyi, L. Zinc modulates A-type potassium currents and neuronal excitability in snail neurons. Cellular and Molecular Neurobiology 14(6):689-700, 1994.

Frankenhauser, B. and Hodgkin, A. L. The action of calcium on the electrical properties of

squid axons. *J. Gen. Physiol.* 137:218-244, 1957.

Frederickson, C. J., Hernandez, M. D., Goik, S. A., Morton, J. D., and McGinty, J. D. Loss of zinc staining form hippocampal mossy fibers during kainic acid induced seizure: a histofluorescence study.. *Brain Res.* 446:383-386, 1988.

Frederickson, D. J., Klitenick, M. A., Manton, W. I., and Kirkpatrick, J. B. Cytoachitechtronic distribution of zinc in the hippocampus of man and the rat. *fr* 273:335-339, 1983.

Friedman, B. and Price, J. L. Firber systems in the olfactory bulb and cortex: A study in adult and developing rats, using the Timm method with the light and electron microscope. *J. Comp. Neurol.* 223:88-109, 1984.

Frye, G. D., Fincher, A. S., Grover, C. A., and Griffith, W. H. Interaction of ethanol and allosteric modulators with $GABA_A$-activated currents in adult medial septum/diagonal band neurons. *Brain Res.* 635:283-292, 1994.

Gerstberger, R. And Fahrenholz., F. Autoradiographic localization of V_1 vasopressin binding sites in rat brain and kidney. *Eur. J. Pharmacol.* 167:105-116, 1989.

Gilly, W. M. F. and Armstrong, C. M. Divalent cations and the activation kinetics of potassium channels in squid giant axons. *J. Gen. Physiol.* 79:965-996, 1982.

Gilly, W. M. F. and Armstrong, C. M. Slowing of sodium channel opening kinetics in squid axon by extracellular zinc. *J. Gen. Physiol.* 79:935-964, 1982.

Givens, B.S. and Olton, D.S. Cholinergic and GABAergic modulation of medial septal area: effect on working memory. *Beh. Neurosci.* 104(6):849-855, 1990.

Goh, J. W., Kelly, M. E., and Pennefather, P. S. Electrophysiological function of the delayed

rectifier (I_K) in bullfrog sympathetic ganglion neurones. *Pflugers Arch Eur. J. Physiol.* 413(5):482-486, 1989.

Goh, J.W., Kelly, M.E, Pennefather, P.S, Chicchi, G.G., Cascieri, M.A., Garcia, M.L., Kaczorwski, G.J. Effect of chaybdotoxin and leuirotoxin on potassium currents in bullfrog sympathetic ganglion and hippocampal neurons. *Br. Res.* 59(1):165-170, 1992.

Griffith, W. H. and Sim, J. A. Comparison of 4-aminopyridine and tetrahyroaminoacridine on basal forebrain neurons. *J. Pharm. Exp. Ther.* 255(3):986-993, 1990.

Harrison, N. L. and Gibbons, S. J. Zn^{2+}: an endogenous modulator of ligand- and voltage-gated ion channels. *Neuropharm.* 33(8):935-952, 1994.

Holm, I. E., Andreasen, A., Danscher, G., Perez-Clausell, J., and Nielsen, H. Quantification of vesicular zinc in the rat brain. *Histochem.* 89:289-293, 1988.

Huang, R., Peng, Y., and Yau, K. Zinc modulation of a transient potassium current and histochemical localization of the metal in neurons of the suprachiasmatic nucleus. *PNAS* 90:11806-11810, 1993.

Ibata, Y. and Otsuka, N. Electron microscope demonstration of zinc in the hippocampal formation using Timm's sulphide silver technique. *J. Hist. Cyto.* 17:171-175, 1969.

Jard, S. Vasopressin isoreceptors in mammals: Relation to cyclic AMP-independent transduction mechanisms. *Curr. Topics membr. Transp.* 18:255-285, 1983.

Jassar, B. S. and Jhamandas, J. H. Effects of neurotensin on acutely dissociated neurons from the horizontal limb of the diagonal band of Broca (hDBB) in the rat. *Soc. Neurosci. Abstr.* 21:90, 1995.

Jassar, B. S., Pennefather, P. S., and Smith, P. A. Changes in sodium and calcium channel activity following axotomy of B-cells in bullfrog sympathetic ganglion. *J. Physiol.* 472:203-231, 1993.

Jassar, B. S., Pennefather, P. S., and Smith, P. A. Changes in potassium channel activity following axotomy of B-cells in bullfrog sympathetic ganglion. *J. Physiol.* 479(Pt 3):353-370, 1994.

Jhamandas, J. H. and Renaud, L. P. A GABA-mediated baroreceptor input to supraoptic vasopressin neurones in the rat. *J. Physiol.* 381:595-606, 1986a.

Jhamandas, J. H. and Renaud, L. P. Diagonal band neurons may mediate arterial baroreceptor input to hypothalamic vasopressin-secretin neurons. *Neurosci. Lett.* 65:214-218, 1986a.

Johnston, A.R., MacLeod, N.K., Dutia, M.B. Ionic conductances contributing to repolarizationand after protentials in rat medial vestibular neurons. *J. Physiol.* 481(1):61-77, 1994.

Jurzak,M., Muller, A.R., and Gerstberger, R. Characterization of vasopressin receptors in cultured cells derived from the region of rat brain circumventricular organs. *Neurosci.* 65(4):1145-1159, 1995.

Kang, J., Richards, E.M., Posner, P. And Sumners, C. Modulation of the delayed rectifier K^{++} current in neurons by an angiotensin II type 2 receptor fragment. *Am. J. Physiol.* 268(Cell Physiol. 37):C278-C282, 1995.

Kesner, R. P., Berman, R. F., and Tardif, R. Place and taste aversion learning: role of basal forebrain, parietal cortex, and amygdala. *Br. Res. Bull.* 29:345-353, 1992.

Kirk, C.J. and Mitchell, R.H. Phosphatidylinositol metabolism in rat hepatocytes stimulated by vasopressin. Biochem J. 194:155-165, 1981.

Kiss, T. and Osipenko, O. Metal ion-induced permeability changes in cell membranes: a minireview. *Cellular and Molecular Neurobiology* 14(6):781-789, 1994.

Koh, J. and Choi, D. W. Zinc alters excitatory amino acid neurotoxicity on cortical neurons. *J. Neurosci.* 8:2164-2171, 1988.

Landgraf, R., Ramirez, A.D., Ramirez V.D. The positive feedback action of vasopressin on its own release from rat septal tissue *in vitro* is receptor-mediated. *Br. Res.* 545:137-141, 1991.

Ma, M. and Koester, J. Consequences and mechanics of spike broadening of R20 cells in *Aplysia californica*. *J. Neurosci.* 15(10):6720-6734, 1995.

Mandava, P., Howell, G. A., and Frederickson, C. J. Zinc-containing neuronal innervation of the septal nuclei. *Brain Res.* 608:115-122, 1993.

Miralles, F., Canti, C., Marsal, J., Peres, J., and Solsona, C. Zinc ions block rectifier potassium channels and calcium activated potassium channels at the frog motor nerve endings. *Brain Res.* 641(2):279-284, 1994.

Moos, T. Simultaneous application of Timm's sulphide silver method and immunofluorescence histochemistry. *J. Neurosci. Meth.* 48:149-156, 1993.

Morel, A., O'Carroll, A.M., Brownstein, M.J. and Lolait, S.J. Molecular cloning and expression of a rat V_1 arginine vasopressin receptor. *Nature* 356:523-526, 1992.

Noszyczyk, B., Lon, S., and Szdzepanska-Sadowska,S. Central cardiovascular effects of AVP and AVP analogs with V_1, V_2, and "V_3" agonistic or antagonist properties in

conscious dog. *Brain Res.* 610:115-126, 1993.

Palouzier-Paulignan, B., Dubois-Dauphin, M., Tribollet, E., Dreifuss, J.J., Ragenbass, M. Action of vasopressin on hypoglossal motoneurons of the rat: presynaptic and postsynaptic effects. *Br. Res.* 650:117-126, 1994.

Paolini, A. G. and Mckenzie, J. S. Effects of lesions in the horizontal diagonal band nucleus on olfactory habituation in the rat.. *Neurosci.* 57(3):717-724, 1994.

Penner, R., Pusch, M., and Neher, E. Washout phenomena in dialyzed mast cells allow discrimination of different steps in stimulus-secretion coupling. *Biosci. Reports* 7(4):313-321, 1987.

Perez-Clausell, J., Frederickson, C. J., and Danscher, G. Amygdaloid efferents through the stria terminalis in the rat give origin to zinc-containing boutons. *J. Comp. Neurol.* 290(2):201-212, 1989.

Pittman, Q.J., Naylor, A., Poulin, P., Disturnal, J., Veale, W.L., Martin, S.M., Malkinson, T.J., and Mathieson, B. The role of vasopressin as an antipyretic agent in the ventral septal area and its possible involvement in convulsive disorders. *Brain Res. Bull.* 20, 887-892, 1988.

Pohle, W. and Rauca, C. Hypoxia protects against the neurotoxicity of kainic acid. *Brain Res.* 644:297-304, 1994.

Raggenbass, M., Goumaz, M., Sermasi, E., Tribollet, E., and Dreifuss, J.J. Vasopressin generates a persistent voltage-dependent sodium current in a mammalian motoneuron. *J.Neurosci.* 11(6):1609-1616, 1991.

Robitaille, R., Garcia, M.L., Kaczorowski, G.J., Charlton, M.P. Functional colocalization

of calcium and calcium-gated potassium channels in control of transmitter release. Neuron 11(4):465-655, 1993.

Roman, F. S., Simonetto, I., and Soumireu-Mourat, B. Learning and memory of odor-reward association: selective impairment following horizontal diagonal band lesions. *Behav. Neurosci.* 107(1):72-81, 1993.

Rudy, B. Diversity and ubiquity of K channels. *Neurosci.* 25:729-749, 1988.

Sah, P., McLachlan, E.M. Potassium currents contributing to the action potential repolarization and the afterhyperpolarization in rat vagal motoneurons. *J. Neurophys.* 68(5):1834-1841, 1992.

Shewey, L.M. and Dorsa, D.M. V_1-type vasopressin receptors in rat brain septum: binding characteristics and effects on inositol phospholipid metabolism. *J. Neurosci.* 8:1671-1677.

Smart, T. G., Xie, X., and Krishek, B. J. Modulation of inhibitory and excitatory amino acid receptor ion channels by zinc. *Prog. Neurobiol.* 42:393-441, 1994.

Sorensen, J. C., Slomianka, L., Christensen, J., and Zimmer, J. Zinc-containing telencephalic connections to the rat striatum: a combined Fluoro-Gold tracing and histochemical study. *Exp. Brain. Res.* 105:370-382, 1995.

Spires, S. and Begenish, T. Chemical properties of the divalent cation binding site on potassium channels. *J. Gen. Physiol.* 100:181-193, 1992.

Standen, N. B. Separation and analysis of ionic currents. In: *Microelectrode Techniques: The Plymouth Workshop Handbook*, edited by N. B. Standen, P. T. A. Gray and M. J. Whitaker. Cambridge: The Company of Biologists, Ltd., 1988, p. 29-40.

Takahashi, K. and Aaike, N. Calcium antaonist effects on low-threshold (T-type) calcium current in rat isolated hippocampal CA1 pyramidal neurons. *PNAS* 256:169-175, 1991.

Talukder, G. and Harrison, N. L. On the mechanism of modulation of transient outward current in cultured rat hippocampal neurons by di- and trivalent cations. *J. Neurophys.* 73(1):73-79, 1995.

Ulfig, N., Braak, E . Ohm, T., and Pool, C.W. Vasopressinergic neurons in the magnocellular nuclei of the human basal forebrain. *Brain Res.* 530:176-180, 1993.

Urban, I.J.A. and DeWied, D. Effect of vasopressin, oxytocin and peptides derived from these hormones on field potential induced in lateral septum of rats by stimulation of the fimbria fornix. *Neuropeptides* 7:41-49, 1986.

van Eerdenburg, F.J.C.M., Pittman, Q.J. Vasopressin modulates glutamate action in the medial septum and diagonal band of Broca of the rat. Soc. Neurosci. Abstr. 17:805, 1991.

Viana, F., Bayliss, D. A., and Berger, A. J. Multiple potassium conductances and their role in action potential repolarization and repetitive firing behavior of neonatal rat hypoglossal motoneurons. *J. Neurophysiol.* 69(6):2150-2163, 1993.

Wallwork, J. C. Zinc and the central nervous system. *Prog. Food Nutr. Sci.* 11(2):203-247, 1987.

Walsh, K. B., Cannon, S. D., and Wuthier, R. E. Characterization of a delayed rectifier potassium curent in chicken growth plate chondrocytes. *Am.J.Physiol.* 262(5 Pt 1):C1335-C1340, 1992.

Weiss, J. H., Hartley, D. M., Koh, J. Y., and Choi, D. W. AMPA receptor activation potentiates zinc neurotoxicity. *Neuron* 10(1):43-49, 1993.

White, J. A., Alonso, A., and Kay, A. R. A heart like Na^+ current in the medial entorhinal cortex. *Neuron* 11:1037-1047, 1993.

Womble, M.D. and Moises, H.C. Muscarinic modulation of conductances underlying the afterhyperpolarization in neurons of the rat basolateral amygdala. Br. Res. 621(1):87-96, 1993.

Wu, R. L. and Barish, M. E. Two pharmacologically and kinetically distinct transient potassium currents in cultured embryonic mouse hippocampal neurons. *J. Neurosci.* 12(6):2235-2246, 1992.

Zhang, L. and McBain, C. J. Potassium conductances underlying repolarization and afterhyperpolarization in rat CA1 hippocampal interneurons. *J. Physiol* 488(3):661-672, 1995.

CHAPTER 6

ZINC MODULATION OF IONIC CURRENTS IN THE HORIZONTAL LIMB OF THE DIAGONAL BAND OF BROCA (hDBB)

ABSTRACT

Zinc (Zn^{++}) is an endogenous cation within the brain. While it subserves important physiological roles, it may also mediate various pathophysiological processes underlying conditions such as Alzheimer's disease (AD). The horizontal limb of the diagonal band of Broca (hDBB) is a basal forebrain region that is severely affected in Alzheimer's disease (AD). In this study, we examined the ability of Zn^{++} to modulate ionic currents in acutely dissociated hDBB neurons using the whole cell patch clamp technique.

50μM Zn^{++} increased the amplitude of the transiently-activated potassium current, I_A by over 300pA (n=27). This response was reversible and could be reproduced in 0 Ca^{++}/1μM TTX (n=15). Analysis of the activation and inactivation characteristics of I_A revealed that Zn^{++} shifts the inactivation curve to the right (n=11) and has no effect on the activation of this current (n=15). In contrast to its effects of I_A, Zn^{++} reduced the amplitude of the delayed rectifier potassium current (I_K). In 16 neurons, Zn^{++} reduced I_K by over 600pA. This reduction was reproducible when cells were perfused with an ACSF solution lacking Ca^{++} and containing 1μM TTX. These observations indicate that Zn^{++} is a potent modulator of potassium currents in hDBB neurons.

Zn^{++} also reduced the amplitude of sodium currents (I_{Na}) in these cells. This reduction was modest (~10%) but observed in every cell examined (n=10). This response could be blocked by 1μM TTX.

Zn^{++} potently modulated currents passing through calcium channels. Using Ba^{++} as the charge carrier, Zn^{++} reversibly reduced I_{Ba} by 85% (n=14). This reduction has important implications in hDBB neurons as blockade of calcium currents would also result in a

significant attenuation of calcium-dependent potassium currents.

These results demonstrate that Zn^{++} is a potent modulator of ionic currents within the hDBB.

INTRODUCTION

With the exception of Ca^{++} and Mg^{++}, the transition metal, zinc (Zn^{++}) is the most abundant divalent cations in the brain (Ebadi et al., 1995).This divalent cation mediates important roles in various intra- and intercellular physiological processes. Its integral roles as a cofactor and structural component in several enzymatic proteins are well documented (Wallwork, 1987; Kiss and Osipenko, 1994). The histological identification of Zn^{++} within central neurons and nerve terminals prompted investigators to examine possible neuromodulatory actions of this cation (Ibata and Otsuka, 1969; Friedman and Price, 1984; Holm et al., 1988). Subsequent studies demonstrated that Zn^{++} fulfills many of the requirements of a neuromodulatory compound as it is localized in terminals (Sorensen et al., 1995), released from terminals in a Ca^{++}-dependent manner (Assaf and Chung, 1984), and exerts actions at postsynaptic sites (Harrison and Gibbons, 1994). There is considerable evidence to indicate that Zn^{++} modulates the activity of several voltage-gated ion channels. These include the delayed rectifier (I_K)(Gilly and Armstrong, 1982) and the transiently activating K^+ currents (I_A)(Talukder and Harrison, 1995; Huang et al., 1993; Constanti and Smart, 1987). In addition, Zn^{++} also influences sodium currents (I_{Na})(Gilly and Armstrong, 1982), and calcium currents (I_{Ca}) (Kiss and Osipenko, 1994; Busselberg et al., 1992; Busselberg et al., 1991). Thus, Zn^{++} appears to function as a potent regulator of neuronal excitability within the CNS.

In addition to its physiological roles, Zn^{++} is also implicated in neurological disorders such as AD. In high concentrations, Zn^{++} is consistently neurotoxic to neurons (Koh and Choi, 1988; Duncan et al., 1992; Choi et al., 1988). This metal is principally localized in

glutamate-containing cells (Moos, 1993; Beaulieu et al., 1992) and, in some cases, potentiates the excitotoxic effects of glutamatergic agonists on neurons (Weiss et al., 1993). Furthermore, as shown by postmortem examination of brains from patients afflicted with epilepsy (Frederickson et al., 1988), Zn^{++} levels are also decreased in AD (Constantinidis, 1991). The loss of Zn^{++} observed under neuropathological examination may arise due to excessive stimulation of the Zn^{++}-containing terminals which would result in a depletion of this ion within the neuropil (Pohle and Rauca, 1994). Thus, although Zn^{++} appears to serve important physiological processes under normal conditions, in certain neuropathological conditions this cation can be neurotoxic.

Zn^{++}-positive fibers permeate the basal forebrain which is the region most severely afflicted in AD (Perez-Clausell et al., 1989; Mandava et al., 1993). The horizontal limb of the diagonal band of Broca (hDBB), a basal forebrain region, is an important site in memory and learning processes (Roman et al., 1993; Kesner et al., 1992) and is particularly susceptible to neuronal death in AD (Paolini and Mckenzie, 1994). In this study, we have endeavored to characterize Zn^{++}-mediated neuromodulation of voltage-gated ionic currents in hDBB cells to gain insight into how this metal may be of physiological significance in this region.

RESULTS

hDBB neurons contain a variety of ionic conductances. We have examined actions of Zn^{++} on I_A, I_K, I_{Na}, and I_{Ba} on 81 acutely dissociated hDBB neurons. The cells from which recordings were made had an average membrane capacitance of 17.9±1.3pF.

Zn^{++} effects on A-current

We examined the effects of Zn^{++} on the transiently activated outward K^+ current, I_A, in hDBB cells. Since activation of I_A is a voltage and time-dependent process, it is possible to isolate I_A from the other ionic currents by utilizing its unique biophysical characteristics. I_A was studied using a voltage protocol modified from protocols of Connor and Stevens (1971), Belluzzi et al. (1985) and Standen (1988) (inset of Fig. 6-1A). Cells were hyperpolarized from a holding potential of -80 to -120mV for 150ms to remove inactivation of I_A. Subsequent depolarization from -40mV (increment 10mV to a maximum of +30mV/step; duration 100ms) was applied to evoke voltage-activated currents. Currents evoked by this protocol include I_A, I_K, I_{Na}, and I_{Ca} (Fig. 6-1). The second protocol utilized is shown in the inset of Fig. 6-1B. Cells were depolarized from a holding level of -80mV to -40mV for 150ms, and then stepped to a command voltage of -40mV for 100ms (increment 10mV/step to a maximum of 30mV). Since I_A inactivates beyond -50mV, the current generated by the second protocol lacked I_A but still contains I_K, I_{Na}, and I_{Ca} all of which activate at potentials depolarized to -40mV (Fig. 6-1B)(Belluzzi et al., 1985; Adams et al., 1982; Jassar et al., 1993). The currents generated by the second protocol (Fig. 6-1B) were subtracted from those elicited by the first protocol (Fig. 6-1A) to obtain a relatively pure I_A (Fig. 6-1C_1). When this protocol was applied in the presence of 50μM of Zn^{++}, an increase in the amplitude of I_A was observed (Fig. 6-1C_2). The effect of Zn^{++} was fully reversible as the currents returned to control levels within 10 minutes after the perfusion of solution was changed to normal ACSF (Fig. 6-1C_3).

It is possible that the increase in I_A may actually be the result of Zn^{++} modulation of

non-potassium currents, namely I_{Na} and I_{Ca}. To address this issue, it was necessary to examine Zn^{++} modulation of I_A in the absence of Ca^{++} and Na^+ influx (Huang et al., 1993). Na^+ and Ca^{++} influx into hDBB neurons can be completely blocked by exogenous perfusion of 1μM TTX and Ca^{++}-free extracellular medium, respectively. The effect of blocking these ionic fluxes on Zn^{++}-mediated enhancement of I_A is illustrated in Fig. 6-2 which shows the peak I_A evoked in each step using the protocol shown in Fig. 6-1 plotted versus command voltage. Averaged data from 27 hDBB neurons is shown in Fig. 6-2A. The peak I_A at +30mV was 2.20±0.08nA under control conditions. In the presence of Zn^{++}, outward current at +30mV increased to 2.57±0.11nA ($P<0.01$). Fig. 6-2B is the averaged data from 15 cells where I_A was studied in 0 Ca^{++}/1μM TTX solutions in in the presence and absence of Zn^{++}. Under these recording conditions, the Zn^{++}-induced increase in I_A was observed (0 Ca^{++} + 1μM TTX: peak=2.20±0.07nA; 0 Ca^{++} + 1μM TTX +Zn^{++}: peak=2.53±0.09nA; $P<0.01$). The magnitude of the potentiation by Zn^{++} was similar in control conditions and in the presence of TTX/0 Ca^{++}. These data support the contention that Zn^{++} increased I_A independently of any modulation of I_{Na} and I_{Ca}.

The effects of Zn^{++} on the activation and inactivation kinetics of I_A were also examined. The voltage protocol used to investigate whether Zn^{++} modulated the activation of I_A is shown in the inset of Fig. 6-3A. Cells were initially held at -80mV, hyperpolarized to -100mV for 1s, then depolarized for 2s (increment 15mV per step), and returned to -80mV. The maximum depolarizing step was +65mV. The currents evoked by each step command were normalized to the peak currents in 14 cells and plotted against the command voltage. The activation curve (Fig. 6-3A) was fitted with Boltzmann's equation. The half-

activation voltage (V_a) was -2.3±2.6mV and the current increased e-fold per 18.0±1.9mV under control conditions. The presence of Zn^{++} in the external solution did not significantly affect V_a (-4.8±2.5mV; P>0.5) or the voltage gradient required for e-fold change in current (e-fold per 16.7±1.8mV; P>0.5). Thus, Zn^{++} did not affect activation of I_A in hDBB neurons.

The inactivation characteristics of I_A in these cells were identified using the following voltage protocol: from a holding potential of -80mV, a conditioning step to -110mV (increment 15mV/step) was applied for 900ms, followed by a depolarizing step to +55mV for 100ms. The normalized current from 11 cells was plotted versus conditioning voltage commands and fitted using the Boltzmann equation. Under control conditions, the half-inactivation (Fig. 6-3B) voltage was -76.4±2.2mV and current changed e-fold per 12.9±1.1mV. There was a significant shift to the right in the presence of Zn^{++} as the half-inactivation voltage was -53.4±2.0mV (P<0.001) and current changed e-fold per 7.2±2.0mV (P<0.02).

Modulation of I_K by Zn^{++}

The voltage protocol used in Fig. 6-1B elicits outward currents mediated principally by delayed rectifier (I_K) and calcium-activated K^+ currents ($I_{K(Ca)}$). The outward currents generated by this protocol were reduced in the presence of Zn^{++} (Fig. 6-4A_2) compared to those elicited under control conditions (Fig. 6-4A_1). Fig. 6-4b illustrates the difference currents from an hDBB neuron after currents evoked in the presence of Zn^{++} were subtracted from control currents. The difference currents represent the portion of I_K which was modulated by Zn^{++}. This response was observed in a total of 16 hDBB cells where Zn^{++} clearly reduced outward currents (Fig. 6-4B). To eliminate the possibility of contamination

of the outward currents by inward currents (I_{Na}, I_{Ca}) I_K was also evoked in a solution containing 0 Ca^{++} and 1μM TTX to occlude Ca^{++} and Na^+ influx. Since the other ionic fluxes are blocked, this current likely represents a more accurate representation of the Zn^{++}-induced decrease in I_K (Fig. 6-4C). Zn^{++} reduced I_K by approximately 600pA in this neuron. The Zn^{++}-mediated reduction of I_K was largely eliminated when 5mM TEA was added to the external solution. TEA at these concentrations is a highly potent blocker of I_K in these cells further confirming that Zn^{++} modulates I_K (Jassar and Jhamandas, 1995)(Fig. 6-4D).

Zn^{++} modulation of I_{Na}

Longer pulses used to evoke I_A and I_K provide a poor resolution (digital sampling rate: 6kHz) of the initial inward component of whole cell current that is principally mediated by Na^+. In order to examine whether these currents with early onset are subject to modulation by Zn^{++}, we used a higher digital sampling rate (111kHz). The currents evoked by brief depolarizing pulses (10mV increment/step) from -80 to +60mV under control conditions in a hDBB neuron are shown in Fig. 6-5A. When the same neuron was perfused with solution containing 50μM Zn^{++}, there was an obvious decrease in inward current (Fig. 6-5B). When the control currents were subtracted from currents elicited in the presence of Zn^{++}, the result was a bimodal I-V relationship (Fig. 6-5C). The first current was maximally activated within 0.5-1ms and the second appears to reach a maximum within 2.5-3ms (Fig. 6-5C; n=22). Application of TTX completely eliminated the first peak identifying it as a TTX-sensitive Na^+ current (Fig. 6-5D; n=8). The reason that Zn^{++}-induced decrease in Na^+ currents is in the positive direction is because control inward current (which has a negative value) subtracted from the Zn^{++}-induced reduction in inward current elicits a positive

difference current. For example, using the data from Fig. 6-6A and 6-6B, the I_{Na} at 0mV (time:2.74ms) is -2.20, but in Zn^{++}, this is reduced to -1.69nA therefore: (-1.69)-(-2.20)=+0.51nA. When this protocol was performed in the presence of 50μM 4-AP, the second peak was largely eliminated (Fig. 6-5E; n=5). A previous report suggests that 4-AP blocks I_A in guinea pig DBB cells (Griffith and Sim, 1990). However, in our preparation, 50μM 4-AP blocks both I_A and I_K. Since I_K is slower to activate, typically activated after 3ms (Belluzzi et al., 1985; Jassar et al., 1994), we postulate that 4-AP is only blocking I_A in this protocol. These results confirm our earlier observation that I_A is modulated by Zn^{++} and also suggest that I_{Na} is affected by Zn^{++}.

Neurons were perfused with an external ACSF and recorded using an internal solution designed to isolate I_{Na}. This current was evoked by voltage steps from -80 to +60mV (increment 10mV; 3ms/step) in the presence and absence of Zn^{++}. The data in Fig. 6-6A and 6-6B are from an individual hDBB cell where perfusion of a cell with Zn^{++} reversibly decreased peak I_{Na} compared to the control. Fig. 6-6C shows the average steady state currents obtained from 10 neurons plotted versus the command voltage steps. This I-V relationship indicates that the maximal decrease elicited by Zn^{++} occurs at 10mV (-4.63±0.24nA under control conditions and -4.28±0.24nA in the presence of Zn^{++}). This decrease is not significant (P>0.5).

Effects of Zn^{++} on I_{Ba}

Ba^{++} was used as the charge carrier in experiments examining the effects of Zn^{++} on currents through calcium channels. Depolarizing voltage steps from -80 to +70mV (increment 10mV; 20ms/step) were applied to voltage clamped hDBB cells under control

conditions and in the presence of Zn^{++}. Fig. 6-7A shows I_{Ba}-evoked in an hDBB neuron under control conditions. In this cell, I_{Ba} is reversibly attenuated by Zn^{++} (Fig. 6-7B and 6-7C). In Fig. 6-7B, the steady state currents from 12 cells were averaged and plotted against the command step voltages. Under control conditions, the peak I_{Ba} at -10mV was -1.03±.07nA. In the presence of Zn^{++}, I_{Ba} was attenuated by approximately 85% to -0.15±.05 nA at -10mV (Fig. 6-7B; n=14; $P<0.001$). This potent inhibition typically required ≤ 2 minutes to reach its maximum effect and recovered within 10 minutes. Activation and inactivation kinetics of calcium currents were not examined as there were very little calcium currents left following the application of Zn^{++}.

Effects of Zn^{++} on the discharge rate of APs in the forebrain slice

We examined the ability of Zn^{++} to modulate excitation of hDBB cells in forebrain slices using the whole cell patch clamp technique. APs were elicited by applying 800-1600ms depolarizing steps (0.03-0.15nA) to current clamped neurons. We observed that these neurons consistently increased their firing rate upon exposure to exogenously applied 50μM Zn^{++} (9/12 cells; Fig. 6-8A). In the remaining cells, Zn^{++} caused a reduction in the firing rate (3/12 cells; Fig. 6-8B).

DISCUSSION

We have characterized the actions of Zn^{++} on voltage-activated conductances in hDBB neurons. Our results provide evidence that Zn^{++} modulates I_A, I_K, I_{Na} and I_{Ca} in this nucleus. This is the first comprehensive analysis of the actions of Zn^{++} on currents through

K^+, Na^+, and Ca^{++} channels in a single neuronal system. These findings are now discussed in context of conductances that govern excitability of hDBB neurons and the potential physiological role of Zn^{++} modulation in this region of the brain.

Concentration of Zn^{++}

Previous reports have described that concentrations of Zn^{++} in the high millimolar range modulate neuronal ionic currents (Busselberg et al., 1991; Gilly and Armstrong, 1982). However, the highest concentration of Zn^{++} identified within the nerve terminals is 100-300μM (Frederickson et al., 1983; Assaf and Chung, 1984) and therefore it may be argued that these previous observations may be of dubious physiological relevance. Furthermore, at millimolar concentrations, Zn^{++} is thought to modulate ion channel activity via a non-specific screening of membrane surface charges (Frankenhauser and Hodgkin, 1957). One of the significant observations in this study is that Zn^{++} exerts its effects on these neurons at a relatively low concentration (50μM) which falls well within the concentration range of Zn^{++} identified in CNS neurons (Frederickson et al., 1983). The concentration of Zn^{++} utilized in the present study was also based, in part, on studies that have examined the actions of Zn^{++} on ligand (Smart et al., 1994) and voltage-gated channels (Huang et al. 1993) in other neuronal systems. At this low concentration, it is unlikely that Zn^{++} exerts a large charge screening effect (Busselberg et al. 1992; Kiss and Osipenko, 1994). Therefore, the observed effects of Zn^{++} on ionic conductances in the present study are likely physiologically relevant.

Zn^{++} modulation of A-current

Zn^{++} increased the amplitude of I_A in hDBB cells. When Ca^{++} and Na^+ influxes were blocked during depolarizing steps, Zn^{++} increased the amplitude of I_A by over 300pA. This

value likely represents the actual effect of Zn^{++} enhancement of I_A in hDBB neurons as contamination from other the ion currents was eliminated (as with 0 Ca^{++}/TTX). Our results also show that Zn^{++} shifts the inactivation curve to the right with no effect on the activation kinetics. Since the inactivation plot is a measure of the probability that channels are available for opening, this result suggests that more I_A channels are available for opening at depolarized membrane potentials in the presence of Zn^{++}. These findings are similar to these reported by Huang et al. (1993) in suprachiasmatic neurons where 50μM Zn^{++} also increased I_A amplitude and shifted the inactivation curve to the right with no concomitant effect on activation. On the contrary, others have described Zn^{++}-mediated reductions of I_A in cultured sympathetic neurons (Constanti and Smart, 1987) and invertebrate neurons (Erdelyi, 1994).

Physiologically, I_A is modulates AP by increasing both the rate of AP repolarization and outward K^+ conductance as the cell depolarized to threshold (Rudy, 1988; Viana et al., 1993; Wu and Barish, 1992; Zhang and McBain, 1995). Increasing I_A would likely decrease the firing rate and putatively decrease AP duration (Ma and Koester, 1995; Zhang and McBain, 1995). Thus, the net effect of an increased I_A in hDBB cells would likely be a reduction in the overall excitability of these neurons.

Decrease in delayed rectifier by Zn^{++}

Zn^{++} decreases I_K currents in hDBB neurons. The block appears to be voltage dependent as the decrease in current becomes more pronounced with increasing voltage. Zn^{++}-reduction of I_K has also been observed in other systems including squid giant axon (Gilly and Armstrong, 1982), squid stellate ganglion (Spires and Begenish, 1992), frog motor nerve endings (Miralles et al. 1994), and chick growth plate chondrocytes (Walsh et al.,

1992). However, this is the first report of Zn^{++} modulation of I_K in central mammalian neurons. Functionally, I_K channels appear to augment AP repolarization (Goh et al., 1989). Thus, in light of previous observations, the physiological significance of a reduction in I_K mediated by Zn^{++} would be seen as an increase in the AP width and thus may contribute to an overall slowing of AP firing rates. Therefore, similar to increasing I_A, the decrease in I_K would ultimately result in a reduction of the excitability of hDBB cells.

Sodium Current modulation by Zn^{++}

Na^+ currents in hDBB neurons are TTX-sensitive and activate completely within 0.5-1ms at most voltages (Fig. 6-5 and 6-6). Inactivation is primarily voltage dependent as the currents inactivate largely in 2-3ms with maintained depolarization. Zn^{++} reduced I_{Na} in every cell examined using the protocols in Fig. 6-5 (n=22) and in Fig. 6-6 (n=10). The Zn^{++}-mediated decrease in I_{Na} was not statistically significant. The maximum blockade by Zn^{++} was observed at 10mV where I_{Na} was reduced by approximately 350pA. This contrasts with the observations made in in adult entorhinal cortical neurons where micromolar concentrations of Zn^{++} completely blocked slow TTX-insensitive Na^+ currents (White et al., 1993). The small effect of Zn^{++} on I_{Na} in hDBB neurons may be physiologically relevant as this small decrease in I_{Na} may raise the threshold required to fire APs. This would be consistent with the Zn^{++}-induced increase in I_A and decrease in I_K which would likely serve to decrease overall cellular excitability.

Calcium Current modulation by Zinc

Perfusion of 50μM Zn^{++} reversibly reduced I_{Ba} in hDBB cells. Analysis of I_{Ba} elicited by voltage steps (Fig. 6-7A, 6-7B, 6-7C) suggest that T-type (LVA) Ca^{++} channels were not

present in the cells examined in this study. Acutely dissociated large, putatively cholinergic DBB cells from guinea pig (>20μM) express HVA (L and N-type Ca^{++} channels) and LVA channels whereas the smaller, putatively GABAergic neurons (10-15μM) only possess HVA channels (Frye et al. 1994). Thus, given the lack of LVA-type current in these cells, the hDBB neurons examined in this study may belong to the GABAergic cell type.

Others have also characterized Zn^{++}- mediated attenuation of I_{Ca}. Busselberg et al. (1992) demonstrated that Zn^{++} reduce HVA I_{Ca} currents in cultured chick DRG neurons. However, unlike the results from our study, they were unable to attain a complete recovery of the calcium currents after washout of Zn^{++}. HVA channels, however, are not the only Ca^{++} channels modulated by Zn^{++}. Potent reductions of T-type currents by micromolar concentrations of Zn^{++} have been reported in acutely isolated rat hippocampal neurons (Takahashi and Akaike, 1991), acutely isolated embryonic chick DRG neurons (Harrison and Gibbons, 1994), and cultured chick DRG cells (Busselberg et al., 1992).

Modulation of I_C and I_{AHP}

There are two main families of calcium activated potassium channels: the voltage-dependent, large conductance I_C channels and the voltage-independent, small conductance I_{AHP} channels. Functionally, I_C participates in AP repolarization and in the early component of the AHP whereas I_{AHP} contributes to the slower component of AP AHP. We have previously demonstrated that apamin has no effect on voltage-activated K^+ conductances in hDBB neurons whereas charybdotoxin, the selective blocker for I_C channels consistently reduces outward currents (Chapter 5). Since Zn^{++} causes a profound blockade of Ca^{++} channels in hDBB cells, it follows that I_C would also be blocked. Blockade of this ionic

current would account for the increased excitability observed when this cation is applied (Fig. 6-8A, B). However, in some cells, we observed a marked decrease in cellular activity (Fig. 6-8C, D). In Fig. 6-8D, it is clear that there is an increase in accomodation over the duration of the depolarizing step. It is likely that the Zn^{++}-mediated increase in I_A and possibly the reduced I_K and I_{Na} mediate this decrease in AP discharge rate. However, further studies must be conducted to specifically elucidate the contribution of the various ionic currents to hDBB AP architecture.

Pathophysiological consequences of Zn^{++} actions on hDBB cells

Under physiological conditions, Zn^{++} regulates voltage-gated ionic channels and ligand-gated GABA and NMDA channels (Smart et al., 1994). Pathophysiologically, our results may have significant implications regarding the actions of Zn^{++} in AD. When released in excessive quantities, Zn^{++} is excitotoxic (Koh and Choi, 1988; Duncan et al., 1992; Choi et al., 1988). This correlates with our observation that despite modulating certain voltage-gated ionic currents in a manner that would reduce excitability, the principal effect of Zn^{++} on these cells is excitatory (Fig. 6-8). Furthermore, Zn^{++} is almost exclusively co-localized in glutamatergic cells (Moos, 1993; Beaulieu et al., 1992) and is capable of potentiating glutamate-mediated excitotoxicity (Weiss et al., 1993). Constantinidis (1991) indicates that Zn^{++} levels are significantly reduced in the brains of patients with AD. This decrease has been associated with other neurodegenerative diseases such as epilepsy (Frederickson et al., 1988; Pohle and Rauca, 1994) and Pick's disease (Ebadi, 1984). It is postulated that AD may arise due to the depletion of Zn^{++} from nerve terminals consequent to excessive stimulation and release from these terminals (Pohle and Rauca, 1994). The

results of this study support this hypothesis and are consistent with the notion that this cation may participate in neurodegenerative disorders affecting this region.

Figure 6-1. Effect of Zn^{++} on I_A. **A.** The voltage protocol used for evoking currents is shown in the inset. The holding potential was -80mV. A 150ms hyperpolarizing command to -120mV was applied to remove inactivation of currents. This was followed by depolarizing 100ms step command (increment 10mV/step starting from -40mV to a maximum of +30mV) to evoke currents. The voltage-dependent currents elicited by using this protocol in a hDBB neuron are shown here. These currents include I_A, I_K, I_{Na}, and I_{Ca}. **B.** The voltage protocol used for evoking currents is shown in the inset. The holding potential was -80mV. A 150ms depolarizing command to -40mV was applied. This was followed by depolarizing 100ms step command (increment 10mV/step starting from -40mV to a maximum of +30mV) to evoke currents. The currents evoked by using this protocol are in the same neuron as in Fig. 6-1A. The currents activated by this protocol are devoid of the transiently-activated I_A which is inactivated at voltages positive to-50mV. However, I_{Na}, I_{Ca}, and I_K are all still present as they activate at potentials positive to -50mV. $\mathbf{C_1}$. The difference currents generated by subtraction of currents generated in Fig. 6-1B from Fig. 6-1A are plotted. The currents in this plot represent relatively pure I_A, isolated under control condition. $\mathbf{C_2}$. The difference currents generated by subtraction in the presence of 50μM Zn^{++}. The difference currents were larger in the presence of Zn^{++} as compared to those under control conditions. $\mathbf{C_3}$. The difference currents generated by subtraction after Zn^{++} has been washed out. This plot shows that I_A recovered to control levels.

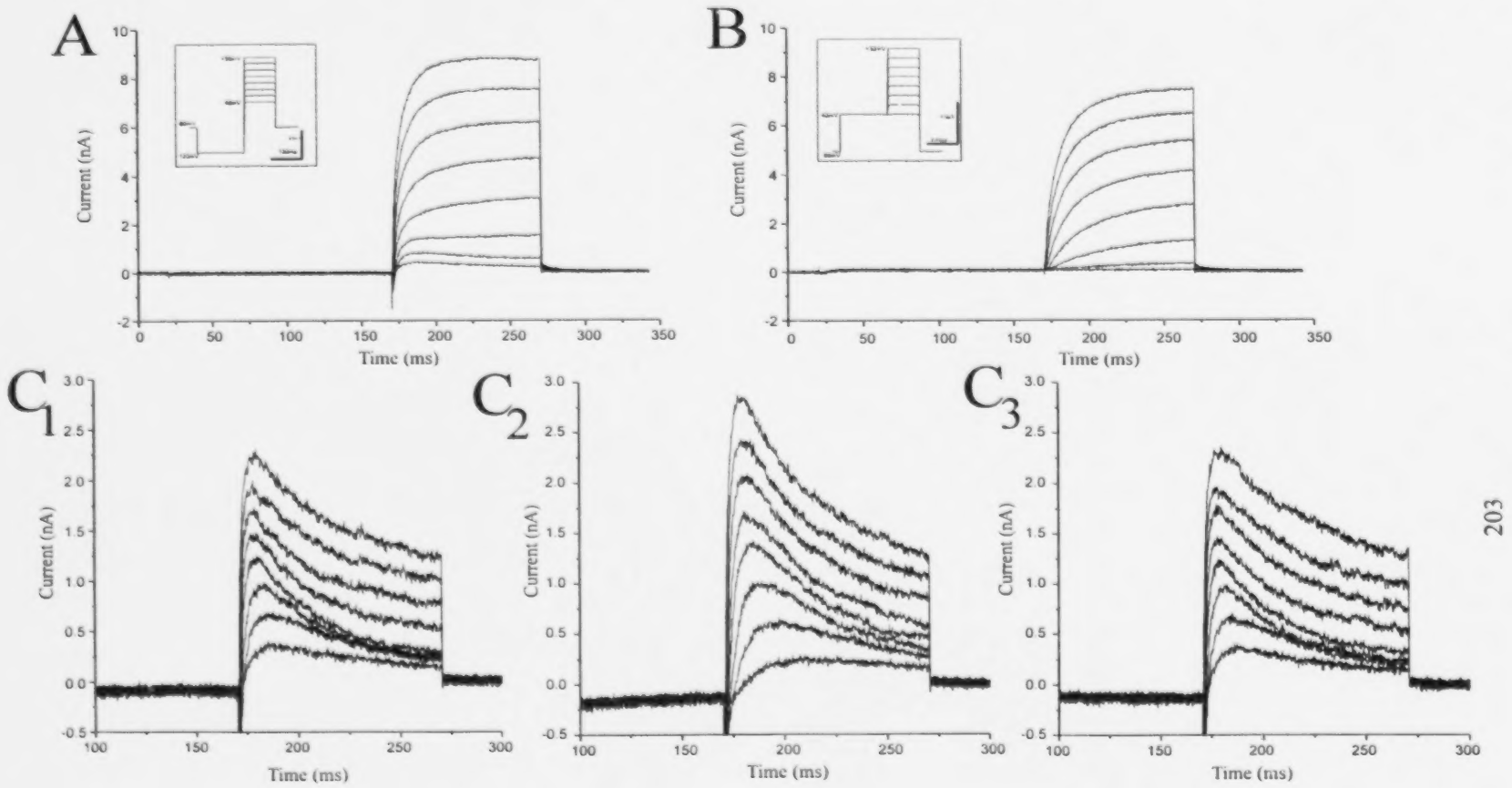
A
B
C1
C2
C3
Current (nA)
Time (ms)

Figure 6-2. Effect of Zn^{++} on I_A under control conditions and under conditions when Na^+ and Ca^{++} influx was blocked. A. Peak currents (generated as in Fig. 6-1C) were plotted against command voltage steps. Application of 50μM Zn^{++} in control ACSF increased I_A by approximately 300pA. **B.** I-V relationship of peak difference currents (generated as in Fig. 6-1D) in 0 Ca^{++} and 1μM TTX external solution in the presence and absence of 50μM Zn^{++} I_A was still augmented by Zn^{++} by about the same amount as under control conditions.

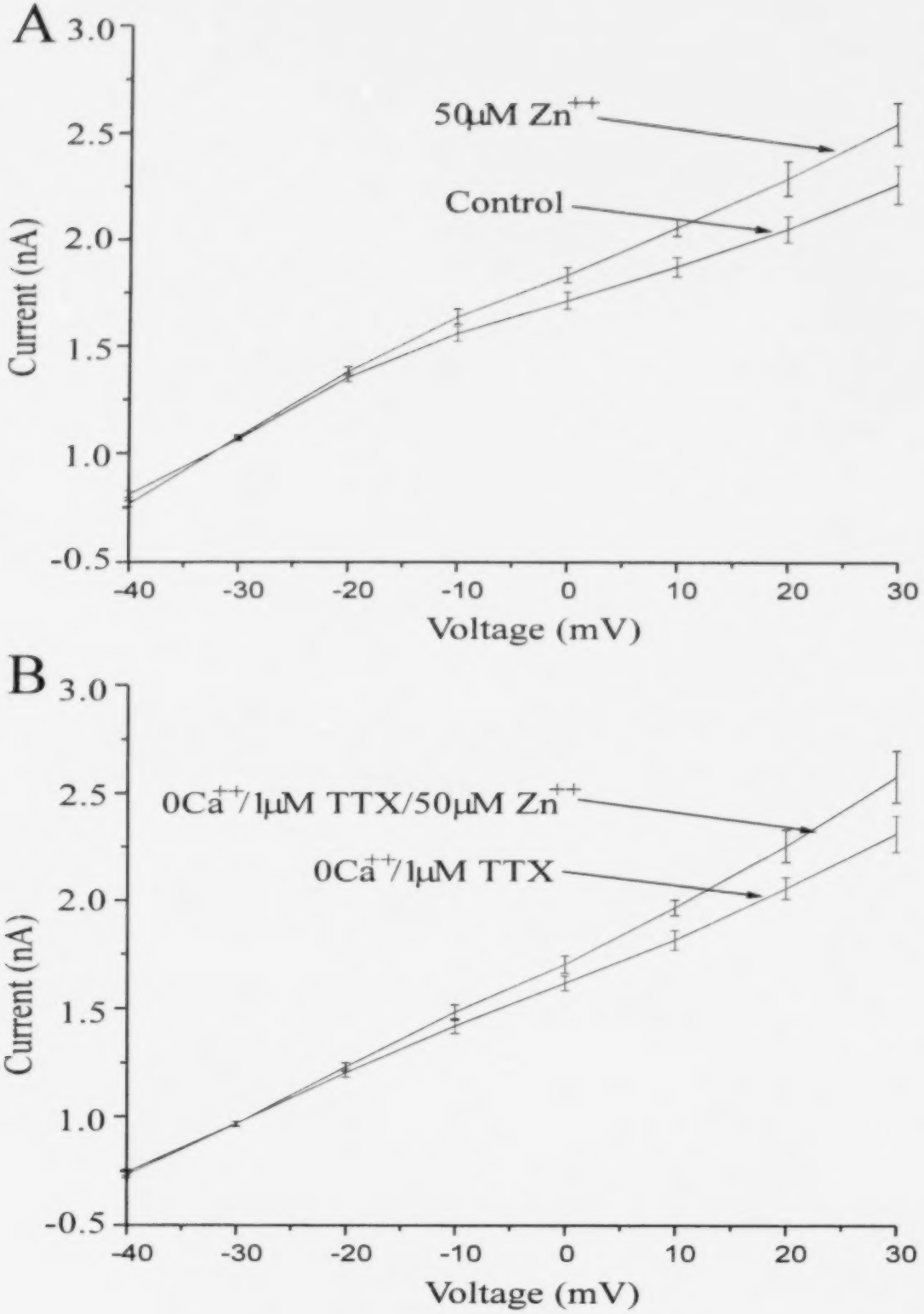
A
3.0
2.5
2.0
1.5
1.0
-0.5
Current (nA)
50μM Zn++
Control
-40
-30
-20
-10
0
10
20
30
Voltage (mV)
B
3.0
2.5
2.0
1.5
1.0
-0.5
Current (nA)
0Ca++/1μM TTX/50μM Zn++
0Ca++/1μM TTX
-40
-30
-20
-10
0
10
20
30
Voltage (mV)

Figure 6-3. Effect of Zn^{++} on the activation and inactivation of I_A. A. Normalized currents were plotted against command voltage to study the voltage-dependence of activation of I_A under control conditions and in the presence of 50μM Zn^{++} (see text for detailed explanation of voltage protocol). Data points were fitted with the Boltmann equation. The half-activation voltage (V_a) was -2.3±2.6mV and the current increased e-fold per 18.0±1.9mV under control conditions. The presence of Zn^{++} in the external solution did not significantly affect V_a (-4.8±2.5mV; P>0.5) and the change in voltage for e-fold change in current was 16.7±1.8mV (P>0.5). Error bars represent s.e.m.. **B.** Normalized currents were plotted against the command voltage to study the voltage-dependence of inactivation of I_A in the presence and absence of 50μM Zn^{++} (see text for detailed explanation of voltage protocol). Zn^{++} shifted inactivation plot to the right. Under control conditions, the half-inactivation voltage was -76.4±2.2mV and current changed e-fold per 12.9±1.1mV. There was a significant shift to the right in the presence of Zn^{++}. The half-inactivation voltage was -53.4±2.0mV (P<0.001) and current changed e-fold per 7.2±2.0mV (P<0.02) . Error bars represent s.e.m.

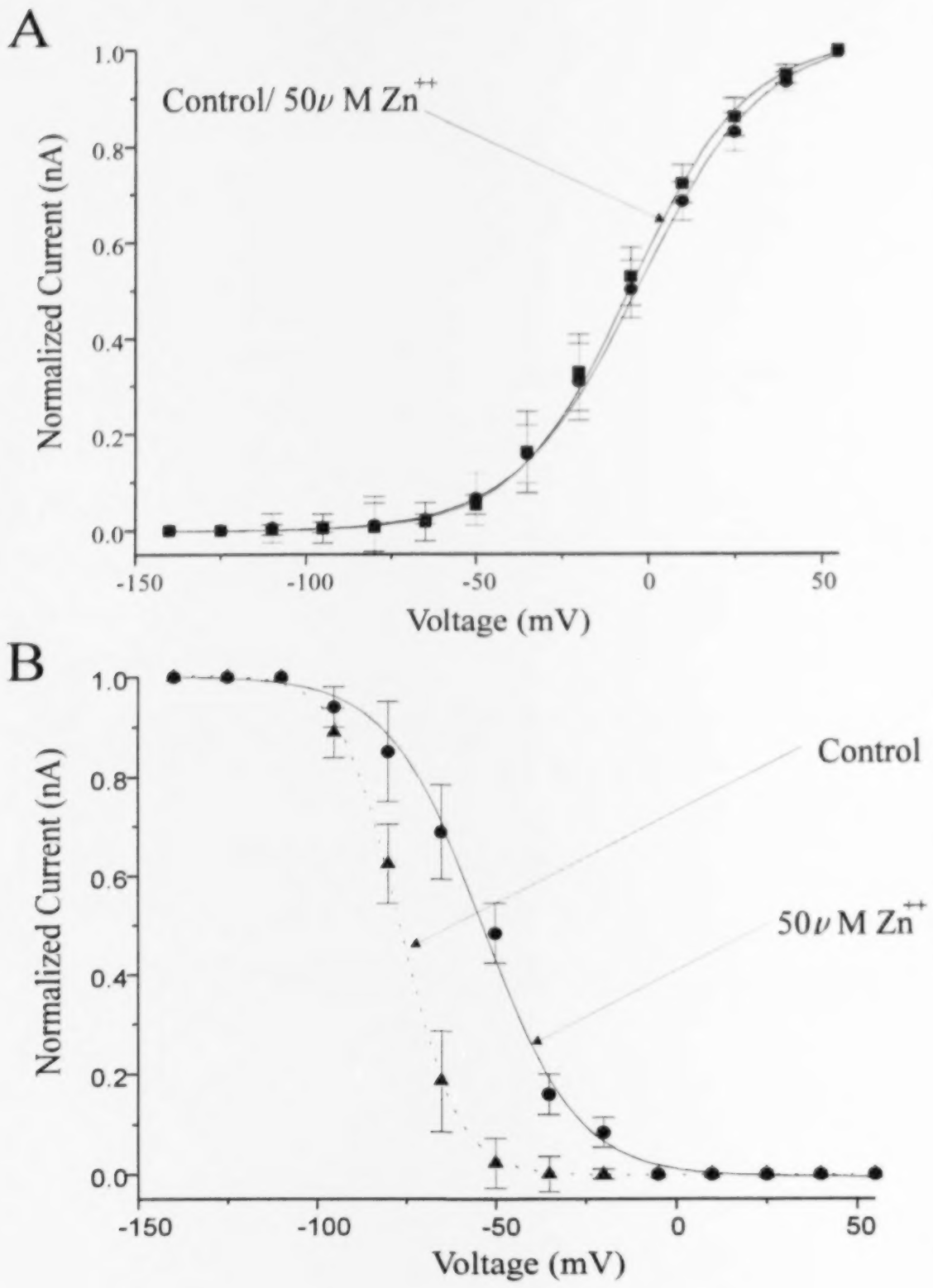
A
Control/ 50ν M Zn++
Normalized Current (nA)
1.0
0.8
0.6
0.4
0.2
0.0
-150
-100
-50
0
50
Voltage (mV)
B
Control
50ν M Zn++
Normalized Current (nA)
1.0
0.8
0.6
0.4
0.2
0.0
-150
-100
-50
0
50
Voltage (mV)

Figure 6-4. Effect of Zn^{++} on I_K in hDBB cells. A_1. Voltage protocol utilized to evoke currents was the same as in Fig. 6-1B under control conditions. The holding potential was -80mV. A 150ms depolarizing command to -40mV was applied. This was followed by depolarizing 100ms step command (increment 10mV/step starting from -40mV) to evoke currents. The currents elicited by using this protocol in a hDBB neuron are shown here. In this protocol, the outward currents are likely mediated by I_K and $I_{K(Ca)}$. A_2. In the same neuron, outward currents evoked in the presence of 50μM Zn^{++} were decreased. **B.** Difference currents (obtained by subtraction of currents evoked in the presence of Zn^{++} from those evoked under control conditions) are shown in this panel. **C.** Difference currents obtained in 0 Ca^{++}, 1μM TTX external solution in the same neuron in the presence and absence of Zn^{++}. **D.** Zn^{++}-modulated outward currents in an external solution containing 0 Ca^{++} external solution in the presence of 1μM TTX were completely blocked by 5mM TEA.

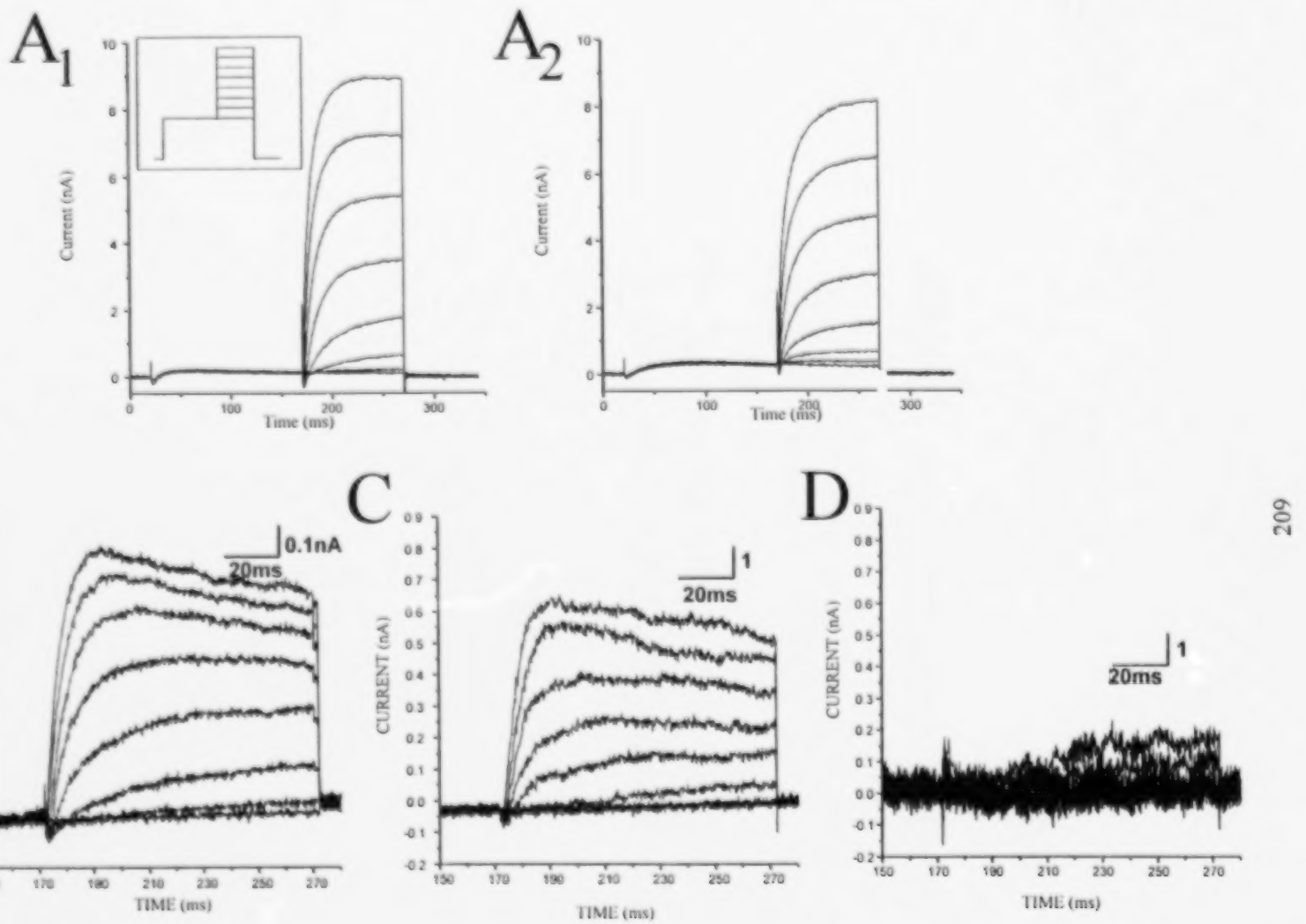
A1
Current (nA)
Time (ms)
A2
Current (nA)
Time (ms)
B
0.1nA
20ms
CURRENT (nA)
TIME (ms)
C
1
20ms
CURRENT (nA)
TIME (ms)
D
1
20ms
CURRENT (nA)
TIME (ms)

Figure 6-5. Effect of Zn^{++} on whole cell currents evoked by brief voltage steps. **A.** The currents elicited by 3ms depolarizing voltage commands from a holding potential of -80mV to a maximum of +55mV (increment 15mV/step) under control conditions. **B.** The currents elicited in the same neuron in the presence of 50μM Zn^{++}. **C.** Difference currents obtained by subtracting currents evoked in the presence of Zn^{++} from those evoked under control conditions. **D.** Difference currents obtained in the presence of 1uM TTX. **E.** Difference currents obtained in the presence of 50μM 4-AP.

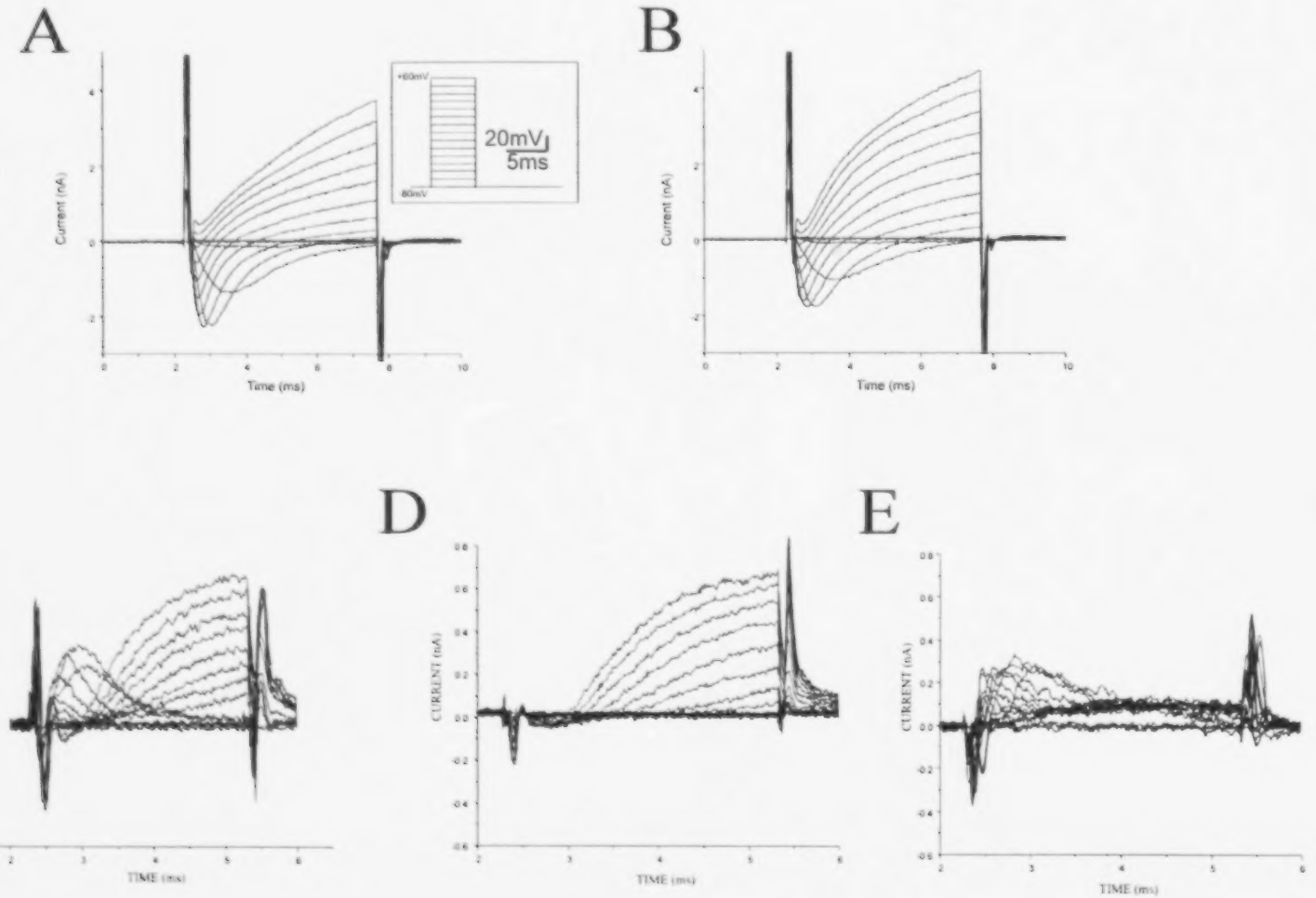
A
B
C
D
E
Current (nA)
Time (ms)
+60mV
-80mV
20mV
5ms
CURRENT (nA)
TIME (ms)

Figure 6-6. Effect of Zn^{++} on I_{Na}. **A.** I_{Na} evoked from an hDBB neuron under control conditions by applying brief depolarizing step commands (increment 15mV/step; 9ms) from a holding potential of -80mV to a maximum of +55mV. **B.** I_{Na} evoked in the presence of 50uM Zn^{++}. A slight decrease in peak I_{Na} current was observed. **C.** I-V relationships of I_{Na} in the presence and absence of Zn^{++}.

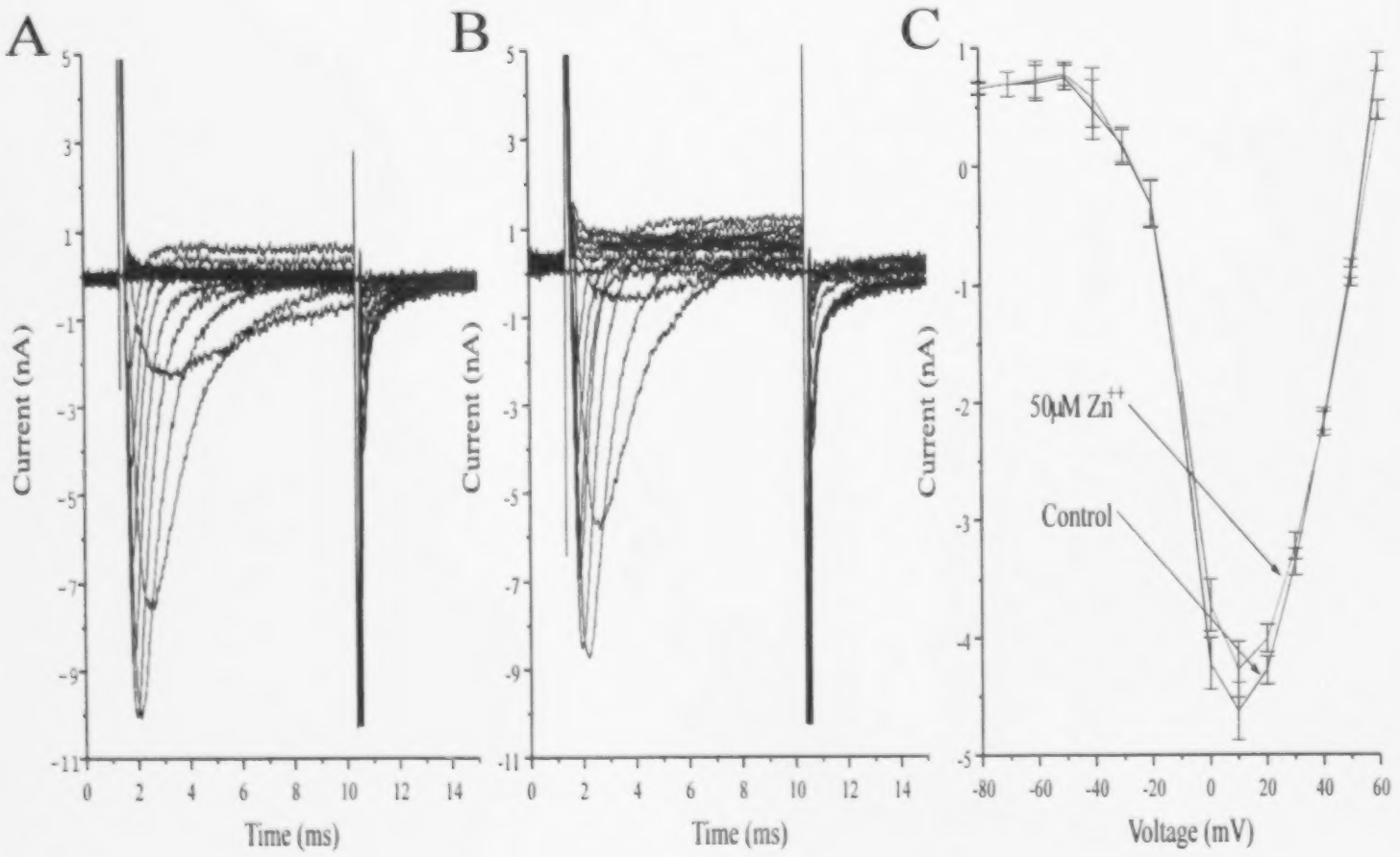
A
B
C
Current (nA)
Time (ms)
Voltage (mV)
50μM Zn++
Control

Figure 6-7. Effect of Zn^{++} on I_{Ba}. A_1. I_{Ba} evoked from an hDBB neuron under control condition by applying 20ms depolarizing voltage command steps from a holding potential of -80mV (increment 10mV/step) to a maximium of +70mV. Tail curents were recorded at -40mV. **B.** I_{Ba} evoked in the presence of 50uM Zn^{++} was significantly reduced (by approximately 85%) as compared to that under control conditions. **C.** Currents recovered to control levels on washout of Zn^{++}. **D.** I-V relationships of I_{Ba} under control conditions and in the presence of Zn^{++}. I_{Ba} was significantly attenuated by Zn^{++}.

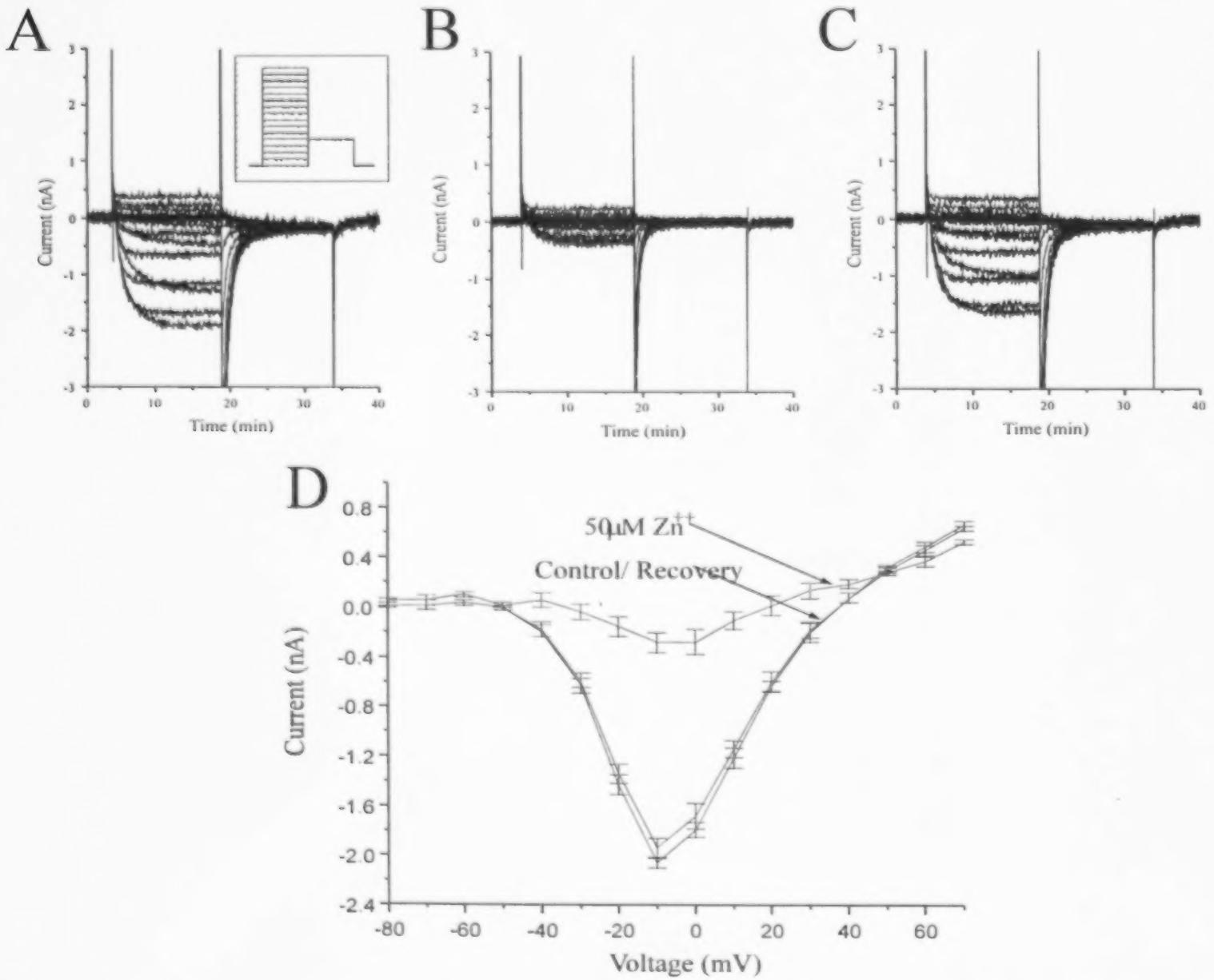
A
B
C
D
Current (nA)
Time (min)
50μM Zn++
Control/ Recovery
Voltage (mV)

Figure 6-8. Zn^{++} modulation of hDBB excitability. A, B. In an hDBB cell held at -76mV, perfusion of 50μM Zn^{++} increased the firing frequency (B) compared to control (A). The depolarization step was 0.13nA in amplitude and 1600ms in duration (rmp=-76mV). Averaged data: *Control:* AP height: 64±9mV; AP width: 2.4±0.8ms; AHP duration: 53.6±10.1ms; AHP amplitude: 4.9±1.1mV (n=9). *Zn^{++}:* AP height: 65±8mV; AP width: 2.4±1.5ms; AHP duration: 148.8±26.0ms; AHP amplitude: 7.32±1.3mV (n=9). **C, D.** In another hDBB cell, perfusion of 50μM Zn^{++} reduced the AP discharge rate (D) compared to control (C). The depolarization step was 0.15nA in amplitude and 1500ms in duration (rmp=-76mV). Averaged data: *Control:* AP height: 65±4.1mV; AP width: 2.4±1.3ms; AHP duration: 88.8±5.1ms; AHP amplitude: 6.4±1.4mV (n=9). *Zn^{++}:* AP height: 69.8±5.3mV; AP width: 3.2±1.5ms; AHP duration: 204.4±22.4ms; AHP amplitude: 5.32±1.1mV (n=9).

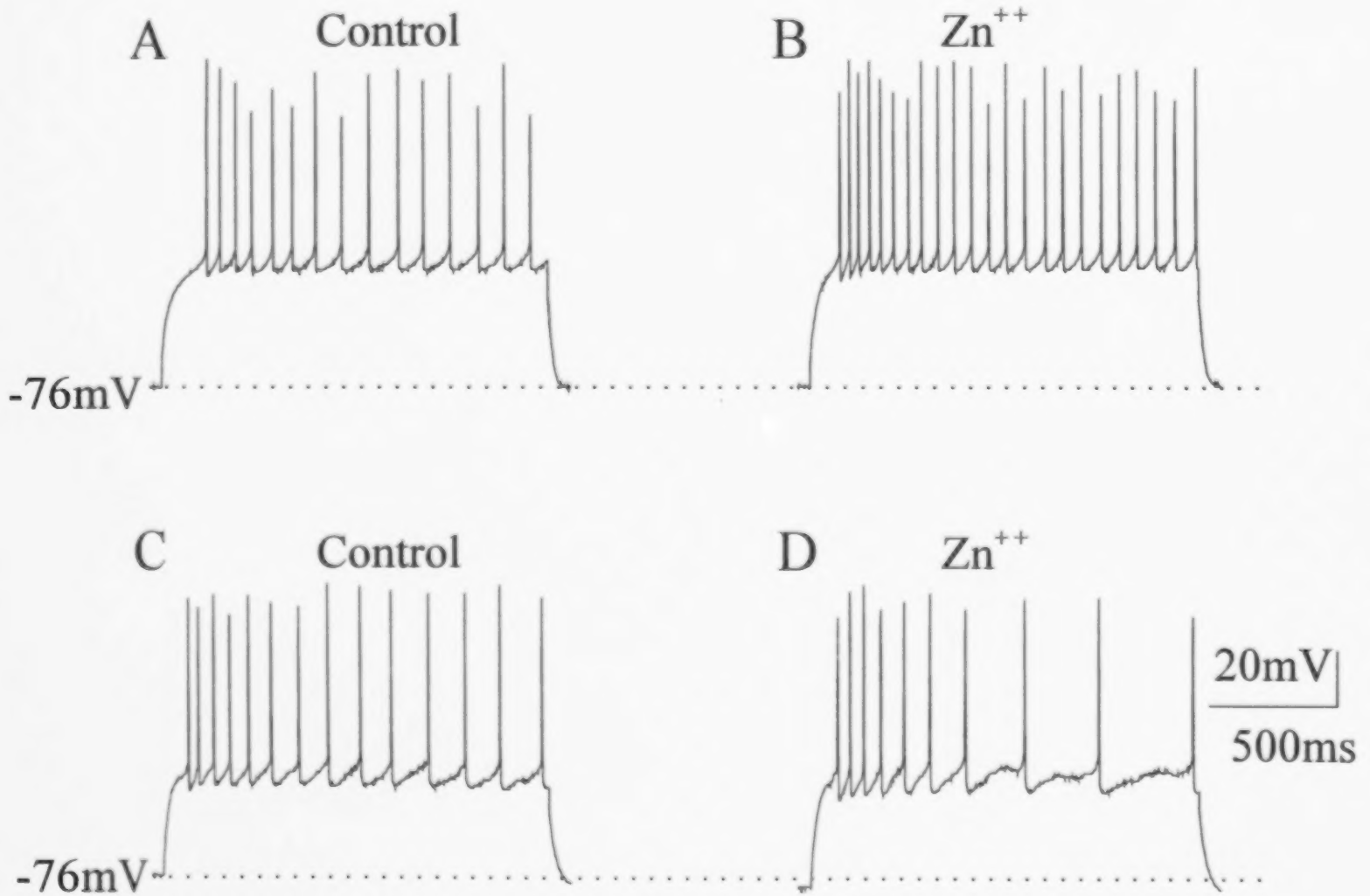
A
Control
B
Zn++
-76mV
C
Control
D
Zn++
20mV
500ms
-76mV

REFERENCES

Adams, P. R., Brown, D. A., and Constanti, A. M-currents and other potassium currents in bullfrog sympathetic neurones. *J. Physiol.* 330:537-572, 1982.

Assaf, S. Y. and Chung, S. -H. Release of endogenous Zn^{2+} from brain tissue during activity. *Nature* 308:734-736, 1984.

Beaulieu, C., Dyck, R., and Cynader, M. Enrichment of glutamate in zinc-containing terminals of the cat visual cortex. *Neuroreport* 3:861-864, 1992.

Belluzzi, O., Sacchi, O., and Wanke, E. A fast transient outward current in the rat sympathetic neurone studied under voltage-clamp conditions. *J. Physiol.* 358:91-108, 1985.

Belluzzi, O., Sacchi, O., and Wanke, E. Identification of delayed potassium and calcium currents in the rat sympathetic neurone under voltage clamp. *J. Physiol. Lond* 358:109-129, 1985.

Busselberg, D., Evans, M. L., Rahmann, H., and Carpenter, D. O. Lead and zinc block a voltage-activated calcium channel of *Aplysia* neurons. *J. Neurophys.* 65(4):786-795, 1991.

Busselberg, D., Michael, D., Evans, M. L., Carpenter, D. O., and Haas, H. L. Zinc blocks voltage gated calcium channels in cultured rat dorsal rool ganglion cells. *Brain Res.* 593:77-81, 1992.

Choi, D. W., Yokoyama, M., and Koh, J. Zinc neurotoxicity in cortical cell culture. *Neurosci.* 24:67-79, 1988.

Connor, J. A. and Stevens, C. F. Voltage clamp studies of a transient outward membrane

current in gastropod neural somata. *J. Physiol.* 299:289-307, 1971.

Constanti, A. and Smart, T. G. Zinc blocks the A-current in cultured rat sympathetic neurones. *J. Physiol.* 396:159P1987.

Constantinidis, J. Hypothesis regarding amyloid and zinc in the pathogenesis of Alzheimer disease: potential for preventive intervention. *Alzhiemer Disease and Associated Disorders* 5(1):31-35, 1991.

Duncan, M. W., Marini, A. M., Watters, R., Kopin, I. J., and Markey, S. P. Zinc, a neurotoxin to cultured neurons, contaminates cycad flour prepared by traditional Guamanian methods. *J. Neurosci.* 12:1523-1537, 1992.

Ebadi, M. The presence of metallotheionein-like protein (MLT) in rat brain. *Fed. Proc.* 43:3317, 1984.

Ebadi, M., Iverson, P. L., Hao, R., Cerutis, D. R., Rojas, P., Happe, H. K., Murrin, L. C., and Pfeiffer, R. F. Expression and regulation of brain metallothionein. *Neurochem. Int.* 27(1):1-22, 1995.

Erdelyi, L. Zinc modulates A-type potassium currents and neuronal excitability in snail neurons. *Cell.Mol. Neurobiol.* 14(6):689-700, 1994.

Frankenhauser, B. and Hodgkin, A. L. The action of calcium on the electrical properties of squid axons. *J. Gen. Physiol.* 137:218-244, 1957.

Frederickson, C. J., Hernandez, M. D., Goik, S. A., Morton, J. D., and McGinty, J. D. Loss of zinc staining form hippocampal mossy fibers during kainic acid induced seizure: a histofluorescence study.. *Brain Res.* 446:383-386, 1988.

Frederickson, C. J., Klitenick, M. A., Manton, W. I., and Kirkpatrick, J. B.

Cytoachitechtronic distribution of zinc in the hippocampus of man and the rat. *Brain Res.* 273:335-339, 1983.

Friedman, B. and Price, J. L. Firber systems in the olfactory bulb and cortex: A study in adult and developing rats, using the Timm method with the light and electron microscope. *J. Comp. Neurol.* 223:88-109, 1984.

Frye, G. D., Fincher, A. S., Grover, C. A., and Griffith, W. H. Interaction of ethanol and allosteric modulators with $GABA_A$-activated currents in adult medial septum/diagonal band neurons. *Brain Res.* 635:283-292, 1994.

Gilly, W. M. F. and Armstrong, C. M. Divalent cations and the activation kinetics of potassium channels in squid giant axons. *J. Gen. Physiol.* 79:965-996, 1982.

Gilly, W. M. F. and Armstrong, C. M. Slowing of sodium channel opening kinetics in squid axon by extracellular zinc. *J. Gen. Physiol.* 79:935-964, 1982.

Goh, J. W., Kelly, M. E., and Pennefather, P. S. Electrophysiological function of the delayed rectifier (IK) in bullfrog sympathetic ganglion neurones. *Pflugers Arch. Eur. J. Physiol.* 413(5):482-486, 1989.

Griffith, W. H. and Sim, J. A. Comparison of 4-aminopyridine and tetrahyroaminoacridine on basal forebrain neurons. *J. Pharm. Exp. Ther.* 255(3):986-993, 1990.

Harrison, N. L. and Gibbons, S. J. Zn^{2+}: an endogenous modulator of ligand- and voltage-gated ion channels. *Neuropharm.* 33(8):935-952, 1994.

Holm, I. E., Andreasen, A., Danscher, G., Perez-Clausell, J., and Nielsen, H. Quantification of vesicular zinc in the rat brain. *Histochem.* 89:289-293, 1988.

Huang, R., Peng, Y., and Yau, K. Zinc modulation of a transient potassium current and

histochemical localization of the metal in neurons of the suprachiasmatic nucleus. *PNAS* 90:11806-11810, 1993.

Ibata, Y. and Otsuka, N. Electron microscope demonstration of zinc in the hippocampal formation using Timm's sulphide silver technique. *J. Hist. Cyto.* 17:171-175, 1969.

Jassar, B. S. and Jhamandas, J. H. Effects of neurotensin on acutely dissociated neurons from the horizontal limb of the diagonal band of Broca (hDBB) in the rat. *Soc. Neurosci. Abstr.* 21:901995.(Abstract)

Jassar, B. S., Pennefather, P. S., and Smith, P. A. Changes in sodium and calcium channel activity following axontomy of B-cells in bullfrog sympathetic ganglion. *J. Physiol.* 472:203-231, 1993.

Jassar, B. S., Pennefather, P. S., and Smith, P. A. Changes in potassium channel activity following axotomy of B-cells in bullfrog sympathetic ganglion. *J. Physiol.* 479(Pt 3):353-370, 1994.

Kesner, R. P., Berman, R. F., and Tardif, R. Place and taste aversion learning: role of basal forebrain, parietal cortex, and amygdala. *Br. Res. Bull.* 29:345-353, 1992.

Kiss, T. and Osipenko, O. Metal ion-induced permeability changes in cell membranes: a minireview. *Cellular and Molecular Neurobiology* 14(6):781-789, 1994.

Koh, J. and Choi, D. W. Zinc alters excitatory amino acid neurotoxicity on cortical neurons. *J. Neurosci.* 8:2164-2171, 1988.

Ma, M. and Koester, J. Consequences and mechanics of spike broadening of R20 cells in *Aplysia californica*. *J. Neurosci.* 15(10):6720-6734, 1995.

Mandava, P., Howell, G. A., and Frederickson, C. J. Zinc-containing neuronal innervation

of the septal nuclei. *Brain Res.* 608:115-122, 1993.

Miralles, F., Canti, C., Marsal, J., Peres, J., and Solsona, C. Zinc ions block rectifier potassium channels and calcium activated potassium channels at the frog motor nerve endings. *Brain Res.* 641(2):279-284, 1994.

Moos, T. Simultaneous application of Timm's sulphide silever method and immunoflurorescence histochemistry. *J. Neurosci. Meth.* 48:149-156, 1993.

Paolini, A. G. and Mckenzie, J. S. Effects of lesions in the horizontal diagonal band nucleus on olfactory habituation in the rat.. *Neurosci.* 57(3):717-724, 1994.

Perez-Clausell, J., Frederickson, C. J., and Danscher, G. Amygdaloid efferents through the stria terminalis in the rat give origin to zinc-containing boutons. *J. Comp. Neurol.* 290(2):201-212, 1989.

Pohle, W. and Rauca, C. Hypoxia protects against the neurotoxicity of kainic acid. *Brain Res.* 644:297-304, 1994.

Roman, F. S., Simonetto, I., and Soumireu-Mourat, B. Learning and memory of odor-reward association: selective impairment following horizontal diagonal band lesions. *Beh. Neurosci.* 107(1):72-81, 1993.

Rudy, B. Diversity and ubiquity of K channels. *Neurosci.* 25:729-749, 1988.

Smart, T. G., Xie, X., and Krishek, B. J. Modulation of inhibitory and excitatory amino acid receptor ion channels by zinc. *Prog. Neurobiol.* 42:393-441, 1994.

Sorensen, J. C., Slomianka, L., Christensen, J., and Zimmer, J. Zinc-containing telencephalic connections to the rat striatum: a combined Fluro-Gold tracing and histochemical study. *Exp. Br. Res.* 105:370-382, 1995.

Spires, S. and Begenish, T. Chemical properties of the divalent cation binding site on potassium channels. *J. Gen. Physiol.* 100:181-193, 1992.

Standen, N. B. Separation and analysis of ionic currents. In: *Microelectrode Techniques: The Plymouth Workshop Handbook*, edited by N. B. Standen, P. T. A. Gray and M. J. Whitaker. Cambridge: The Company of Biologists, Ltd., 1988, p. 29-40.

Takahashi, K. and Aaike, N. Calcium antaonist effects on low-threshold (T-type) calcium current in rat isolated hippocampal CA1 pyramidal neurons. *PNAS* 256:169-175, 1991.

Talukder, G. and Harrison, N. L. On the mechanism of modulation of transient outward current in cultured rat hippocampal neurons by di- and trivalent cations. *J. Neurophys.* 73(1):73-79, 1995.

Viana, F., Bayliss, D. A., and Berger, A. J. Multiple potassium conductances and their role in action potential repolarization and repetitive firing behavior of neonatal rat hypoglossal motoneurons. *J. Neurophysiol.* 69(6):2150-2163, 1993.

Wallwork, J. C. Zinc and the central nervous system. *Prog. Food Nutr. Sci.* 11(2):203-247, 1987.

Walsh, K. B., Cannon, S. D., and Wuthier, R. E. Characterization of a delayed rectifier potassium current in chicken growth plate chondrocytes. *Am.J.Physiol.* 262(5 Pt 1):C1335-C1340, 1992.

Weiss, J. H., Hartley, D. M., Koh, J. Y., and Choi, D. W. AMPA receptor activation potentiates zinc neurotoxicity. *Neuron* 10(1):43-49, 1993.

White, J. A., Alonso, A., and Kay, A. R. A heart like Na^+ current in the medial entorhinal

cortex. *Neuron* 11:1037-1047, 1993.

Wu, R. L. and Barish, M. E. Two pharmacologically and kinetically distinct transient potassiumcurrents in cultured embryonic mouse hippocampal neurons. *J. Neurosci* 12(6):2235-2246, 1992.

Zhang, L. and McBain, C. J. Potassium conductances underlying repolarization and AHP in rat CA1 hippocampal interneurons. *J. Physiol.* 488(3):661-672, 1995.

CHAPTER 7

GENERAL DISCUSSION

The work described in this thesis has examined the biophysical properties and the actions of various neurotransmitters within the hDBB. This region is also a major site for pathology in the context of neurodegenerative disease. My results show that the neurotransmitter/neuromodulatory compounds examined in this thesis utilize highly selective and specific mechanisms to regulate the behavior of hDBB neurons. This chapter will summarize my findings and discuss how these findings may be relevant in the context of the physiological and pathophysiological processes involving the hDBB.

The investigation into the role of glutamate in excitatory neurotransmission within the hDBB was described in Chapter 3. Our results indicate that glutamate is a prominent excitatory neurotransmitter in this region. Exogenous application of specific glutamate agonists revealed that AMPA, kainate, mGluR, and NMDA receptors are all present on postsynaptic hDBB neurons. Furthermore, the use of various selective glutamate antagonists revealed that each of these receptor subtypes participates in excitatory neurotransmission. In addition to mediating actions postsynaptically, mGluR receptors also reduced glutamate release via a presynaptic mechanism (summarized in Fig. 7-1). Taken together, these results indicate that glutamate is an important modulator of hDBB neurons.

These findings may lay the foundation to explain the hDBB's participation within various physiological and pathophysiological processes. Anatomical data demonstrate that dense glutamate-positive fibers are present within the hDBB (Carnes et al., 1990) and originate principally from the hippocampal CA1 region (Jakab and Leranth, 1995). Glutamate-mediated connectivity between the hippocampal CA1 area and the hDBB is believed to underly important physiological processes such as theta rhythm (Sainsbury and

Bland, 1981; Bland and Colom, 1993; Mitchell and Ranck, 1980) and memory mechanisms (Oka and Yoshida, 1985; Kesner et al., 1992). Pathophysiologically, it has been hypothesized that the massive death of hDBB cholinergic neurons in AD may arise due to glutamate-mediated excitotoxicity. Our demonstration of a prominent glutamate input onto these cells lends credence to this hypothesis.

I also examined the biophysical profiles of hDBB neurons recorded in this study. Analysis of specific cable properties including H, R_m, ρ, and L demonstrates that hDBB neurons are electrotonically compact. This observation suggests that these cells are capable of efficient transfer for distal afferent inputs.

The investigation into the actions of the monocarboxylic amino acid GABA was reported in Chapter 4. GABA was demonstrated to mediate its effects via two pharmacologically distinct receptors: $GABA_A$ and $GABA_B$ receptors. The $GABA_A$ receptors were found on postsynaptic membranes and act through a chloride conductance. $GABA_B$ receptors, members of the G-protein coupled receptor family, were mostly present presynaptically and modulated the ability of glutamate to exert an effect on postsynaptic membranes (summarized in Figure 7-1).

The presence of GABA receptors on these cells may mediate several physiological processes and may also serve as a neuroprotective agent. GABAergic hDBB cells receive particularly dense GABAergic inputs from the hippocampus (Hofer et al., 1990). These cells, in turn, project back to the hippocampus (Freund and Antal, 1988). This reciprocal connectivity may underlie the actions of these two regions in processes associated with theta rhythm and memory (Bland and Colom, 1993; Bland, 1986; Toth et al., 1993; Alonso and

Kohler, 1984; Zaborszky et al., 1991).

Furthermore, the multi-layered inhibitory system mediated by $GABA_A$, $GABA_B$, and mGluR receptors may act to balance excitatory inputs and prevent excessive glutamatergic input of these cells. This is confirmed by the observation that GABAergic receptors blunt postsynaptic glutamate-mediated EPSPs (Fig. 4-1C). Any reduction of inhibitory inputs to the hDBB would potentially allow glutamate innervation of these cells to become unbalanced, thereby predisposing neurons to excitotoxicity (Pohle and Rauca, 1994). Therefore, the clinical relevance of my findings is that GABAergic inputs may constitute an intrinsic neuroprotective system for hDBB neurons.

The neuromodulatory actions of VP were investigated using both the brain slice and the acutely dissociated preparation of hDBB neurons (Chapter 5). My results show that VP differentially and modulated I_C by activation of specific VP receptor subtypes (Fig. 7-2). Specifically, activation of the V_1 receptors selectively decreased I_C whereas activation of V_2 receptors increased I_C. Our observed lack of VP effects on calcium currents provide strong evidence for direct modulation of the I_C channel by this peptide.

I_C plays a critical role in AP repolarization and determines the duration and amplitude of the fast AHP (Womble and Moises, 1993). Increasing I_C will increase the duration of the AHP and decrease cellular firing frequency (Zhang and McBain, 1995) thereby reducing neuronal excitability. In contrast, decreasing I_C has the opposite effect by reducing the duration of the fast AHP and increasing the overall firing rate of the cell (Zhang and McBain, 1995). The net effect of a decrease in I_C is therefore an increase in cellular excitability. As a consequence, it is clear that the differential activation of V_1 and V_2 receptors represents a

potent mechanism whereby VP can modulate the excitability of hDBB neurons and thereby regulate the activity of target neurons.

Physiologically, VP may be an integral component in the DBB's participation in memory mechanisms and central cardiovascular processes. Intracellular levels of VP are considerably reduced in aged animals which typically show memory deficits (Fischer et al., 1987). In contrast, injection of VP into the septal area improves the ability of rats to perform specific memory-related tasks (Fliers et al., 1985).

In addition to a role in memory, VP modulation of hDBB neurons may also mediate their role in autonomic cardiovascular regulation. Dense VP afferents to the DBB have been anatomically identified as originating from the ACE and BST. Both of these regions respond to changes in blood pressure (Ciriello and Janssen, 1993; Sanders and Shekhar, 1991). Thus, in the context of my results, the presence of both V_1 and V_2 receptors may allow VP to differentially regulate the activity of baroreceptor-sensitive DBB neurons which, in turn, inhibit the activity of VP-synthesizing neurons within the hypothalamic SON (Jhamandas and Renaud, 1986; 1986).

The actions of Zn^{++} on DBB neurons were described in Chapter 6. Analysis of Zn^{++} on voltage-dependent ionic currents in the hDBB revealed that this metal significantly increases I_A and decreases I_K and I_{Ca}. The blockade of I_{Ca} would lead to a concomitant loss of I_C and I_{AHP} which would result in an overall increase in excitability (Sacchi et al., 1995; Zhang and McBain, 1995) (Fig. 7-3). This concurs with our results in the brain slice where exogenous application of Zn^{++} increased the firing frequency of APs in the hDBB.

Zn^{++} is known to subserve important roles in enzymatic processes and also functions

as a neuromodulatory compound in the CNS (Smart et al., 1994; Wallwork, 1987; Westbrook and Mayer, 1987). Pathologically, however, excessive release of Zn^{++} is neurotoxic (Koh and Choi, 1988; Duncan et al., 1992; Choi et al., 1988). Zn^{++} is reported to coexist primarily with glutamatergic neurons (Moos, 1993; Beaulieu et al., 1992) and at high concentrations, this cation potentiates the excitotoxic effects of glutamate in cortical neurons (Weiss et al., 1993). In addition to its interactions with glutamate, Zn^{++} also potently inhibits $GABA_A$ receptors (Narahashi et al., 1994; Smart, 1992; Mayer and Vyklicky, 1989). Ebadi et al. (1995). Buhl et al. (1996) speculate that this may be a further mechanism whereby Zn^{++} contributes to excitotoxicity as they demonstrated that Zn^{++} inhibition of GABA permits glutamate-mediated excitotoxicity in a temporal lobe model of epilepsy. Collectively, these results suggest that Zn^{++} may interact with both GABA and glutamate channels to mediate excitotoxic insult to neurons, particularly those within the basal forebrain.

CONCLUSIONS AND FUTURE EXPERIMENTS

The results of this thesis show that classical neurotransmitters such as glutamate and GABA, neuropeptides such as VP, and non-classical transmitters such as Zn^{++} all potently modulate hDBB cell behavior. Glutamate appears to provide the majority of excitatory input as judged by the contribution of this amino acid to excitatory neurotransmission. Conversely, GABA inhibits hDBB cells postsynaptically and reduces postsynaptic glutamate inputs via a presynaptic mechanism. VP differentially modulates I_C channels via the V_1 and V_2 receptors. The I_C channel likely contributes to the repolarization and the fast component

of the AHP therefore modulation of this ionic current may play a critical role in the regulation of hDBB cell excitability. Finally, Zn^{++} modulates several ionic currents in these cells, however, the most potent effect of this cation appears to be directed at I_{Ca}. The Zn^{++}-mediated decrease in I_{Ca} and consequent decrease in Ca^{++}-dependent K^+ currents such as I_C and I_{AHP} may explain why perfusion of this metal significantly increases the firing frequency of these cells.

The results presented in this thesis have lead to other questions that will be addressed in future studies. A study of the various ionic currents that compose AP's in the hDBB may permit a better understanding of how VP and Zn^{++}-induced modulation of ionic currents can modulate cellular excitability. Recent studies indicate that application of Zn^{++} can enhance excitotoxic actions of glutamate releasing agents in the rat nucleus basalis, a cholinergic nucleus in the basal forebrain (Lee et al, in press). Furthermore, they observe that picolinic acid, an endogenous compound in the brain, potently chelates Zn^{++} and protects against its excitotoxic actions. The study of the actions of Zn^{++} in the basal forebrain and its potentially excitotoxic actions on neurons in this region will clearly be an important focus of study in the years to come.

Another important issue that remains to be addressed are the efferent targets of hDBB cells which receive VP input. Given that hDBB cells potently modulate the release of VP from the SON, an important question to be addressed is whether the hDBB neurons which receive VP input are the same cells which innervate the SON. Microinjection of retrograde tracers into the PNZ and the SON and subsequent study of VP actions on acutely dissociated and retrogradely labelled hDBB neurons could serve as a useful approach.

Figure 7-1. Distribution of GABAergic and glutamatergic receptor subtypes within the hDBB. This figure illustrates two presynaptic terminals containing GABA and glutamate vesicles. GABA interacts with postsynaptic $GABA_A$ and $GABA_B$ receptors and presynaptic $GABA_B$ receptors. Glutamate acts at postsynaptic NMDA, kainate, AMPA, and mGlurR receptors on postsynaptic membranes and mGluR receptors presynaptically.

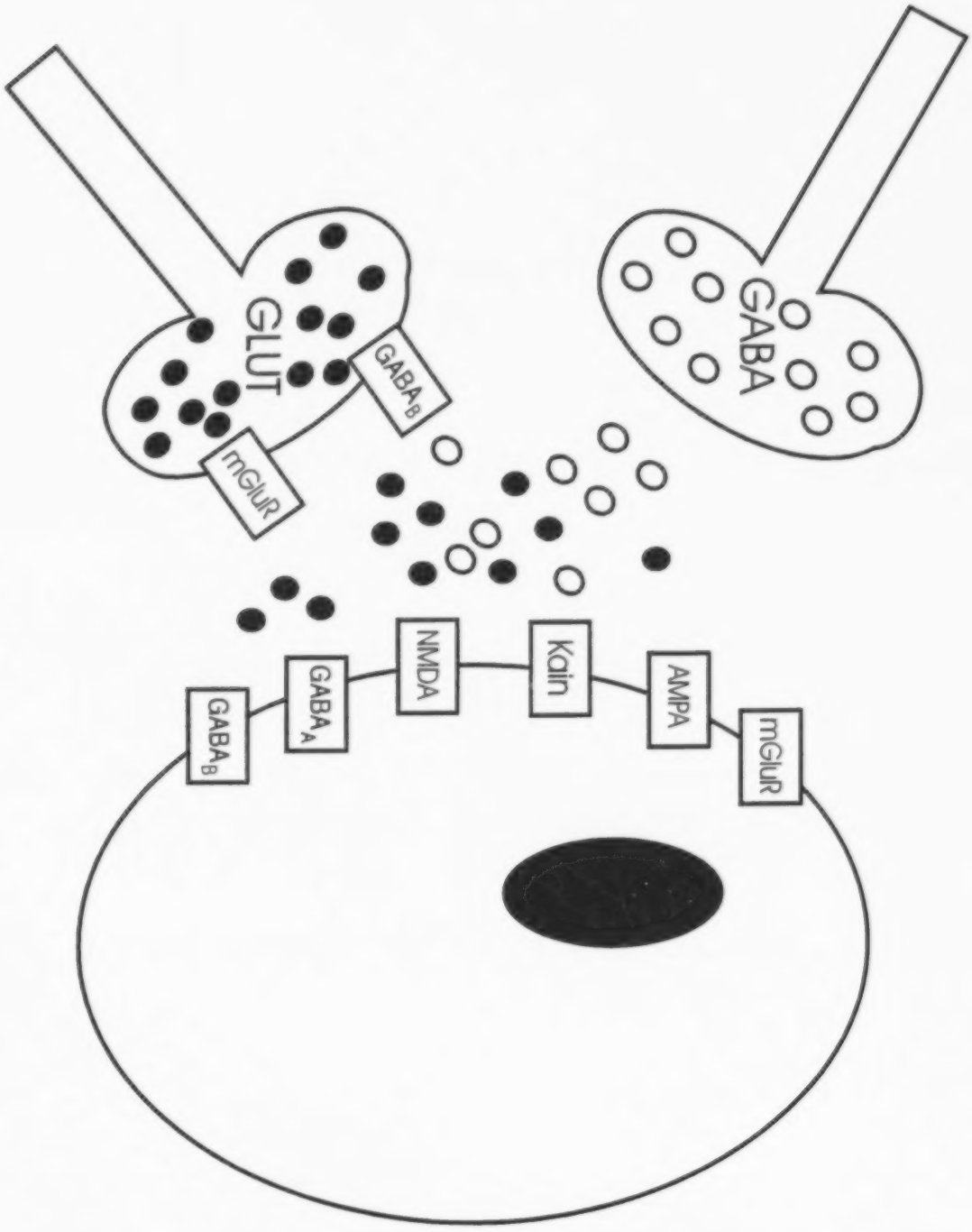
GABA
GLUT
GABA$_B$
mGluR
GABA$_B$
GABA$_A$
NMDA
Kain
AMPA
mGluR

Figure 7-2. VP released from presynaptic terminals acts at postsynaptic V_1 and V_2 receptors. VP activation of V_1 receptors results in the decrease (shown by "-") in I_C whereas VP activation of V_2 receptors elicits an increase in I_C (shown by the "+").

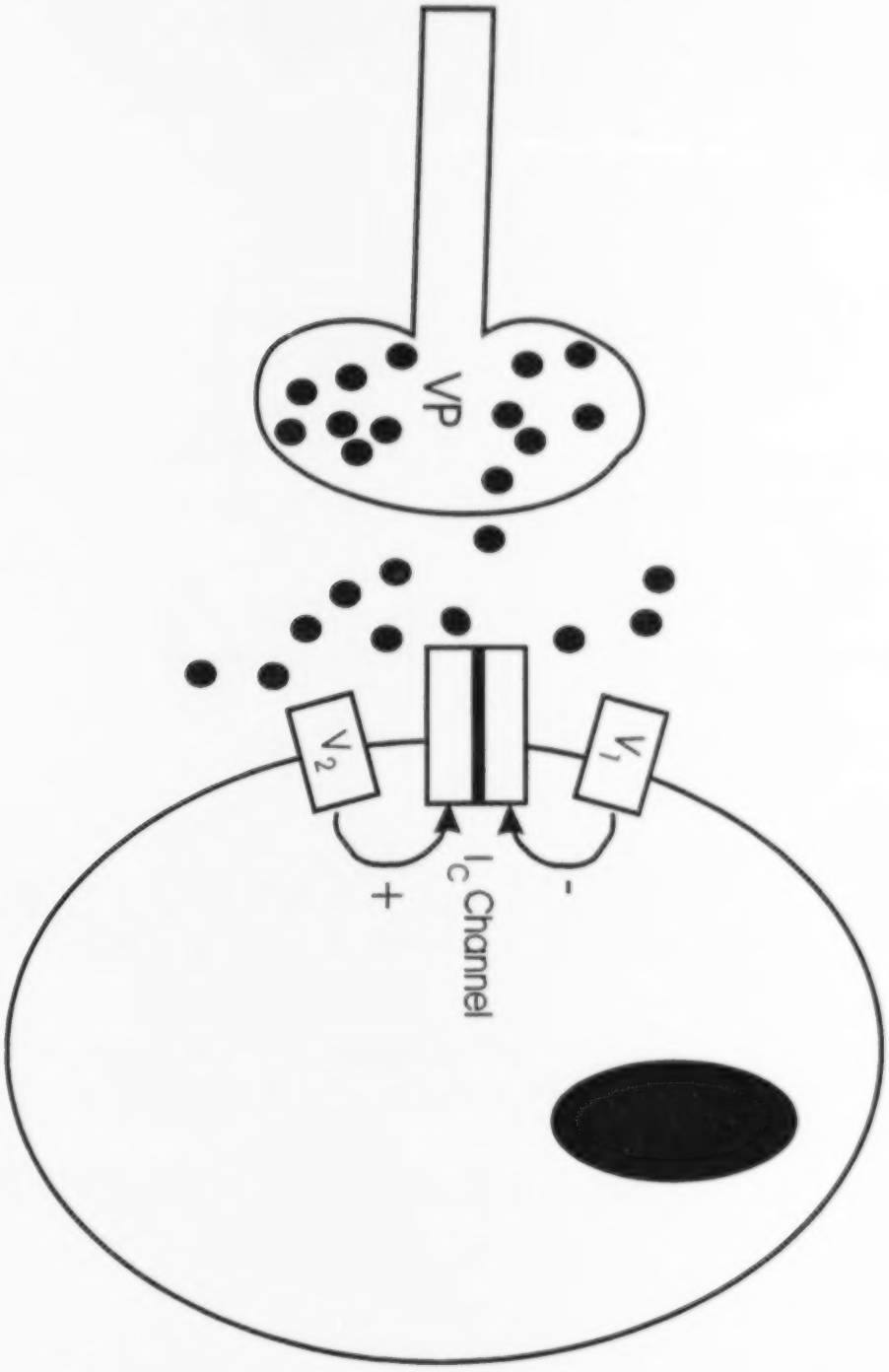
VP
V_2
V_1
+
I_C Channel
-

Figure 7-3. Zn^{++} released from presynaptic terminals modulates voltage-gated ion channels postsynaptically. Specifically, this cation increases I_A (shown by "+"), decreases I_K and I_{Ca} (shown by "-") and has no significant effect on I_{Na}. Both I_C and I_{AHP} channels are blocked consequent to the reduction in Ca^{++} influx (shown by "-" inside cell).

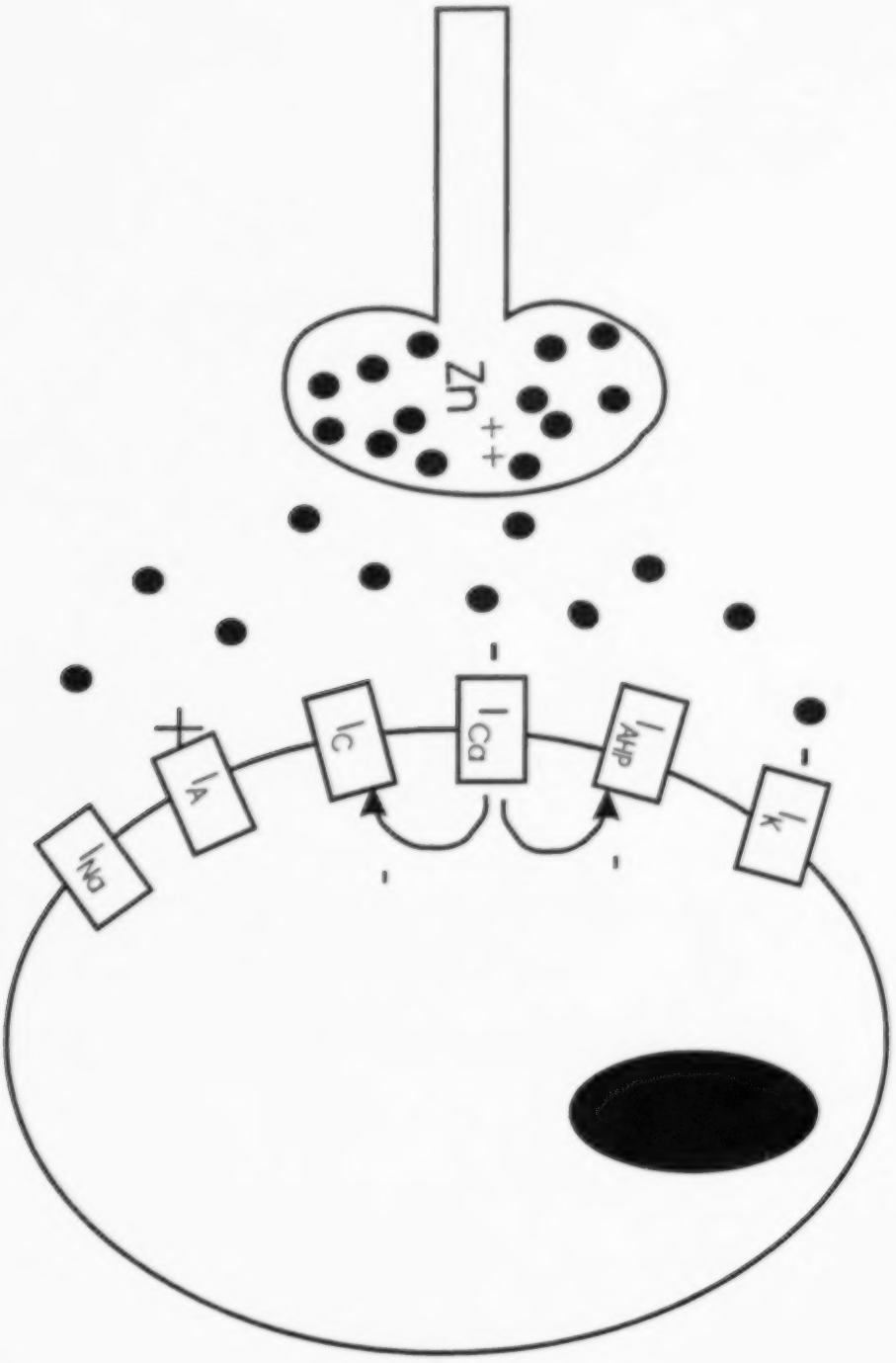
Zn
++
+
-
I_{NA}
I_A
I_C
I_{Ca}
I_{AHP}
I_K

REFERENCES

Alonso, A. and Kohler, C. A study of the reciprocal connections between the septum and the entorhinal area using anterograde and retrograde axonal transport methods in the rat brain. *J. Comp. Neurol.* 225:327-343, 1984.

Barger, S. W., Smith-Swintosky, V. L., Rydel, R. E., and Mattson, M. P. Beta-amyloid precursor protein mismetabolism and loss of calcium homeostasis in Alzheimer's disease. *Ann. N.Y. Acad. Sci.* 695:158-164, 1993.

Beaulieu, C., Dyck, R., and Cynader, M. Enrichment of glutamate in zinc-containing terminals of the cat visual cortex. *Neuroreport* 3:861-864, 1992.

Bland, B. H. The physiology and pharmacology of hippocampal formation theta rhythms. *Prog. Neurobiol.* 26:1-54, 1986.

Bland, B. H. and Colom, L. V. Extrinsic and intrinsic properties underlying oscillation and synchrony in limbic cortex. *Prog. Neurobiol.* 41:157-208, 1993.

Buhl, E. H., Otis, T. S., and Mody, I. Zinc-induced collapse of augmented inhibition by GABA in a temporal lobe epilepsy model. *Science* 271:369-372, 1996.

Carnes, K. M., Fuller, T. A., and Price, J. L. Sources of presumptive glutamatergic/aspartatergic afferents to the magnocellular basal forebrain in the rat. *J.Comp.Neurol.* 302:824-852, 1990.

Choi, D. W., Yokoyama, M., and Koh, J. Zinc neurotoxicity in cortical cell culture. *Neurosci.* 24:67-79, 1988.

Ciriello, J. and Janssen, S. A. Effect of glutamate stimulation of bed nucleus of the stria terminalis on arterial pressure and heart rate. *Am.J.Physiol.* 265(5 Pt

2):H1516-H1522, 1993.

Constantinidis, J. Hypothesis regarding amyloid and zinc in the pathogenesis of Alzheimer disease: potential for preventive intervention. *Alzhiemer Disease and Associated Disorders* 5(1):31-35, 1991.

Duncan, M. W., Marini, A. M., Watters, R., Kopin, I. J., and Markey, S. P. Zinc, a neurotoxin to cultured neurons, contaminates cycad flour prepared by traditional Guamanian methods. *J. Neurosci.* 12:1523-1537, 1992.

Ebadi, M. The presence of metallotheionein-like protein (MLT) in rat brain. *Fed. Proc.* 43:3317, 1984.

Ebadi, M., Iverson, P. L., Hao, R., Cerutis, D. R., Rojas, P., Happe, H. K., Murrin, L. C., and Pfeiffer, R. F. Expression and regulation of brain metallothionein. *Neurochem. Int.* 27(1):1-22, 1995.

Fischer, W., Wictorin, K., Bjorklund, A., Williams, L. R., Varon, S., and Gage, F. H. Amelioration of cholinergic neuron atrophy and spatial memory impairment in aged rats by nerve growth factor. *Nature* 329:65-68, 1987.

Fliers, E., DeVries, G. J., and Swaab, D. F. Changes with aging in the vasopressin and oxytocin innervation of the rat brain. *Brain Res.* 348(1):1-8, 1985.

Frederickson, C. J., Hernandez, M. D., Goik, S. A., Morton, J. D., and McGinty, J. D. Loss of zinc staining form hippocampal mossy fibers during kainic acid induced seizure: a histofluorescence study.. *Brain Res.* 446:383-386, 1988.

Freund, T. F. and Antal, M. GABA-containing neurons in the septum control inhibitory interneurons in the hippocampus. *Nature* 336(6195):170-173, 1988.

Hofer, M., Pagliusi, S. R., Hohn, A., Leibrock, J., and Barde, Y. Regional distribution of brain-derived neurotrophic factor mRNA in the adult mouse brain. *EMBO* 9(8):2459-2464, 1990.

Jakab, R. L. and Leranth, C. Septum. In: *The Rat Nervous System*, edited by G. Paxinos. New York: Academic Press, 1995, p. 405-442.

Jhamandas, J. H. and Renaud, L. P. Diagonal band neurons may mediate arterial baroreceptor input to hypothalamic vasopressin-secreting neurons. *Neurosci. Lett.* 65:214-218, 1986.

Jhamandas, J. H. and Renaud, L. P. A gamma-amminobutyric-acid mediated baroreceptor input to supraoptic vasopressin neurons in the rat. *J. Physiol.* 381:595-606, 1986.

Kesner, R. P., Berman, R. F., and Tardif, R. Place and taste aversion learning: role of basal forebrain, parietal cortex, and amygdala. *Br. Res. Bull.* 29:345-353, 1992.

Koh, J. and Choi, D. W. Zinc alters excitatory amino acid neurotoxicity on cortical neurons. *J. Neurosci.* 8:2164-2171, 1988.

Lee, P.J., Jhamandas, K., Boegman, R.J., and Beninger, R.J. Zinc chelating agents inhibit excitotoxic action of quinolinic acid on basal forebrain cholinergic neurons. Soc. Neurosci. Abstr. 1996 (Submitted)

Mayer, M. L. and Vyklicky, L. The action of zinc on synaptic transmission and neuronal excitability in cultures of mouse hippocampus. *J. Physiol.* 415:315-365, 1989.

Mitchell, S. J. and Ranck, J. B. Generation of theta rhythm in medial entorhinal cortex of freely moving rat. *Brain Res.* 189:49-66, 1980.

Mohanakrishnan, P., Fowler, A. H., Vonsattel, J. P., Husain, M. M., Jolles, P. R., Liem, P.,

and Komoroski, R. A. An *in vitro* 1H nuclear magnetic resonance study of the temporopatietal cortex of Alzheimer brains. *Exp. Br. Res* 102(3):503-510, 1995.

Moos, T. Simultaneous application of Timm's sulphide silver method and immunofluroresccence histochemistry. *J. Neurosci. Meth.* 48:149-156, 1993.

Narahashi, T., Ma, J. Y., Arakawa, O., Reuveny, E., and Nakahiro, M. GABA receptor-channel complex as a target site of mercury, copper, zinc, and lanthanides. *Cellular and Molecular Neurobiology* 14(6):599-620, 1994.

Oka, H. and Yoshida, K. Septohippocampal connectons to field CA1 of the rat identified with field potential analysis an retrograde labeling by horseradish peroxidase. *Neurosci. Lett.* 58:19-24, 1985.

Phillips, S., Sangalang, V., and Sterns, G. Basal forebrain infarction. A clinicopathologic correlation.. *Arch.Neurol.* 44(11):1134-1138, 1987.

Pohle, W. and Rauca, C. Hypoxia protects against the neurotoxicity of kainic acid. *Brain Res.* 644(2):297-304, 1994.

Pohle, W. and Rauca, C. Hypoxia protects against the neurotoxicity of kainic acid. *Brain Res.* 644:297-304, 1994.

Sacchi, O., Rossi, M. L., and Canella, R. The slow Ca^{2+}-activated K^+ current, I_{AHP}, in the rat sympathetic neurone. *J. Physiol.* 483(Pt 1):15-27, 1995.

Sainsbury, R. S. and Bland, B. H. The effects of selective septal lesions on theta production in CA1 and the dentate gyrus of the hippocampus. *Physiol. Behav.* 26:1097-1101, 1981.

Sanders, S. K. and Shekhar, A. Blockade of $GABA_A$ receptors in the region of the anterior

basolateral amygdala of rats elicits increases in heart rate and blood pressure. *Brain Res.* 567(1):101-110, 1991.

Sasaki, H., Muramoto, O., Kanazawa, I., Arai, H., Kosaka, K., and Iizuka, R. Regional distribution of amino acid transmitters in postmortem brains of presenile and senile dementia of Alzheimer type. *Ann. Neurol.* 19(3):263-269, 1986.

Scott, H. L., Tannenberg, A. E., and Dodd, P. R. Variant forms of neuronal glutamate transporter sites in Alzheimer's disease cerebral cortex. *J. Neurochem.* 64(5):2193-2202, 1995.

Shaw, P. J. Excitatory amino acid neurotransmission, excitotoxicity, and excitotoxins. *Curr. Op. Neurol. Neurosurg.* 5(3):383-390, 1992.

Smart, T. G. A novel moduexcitability site for zinc on the $GABA_A$ receptor complex in cultured rat neurones. *J. Physiol.* 447:587-625, 1992.

Smart, T. G., Xie, X., and Krishek, B. J. Modulation of inhibitory and excitatory amino acid receptor ion channels by zinc. *Prog. Neurobiol.* 42:393-441, 1994.

Smith-Swintosky, V. L. and Mattson, M. P. Glutamate, beta-amyloid precursor proteins, and calcium mediated neurofibrillary degeneration. *J. Neural Transm. Suppl.* 44:29-45, 1994.

Toth, K., Borhegyi, Z., and Freund, T. F. Postsynaptic targets of GABAergic hippocampal neurons in the medial septum-diagonal band of Broca complex. *J. Neurosci.* 13(9):3712-3724, 1993.

Wallwork, J. C. Zinc and the central nervous system. *Prog. Food Nutr. Sci.* 11(2):203-247, 1987.

Weiss, J. H., Hartley, D. M., Koh, J. Y., and Choi, D. W. AMPA receptor activation potentiates zinc neurotoxicity. *Neuron* 10(1):43-49, 1993.

Wenk, G., Hughey, D., Boundry, V., Kim, A., and Walker, L. Neurotransmitters and memory: role of cholinergic, serotonergic, and noradrenergic systems. *Behav. Neurosci.* 101:325-332, 1987.

Westbrook, G. L. and Mayer, M. L. Micromolar concentrations of Zn^{++} antagonize NMDA and GABA responses of hippocampal neurons. *Nature* 328(6131):640-643, 1987.

Womble, M. D. and Moises, H. C. Muscarinic modulation of conductances underlying the afterhyperpolarization in neurons of the rat basolateral amygdala. *Brain Res.* 621:87-96, 1993.

Young, A. B. Cortical amino acidergic pathways in Alzheimer's disease. *J. Neural Transm. Suppl.* 24:147-152, 1987.

Zaborszky, L., Cullinan, W. E., and Braun, A. Afferents to basal forebrain cholinergic projection neurons: an update. In: *The Basal Forebrain*, edited by T.C.Napier et al., New York: Plenum Press, 1991, p. 43-100.

Zhang, L. and McBain, C. J. Potassium conductances underlying repolarization and afterhyperpolarization in rat CA1 hippocampal interneurons. *J. Physiol* 488(3):661-672, 1995.